(19) DANMARK

(10) DK/EP 3820569 T3

(12) Oversættelse af europæisk patentskrift

Patent- og Varemærkestyrelsen

(51) Int.Cl.: *A 61 P 35/00 (2006.01)* *A 61 K 39/00 (2006.01)* *C 07 K 16/28 (2006.01)*

(45) Oversættelsen bekendtgjort den: **2025-01-02**

(80) Dato for Den Europæiske Patentmyndigheds bekendtgørelse om meddelelse af patentet: **2024-11-20**

(86) Europæisk ansøgning nr.: **19740347.0**

(86) Europæisk indleveringsdag: **2019-07-12**

(87) Den europæiske ansøgnings publiceringsdag: **2021-05-19**

(86) International ansøgning nr.: **EP2019068793**

(87) Internationalt publikationsnr.: **WO2020011964**

(30) Prioritet: **2018-07-12 GB 201811405**
2018-11-09 GB 201818283
2019-02-26 GB 201902594

(84) Designerede stater: **AL AT BE BG CH CY CZ DE DK EE ES FI FR GB GR HR HU IE IS IT LI LT LU LV MC MK MT NL NO PL PT RO RS SE SI SK SM TR**

(73) Patenthaver: **invoX Pharma Limited, Suite 2, First Floor, The Westworks, 195 Wood Lane, White City Place, London W12 7FQ, Storbritannien**

(72) Opfinder: **LAKINS, Matthew, c/o F-star Biotechnology Limited Eddeva B920 , Babraham Research Campus, Cambridge Cambridgeshire CB22 3AT, Storbritannien**
MUNOZ-OLAYA, Jose, c/o F-star Biotechnology Limited Eddeva B920 , Babraham Research Campus, Cambridge Cambridgeshire CB22 3AT, Storbritannien
WOLLERTON, Francisca, c/o F-star Biotechnology Limited Eddeva B920 , Babraham Research Campus, Cambridge Cambridgeshire CB22 3AT, Storbritannien
BATEY, Sarah, c/o F-star Biotechnology Limited Eddeva B920 , Babraham Research Campus, Cambridge Cambridgeshire CB22 3AT, Storbritannien
TUNA, Mihriban, c/o F-star Biotechnology Limited, Eddeva B920, Babraham Research Campus, Cambridge, Cambridgeshire CB22 3AT, Storbritannien
KOERS, Alexander, c/o F-star Biotechnology Limited Eddeva B920 , Babraham Research Campus, Cambridge Cambridgeshire CB22 3AT, Storbritannien

(74) Fuldmægtig i Danmark: **Dennemeyer & Associates S.A, P.O. Box 700425, DE-81304 Munich, Tyskland**

(54) Benævnelse: **ANTISTOFMOLEKYLER DER BINDER PD-L1 OG CD137**

(56) Fremdragne publikationer:
WO-A1-2018/056821
WO-A1-2019/025545
WO-A2-2017/123650
LAKINS ET AL.: "A Novel CD137/PD-L1 Bispecific Antibody Modulates the Tumour Microenvironmentby Activating CD8+ T cells and Results in Tumour Growth Inhibition", 7 November 2018 (2018-11-07), XP002794172, Retrieved from the Internet <URL:http://www.f-star.com/media/87488/201811-SITC-2018-F-star-

Fortsættes ...

FS222-Poster-ONLINE.pdf> [retrieved on 20190908]
WOZNIAK-KNOPP G ET AL: "Introducing antigen-binding sites in structural loops of immunoglobulin constant domains: Fc fragments with engineered HER2/neu-binding sites and antibody properties", PROTEIN ENGINEERING, DESIGN AND SELECTION, vol. 23, no. 4, 1 April 2010 (2010-04-01), OXFORD JOURNAL, LONDON, GB, pages 289 - 297, XP009137665, ISSN: 1741-0126, [retrieved on 20100211], DOI: 10.1093/PROTEIN/GZQ005
SHINDO Y ET AL: "Combination immunotherapy with 4-1BB activation and PD-1 blockade enhances antitumor efficacy in a mouse model of subcutaneous tumor", ANTICANCER RESEARCH - INTERNATIONAL JOURNAL OF CANCER RESEARCH AND TREATMENT, INTERNATIONAL INSTITUTE OF ANTICANCER RESEARCH, GR, vol. 35, no. 1, 1 January 2015 (2015-01-01), pages 129 - 136, XP002746546, ISSN: 0250-7005
RAMELET M ET AL: "Beneficial outcome of combination therapy with 4-1BB targeting antibody", EUROPEAN JOURNAL OF CANCER, vol. 69, 29 November 2016 (2016-11-29), XP029843751, ISSN: 0959-8049, DOI: 10.1016/S0959-8049(16)32886-6

DESCRIPTION

Description

Field of the invention

[0001] The present invention relates to antibody molecules that bind both PD-L1 and CD137 and are able to induce agonism of CD137. The antibody molecules comprise a CDR-based binding site for PD-L1, and a CD137 antigen-binding site that is located in a constant domain of the antibody molecule. The antibody molecules of the invention find application, for example, in the treatment of diseases, such as cancer.

Background to the invention

[0002] Programmed cell death 1 (PD-1) and its ligands PD-L1 (CD274, B7-H1) and PD-L2 (B7-DC) deliver inhibitory signals that regulate the balance between T cell activation, tolerance, and immunopathology. PD-L1 is transiently expressed on all immune cells and some tumour cells. PD-L1 is a member of the B7 protein family and shares approximately 20% amino acid sequence identity with B7.1 and B7.2. Human PD-L1 shares 70% and 93 % amino acid identity with the murine and cynomolgus orthologs of PD-L1, respectively.

[0003] PD-L1 binds to its receptor PD-1 with an affinity (K_D) of 770 nM. PD-1 is expressed on activated T cells, B cells and myeloid cells, and modulates activation or inhibition of cellular immune responses. Binding of PD-L1 to PD-1 delivers an inhibitory signal, reducing cytokine production and proliferation of T cells. Consequently, PD-L1 expression by cells can mediate protection against cytotoxic T lymphocyte (CTL) killing and is a regulatory mechanism that dampens chronic immune responses during viral infections. Cancer, as a chronic and pro-inflammatory disease, subverts this immune-protective pathway through up-regulation of PD-L1 expression to evade the host immune response. In the context of an active immune response, interferon-gamma (IFN-y) also upregulates the expression of PD-L1.

[0004] PD-L1 also mediates immune suppression through interaction with another protein, B7.1 (also known as CD80), blocking its ability to deliver one of the secondary signals of activation on T cells through CD28. In terms of PD-L1 expression on tumour cells and its engagement with B7.1, the relevance of this specific interaction in tumour immune resistance is still unclear.

[0005] PD-L1 expression has been shown in a wide variety of solid tumours. Of 654 samples

examined in one study, spanning 19 tumours from different sites, 89 (14%) were PD-L1 positive (≥5% frequency). The highest PD-L1 positive frequencies were seen in head and neck (17/54; 31%), cervical (10/34; 29%), cancer of unknown primary origin (CUP; 8/29; 28%), glioblastoma multiforme (GBM; 5/20; 25%), bladder (8/37; 21%), oesophageal (16/80; 20%), triple negative (TN) breast (6/33; 18%), and hepatocarcinoma (6/41; 15%) (Grosso *et* al, 2013). Tumour-associated expression of PD-L1 has been shown to confer immune resistance and potentially protect tumour cells from T cell mediated apoptosis.

[0006] Clinical trials have shown the clinical benefit of targeting PD-L1 in patients leading to the approval of three anti-PD-L1 targeting monoclonal antibodies to date. Atezolizumab (MPDL3280A, RG7466, Tecentriq™), a humanised IgG1 antibody which binds PD-L1, is approved for first line treatment of non-small-cell lung carcinoma (NSCLC) and first and second line treatment of bladder cancer after clinical trials showed objective response rates (ORR) of 38% and 43%, respectively, in patients with PD-L1 positive tumours (Iwai *et al.,* 2017). Avelumab (MSB0010718C, Bavencio™) is a fully human IgG1 antibody which binds to PD-L1 and is approved for the treatment of Merkel-cell carcinoma and second line treatment of bladder cancer, whereas the fully human IgG1 antibody durvalumab (MEDI4736, Imfinzi™) is approved for the treatment of second line bladder cancer. Additional trials with these antibodies and other anti-PD-L1 therapeutics are ongoing focusing on expanding the range of solid cancers that can be treated, including colorectal cancer, gastric cancer, breast cancer, head and neck, pancreatic, ovarian and renal cell carcinoma.

[0007] CD137 (4-1 BB; TNFRSF9) is a co-stimulatory molecule of the tumour necrosis factor receptor superfamily (TNFRSF). CD137 is widely known to be upregulated on $CD8^+$ T cells following activation, and can also be expressed on activated $CD4^+$ helper T cells, B cells, regulatory T cells, natural killer (NK) cells, natural killer T (NKT) cells and dendritic cells (DCs) (Bartkowiak & Curran, 2015). The primary functional role of CD137 in enhancing T cell cytotoxicity was first described in 1997 (Shuford *et al.,* 1997), and soon thereafter anti-CD137 mAbs were proposed as anti-cancer therapeutics.

[0008] CD137 is a transmembrane protein with four extracellular cysteine-rich domains, referred to as CRD1-4, and a cytoplasmic region responsible for CD137 signalling. The ligand for CD137 is CD137L. Although no crystal structure exists for the CD137/CD137L complex, it is predicted that CD137 forms a trimer/trimer complex with CD137L (Won *et al.,* 2010). Engagement of CD137L results in receptor trimer formation and subsequent clustering of multiple receptor trimers, and leads to the activation of the CD137 signalling cascade. This signalling cascade provides a survival signal to T cells against activation-induced cell death (Hurtado *et al.,* 1997) thereby playing a critical role in sustaining effective T cell immune responses and generating immunological memory (Bartkowiak & Curran, 2015).

[0009] CD137 is expressed by activated T cells and has been used as a marker to identify antigen-specific $CD4^+$ and $CD8^+$ T cells (Wolfl *et al.,* 2007; Ye *et al.,* 2014). Typically,

expression of CD137 is higher on $CD8^+$ T cells than $CD4^+$ T cells (Wen *et al.,* 2002). In the case of $CD8^+$ T cells, proliferation, survival and cytotoxic effector function via the production of interferon gamma and interleukin 2 have been attributed to CD137 crosslinking. CD137 crosslinking also contributes to the differentiation and maintenance of memory $CD8^+$ T cells (Chacon *et al.,* 2013). In some subsets of $CD4^+$ T cells, CD137 crosslinking similarly leads to proliferation and activation and results in the release of cytokines such as interleukin 2 (Makkouk *et al.,* 2016). CD137 has also been demonstrated to be expressed on tumour-reactive subsets of tumour-infiltrating lymphocytes (TILs). CD137 monotherapy has been shown to be efficacious in several preclinical immunogenic tumour models such as MC38, CT26 and B cell lymphomas.

[0010] Clinical development of CD137 mAbs has been slow due to dose-limiting high-grade liver inflammation associated with CD137 agonist antibody treatment. Urelumab (BMS-663513), a non-ligand blocking human IgG4 isotype antibody (Chester *et al,* 2018), was the first anti-CD137 antibody to enter clinical trials but these were halted after significant, on target, dose-dependent liver toxicity was observed (Chester *et al.,* 2018; Segal *et al.,* 2017; and Segal *et al.,* 2018). More recently, clinical trials of urelumab in the treatment of solid cancers was recommenced in which urelumab treatment was combined with radiotherapy (NCT03431948) or with other therapeutic antibodies, such as rituximab (NCT01775631), cetuximab (NCT02110082), anti-PD-1 antibody nivolumab (NCT02253992, NCT02534506, NCT02845323), and a combination of nivolumab and the anti-LAG-3 antibody BMS986016 (NCT02658981). However, to reduce liver toxicity associated with urelumab treatment, dosing of urelumab in these trials had to be limited and efficacy results were disappointing (Chester *et al.,* 2018).

[0011] No dose-limiting toxicity has been observed with Pfizer's anti-CD137 antibody utomilumab (PF-05082566), a human IgG2 isotype antibody, in the dose range 0.03 mg/kg up to 10 mg/kg in Phase I clinical trials of advanced cancer (Chester *et al.* 2016; Segal *et al.,* 2018). However, the overall objective response rate with this antibody was only 3.8% in patients with solid tumours, potentially indicating that utomilumab has a weaker potency and clinical efficacy than urelumab, whilst having a more favourable safety profile (Chester *et al.,* 2018; Segal *et al.,* 2018). Utomilumab has been tested in combination with radiotherapy (NCT03217747) or chemotherapy, as well as in combination with other antibody therapies, including anti-PD-L1 antibody avelumab (NCT02554812), and anti-PD-1 antibody pembrolizumab (NCT02179918), to assess the safety, tolerability, dose-limiting toxicities (DLTs), maximum tolerated dose (MTD) and efficacy of the different treatment combinations. These trials are ongoing with early results showing no DLTs for doses up to 5 mg/kg and a 26% patient response rate for the combination of utomilumab and pembrolizumab. (Tolcher *et al.,* 2016) (Pérez-Ruiz *et al,* 2017).

[0012] Clinical trials are ongoing to test anti-CD137 antibody, utomilumab, in combination with anti-PD-L1 antibody, avelumab (NCT02554812, NCT3390296). Triple combinations of utomilumab with avelumab and other therapies are also being tested (NCT02554812,

NCT03217747, NCT03440567, NCT03414658).

[0013] A number of bispecific molecules targeting CD137 are also in early stage development, for example those targeting CD137 as well as FAP-alpha (Link *et al.,* 2018; Reichen *et al.,* 2018), HER2 (Hinner *et al.,* 2015 and WO 2016/177802 A1), or EphA2 (Liu *et al.,* 2017). CD137L fusion proteins which target tumours for example via FAP-alpha (Claus *et al.,* 2017) are also being developed. The most clinically advanced CD137 bispecific is PRS-343, a CD137/HER2 bispecific molecule which has recently entered Phase I clinical trials for treatment of a range of solid tumours to assess its safety, tolerability and efficacy (NCT03330561).

[0014] There are other approaches to combine anti-CD137 activity and anti-PD-L1 activity into bispecific therapies. One approach utilized the biclonics technology to produce a full length heterodimeric human IgG with monovalent binding to both CD137 and PD-L1 (WO2018056821) resulting in a molecule that can bind to both CD137 and PD-L1 and induce CD137 agonism in the presence of high levels of PD-L1. A second approach has been described using sdAb-Fc fusions to target both CD137 and PD-L1 (WO2017123650). Both approaches are capable of binding CD137 in the absence of PD-L1 binding and induce low levels of CD137 agonism in the absence of PD-L1, this agonism is increased in the presence of high levels of PD-L1. A further heterodimeric bispecific antibody has been described with monovalent binding to both CD137 and PD-L1 (WO2019/025545 A1), containing a humanised anti-CD137 binding region and a human anti-PD-L1 region that induces CD137 agonism in the presence of levels of PD-L1.

[0015] Current data shows that overall treatment with anti-PD-L1 monotherapy results in a response in less than 50% of cancer patients. Thus, there remains a need in the art for additional molecules which can target PD-L1 and which find application in cancer therapy. PD-1/PD-L1 blockade has strong clinical validation however less than 50% of patients respond in a monotherapy setting. Combinations of PD-L1 and additional immune modulators are expected to demonstrate improved efficacy. However, such combinations may be linked to an increase in treatment related adverse events and as a result the efficacy can be restricted by the limited therapeutic window. CD137-targetting agonistic molecules have yet to demonstrate significant responses in cancer patients, this may in part be due to relatively low dose levels due to a limited therapeutic index. Thus, there remains a need in the art to develop treatments which combine PD-L1 blockade and elicit CD137 agonism in safe and efficacious therapies.

Statements of invention

[0016] As explained in the background section above, clinical development of CD137 agonist molecules has been held back due to treatment being either associated with dose-limiting high-grade liver inflammation (urelumab) or low clinical efficacy (utomilumab).

[0017] The present inventors recognised that there is a need in the art for CD137 agonist molecules which exhibit high activity and where agonism can be localised to the tumour

microenvironment. Such molecules could be administered to individuals at doses which optimize the potency and therefore efficacy of the molecule, and could be employed in the treatment of cancer as immunotherapeutic agents, for example.

[0018] The antibody molecules of the present invention comprise a CD137 antigen-binding site that is located in a constant domain of the antibody molecule. The present inventors performed an extensive selection and affinity maturation program to isolate a panel of CD137 antigen-binding site containing molecules (also referred to as "Fcabs" herein) which bind to dimeric CD137 with a higher affinity than to monomeric CD137.

[0019] 'Affinity' as referred to herein may refer to the strength of the binding interaction between an antibody molecule and its cognate antigen as measured by K_D. As would be readily apparent to the skilled person, where the antibody molecule is capable of forming multiple binding interactions with an antigen (e.g. where the antibody molecule is capable of binding the antigen bivalently and, optionally, the antigen is dimeric) the affinity, as measured by K_D, may also be influenced by avidity, whereby avidity refers to the overall strength of an antibody-antigen complex.

[0020] Expression of CD137 by T cells is upregulated on activation. Without wishing to be bound by theory, it is thought that due to the high expression of CD137 on activated T cells, CD137 will be in the form of dimers, trimers and higher-order multimers on the surface of such cells. In contrast, naive immune cells, such as naive T cells, express low or negligible levels of CD137 on their cell surface and any CD137 present is therefore likely to be in monomeric form. It is therefore expected that antibody molecules comprising a CD137 antigen-binding site which bind to dimeric or multimeric CD137 with high avidity, will preferentially bind to activated immune cells, such as activated T cells, as opposed to naive immune cells, for example.

[0021] These features of the CD137 antigen-binding site are believed to distinguish the antibody molecules of the present invention from known antibodies that bind CD137, for example, the antibody described in WO2018056821. WO2018056821 describes an antibody containing a monovalent CD137 binding domain that binds to CD137 with a high affinity (low nM range, see Table 6 of WO2018056821). Since these antibodies do not distinguish between monomeric and dimeric or multimeric CD137, it is not expected that these prior art antibodies would display the same preferential binding to activated immune cells.

[0022] As described in the background section above, it is thought that initial ligation of CD137 ligand to CD137 initiates a chain of events that leads to receptor trimerisation, followed by receptor clustering, activation and subsequent initiation of potent anti-tumour T cell activity. For a therapeutic agent to efficiently achieve activation of CD137, it is therefore expected that several receptor monomers need to be bridged together in a way that mimics bridging by the trimeric ligand.

[0023] Utomilumab is an IgG2 molecule and is dependent on crosslinking by Fcγ receptors for its agonist activity. Urelumab is an IgG4 molecule with constitutive activity and so does not

require crosslinking by Fcγ receptors for activity, although its agonist activity is enhanced on crosslinking by some Fcγ receptors. Fcγ receptors are found throughout the human body. The immune cell activation activity of utomilumab and urelumab is therefore not limited to particular sites in the body and thus may occur in locations other than the tumour microenvironment, such as the liver.

[0024] The present inventors have shown that the CD137 antigen-binding site present in the antibody molecules of the invention requires crosslinking in order to cluster and activate CD137. However, it should be noted that this is not an intrinsic feature of CD137 binders.

[0025] Rather, many of the CD137 binders isolated during the screening program bound to CD137 but did not require crosslinking for CD137 clustering and activation or induced limited CD137 clustering and activation in the absence of crosslinking.

[0026] As mentioned above, Fcγ receptor-mediated crosslinking has the disadvantage that Fcγ receptors are found throughout the human body and thus CD137 activation is not limited to a particular site. The present inventors therefore introduced mutations into the CH2 domain of the Fcabs to reduce or abrogate Fcγ receptor binding. Thus, in the absence of crosslinking through an agent other than Fcγ receptors, the antibody molecules of the invention do not exhibit CD137 agonist activity. Further, it is expected that these mutations will result in the antibody molecules of the present invention being unable to induce antibody cellular cytotoxicity, so the antibody molecules will not elicit killing of the immune cells they activate.

[0027] The present inventors have demonstrated that antibody molecules which contain the CD137 antigen-binding site described above and a CDR-based binding site for PD-L1 are highly effective in activating immune cells in locations where CD137 and PD-L1 are co-expressed, for example in a tumour microenvironment. Co-expression in this sense encompasses situations where CD137 and PD-L1 are expressed on the same cells, e.g. a T cell, and situations where CD137 and PD-L1 are expressed on different cells, for example a T cell and a tumour cell, respectively.

[0028] The antibody molecules are capable of binding simultaneously to CD137 and PD-L1. Thus, in locations where PD-L1 and CD137 are co-expressed, it is thought that binding of the antibody molecules to PD-L1 causes crosslinking of the antibody molecules, which in turn leads to clustering and activation of bound CD137 on the T cell surface.

[0029] As demonstrated by the present inventors, by reducing or abrogating Fcγ receptor binding, the agonistic activity of the antibody molecules is dependent on both the PD-L1 and CD137 being present. In other words, the agonistic activity is conditional and the antibody molecules are therefore expected to be capable of only activating immune cells in locations where PD-L1 is present, such as in the tumour microenvironment. This targeted activation of immune cells is expected to be beneficial in avoiding the liver inflammation seen with urelumab treatment, for example.

[0030] Indeed, the present inventors demonstrate that antibody molecules having the features described above do not show exhibit severe hepatoxicity when administered in a mouse model at therapeutic doses. Only minimal liver pathology was observed in mice that had been administered with these antibody molecules, which was not deemed to represent the severe hepatoxicity that has been previously reported for other anti-CD137 agonist antibodies. Preliminary studies in cynomolgus monkeys also showed that the antibody molecules are safe and well tolerated up to 30mg/kg. Without wishing to be bound by theory, it is expected that the results from these animal models will translate to the clinic in predicting the risk of hepatoxicity in human patients and therefore that the antibody molecules of the invention would have low risk of inducing hepatoxicity in human patients treated at therapeutic doses.

[0031] The present inventors also provide *in vitro* evidence that the level of CD137 agonistic activity induced by the antibody molecule correlates with the amount of PD-L1 expression on the cell surface. The inventors demonstrate that the antibody molecule is capable of agonising CD137 even where there is a low level of PD-L1 expression and that as the level of PD-L1 in the system increases, so does the CD137 agonistic activity. This result further supports the evidence that CD137 agonistic activity is dependent on PD-L1 expression and suggests that the antibody molecules of the invention will have a broad range of activity on tumours that express varying levels of PD-L1 on the tumour cell surface.

[0032] The CDR-based binding sites for PD-L1 described above are able to efficiently block binding of PD-L1 to its receptor PD-1. PD-1 is expressed on activated T cells, B cells, and myeloid cells, and modulates activation or inhibition of cellular immune responses. Binding of PD-L1 to PD-1 delivers an inhibitory signal, reducing cytokine production and proliferation of T cells, thereby dampening the immune response. In cancer, the interaction of PD-L1 on a tumour cell with PD-1 on a T cell reduces T cell activity to prevent the immune system from attacking the tumour cells. Therefore, it is expected that by blocking the binding of PD-L1 to PD-1, the antibody molecules of the invention can prevent the tumour cells from evading the immune system in this way. Without wishing to be bound by theory, it is believed that this efficient blocking of PD-L1 binding to PD-1 functions together with the CD137 agonistic activity described above to increase anti-tumour potency of the antibody molecule.

[0033] The present inventors have also shown that such bispecific antibody molecules comprising the CD137 antigen-binding site and CDR-based binding site for PD-L1 described above are capable of supressing tumour growth *in vivo.* Furthermore, more effective tumour growth suppression was observed with the bispecific antibody molecules as compared to a combination of two monospecific antibody molecules where one of the antibody molecules comprised a CDR-based antigen-binding site for PD-L1 and the other molecule comprised a CDR-based antigen-binding site for CD137, demonstrating that enhanced clustering and signalling of CD137, and thus T cell activation and corresponding anti-tumour effects, are seen with the antibody molecules of the invention.

[0034] Antibody molecules comprising a CD137 antigen-binding site of the invention may additionally be able to bind PD-L1 bivalently, such that the antibody molecules bind both

CD137 and PD-L1 bivalently. This is expected to be advantageous, as the bivalent binding of both targets is expected to make the bridging between the T cell expressing CD137 and the PD-L1 expressing cell more stable and thereby extend the time during which the T cell is localised at sites where PD-L1 is co-expressed with CD137, such as in the tumour microenvironment, and can act on the disease, e.g. the tumour. This is different to the vast majority of conventional bispecific antibody formats which are heterodimeric and bind each target antigen monovalently via one Fab arm. Such a monovalent interaction is expected to not only be less stable but also to be less efficient at inducing clustering of TNF receptors such as CD137 and/or to require higher expression of one or both targets to induce such clustering, and thus T cell activation. This is supported by experiments conducted by the present inventors, which showed that mAb^2 molecules comprising a bivalent Fab binding site for PD-L1 and a monovalent binding site for CD137 in one of the CH3 domains of the molecule induced lower levels of T cell activation, as measured by IFN-y release, than a mAb^2 binding both targets bivalently.

[0035] A further feature of the antibody molecules identified by the inventors is that the antigen-binding site for CD137 and the CDR-based binding site for PD-L1 are both contained within the antibody structure itself. In particular, the antibody molecules do not require other proteins to be fused to the antibody molecule via linkers or other means to result in molecule that binds bivalently to both of its targets. This has a number of advantages. Specifically, the antibody molecules can be produced using methods similar to those employed for the production of standard antibodies, as they do not comprise any additional fused portions. The structure is also expected to result in improved antibody stability, as linkers may degrade over time, resulting in a heterogeneous population of antibody molecules. In such heterogeneous populations, those antibodies in the population having only one protein fused to them, and thus binding one target only monovalently, are expected not to induce conditional agonism of TNF receptors such as CD137 as efficiently, as those antibodies which have two proteins fused to them and which are thus capable of binding both targets bivalently. Cleavage/degradation of the linker could take place prior to administration or after administration of the therapeutic to the patient (e.g. through enzymatic cleavage or the *in vivo* pH of the patient), thereby resulting in a reduction of its effectiveness whilst circulating in the patient. As there are no linkers in the antibody molecules of the invention, the antibody molecules are expected to retain the same number of binding sites both before and after administration. Furthermore, the structure of the antibody molecules is also preferred from the perspective of immunogenicity of the molecules, as the introduction of fused proteins or linkers or both may induce immunogenicity when the molecules are administered to a patient, resulting in reduced effectiveness of the therapeutic.

[0036] Thus, the present invention provides:

1. [1] An antibody molecule that binds to programmed death-ligand 1 (PD-L1) and CD137, comprising
    1. (a) a complementarity determining region (CDR)-based antigen-binding site for PD-L1; and
    2. (b) a CD137 antigen-binding site located in a CH3 domain of the antibody

molecule, wherein the CD137 antigen-binding site comprises a first sequence and a second sequence located in the AB and EF structural loops of the CH3 domain, respectively, wherein the first sequence is located between positions 14 and 17 of the CH3 domain and the second sequence is located between positions 91 and 99 of the CH3 domain, wherein the amino acid residue numbering is according to the IMGT numbering scheme, and

wherein the antibody molecule comprises the VH domain, VL domain, first sequence and second sequence set forth in:

1. (i) SEQ ID NOs **12, 14, 113** and **114,** respectively **[FS22-172-003-AA/E12v2];**
2. (ii) SEQ ID NOs **23, 25, 113** and **114,** respectively **[FS22-172-003-AA/E05v2];**
3. (iii) SEQ ID NOs **23, 30, 113** and **114,** respectively **[FS22-172-003-AA/G12v2];**
4. (iv) SEQ ID NOs **12, 14, 79** and **80,** respectively **[FS22-053-008-AA/E12v2];**
5. (v) SEQ ID NOs **23, 25, 79** and **80,** respectively **[FS22-053-008-AA/E05v2];**
6. (vi) SEQ ID NOs **12, 14, 79** and **89,** respectively **[FS22-053-017-AA/E12v2];**
7. (vii) SEQ ID NOs **23, 25, 79** and **89,** respectively **[FS22-053-017-AA/E05v2];** or
8. (viii) SEQ ID NOs **23, 30, 79** and **89,** respectively **[FS22-053-017-AA/G12v2].**

2. [2] The antibody molecule according to [1], wherein the antibody molecule comprises an immunoglobulin heavy chain and/or an immunoglobulin light chain, preferably an immunoglobulin heavy chain and an immunoglobulin light chain.
3. [3] The antibody molecule according to [1] or [2], wherein the antibody molecule comprises the VH domain and VL domain set out in (i) or (ii).
4. [4] The antibody molecule according to [3], wherein the antibody molecule comprises the VH domain and VL domain set out in (i).
5. [5] The antibody molecule according to any one of [1] to [4], wherein the first sequence is located at positions 15, 16, 16.5, 16.4, 16.3, 16.2, and 16.1 of the CH3 domain of the antibody molecule, wherein the amino acid residue numbering is according to the IMGT numbering scheme.
6. [6] The antibody molecule according to any one of [1] to [5], wherein the second sequence is located at positions 92 to 98 of the CH3 domain of the antibody molecule, wherein the amino acid residue numbering is according to the IMGT numbering scheme.
7. [7] The antibody molecule according to any one of [1] to [6], wherein the antibody molecule further comprises a third sequence located in the CD structural loop of the CH3 domain.
8. [8] The antibody molecule according to [7], wherein the third sequence is located at positions 43 to 78 of the CH3 domain of the antibody molecule, wherein the amino acid residue numbering is according to the IMGT numbering scheme.
9. [9] The antibody molecule according to any one of [7] to [8], wherein the third sequence

has the sequence set forth in SEQ ID NO: 73.

10. [10] The antibody molecule according to any one of [1] to [9], wherein the antibody molecule comprises the CH3 domain sequence set forth in:
    1. (i) SEQ ID NO: **115 [FS22-172-003];** or
    2. (ii) SEQ ID NO: **81 [FS22-53-008].**
11. [11] The antibody molecule according to any one of [1] to [10], wherein the first and second sequence have the sequence set forth in SEQ ID NOs **113** and **114 [FS22-172-003],** respectively.
12. [12] The antibody molecule according to any one of [1] to [9] and [11], wherein the antibody molecule comprises the CH3 domain sequence set forth in SEQ ID NO: **115 [FS22-172-003].**
13. [13] An antibody molecule according to any one of [1] to [12], wherein the antibody molecule is a human IgG1 molecule.
14. [14] The antibody molecule according to any one of [1] to [13], wherein the antibody molecule comprises the heavy chain and light chain of antibody:
    1. (i) **FS22-172-003-AA/E12v2** set forth in SEQ ID NOs **134** and **17,** respectively;
    2. (ii) **FS22-172-003-AA/E05v2** set forth in SEQ ID NOs **137** and **28,** respectively;
    3. (iii) **FS22-172-003-AA/G12v2** set forth in SEQ ID NOs **140** and **33,** respectively;
    4. (iv) **FS22-053-008-AA/E12v2** set forth in SEQ ID NOs **143** and **17,** respectively;
    5. (v) **FS22-053-008-AA/E05v2** set forth in SEQ ID NOs **146** and **28,** respectively;
    6. (vi) **FS22-053-017-AA/E12v2** set forth in SEQ ID NOs **152** and **17,** respectively;
    7. (vii) **FS22-053-017-AA/E05v2** set forth in SEQ ID NOs **153** and **28,** respectively; or
    8. (viii) **FS22-053-017-AA/G12v2** set forth in SEQ ID NOs **154** and **33,** respectively.
15. [15] The antibody molecule according to [14], wherein the antibody molecule comprises light chain and heavy chain set out in any one of (i) - (iv) of [14].
16. [16] The antibody molecule according to [14], wherein the antibody molecule comprises light chain and heavy chain set out in (i) of [14].
17. [17] The antibody molecule according to any one of [14] to [16], wherein the proline (P) at position **114** of the CH2 domain of the antibody is substituted with alanine (A), and wherein the amino acid residue numbering is according to the IMGT numbering scheme.
18. [18] The antibody molecule according to any one of [1] to [17], wherein the antibody molecule binds human PD-L1 and human CD137.
19. [19] The antibody molecule according to [18], wherein the PD-L1 consists of or comprises the sequence set forth in SEQ ID NO: **180.**
20. [20] The antibody molecule according to [18] or [19], wherein the human CD137 consists of or comprises the sequence set forth in SEQ ID NO: **186.**
21. [21] The antibody molecule according to any one of [1] to [20], wherein the antibody molecule has been modified to reduce or abrogate binding of the CH2 domain of the antibody molecule to one or more Fcγ receptors.
22. [22] The antibody molecule according to any one of [1] to [21], wherein the antibody molecule does not bind to one or more Fcγ receptors.
23. [23] The antibody molecule according to [21] or [22], wherein the Fcγ receptor is selected from the group consisting of: FcγRI, FcγRIIa, FcγRIIb and FcγRIII.

24. [24] A conjugate comprising the antibody molecule according to any one of [1] to [23] and a bioactive molecule.
25. [25] A conjugate comprising the antibody molecule according to any one of [1] to [23] and a detectable label.
26. [26] A nucleic acid molecule or molecules encoding the antibody molecule according to any one of [1] to [23].
27. [27] A nucleic acid molecule or molecules encoding the antibody molecule according to any one of [1] to [2], [5] to [10], [13] to [14] and [17] to [23], wherein the nucleic acid molecule(s) comprise(s) the heavy chain nucleic acid sequence and/or light chain nucleic acid sequence of:
    1. (i) **FS22-172-003-AA/E12v2** set forth in SEQ ID NOs **32** and **39,** or **135** and **136,** respectively, preferably SEQ ID NOs **32** and **39,** respectively;
    2. (ii) **FS22-172-003-AA/E05v2** set forth in SEQ ID NOs **138** and **139,** respectively;
    3. (iii) **FS22-172-003-AA/G12v2** set forth in SEQ ID NOs **141** and **142,** respectively;
    4. (iv) **FS22-053-008-AA/E12v2** set forth in SEQ ID NOs **144** and **145,** respectively; or
    5. (v) **FS22-053-008-AA/E05v2** set forth in SEQ ID NOs **147** and **148,** respectively.
28. [28] A vector or vectors comprising the nucleic acid molecule or molecules according to any one of [26] to [27].
29. [29] A recombinant host cell comprising the nucleic acid molecule(s) according to any one of [26] to [27], or the vector(s) according to [28].
30. [30] A method of producing the antibody molecule according to any one of [1] to [23] comprising culturing the recombinant host cell of [29 under conditions for production of the antibody molecule.
31. [31] The method according to [30] further comprising isolating and/or purifying the antibody molecule.
32. [32] A pharmaceutical composition comprising the antibody molecule or conjugate according to any one of [1] to [25] and a pharmaceutically acceptable excipient.
33. [33] The antibody molecule or conjugate according to any one of [1] to [25] for use in a method of treating cancer in an individual.
34. [34] The antibody molecule or conjugate for use according to [33], wherein the cancer is selected from the list consisting of: melanoma, bladder cancer, brain cancer, breast cancer, ovarian cancer, lung cancer, colorectal cancer, cervical cancer, liver cancer, head and neck cancer, pancreatic cancer, renal cancer, stomach cancer and Gastrointestinal Stromal Tumours (GISTs).
35. [35] The antibody molecule or conjugate for use according to [33], where the treatment comprises administering the antibody molecule or conjugate to the individual in combination with a second therapeutic.

Brief Description of the Figures

[0037]

Figure 1: Figures 1A, B and C show an alignment of the sequences of the CH3 domains of Fcabs FS22-053, FS22-053-008, FS22-053-009, FS22-053-010, FS22-053-011, FS22-053-012, FS22-053-013, FS22-053-014, FS22-053-015, FS22-053-016, FS22-053-017, FS22-172, FS22-172-001, FS22-172-002, FS22-172-003, FS22-172-004, FS22-172-005 and FS22-172-006 as well as the wild-type (WT) Fcab. The numbers of the residues according to the IMGT, IMGT exon (consecutive numbering), EU and Kabat numbering systems is indicated.

Figure 2 shows that the CD137/PD-L1 mAb^2 FS22-172-003-AA/E12v2 is capable of binding to activated $CD4^+$ **(Figure 2A)** and $CD8^+$ **(Figure 2B)** T cells. The anti-human CD137/PD-L1 mAb^2 FS22-172-003-AA/E12v2 bound activated T cells with EC_{50} values of 0.8 nM in the case of $CD4^+$ T cells and 0.9 nM in the case of $CD8^+$ T cells. The positive control anti-human PD-L1 antibody (G1-AA/E12v2) showed very similar affinity to the mAb^2 with EC_{50} values of 0.8 nM for both cell types. The positive control anti-human CD137 antibody (G1-AA/MOR7480.1) showed low binding to $CD4^+$ and $CD8^+$ cells, indicating the low level of CD137 expression on these cell types.

Figure 3 shows that anti-human CD137/PD-L1 mAb^2 FS22-172-003-AA/E12v2 does not bind to Fcγ receptor over-expressing CHO cells. Anti-human CD137/PD-L1 mAb^2 FS22-172-003-AA/E12v2, the positive control antibody for Fey receptor binding, G1/4420, and the negative control antibody for no Fcγ receptor binding, G1-AA/4420, were tested in a cell binding assay against five different Fcγ receptor over-expressing CHO cell lines expressing (A) FcgRIIA 131H, (B) FcgRIIA 131E, (C) FcgRIIB, (D) FcgRIIIA 158F, (E) FcgRIIIA 158V, as well as (F) a CHO WT cell line used as a negative control. The anti-human CD137/PD-L1 mAb^2, which contained the LALA mutation in the CH2 region, did not bind any of the Fcγ receptors tested and neither did it bind non-specifically to CHO WT cells (closed black triangles). The positive control antibody bound Fcγ receptors (closed black circles) and the negative control antibody G1-AA/4420, which contained the LALA mutation in the CH2 region, did not bind Fcγ receptors (open grey squares), as expected.

Figure 4 shows release of human IL-2 (hIL-2) in a human primary $CD8^+$ T cell activation assay in the presence of anti-human CD137/PD-L1 mAb^2 or positive control anti-human CD137 antibody G1-AA/20H4.9. All mAb^2 tested drove CD137 clustering and activation of $CD8^+$ T cells only when the mAb^2 were crosslinked by HEK cells overexpressing human PD-L1 leading to release of human IL-2. The EC_{50} values of the anti-human CD137/PD-L1 mAb^2 were smaller than the EC_{50} value of the positive control anti-human CD137 antibody, G1-AA/20H4.9 when crosslinked with anti-human CH2 secondary antibody (closed black circles, dotted line), indicating that improved T cell activation was achieved with the mAb^2. All showed an increase in hIL-2 release and there was a larger release of IL-2 (E_{max}) with the positive control antibody than with the anti-human CD137/PD-L1 mAb^2.

Figure 5 shows release of human IL-2 (hIL-2) in a human primary $CD8^+$ T cell activation assay in the presence of anti-human CD137/PD-L1 mAb^2 or positive control anti-human CD137 antibody G1-AA/20H4.9. All mAb^2 tested drove CD137 clustering and activation of $CD8^+$ T cells only when the mAb^2 were crosslinked by MDA-MD-231 cells endogenously expressing human PD-L1 leading to release of human IL-2. The EC_{50} values of the anti-human CD137/PD-L1 mAb^2 were smaller than the EC_{50} value of the positive control anti-human CD137 antibody, G1-AA/20H4.9 when crosslinked with anti-human CH2 secondary antibody (closed black circles, dotted line) indicating that better activity was achieved with the mAb^2. All showed an increase in hIL-2 release and there was a larger release of IL-2 (E_{max}) with the positive control antibody than with the anti-human CD137/PD-L1 mAb^2.

Figure 6 shows release of human IL-2 (hIL-2) in a human primary $CD8^+$ T cell activation assay in the presence of anti-human CD137/PD-L1 mAb^2 FS22-172-003-AA/E12v2 or positive control anti-human CD137 antibody G1-AA/20H4.9. All mAb^2 tested drove CD137 clustering and activation of $CD8^+$ T cells only when the mAb^2 were crosslinked by HEK.hPD-L1 cells that comprised at least 6.5% of the total HEK cell population leading to release of human IL-2. The EC_{50} values of the anti-human CD137/PD-L1 mAb^2 remained similar when modulating the percentage of HEK.hPD-L1 cells present in the assay, but the maximal activation (E_{max}) increased in relation to an increasing percentage of HEK.hPD-L1 crosslinking cells in the assay. This indicated that better maximum activity was achieved with the mAb^2 overall when 100% of HEK cells express PD-L1.

Figure 7 shows that anti-human CD137/PD-L1 mAb^2 are capable of activating T cells. **(A)** and **(B):** Release of IFN-γ in a primary human Mixed Lymphocyte Reaction (MLR) assay was tested in the presence of anti-human CD137/PD-L1 mAb^2, anti-human PD-L1 positive control antibody G1/S70 or anti-human CD137 positive control antibody G1-AA/20H4.9 (crosslinked with an anti-human CH2 antibody). **(A)** FS22-053-008 Fcab-based mAb^2 and **(B)** FS22-172-003 Fcab-based mAb^2 showed higher activity in this assay than either of the positive control antibodies, indicating that PD-L1 blockade and CD137 agonism in the same molecule elicits greater T cell activation, presumably through PD-L1-based clustering and activation of CD137. **(C)** Release of IFN-γ in a primary human MLR assay was tested in the presence of anti-human CD137/PD-L1 mAb^2, anti-human PD-L1 antibody G1-AA/E12v2, anti-human CD137 positive control antibody G1-AA/20H4.9 (crosslinked with an anti-human CH2 antibody), or anti-human CD137 Fcab in mock mAb^2 format (FS22-172-003-AA/D1.3). FS22-172-003-AA/E12v2 mAb^2 showed higher T cell activation activity in this assay than either of the positive control antibodies or its component Fcab in mock mAb^2 format, indicating that PD-L1 blockade and CD137 agonism in the same molecule elicits greater T cell activation, presumably through PD-L1-based crosslinking leading to clustering and activation of CD137.

Figure 8 shows IL-2 release in a T cell activation assay, wherein the T cells have been engineered to overexpress cynomolgus CD137, in the presence of anti-human CD137/PD-L1 mAb^2 and positive control anti-human CD137antibody G1-AA/MOR7480.1. All mAb^2 tested drove clustering and activation of CD137 only when crosslinked with HEK cells overexpressing cynomolgus PD-L1 (open and closed black and grey symbols with solid connecting lines) leading to a release of mouse interleukin-2 (mIL-2) in a DO11.10 T cell activation assay. At increasing concentrations, the positive control anti-human CD137 antibody, G1-AA/MOR7480.1 which has previously been shown by others to by cynomolgus cross-reactive to cynomolgus CD137, shows an increase in mIL-2 release (solid black circles, dotted line), however the maximal release was significantly less than that of all anti-human CD137/PD-L1 mAb^2. All anti-human CD137/PD-L1 mAb^2 without HEK cells overexpressing PD-L1 to crosslink show significantly lower mIL-2 release compared to when crosslinked (data not shown).

Figure 9 shows IL-2 release at day 2 **(Figure 9A)** or IFN-y release at day 6 **(Figure 9B)** from cynomolgus $CD4^+$ T cells cultured with allogeneic cynomolgus monocytes in the presence of a titration of anti-human CD137/PD-L1 mAb^2 FS22-053-008-AA/E12v2 or 172-003-AA/E12v2 or anti-human PD-L1 positive control antibody G1-AA/E12v2 or isotype control antibody G1-AA/HelD1.3.

Figure 10 shows mouse IL-2 release in a DO11.10 mouse CD137 T cell activation assay testing the mouse and human cross-reactive CD137 Fcabs FS22-053-014 and FS22-053-017 in mock mAb^2 format when crosslinked with Protein L. FS22-053-014 and FS22-053-017, and anti-mouse CD137 Fcab FS22m-063, all in HelD1.3 mock mAb^2 format activated CD137 when crosslinked with Protein L leading to a release of mIL-2. The positive control anti-mouse CD137 mAb, Lob12.3, showed an increase in mIL-2 release as expected. All anti-CD137 Fcabs in mock mAb^2 format without Protein L to crosslink (dotted lines) showed greatly reduced mIL-2 release compared to when crosslinked. FS22-053-017 had lower activity in this assay (8-fold worse EC_{50} compared to FS22-053-014) but still showed activity in the assay.

Figure 11 shows release of mouse IFNy which is an indication of $CD8^+$ T cell activation. The anti-mouse CD137/PD-L1 mAb^2 shows the greatest potency in this assay above either of the positive control antibodies against human CD137 and PD-L1, or the combination of the two. As expected, the FS22m-063-AA Fcab in mock mAb^2 format (FS22m-063-AA/HelD1.3) does not show any activity.

Figure 12 shows tumour volume measurements of the CT26 syngeneic tumour model grown subcutaneously in Balb/c mice treated with G1-AA/4420 (IgG control), G1/S70 (PD-L1 positive control), G1-AA/Lob12.3 and G1/Lob12.3 (CD137 positive control with the LALA mutation and without), the combination of G1/S70 plus G1-AA/Lob12.3 and FS22m-063-AA/S70 (the anti-mouse CD137 Fcab FS22m-063 in a model PD-L1 mAb^2 format). The mean tumour volume plus or minus 95% confidence interval is plotted. FS22m-063-AA/S70 is able to significantly reduce tumour growth in a CT26 syngeneic tumour model compared to IgG control treated

mice and anti-PD-L1 positive control mAb. Statistical significance shown pairwise for growth rates over the full time of study using the Mixed Model analysis. Mean tumour volume shown as geometric or arithmetic mean as appropriate based on data normality testing. * P ≤ 0.05; ** P ≤ 0.01; *** P ≤ 0.001; **** P ≤ 0.0001.

Figure 13 shows the results of a dose-response study of anti-mouse CD137/PD-L1 mAb^2 in a CT26 syngeneic mouse tumour model. **A:** shows tumour volume measurements of the CT26 syngeneic tumour model grown subcutaneously in Balb/c mice treated with 3 doses of G1-AA/4420 (IgG control, 10 mg/kg), G1/Lob12.3 (CD137 positive control, 1 mg/kg), and the anti-mouse CD137/PD-L1 mAb^2 FS22m-063-AA/S70 at 4 different doses (0.1 mg/kg, 0.3 mg/kg, 1.0 mg/kg, and 10.0 mg/kg). Each dose is indicated by a vertical black arrow on the x-axis. The mean tumour volume plus or minus 95% confidence interval is plotted. FS22m-063-AA/S70 is able to significantly reduce tumour growth in a CT26 syngeneic tumour model compared to IgG control treated mice and anti-PD-L1 positive control mAb. Statistical significance shown pairwise for growth rates over the full time of study using the Mixed Model analysis. Mean tumour volume shown as geometric or arithmetic mean as appropriate based on data normality testing. ** P ≤ 0.01; *** **** P ≤ 0.0001. **B:** shows a Kaplan Meier plot of the CT26 syngeneic tumour model grown subcutaneously in Balb/c mice treated with 3 doses of G1-AA/4420 (IgG control, ~10 mg/kg) and the anti-mouse CD137/PD-L1 mAb^2 FS22m-063-AA/S70 at 4 different doses 2µg, 6µg, 20µg, and 200µg (equivalent to approximately 0.1 mg/kg, 0.3 mg/kg, 1.0 mg/kg, and 10.0 mg/kg). FS22m-063-AA/S70 induces a dose dependent increase of survival in a CT26 syngeneic tumour model compared to IgG control treated mice.

Figure 14 shows a dose dependent increase in $CD8^+$:$CD4^+$ percentage ratio in tumour and blood of mice administered q2dx3 with anti-mouse CD137/PD-L1 mAb^2 FS22m-063-AA/S70 at four different dose levels is shown in panel A and B and Ki67 expression on $CD8^+$ T cells is shown in panels C and D.

Figure 15 shows tumour volume measurements of the MC38 syngeneic tumour model grown subcutaneously in C57BL/6 mice treated with G1-AA/4420 (isotype control), G1-AA/S70 (PD-L1 positive control), G1-AA/Lob12.3 (CD137 positive control), the combination of G1-AA/S70 plus G1-AA/Lob12.3, and FS22m-063-AA/S70 (the anti-mouse CD137 Fcab FS22m-063 in a model PD-L1 mAb^2 format). The mean tumour volume [in mm^3] plus or minus the 95% Confidence Interval is plotted. FS22m-063-AA/S70 is able to significantly reduce tumour growth in a MC38 syngeneic tumour model compared to IgG control treated mice, anti-PD-L1 positive control mAb treated mice, anti-CD137 positive control treated mice. Statistical significance shown pairwise for growth rates over the full time of study using the Mixed Model analysis. **** ≤ 0.0001 p-value.

Figure 16 shows tumour volume measurements of the B16.F10 syngeneic tumour model grown subcutaneously in C57BL/6 mice treated with G1-AA/4420 (isotype control) and the anti-mouse CD137/PD-L1 mAb^2 FS22m-063-AA/S70. Both compositions were dosed at 1mg/kg. The mean tumour volume [in mm^3] plus or minus the 95% Confidence Interval is plotted.

FS22m-063-AA/S70 treatment significantly reduced tumour growth in a B16.F10 syngeneic tumour model compared to IgG control treated mice. Statistical significance shown pairwise for growth rates over the full time of study using the Mixed Model analysis. Mean tumour volume shown as geometric or arithmetic mean as appropriate based on data normality testing. * $P \leq 0.05$; ** $P \leq 0.01$; *** $P \leq 0.001$; **** $P \leq 0.0001$.

Figure 17 shows the spaghetti plots for individual mice in the CT26 syngeneic tumour model grown subcutaneously in Balb/c mice treated with (A) G1-AA/4420 (IgG control), (C) G1/S70 (anti-PD-L1 positive control), (B) G1-AA/Lob12.3 and (D) G1/Lob12.3 (anti-CD137 positive control with and without the LALA mutation), or (E) a combination of G1/S70 plus G1-AA/Lob12.3 and (F) FS22m-063-AA/S70 (the anti-mouse CD137 Fcab FS22m-063 in a model PD-L1 mAb^2 format). FS22m-063-AA/S70 induced significant tumour growth inhibition in a CT26 syngeneic tumour model compared to IgG control treated mice.

Figure 18 shows a Kaplan Meier plot of the CT26 syngeneic tumour model grown subcutaneously in Balb/c mice treated with G1-AA/4420 (IgG control), the combination of G1/S70 plus G1-AA/Lob12.3, and FS22m-063-AA/S70 (the anti-mouse CD137 Fcab FS22m-063 in a model PD-L1 mAb^2 format) all at 1mg/kg. FS22m-063-AA/S70 induced significant survival in a CT26 syngeneic tumour model compared to IgG control treated mice.

Figure 19 shows tumour volume measurements of the CT26 syngeneic tumour model grown subcutaneously in Balb/c mice treated with G1-AA/HelD1.3 (IgG control), G1/S70 (anti-PD-L1 positive control), G1-AA/Lob12.3 (anti-CD137 positive control), and FS22m-063-AA/S70 (the anti-mouse CD137 Fcab FS22m-063 in a model PD-L1 mAb^2 format). The mean tumour volume plus or minus 95% confidence interval is plotted. FS22m-063-AA/S70 was able to significantly reduce tumour growth in a CT26 syngeneic tumour model compared to IgG control treated mice, anti-PD-L1 positive control mAb treated mice and anti-CD137 positive control treated mice. Statistical significance shown pairwise for growth rates over the full time of study using the Mixed Model analysis. Mean tumour volume shown as geometric or arithmetic mean as appropriate based on data normality testing. * $P \leq 0.05$; ** $P \leq 0.01$; *** $P \leq 0.001$; **** $P \leq 0.0001$.

Figure 20 shows a Kaplan Meier plot of the CT26 syngeneic tumour model grown subcutaneously in Balb/c mice treated with G1-AA/HelD1.3 (IgG control), G1/S70 (anti-PD-L1 positive control), G1-AA/Lob12.3 (anti-CD137 positive control) and FS22m-063-AA/S70 (the anti-mouse CD137 Fcab FS22m-063 in a model PD-L1 mAb^2 format). FS22m-063-AA/S70 induces significant survival in a CT26 syngeneic tumour model compared to IgG control treated mice and CD137 positive control treated mice.

Figure 21 shows the spaghetti plots for individual mice in the MC38 syngeneic tumour model grown subcutaneously in C57BL/6 mice treated with 3 doses of (A) G1-AA/4420 (isotype control), (B) G1-AA/S70 (anti-PD-L1 positive control), (C) G1-AA/Lob12.3 (anti-CD137 positive control), (D) the combination of G1-AA/S70 plus G1-AA/Lob12.3, and (E) FS22m-063-AA/S70 (the anti-mouse CD137 Fcab FS22m-063 in a model PD-L1 mAb^2 format). FS22m-063-AA/S70 induces full tumour growth inhibition, resulting in 100% tumour-free mice, in a MC38 syngeneic

tumour model compared to IgG control treated mice.

Figure 22 shows a Kaplan Meier plot of the MC38 syngeneic tumour model grown subcutaneously in C57BL/6 mice treated with 3 doses of G1-AA/4420 (isotype control), G1-AA/S70 (anti-PD-L1 positive control), G1-AA/Lob12.3 (anti-CD137 positive control), the combination of G1-AA/S70 plus G1-AA/Lob12.3, and FS22m-063-AA/S70 (the anti-mouse CD137 Fcab FS22m-063 in a model PD-L1 mAb^2 format). FS22m-063-AA/S70 induces full survival in a MC38 syngeneic tumour model compared to IgG control treated mice.

Figure 23 shows the spaghetti plots for individual mice in the B16.F10 syngeneic tumour model grown subcutaneously in C57BL/6 mice treated with G1-AA/4420 (isotype control) **(Figure 23A)** and the anti-mouse CD137/PD-L1 mAb^2 FS22m-063-AA/S70 **(Figure 23B).** FS22m-063-AA/S70 induced partial tumour growth inhibition in a B16.F10 syngeneic tumour model compared to IgG control treated mice.

Figure 24 shows anti-mCD137/PD-L1 mAb^2 binding data to T cells *ex vivo,* determined by flow cytometry. The Mean Fluorescent Intensity (MFI) values were measured from anti-human Fc secondary antibody conjugated with Alexa Fluor 488 that detected the human Fc region of the anti-mCD137/PDl-L1 mAb^2 bound to cells. Positive cells that had an MFI greater than that of an unstained control sample were identified as positive for anti-mCD137/PD-L1 and the data presented shows the positive population as a percentage of **(A)** all $CD8^+$ or **(B)** all $CD4^+$ T cells from the blood, or **(C)** all $CD8^+$ or **(D)** all $CD4^+$ T cells from the tumour. These results show that anti-mCD137/PD-L1 mAb^2 rapidly binds both $CD8^+$ and $CD4^+$ T cells present in both tumour and blood and that the percentage positive T cell population decreases over time dependent on dose level.

Figure 25 shows Ki67 expression data by T cells *ex vivo,* determined by flow cytometry. The Mean Fluorescent Intensity (MFI) values were measured from anti-Ki67 antibody conjugated with PE-Cy7 bound to cells. Positive cells that had an MFI greater than that of an unstained control sample were identified as positive for Ki67 expression and the data presented shows the positive population as a percentage of **(A)** all $CD8^+$ or **(B)** all $CD4^+$ T cells from the blood, or **(C)** all $CD8^+$ or **(D)** all $CD4^+$ T cells from the tumour. These results show that T cells in mice dosed with anti-mCD137/PD-L1 mAb^2 rapidly express Ki67 both on $CD8^+$ and $CD4^+$ T cells in the blood and that a high percentage of Ki67 positive T cells are already present in a sample from the tumour microenvironment. An increase in Ki67 expression over time dependent on dose level was observed.

Figure 26 shows PD-L1 receptor occupancy relative to a time-matched sample from mice dosed with control antibody G1-AA/4420 that was then spiked with 100nM anti-mCD137/PD-L1 mAb^2 *ex vivo* to saturate all PD-L1 receptors, thus indicating a 100% PD-L1 receptor occupancy level (triangle symbols with dashed line). Free PD-L1 receptors were detected using the Mean Fluorescent Intensity (MFI) values of a competing anti-mPD-L1 antibody conjugated with Bv605. Positive cells that had an MFI greater than that of an unstained control

sample were identified as positive for free PD-L1. The results show the positive population as a percentage of PD-L1 receptor occupancy compared to the 100% saturated sample of **(A)** $CD8^+$ or **(B)** $CD4^+$ T cells from the blood, or **(C)** $CD8^+$ or **(D)** $CD4^+$ T cells from the tumour. These results demonstrate that PD-L1 receptor occupancy reached 100% rapidly in the blood before decreasing in line with dose level over time. PD-L1 receptor occupancy on T cells was maintained longer in the tumour microenvironment than in the blood.

Figure 27 shows the pharmacokinetic profile of anti-CD137/PD-L1 mAb^2 at 25, 10, 3, and 1 mg/kg after a single intravenous single-dose administered to C57BL/6 naive mice. The concentration of CD137/PD-L1 mAb^2 in the mice over time is shown. Figure 27 demonstrates that the rate of clearance of the anti-CD137/PD-L1 mAb^2 at each dose is comparable to clearance of a standard human IgG in mice.

Figure 28 shows that anti-human CD137/PD-L1 mAb^2 FS22-172-003-AA/E12v2 is capable of activating T cells in a PBMC T cell activation assay using **(A)** cynomolgus monkey PBMCs or **(B)** human PBMCs. Release of IFN-γ in a PBMC assay was tested in the presence of anti-human CD137/PD-L1 mAb^2, anti-human CD137 positive control antibody G1-AA/MOR7480.1 (crosslinked with an anti-human CH2 antibody). The mAb2 showed activity in both assays and showed activation levels higher than the positive control antibody, indicating that PD-L1 blockade and CD137 agonism by the same molecule elicits greater T cell activation, presumably through PD-L1-based clustering and activation of CD137, in both cynomolgus monkey and humans.

Detailed Description

[0038] Aspects and embodiments of the present invention will now be discussed with reference to the accompanying figures. Further aspects and embodiments will be apparent to those skilled in the art.

[0039] The present invention relates to antibody molecules which bind both to PD-L1 and CD137. Specifically, the antibody molecules of the present invention comprise a CDR-based antigen-binding site for PD-L1 and a CD137 antigen-binding site located in a constant domain of the antibody molecule. The terms "PD-L1" and "CD137" may refer to human PD-L1 and human CD137, murine PD-L1 and murine CD137, and/or cynomologus monkey PD-L1 and cynomologus monkey CD137, unless the context requires otherwise. Preferably the terms "PD-L1" and "CD137" refer to human PD-L1 and human CD137, unless the context requires otherwise.

[0040] The term "antibody molecule" describes an immunoglobulin whether natural or partly or wholly synthetically produced. The antibody molecule may be human or humanised, preferably

human. The antibody molecule is preferably a monoclonal antibody molecule. Examples of antibodies are the immunoglobulin isotypes, such as immunoglobulin G, and their isotypic subclasses, such as IgG1, IgG2, IgG3 and IgG4, as well as fragments thereof. The antibody molecule may be isolated, in the sense of being free from contaminants, such as antibodies able to bind other polypeptides and/or serum components.

[0041] The term "antibody molecule", as used herein, thus includes antibody fragments, provided said fragments comprise a CDR-based antigen binding site for PD-L1 and a CD137 antigen binding site located in a constant domain. Unless the context requires otherwise, the term "antibody molecule", as used herein, is thus equivalent to "antibody molecule or fragment thereof".

[0042] It is possible to take monoclonal and other antibodies and use techniques of recombinant DNA technology to produce other antibodies or chimeric molecules which retain the specificity of the original antibody. Such techniques may involve introducing the CDRs, or variable regions, and/or the constant domain sequences providing the CD137 antigen binding site, into a different immunoglobulin. Introduction of the CDRs of one immunoglobulin into another immunoglobulin is described for example in EP-A-184187, GB 2188638A or EP-A-239400. Similar techniques could be employed for the relevant constant domain sequences. Alternatively, a hybridoma or other cell producing an antibody molecule may be subject to genetic mutation or other changes, which may or may not alter the binding specificity of antibodies produced.

[0043] As antibodies can be modified in a number of ways, the term "antibody molecule" should be construed as covering antibody fragments, derivatives, functional equivalents and homologues of antibodies, including any polypeptide comprising an immunoglobulin binding domain, whether natural or wholly or partially synthetic. Chimeric molecules comprising an immunoglobulin binding domain, or equivalent, fused to another polypeptide are therefore included. Cloning and expression of chimeric antibodies are described in EP-A-0120694 and EP-A-0125023.

[0044] An example of an antibody fragment comprising both CDR sequences and CH3 domain is a minibody, which comprises an scFv joined to a CH3 domain (Hu et al. (1996), Cancer Res., 56(13):3055-61).

[0045] The antibody molecule of the present invention binds to PD-L1 and CD137. Binding in this context may refer to specific binding. The term "specific" may refer to the situation in which the antibody molecule will not show any significant binding to molecules other than its specific binding partner(s), here PD-L1 and CD137. The term "specific" is also applicable where the antibody molecule is specific for particular epitopes, such as epitopes on PD-L1 and CD137, that are carried by a number of antigens in which case the antibody molecule will be able to bind to the various antigens carrying the epitope.

[0046] The present inventors demonstrated that antibody molecules described herein showed

a high level of specificity for human PD-L1 and did not show any significant binding to other T cells targets PD-L1, CD80, PD-1 or B7-H3. See **Example 9.3.** Thus, in a preferred embodiment, the antibody molecule does not bind, or does not show any significant binding, to any one of, preferably all of, PD-L2, CD80, PD-1, and B7-H3. The present inventors also demonstrated that the CD137 antigen-binding site did not show any significant binding to the human TNFRSF receptors CD40, OX40 and GITR. See **Example 3.6.** Thus, in a more preferred embodiment, the antibody molecule does not bind, or does show any significant binding, to any one of, preferably all of, PD-L2, CD80, PD-1, B7-H3, CD40, OX40 and GITR.

[0047] Antibodies and methods for their construction and use are well-known in the art and are described in, for example, Holliger & Hudson (2005). It is possible to take monoclonal and other antibodies and use techniques of recombinant DNA technology to produce other antibodies or chimeric molecules which retain the specificity of the original antibody. Such techniques may involve introducing CDRs or variable regions of one antibody molecule into a different antibody molecule (EP-A-184187, GB 2188638A and EP-A-239400).

[0048] A CDR-based antigen-binding site is an antigen-binding site in an antibody variable region. A CDR-based antigen-binding site, may be formed by three CDRs, such as the three light chain variable domain (VL) CDRs or three heavy chain variable domain (VH) CDRs. Preferably the CDR-based antigen-binding site is formed by six CDRs, three VL CDRs and three VH CDRs. The contributions of the different CDRs to the binding of the antigen may vary in different antigen binding sites.

[0049] The three VH domain CDRs of the antigen-binding site may be located within an immunoglobulin VH domain and the three VL domain CDRs may be located within an immunoglobulin VL domain. For example, the CDR-based antigen-binding site may be located in an antibody variable region.

[0050] The antibody molecule has one or preferably more than one, for example two, CDR-based antigen binding sites for the first antigen. The antibody molecule thus comprises one VH and one VL domain but preferably comprises two VH and two VL domains, i.e. two VH/VL domain pairs, as is the case in naturally-occurring IgG molecules, for example.

[0051] The CDR-based antigen-binding site comprises the three VH CDRs and the three VL CDRs, of antibody **E12v2, E05v2,** or **G12v2,** preferably **E12v2** or **E05v2,** more preferably **E12v2.**

[0052] The VH and VL domain sequences of these antibodies are set forth as follows:

1. (i) the VH and VL domain sequences for antibody **E12v2** are shown in SEQ ID NOs **12** and **14,** respectively;
2. (ii) the VH and VL domain sequences for antibody **E05v2** are shown in SEQ ID NOs **23** and **25,** respectively; and
3. (iii) the VH and VL domain sequences for antibody **G12v2** are shown in SEQ ID NOs **23**

and **30,** respectively.

[0053] The skilled person would have no difficulty in determining the sequences of the CDRs from the VH and VL domain sequences of the antibodies set out above. The CDR sequences may, for example, be determined according to Kabat (Kabat, E.A et al. (1991). Sequences of Proteins of Immunological Interest, 5th edit., NIH Publication no. 91-3242. U.S. Department of Health and Human Services) or the international ImMunoGeneTics information system (IMGT: Lefranc, M.-P. et al. Nucleic Acids Res. 43, D413-22 (2015)).

[0054] The VH domain CDR1, CDR2 and CDR3 sequences of the antibody molecule according to Kabat numbering may be the sequences at located positions 31-35, 50-65, and 95-102 of the VH domain, respectively.

[0055] The VH domain CDR1, CDR2 and CDR3 sequences of the antibody molecule according to IMGT numbering may be the sequences located at positions 27-38, 56-65, and 105-117, of the VH domain of the antibody molecule, respectively.

[0056] The VL domain CDR1, CDR2 and CDR3 sequences of the antibody molecule according to Kabat numbering may be the sequences at located positions 24-34, 50-56, and 89-97 of the VL domain, respectively.

[0057] The VL domain CDR1, CDR2 and CDR3 sequences of the antibody molecule according to IMGT numbering may be the sequences located at positions 27-38, 56-65, and 105-117, of the VL domain, respectively.

[0058] The antibody molecule comprises the sequence of the VH domain CDR1 of **SYGIS** (SEQ ID NO: 1), the VH domain CDR2 of **WISAYSGGTNYAQKLQG** (SEQ ID NO: **2**), and the VH domain CDR3 of **DLFPTIFGVSYYYY** (SEQ ID NO: **3**) wherein the CDR sequences are defined according to the Kabat numbering scheme.

[0059] The antibody molecule comprises the sequence of the VH domain CDR1, CDR2 and CDR3 of:

1. (i) SEQ ID NOs **7, 8** and **9,** respectively **[E12v2];** or
2. (ii) SEQ ID NOs **21, 8** and **9,** respectively **[E05v2** or **G12v2],**
   wherein the CDR sequences are defined according to the IMGT numbering scheme.

[0060] The CDRs of the VH domain are flanked by framework (FW) sequences (HFW1, HFW2, HFW3 and HFW4). The VH domain comprises the HFW1, HFW2, HFW3 and HFW4 sequences of SEQ ID NO: **55, 56, 57** and **54,** respectively, wherein the FW and CDR sequences are defined according to the IMGT numbering scheme.

[0061] Preferably, the antibody molecule comprises the sequence of the VL domain CDR1 of **RASQSIGNRLA** (SEQ ID NO: **4**), the VL CDR2 of **EASTSET** (SEQ ID NO: **5**), and the VL CDR3 of **QQSYSTPYT** (SEQ ID NO: **6**), wherein the CDR sequences are defined according to the Kabat numbering scheme. The VL domain is derived from a kappa VL domain. Each of the VL domain CDRs are flanked by framework (FW) sequences (LFW1, LFW2, LFW3 and LFW4) that are derived from a kappa VL domain. Specifically, the VL domain may comprise the LFW1, LFW2, LFW3 and LFW4 sequences of SEQ ID NO: **58, 59, 60** and **61,** respectively, wherein the FW sequences are defined according to the Kabat numbering scheme.

[0062] The antibody molecule may comprises the sequence of the VL domain CDR1, CDR2 and CDR3 of:

1. (i) SEQ ID NOs **4, 5** and **6,** respectively **[E12v2];**
2. (ii) SEQ ID NOs **18, 19** and **20,** respectively **[E05v2];** or
3. (iii) SEQ ID NOs **18, 19** and **29,** respectively **[G12v2],**
   wherein the CDR sequences are defined according to the Kabat numbering scheme.

[0063] Preferably, the antibody molecule comprises the sequence of the VL domain CDR1 of **QSIGNR** (SEQ ID NO: **10**), the VL CDR2 of **EAS** (SEQ ID NO: **11**), and the VL CDR3 of **QQSYSTPYT** (SEQ ID NO: **6**), wherein the CDR sequences are defined according to the IMGT numbering scheme. The VL domain is derived from a kappa VL domain. Each of the VL domain CDRs may be flanked by framework (FW) sequences (LFW1, LFW2, LFW3 and LFW4) that are derived from a kappa VL domain. Specifically, the VL domain may comprise the LFW1, LFW2, LFW3 and LFW4 sequences of SEQ ID NO: **62, 63, 64** and **61,** respectively, wherein the FW sequences are defined according to the IMGT numbering scheme.

[0064] The antibody molecule comprises the sequence of the VL domain CDR1, CDR2 and CDR3 of:

1. (i) SEQ ID NOs **10, 11** and **6,** respectively **[E12v2];**
2. (ii) SEQ ID NOs **22, 11** and **20,** respectively **[E05v2];** or
3. (iii) SEQ ID NOs **22, 11** and **29,** respectively **[G12v2],**
   wherein the CDR sequences are defined according to the IMGT numbering scheme.

[0065] The CDR-based antigen-binding site comprises the VH and VL domains of antibody **E12v2, E05v2,** or **G12v2,** preferably **E12v2** or **E05v2,** more preferably **E12v2.**

[0066] The VH domain of antibodies **E12v2, E05v2,** and **G12v2** has the sequence set forth in SEQ ID NOs **12, 23,** and **23,** respectively. The VL domain of antibodies **E12v2, E05v2,** and **G12v2** has the sequence set forth in SEQ ID NOs **14, 25,** and **30,** respectively.

[0067] The antibody molecule of the invention comprises a CD137 antigen-binding site located in the CH3 domain. The CD137 antigen-binding site comprises two or more modified structural loops in a CH3 domain of the antibody molecule. Engineering antibody constant domain structural loops to create antigen-binding sites for target antigens is known in the art and is described, for example, Wozniak-Knopp G *et al.* (2010); WO2006/072620 and WO2009/132876.

[0068] The CD137 antigen-binding site of the antibody molecule comprises a first and second sequence, wherein the first and second sequence are located in the AB and EF structural loops of the CH3 domain, of the antibody molecule, respectively.

[0069] The residues at positions 95 and 96 of the CH3 domain of the antibody molecule are wild-type, i.e. are arginine (R) and tryptophan (W), respectively. Both of these residues are located in the EF structural loop. Amino acid residue positions are numbered herein according to the ImMunoGeneTics (IMGT) numbering scheme, unless otherwise indicated. The IMGT numbering scheme is described in Lefranc *et al.,* 2005.

[0070] The first sequence comprises the sequence PPY (SEQ ID NO: **78**).

[0071] The PPY sequence is located between positions 15 and 17 of the CH3 domain of the antibody molecule. In a preferred embodiment, the PPY sequence is located at positions 16, 16.5 and 16.4 of the CH3 domain. Alternatively, the PPY sequence may be located between positions 16 and 17 of the CH3 domain. In an alternative preferred embodiment, the PPY sequence is located at positions 16.3, 16.2 and 16.1 of the CH3 domain. In the IMGT numbering scheme, inserted residues are numbered according to the direction of the loop in which they are located. If the loop goes "up" the inserted residues take the number of the residue immediately preceding the insertion with the number of the inserted residue in the sequence being indicated by an ascending decimal number, e.g. 16, 16.1, 16.2, 16.3, where there are three mutations following residue 16. If the loop goes "down", the inserted residues take the number of the residue immediately preceding the insertion with the number of the inserted residue in the sequence being indicated by descending decimal number, e.g. 16, 16.3, 16.2, 16.1, where again there are three mutations following residue 16 (LeFranc *et al.,* 2005, and LeFranc *et al.* 2015).

[0072] The AB structural loop comprises an amino acid insertion. The insertion is 5 amino acids in length.

[0073] The insertion is located between positions 16 and 17 of the CH3 domain of the antibody molecule. The insertion is located at positions 16.5 to 16.1 of the CH3 domain of the antibody molecule. **Figure 1** shows Fcabs comprising a CH3 domain where the insertion is located at positions 16.5 to 16.1 of the CH3 domain.

[0074] The majority of the Fcabs identified following affinity maturation comprised a leucine (L) residue at position 97 of the CH3 domain. Many of these Fcabs also comprised an aspartic

acid (D) residue or glutamic acid (E) residue at positions 98 of the CH3 domain. Both of these amino acid changes are located in the EF structural loop. These results suggest that one or both of these residues may be important for CD137 binding. Thus, the second sequence comprises the sequence LE, wherein the LE sequence is located at positions 97 and 98 of the CH3 domain of the antibody molecule.

[0075] The first sequence and second sequence may be a first and second sequence of the CH3 domain of: **FS22-053-008,** or **FS22-053-017,** preferably specific binding member **FS22-053-008.**

[0076] The first sequence and second sequence is a first and second sequence of the CH3 domain of: **FS22-053-008, FS22-053-017,** or **FS22-172-003,** preferably **FS22-053-008** or **FS22-172-003,** more preferably **FS22-172-003.**

[0077] The CH3 domain sequence of **FS22-053-008, FS22-053-017,** and **FS22-172-003** is set forth in SEQ ID NOs: **81, 90** and **115,** respectively.

[0078] The first and second sequence of **FS22-053-008, FS22-053-017** and **FS22-172-003** is the sequence between positions 14 and 17, and positions 91 and 99, of the CH3 domain of **FS22-053-008, FS22-053-017** and **FS22-172-003,** respectively.

[0079] Alternatively, the first and second sequence of **FS22-053-008** may be the sequence between positions 14 and 17, and positions 92 and 99, of the CH3 domain of **FS22-053-008.**

[0080] The CD loop sequence of the antibody molecule is preferably unmodified, i.e. wild type. The CD loop sequence therefore preferably has the sequence set forth in SEQ ID NO: **73.** The CD loop sequence is preferably located at positions 43 to 78 of the CH3 domain.

[0081] The first and second sequences may be the complete AB and EF structural loop sequences, of **FS22-053-008, FS22-053-017** or **FS22-172-003,** respectively. Determination of the location of the AB, CD, and EF structural loops in a CH3 domain sequence, for example in accordance with the IMGT, IMGT exon, EU, or Kabat numbering systems, is within the capabilities of the skilled person and described in Hasenhindl *et al.* (2013). In a preferred embodiment, the AB, CD and EF structural loops according to the IMGT numbering system are located between positions 10 and 19, 42 and 79, and 91 and 102 of the CH3 domain, respectively. In a preferred embodiment, the first, second and third sequence are therefore the sequence between positions 10 and 19, 42 and 79, and 91 and 102 of the CH3 domain of **FS22-053-008, FS22-053-017** or **FS22-172-003,** respectively.

[0082] Thus, in one preferred embodiment, the first and second sequence of the CD137 antigen-binding site comprise the AB and EF loop sequence set forth in SEQ ID NOs **171** and **172 [FS22-172-003],** respectively, or the AB and EF structural loop sequence set forth in SEQ ID NOs **173** and **174 [FS22-53-008],** respectively. In a more preferred embodiment, the first and second sequence of the CD137 antigen-binding site comprise the AB and EF structural

loop set forth in SEQ ID NOs **171** and **172 [FS22-172-003],** respectively.

[0083] In an alternatively preferred embodiment, the first and second sequence of the CD137 antigen-binding site comprise the AB and EF structural loop sequence set forth in SEQ ID NOs **173** and **175 [FS22-053-017],** respectively.

[0084] The CD137 antigen-binding site comprises the first and second sequence set forth in:

1. (i) SEQ ID NOs 79 and 80, respectively **[FS22-053-008];**
2. (ii) SEQ ID NOs 79 and 89, respectively **[FS22-053-017];** or
3. (iii) SEQ ID NOs 113 and 114, respectively **[FS22-172-003];** wherein the first and second sequence are located between positions 14 and 17, and 91 and 99 of the CH3 domain of the antibody molecule, respectively.

[0085] In a preferred embodiment, the CD137 antigen-binding site of the antibody molecule comprises the first and second sequence set forth in SEQ ID NOs **113** and **114 [FS22-172-003],** respectively, or the first and second sequence set forth in SEQ ID NOs **79** and **80 [FS22-53-008],** respectively. In a still more preferred embodiment, the CD137 antigen-binding site of the antibody molecule comprises the first and second sequence set forth in SEQ ID NOs **113** and **114 [FS22-172-003],** respectively. For example, the CD137 antigen-binding site may comprise the AB and EF structural loop sequences set forth in SEQ ID NOs **171** and **172 [FS22-172-003],** respectively.

[0086] As an alternative to IMGT numbering, amino acid residue positions, including the position of amino acid sequences, substitutions, deletions and insertions as described herein, may be numbered according to IMGT exon numbering (also referred to as consecutive numbering), EU numbering, or Kabat numbering. The concordance between IMGT numbering, IMGT exon numbering, EU numbering, and Kabat numbering of the residue positions of the CH3 domain are shown in **Figure 1.** Thus, for example, where the present application refers to the first sequence being located between positions 14 and 17 of the CH3 domain of the clone, respectively, where the residue positions are numbered in accordance with the IMGT numbering scheme, the first sequence is located between positions 18 and 21 of the CH3 domain, where the residue positions are numbered in accordance with the IMGT exon numbering scheme, as shown in **Figure 1.** Alternatively, the position of amino acid residues in the CH3 domain, including the position of amino acid sequences, substitutions, deletions and insertions in the CH3 domain, as described herein, may be defined by reference to their position in the wild-type CH3 domain sequence set forth in SEQ ID NO: **75.** The concordance between IMGT numbering and the wild-type CH3 domain sequence is also shown in **Figure 1.**

[0087] In one embodiment, the antibody molecule comprises a CH3 domain which comprises, has, or consists of the CH3 domain sequence of **FS22-053-008, FS22-053-017,** or **FS22-172-003,** wherein the CH3 domain sequence of **FS22-053-008, FS22-053-017** and **FS22-172-003** is set forth in SEQ ID NOs **81, 90** and **115,** respectively.

[0088] In a preferred embodiment, the antibody molecule comprises a CH3 domain which comprises, has, or consists of the CH3 domain sequence of **FS22-172-003** or **FS22-053-008** set forth in SEQ ID NO **115** and **81,** respectively. In a more preferred embodiment, the antibody molecule comprises a CH3 domain which comprises, has, or consists of the CH3 domain sequence of **FS22-172-003** set forth in SEQ ID NO **115.**

[0089] In an alternatively preferred embodiment, the antibody molecule comprises a CH3 domain which comprises, has, or consists of the CH3 domain sequence of **FS22-053-017** set forth in SEQ ID NO **90,** respectively.

[0090] The CH3 domain of the antibody molecule may optionally comprise an additional lysine residue (K) at the immediate C-terminus of the CH3 domain sequence.

[0091] In addition, the antibody molecule of the invention may comprise a CH2 domain of an immunoglobulin G molecule, such as a CH2 domain of an IgG1, IgG2, IgG3, or IgG4 molecule. Preferably the antibody molecule of the invention comprises a CH2 domain of an IgG1 molecule. The CH2 domain may have the sequence set forth in SEQ ID NO: **76.**

[0092] The CH2 domain is known to bind to Fcγ receptors and complement. Binding of the CH2 domain to Fcγ receptors is required antibody-dependent cell-mediated cytotoxicity (ADCC), while binding to complement is required complement-dependent cytotoxicity (CDC). The CH2 domain of the antibody molecule preferably comprise one or more mutations that reduce or abrogate binding of the CH2 domain to one or more Fcγ receptors, such as FcγRI, FcγRIIa, FcγRIIb, FcγRIII, and/or to complement. The inventors postulate that reducing or abrogating binding to Fcγ receptors will decrease or eliminate ADCC mediated by the antibody molecule. Similarly, reducing or abrogating binding to complement is expected to reduce or eliminate CDC mediated by the antibody molecule. Without wishing to be bound by theory, this is expected to reduce or avoid liver toxicity when the antibody molecule is administered to a patient. In addition, reducing or abrogating binding to Fcγ receptors is expected to be useful where the antibody molecule comprises a second antigen-binding site for an immune cell antigen, where ADCC and/or CDC-mediated killing of immune cells bound by the antibody molecule should be avoided. Mutations to decrease or abrogate binding of the CH2 domain to one or more Fcγ receptors and/or complement are known in the art (Wang *et al.,* 2018). These mutations include the "LALA mutation" described in Bruhns *et al.,* 2009 and Hezareh *et al.,* 2001, which involves substitution of the leucine residues at positions 1.3 and 1.2 of the CH2 domain with alanine (L1.3A and L1.2A). Alternatively, the generation of a-glycosyl antibodies through mutation of the conserved N-linked glycosylation site by mutating the aparagine (N) at position 84.4 of the CH2 domain to alanine, glycine or glutamine (N84.4A, N84.4G or N84.4Q) is also known to decrease IgG1 effector function (Wang *et al.,* 2018). As a further alternative, complement activation (C1q binding) and ADCC are known to be reduced through mutation of the proline at position 114 of the CH2 domain to alanine or glycine (P114A or P114G) (Idusogie *et al.,* 2000; Klein *et* al., 2016). These mutations may also be combined in order to generate antibody molecules with further reduced or no ADCC or CDC activity.

[0093] Thus, the antibody molecule may comprise a CH2 domain, wherein the CH2 domain preferably comprises:

1. (i) alanine residues at positions 1.3 and 1.2; and/or
2. (ii) an alanine or glycine at position 114; and/or
3. (iii) an alanine, glutamine or glycine at position 84.4;

wherein the amino acid residue numbering is according to the IMGT numbering scheme.

[0094] In a preferred embodiment, the antibody molecule comprises a CH2 domain, wherein the CH2 domain comprises:

1. (i) an alanine residue at position 1.3; and
2. (ii) an alanine residue at position 1.2;

wherein the amino acid residue numbering is according to the IMGT numbering scheme.

[0095] For example, the CH2 domain may have the sequence set forth in SEQ ID NO: 77.

[0096] In an alternative preferred embodiment, the antibody molecule comprises a CH2 domain, wherein the CH2 domain comprises:

1. (i) an alanine residue at position 1.3;
2. (ii) an alanine residue at position 1.2; and
3. (iii) an alanine at position 114;

wherein the amino acid residue numbering is according to the IMGT numbering scheme.

[0097] For example, the CH2 domain may have the sequence set forth in SEQ ID NO: 176.

[0098] In a preferred embodiment, the antibody molecule that binds to PD-L1 and CD137 comprises

1. (a) a VH domain and a VL domain comprising the CDR-based antigen-binding site for PD-L1; and
2. (b) a CD137 antigen-binding site located in a CH3 domain of the antibody molecule;

wherein the VH and VL domain comprises, has, or consists of the VH and VL of antibody **E12v2, E05v2,** or **G12v2,** preferably **E12v2;** and

wherein the CD137 antigen-binding site comprises a first sequence and a second sequence located in the AB and EF structural loops of the CH3 domain, respectively; wherein the first and second sequence have the sequence set forth in SEQ ID NOs 113 and **114 [FS22-172-003],** or **79** and **80 [FS22-53-008],** respectively, preferably wherein the first and second sequence have the sequence set forth in SEQ ID NOs **113** and **114 [FS22-172-003],** with the proviso that the antibody molecule does not comprise the VH domain and VL domain of antibody **G12v2** paired

with the CD137 antigen-binding site having the first and second sequence set forth in in SEQ ID NOs **79** and **80 [FS22-053-008].**

[0099] As described in the Examples, an antibody molecule having a CD137 antigen-binding site comprising the first sequence and a second sequence set forth in SEQ ID NOs 79 and 89, respectively **[FS22-053-017]** was able to bind human, cynomolgus and, unexpectedly, mouse CD137. The inventors demonstrated that this antibody molecule had activity in human, cynomolgus and mouse T cell activation assays when crosslinked.

[0100] In an alternatively preferred embodiment, the antibody molecule that binds to PD-L1 and CD137 comprises

1. (a) a VH domain and a VL domain comprising the CDR-based antigen-binding site for PD-L1; and
2. (b) a CD137 antigen-binding site located in a CH3 domain of the antibody molecule;

wherein the VH and VL domain consists of the VH and VL of antibody **E12v2, E05v2,** or **G12v2,** preferably **E12v2;** and

wherein the CD137 antigen-binding site comprises a first sequence and a second sequence located in the AB and EF structural loops of the CH3 domain, respectively, wherein the first and second sequence have the sequence set forth in SEQ ID NOs 79 and **89 [FS22-053-017].**

[0101] In a preferred embodiment, the antibody molecule that binds to PD-L1 and CD137 comprises

1. (a) a VH domain and a VL domain comprising the CDR-based antigen binding site for PD-L1; and
2. (b) a CH3 domain which comprises, has, or consists of the sequence set forth in SEQ ID NOs **115 [FS22-172-003],** or **81 [FS22-53-008],** preferably SEQ ID NO **115 [FS22-172-003];**

wherein the VH and VL domain consists of the VH and VL of antibody **E12v2, E05v2,** or **G12v2,** preferably **E12v2,** with the proviso that the antibody molecule does not comprise the VH domain and VL domain of antibody **G12v2** paired with the CH3 domain which comprises, has, or consists of the sequence set forth in SEQ ID NO: **81 [FS22-53-008].**

[0102] In a yet further alternatively preferred embodiment, the antibody molecule that binds to PD-L1 and CD137 comprises

1. (a) a VH domain and a VL domain comprising the CDR-based antigen binding site for PD-L1; and
2. (b) a CH3 domain which comprises, has, or consists of the sequence set forth in SEQ ID

NO: **90 [FS22-053-017];**

wherein the VH and VL domain comprises, has, or consists of the VH and VL of antibody **E12v2, E05v2,** or **G12v2,** preferably **E12v2.**

[0103] In a further preferred embodiment, the antibody molecule that binds to PD-L1 and CD137 comprises

1. (a) a VH domain and a VL domain comprising the CDR-based antigen binding site for PD-L1;
2. (b) a CH3 domain which comprises, has, or consists of the sequence set forth in SEQ ID NOs **115 [FS22-172-003],** or **81 [FS22-53-008],** preferably SEQ ID NO **115 [FS22-172-003];**
3. (c) a CH2 domain which comprises, has or consists of the sequence set forth in SEQ ID NO: 76, wherein the CH2 domain comprises:
    1. (i) an alanine residue at position 1.3;
    2. (ii) an alanine residue at position 1.2;

    wherein the amino acid residue numbering is according to the IMGT numbering scheme; and

    wherein the VH and VL domain comprises, has, or consists of the VH and VL of antibody **E12v2, E05v2,** or **G12v2,** preferably **E12v2,** with the proviso that the antibody molecule does not comprise the VH domain and VL domain of antibody **G12v2** paired with the CH3 domain which comprises, has, or consists of the sequence set forth in SEQ ID NO: **81 [FS22-53-008].**

[0104] In a further embodiment, the antibody molecule the antibody molecule that binds to PD-L1 and CD137 comprises:

1. (a) a VH and VL domain comprising a CDR-based antigen-binding site for PD-L1, wherein the CDR-based antigen-binding site comprises CDRs 1-6; and
2. (b) a CD137 antigen-binding site located in a CH3 domain of the antibody molecule, the CD137 antigen binding site comprising a first sequence and a second sequence located in the AB and EF structural loops of the CH3 domain;

wherein the VH domain, VL domain, first sequence and second sequence have the sequence set forth in:

1. (i) SEQ ID NOs **12, 14, 113** and **114,** respectively **[FS22-172-003-AA/E12v2];**
2. (ii) SEQ ID NOs **23, 25, 113** and **114,** respectively **[FS22-172-003-AA/E05v2];**
3. (iii) SEQ ID NOs **23, 30, 113** and **114,** respectively **[FS22-172-003-AA/G12v2];**
4. (iv) SEQ ID NOs **12, 14, 79** and **80,** respectively **[FS22-053-008-AA/E12v2];** or
5. (v) SEQ ID NOs **23, 25, 79** and **80,** respectively **[FS22-053-008-AA/E05v2];** or

wherein the VH domain, VL domain, and CH3 domain have the sequence set forth in:

1. (i) SEQ ID NOs **12, 14,** and **115,** respectively **[FS22-172-003-AA/E12v2];**
2. (ii) SEQ ID NOs **23, 25,** and **115,** respectively **[FS22-172-003-AA/E05v2];**
3. (iii) SEQ ID NOs **23, 30,** and **115,** respectively **[FS22-172-003-AA/G12v2];**
4. (iv) SEQ ID NOs **12, 14,** and **81,** respectively **[FS22-053-008-AA/E12v2];** or
5. (v) SEQ ID NOs 23, **25,** and **81,** respectively **[FS22-053-008-AA/E05v2].**

[0105] In a further preferred embodiment, the antibody molecule that binds to PD-L1 and CD137 comprises a heavy chain which comprises, has, or consists of the heavy chain and light chain of antibody:

1. (i) **FS22-172-003-AA/E12v2** set forth in SEQ ID NOs **134** and **17,** respectively;
2. (ii) **FS22-172-003-AA/E05v2** set forth in SEQ ID NOs **137** and **28,** respectively;
3. (iii) **FS22-172-003-AA/G12v2** set forth in SEQ ID NOs **140** and **33,** respectively;
4. (iv) **FS22-053-008-AA/E12v2** set forth in SEQ ID NOs **143** and **17,** respectively; or
5. (v) **FS22-053-008-AA/E05v2** set forth in SEQ ID NOs **146** and **28,** respectively.

[0106] In an even more preferred embodiment, the antibody molecule that binds to PD-L1 and CD137 comprises a heavy chain which comprises, has, or consists of the heavy chain and light chain of antibody:

1. (i) **FS22-172-003-AA/E12v2** set forth in SEQ ID NOs **134** and **17,** respectively;
2. (ii) **FS22-172-003-AA/E05v2** set forth in SEQ ID NOs **137** and **28,** respectively;
3. (iii) **FS22-172-003-AA/G12v2** set forth in SEQ ID NOs **140** and **33,** respectively;
4. (iv) **FS22-053-008-AA/E12v2** set forth in SEQ ID NOs **143** and **17,** respectively; or
5. (v) **FS22-053-008-AA/E05v2** set forth in SEQ ID NOs **146** and **28,** respectively.

[0107] In a still more preferred embodiment, the antibody molecule that binds to PD-L1 and CD137 comprises a heavy chain which comprises, has, or consists of the heavy chain and light chain of antibody:

(i) **FS22-172-003-AA/E12v2** set forth in SEQ ID NOs **134** and **17,** respectively; or

(iv) **FS22-053-008-AA/E12v2** set forth in SEQ ID NOs **143** and **17,** respectively.

[0108] In a yet still more preferred embodiment, the antibody molecule that binds to PD-L1 and CD137 comprises a heavy chain which comprises, has, or consists of the heavy chain and light chain of antibody **FS22-172-003-AA/E12v2** set forth in SEQ ID NOs **134** and **17,** respectively.

[0109] In a yet further alternatively preferred embodiment, the antibody molecule that binds to PD-L1 and CD137 comprises a heavy chain which comprises, has, or consists of the heavy chain and light chain of antibody:

1. (i) **FS22-053-017-AA/E12v2** set forth in SEQ ID NOs **152** and **17,** respectively;
2. (ii) **FS22-053-017-AA/E05v2** set forth in SEQ ID NOs **153** and **28,** respectively; or
3. (iii) **FS22-053-017-AA/G12v2** set forth in SEQ ID NOs **154** and **33,** respectively.

[0110] The antibody molecules of the present invention may also comprise variants of a third sequence, AB, CD or EF structural loop sequence, CH3 domain, CH2 domain, CH2 and CH3 domain, light chain and/or heavy chain sequences disclosed herein. Suitable variants can be obtained by means of methods of sequence alteration, or mutation, and screening. In a preferred embodiment, an antibody molecule comprising one or more variant sequences retains one or more of the functional characteristics of the parent antibody molecule, such as binding specificity and/or binding affinity for PD-L1 and CD137. For example, an antibody molecule comprising one or more variant sequences preferably binds to PD-L1 and/or CD137 with the same affinity, or a higher affinity, than the (parent) antibody molecule. The parent antibody molecule is an antibody molecule which does not comprise the amino acid substitution(s), deletion(s), and/or insertion(s) which have been incorporated into the variant antibody molecule.

[0111] For example, an antibody molecule of the invention may comprise a third sequence, AB, CD or EF structural loop sequence, CH3 domain, CH2 domain, CH2 and CH3 domain, light chain and/or heavy chain sequence which has at least 70%, at least 75%, at least 80%, at least 85%, at least 90%, at least 95%, at least 96%, at least 97%, at least 98%, at least 99%, at least 99.1%, at least 99.2%, at least 99.3%, at least 99.4%, at least 99.5%, at least 99.6%, at least 99.7%, at least 99.8%, or at least 99.9% sequence identity to a structural loop, CH3 domain, CH2 domain, CH2 and CH3 domain, light chain or heavy chain sequence disclosed herein.

[0112] In a preferred embodiment, the antibody molecule of the invention comprises a CH3 domain sequence which has at least 97%, at least 98%, at least 99%, at least 99.1%, at least 99.2%, at least 99.3%, at least 99.4%, at least 99.5%, at least 99.6%, at least 99.7%, at least 99.8%, or at least 99.9% sequence identity to the CH3 domain sequence set forth in SEQ ID NO: **115 [FS22-172-003]** or **81 [FS22-053-008],** preferably SEQ ID NO: **115 [FS22-172-003]**.

[0113] In a further preferred embodiment, the antibody molecule has or comprises a CH2 domain sequence, which has at least 95%, at least 96%, at least 97%, at least 98%, at least 99%, at least 99.1%, at least 99.2%, at least 99.3%, at least 99.4%, at least 99.5%, at least 99.6%, at least 99.7%, at least 99.8%, or at least 99.9% sequence identity to the CH2 domain sequence set forth in SEQ ID NO: **76** or **77.**

[0114] Sequence identity is commonly defined with reference to the algorithm GAP (Wisconsin

GCG package, Accelerys Inc, San Diego USA). GAP uses the Needleman and Wunsch algorithm to align two complete sequences, maximising the number of matches and minimising the number of gaps. Generally, default parameters are used, with a gap creation penalty equalling 12 and a gap extension penalty equalling 4. Use of GAP may be preferred but other algorithms may be used, e.g. BLAST (which uses the method of Altschul *et al.,* 1990), FASTA (which uses the method of Pearson and Lipman, 1988), or the Smith-Waterman algorithm (Smith and Waterman, 1981), or the TBLASTN program, of Altschul *et* al., 1990 supra, generally employing default parameters. In particular, the psi-Blast algorithm (Altschul *et al.,* 1997) may be used.

[0115] An antibody molecule of the invention may also comprise a third sequence, AB, CD or EF structural loop sequence, CH3 domain, CH2 domain, CH2 and CH3 domain, light chain and/or heavy chain which has one or more amino acid sequence alterations (addition, deletion, substitution and/or insertion of an amino acid residue), for example 20 alterations or fewer, 15 alterations or fewer, 10 alterations or fewer, 5 alterations or fewer, 4 alterations or fewer, 3 alterations or fewer, 2 alterations or fewer, or 1 alteration compared with a third sequence, AB, CD or EF structural loop sequence, CH3 domain, CH2 domain, CH2 and CH3 domain, light chain or heavy chain sequence disclosed herein. In particular, alterations may be made in one or more framework regions of the antibody molecule outside the VH and VL domain sequences and/or in one or more framework regions of the CH3 domain. For example, the alterations may be in the CH3 domain outside of the sequences described herein as a first, second and third sequences, or as AB, CD or EF structural loop sequences.

[0116] In a preferred embodiment, the antibody molecule of the invention may comprise a CH3 domain sequence with one or more amino acid sequence alterations (addition, deletion, substitution and/or insertion of an amino acid residue), preferably 20 alterations or fewer, 15 alterations or fewer, 10 alterations or fewer, 5 alterations or fewer, 4 alterations or fewer, 3 alterations or fewer, 2 alterations or fewer, or 1 alteration compared with the CH3 domain sequence set forth in SEQ ID NOs **81, 84, 87, 90, 93, 96, 99, 102, 105, 108, 111, 115, 118, 121, 124, 127, 130,** or **132.** In a more preferred embodiment, the antibody molecule of the invention may comprise a CH3 domain sequence with one or more amino acid sequence alterations (addition, deletion, substitution and/or insertion of an amino acid residue), preferably 20 alterations or fewer, 15 alterations or fewer, 10 alterations or fewer, 5 alterations or fewer, 4 alterations or fewer, 3 alterations or fewer, 2 alterations or fewer, or 1 alteration compared with the CH3 domain sequence set forth in SEQ ID NOs: **115 [FS22-172-003]** or **81 [FS22-053-008],** preferably SEQ ID NO: **115 [FS22-172-003].**

[0117] In a further preferred embodiment, the antibody molecule comprises a CH2 domain sequence, with one or more amino acid sequence alterations (addition, deletion, substitution and/or insertion of an amino acid residue), preferably 20 alterations or fewer, 15 alterations or fewer, 10 alterations or fewer, 5 alterations or fewer, 4 alterations or fewer, 3 alterations or fewer, 2 alterations or fewer, or 1 alteration compared with the CH2 domain sequence set forth in SEQ ID NO: **76** or **77.**

[0118] In preferred embodiments in which one or more amino acids are substituted with another amino acid, the substitutions may conservative substitutions, for example according to the following Table. In some embodiments, amino acids in the same category in the middle column are substituted for one another, i.e. a non-polar amino acid is substituted with another non-polar amino acid for example. In some embodiments, amino acids in the same line in the rightmost column are substituted for one another.

ALIPHATIC	Non-polar	G A P
		I L V
	Polar - uncharged	C S T M
		N Q
	Polar - charged	D E
		K R
AROMATIC		H F W Y

[0119] In some embodiments, substitution(s) may be functionally conservative. That is, in some embodiments the substitution may not affect (or may not substantially affect) one or more functional properties (e.g. binding affinity) of the antibody molecule comprising the substitution as compared to the equivalent unsubstituted antibody molecule.

[0120] Where the antibody molecule comprises a variant of an AB structural loop sequence, CH3 domain, or heavy chain sequence as disclosed herein, the antibody molecule retains the sequence PPY between positions 15 and 17, of the CH3 domain of the antibody molecule. In addition, the antibody molecule retains a 5 amino acid insertion between positions 16 and 17 of the CH3 domain of the antibody molecule. Also disclosed herein, the antibody molecule may retain the sequence at positions 97 and 98 of the CH3 domain of the antibody molecule.

[0121] Where the antibody molecule comprises a variant of CH3 domain, CH2 and CH3 domain, light chain or heavy chain sequence disclosed herein, the variant does not comprise any amino acid alterations in the first and second sequence located in the AB and EF structural loops of the CH3 domain of the antibody molecule. For example, the variant may not comprise any amino acid alterations in the AB and EF structural loops of the CH3 domain of the antibody molecule. Additionally, the variant may not comprise any amino acid alterations in the CD structural loop of the CH3 domain of the antibody molecule. That is, the variant may not comprise any amino acid alterations in the AB and EF structural loops of the CH3 domain of the antibody molecule.

[0122] Where the antibody molecule comprises a variant of a light chain or heavy chain sequence disclosed herein, the antibody molecule does not comprise any amino acid alterations in the CDR sequences. For example, the variant may not comprise any amino acid alterations in the CDR1, CDR2, CDR3, CDR4, CDR5 and/or CDR6 sequences.

[0123] The antibody molecule preferably binds to human PD-L1 and human CD137. Preferably, the antibody molecule is capable of simultaneously binding to human PD-L1 and human CD137, wherein human CD137 and human PD-L1 are co-expressed. As used herein, co-expression means that the two targets are expressed on the surface of a single cell, or on the surface of two separate cells. For example, the antibody molecule may be capable of binding to human PD-L1 and human CD137 when human PD-L1 and human CD137 are co-expressed on a single cell, e.g. an immune cell, as well as being capable of binding to human PD-L1 and human CD137 when human PD-L1 and human CD137 are co-expressed on two separate cells, e.g. an immune cell expressing CD137 and a separate tumour cell expressing PD-L1 in the tumour microenvironment.

[0124] The antibody molecule preferably binds to human PD-L1 with an affinity (K_D) of 8 nM, 7 nM, 6 nM, 5 nM, 4 nM, 3 nM, 2 nM, 1 nM, 0.5 nM, 0.4 nM, or 0.3 nM or with a higher affinity. Preferably, the antibody molecule binds to human PD-L1, with an affinity (K_D) of 0.3 nM, or with a higher affinity.

[0125] The human PD-L1 may, for example, have the sequence set forth in SEQ ID NO: 180. The human PD-L1 may, for example, be recombinant human PD-L1 with an Avi Tag (hPD-L1-Avi-His), available from Aero Biosystems (catalogue number: PD1-H82E5). The recombinant human PD-L1 may be biotinylated.

[0126] The antibody molecule preferably binds to dimeric human CD137 with an affinity (K_D) of 60 nM, 50 nM, 40 nM, 30 nM, 20 nM, 10 nM, 5 nM, 4 nM, 3 nM, or 2 nM, or with a higher affinity. Preferably, the antibody molecule binds to dimeric human CD137, with an affinity (K_D) of 2 nM, or with a higher affinity.

[0127] In a preferred embodiment, the antibody molecule binds to dimeric CD137 with a higher affinity than monomeric CD137. In a preferred embodiment, the antibody molecule binds to dimeric CD137 with an affinity which is at least 50-fold, 60-fold, 70-fold, 80-fold, 90-fold, 100-fold, 110-fold, 120-fold, 130-fold, 140-fold, 150-fold, 160-fold, 170-fold or 200-fold higher than the affinity of the antibody molecule for monomeric CD137.

[0128] The human CD137 may, for example, have the sequence set forth in SEQ ID NO: **186.** Methods for producing dimeric and monomeric CD137 antigens are described in the examples.

[0129] The antibody molecule preferably binds to cynomolgus PD-L1 and cynomolgus CD137. Preferably, the antibody molecule is capable of simultaneously binding to cynomolgus PD-L1 and cynomolgus CD137, wherein cynomolgus PD-L1 and cynomolgus CD137 are expressed on the surface of a single cell, or on the surface of two separate cells.

[0130] In a preferred embodiment, the antibody molecule may bind to cynomolgus PD-L1 with an affinity (K_D) of 8 nM, 7 nM, 6 nM, 5 nM, 4 nM, 3 nM, 2 nM, 1 nM, 0.5 nM, 0.4 nM, or 0.3 nM or with a higher affinity. Preferably, the antibody molecule binds to cynomolgus PD-L1, with an

affinity (K_D) of 1 nM, or with a higher affinity.

[0131] The cynomolgus PD-L1 may, for example, have the sequence set forth in SEQ ID NO: **184.**

[0132] In a preferred embodiment, the antibody molecule may bind to dimeric cynomolgus CD137 with an affinity (K_D) of 60 nM, 50 nM, 40 nM, 30 nM, 20 nM, 10 nM, 5 nM, 4 nM, 3 nM, or 2 nM or with a higher affinity. Preferably, the antibody molecule binds to dimeric cynomolgus CD137, with an affinity (K_D) of 2 nM, or with a higher affinity.

[0133] The antibody molecule may bind to human PD-L1 and cynomolgus PD-L1 with a similar affinity, and/or bind to dimeric human CD137 and dimeric cynomolgus CD137 with similar affinity. This is thought to be beneficial for ensuring that efficacy and toxicity studies carried out with the antibody molecule in cynomolgus monkeys are predictive of the efficacy and toxicity of the antibody molecule in humans.

[0134] Thus, in a preferred embodiment, the antibody molecule binds to cynomolgus PD-L1 with an affinity which is no more than 10-fold, preferably no more than 5-fold lower or higher than the affinity with which the antibody molecule binds to human PD-L1. In a preferred embodiment, the antibody molecule binds to dimeric cynomolgus CD137 with an affinity which is no more than 10-fold, preferably no more than 5-fold lower or higher than the affinity with which the antibody molecule binds dimeric human CD137.

[0135] The binding affinity of an antibody molecule to a cognate antigen, such as human PD-L1, human CD137, cynomolgus PD-L1, or cynomolgus CD137 can be determined by surface plasmon resonance (SPR), such as Biacore, for example. Further details of suitable methods are described in the Examples.

[0136] The ability of an antibody molecule to simultaneously bind to two cognate antigens, e.g. human PD-L1 and human CD137, or cynomolgus PD-L1 and cynomolgus CD137, can be determined by SPR, such as Biacore for example. Further details of suitable methods are described in the Examples.

[0137] The antibody molecule may be capable of blocking the interaction between PD-L1 and its receptor, PD-1, preferably human PD-L1 and human PD-1.

[0138] The PD-1/PD-L1 signalling pathway is known to be important in mediating immune suppression. Thus, antibody molecules that are capable of blocking this pathway are expected to be advantageous in that they may reduce immune suppression and help to increase the anti-tumour response. PD-1/PD-L1 signalling inhibition and CD137 activation may work together in order to increase anti-tumour potency.

[0139] The ability of an antibody molecule to block the binding of PD-L1 to PD-1 may be determined using a bioluminescent cell-based assay, for example using a PD-1/PD-L1

Blockade Bioassay product, e.g. from Promega. The ability of an antibody molecule to block the binding of PD-L1 to PD-1 may be determined using ELISA. Further details of these assays are described in the Examples.

[0140] The ability of an antibody molecule to block the binding of PD-L1 to PD-1, also referred to as the PD-1/PD-L1 blocking activity herein, may be determined by reference to an antibody molecule comprising or consisting of the heavy chain and light chain of antibody **2.14H9OPT** set forth in WO2011/066389 A1, respectively, or the heavy chain and light chain of antibody **G1/280_02_G02** set forth in SEQ ID NOs **177** and **178,** respectively.

[0141] For example, the antibody molecule may have a similar or higher level of PD-1/PD-L1 blocking activity than an antibody molecule comprising or consisting of the heavy chain and light chain of antibody **2.14H9OPT** set forth in WO2011/066389 A1, or the heavy chain and light chain of antibody **G1/280_02_G02** set forth in SEQ ID NOs **177** and **178,** respectively.

[0142] The antibody molecule may have a PD-1/PD-L1 blocking activity that is at least 70%, 80%, or 90% of the PD-1/PD-L1 blocking activity of an antibody molecule comprising or consisting of the heavy chain sequence and light chain sequence of antibody **2.14H9OPT** set forth in WO2011/066389 A1, or the heavy chain and light chain of antibody **G1/280_02_G02** set forth in SEQ ID NOs **177** and **178,** respectively.

[0143] The antibody molecule may have a PD-1/PD-L1 blocking activity that is between 70% and 130%, 80% and 120%, or 90% and 110% of the PD-1/PD-L1 blocking activity of an antibody molecule comprising or consisting of the heavy chain sequence and light chain sequence of antibody **2.14H9OPT** set forth in WO2011/066389 A1, or the heavy chain and light chain of antibody **G1/280_02_G02** set forth in SEQ ID NOs **177** and **178,** respectively.

[0144] As described above, the antibody molecules of the invention are capable of simultaneously binding PD-L1 and CD137, which results in the activation (agonism) of CD137. In a preferred embodiment, the antibody molecule is capable of simultaneously binding to both human PD-L1 and human CD137, wherein such binding causes activation of human CD137. In an additionally preferred embodiment, the antibody molecule is capable of simultaneously binding to both cynomolgus PD-L1 and cynomolgus CD137, wherein such binding causes activation of cynomolgus CD137. Exemplary methods of testing simultaneous binding and activation include T cell activation assays, as described in more detail below.

[0145] The ability of an antibody molecule to activate T cells can be measured using a T cell activation assay. T cells release IL-2 on activation. A T cell activation assay may therefore measure IL-2 release to determine the level of T cell activation induced by the antibody molecule.

[0146] For example, the ability of the antibody molecule to activate T cells is determined by measuring the concentration of the antibody molecule required to achieve half-maximal release of IL-2 by the T cells in a T cell activation assay. This is referred to as the EC_{50} below.

[0147] In a preferred embodiment, the antibody molecule has an EC_{50} in a T cell activation assay which is within 50-fold, 40-fold, 30-fold, 20-fold, 10-fold, 5-fold, 4-fold, 3-fold, or 2-fold of the EC_{50} of **FS22-172-003-AA/E12v2** in the same assay, wherein **FS22-172-003-AA/E12v2** consists of the heavy chain of SEQ ID NO: **134** and the light chain of SEQ ID NO: **17.**

[0148] For example, the antibody molecule may have an EC_{50} in a T cell activation assay of 30 nM or less, 25 nM or less, 20 nM or less, 14 nM or less, 10 nM or less, 5 nM or less, 4 nM or less, 3 nM or less, 2 nM or less, 1.5 nM or less, 1 nM or less, 0.4 nM or less, 0.4 nM or less, or 0.3 nM or less, preferably 1 nM or less, more preferably 1.5 nM or less when the antibody molecule is crosslinked.

[0149] In addition, or alternatively, the ability of an antibody molecule to activate T cells may be determined by measuring the maximum concentration of IL-2 released by the T cells in a T cell activation assay in the presence of the antibody molecule (E_{max}).

[0150] The antibody molecule may have a maximum concentration of IL-2 released by the T cells in a T cell activation assay in the presence of the antibody molecule of at least 1500 pg/ml, 2000 pg/ml, 2500 pg/ml, 3000 pg/ml, or 3250 pg/ml or more, preferably 2500 pg/ml or more.

[0151] In a preferred embodiment, the maximum concentration of IL-2 released by the T cells in a T cell activation assay in the presence of the antibody molecule is within 20%, or 10% of the maximum concentration of IL-2 released by the T cells in the presence of **FS22-172-003-AA/E12v2** in the same assay, wherein **FS22-172-003-AA/E12v2** consists of the heavy chain of SEQ ID NO: **134** and the light chain of SEQ ID NO: **17.**

[0152] The T cell activation assay preferably comprises T cells expressing CD137 and cells expressing PD-L1, for example, HEK293 cells overexpressing human PD-L1 (HEK.hPD-L1) may be prepared and used as described in the Examples. Alternatively, or additionally, cells expressing a different level of PD-L1 may be used, such as the human breast adenocarcinoma cell line MDA-MB-231 (ATCC HTB-26) cells and/or SKBR3 cells. As described in the Examples, HEK.hPD-L1 express a high level of human PD-L1, MDA-MB-231 cells express a medium level of human PD-L1 and SKBR3 cells express a low level of PD-L1.

[0153] In a preferred embodiment, the T cell activation assay does not comprise any agents capable of crosslinking the antibody molecule other than CD137 and PD-L1 expressing cells. Examples of agents capable of crosslinking the antibody molecule include an anti-human CH2 antibody, as described in the Examples.

[0154] The T cell activation assay may be a T cell assay as described herein, such as a pan-T cell assay as described in the present Examples.

[0155] For example, a T cell activation assay may be an IL-2 release assay based on T cells isolated from human Peripheral Blood Mononuclear Cells (PBMCs). For example, the T cell activation assay may comprise isolating human PBMCs from leucocyte depletion cones. Methods for isolating PBMCs are known in the art and described in the present examples. The T cells may then be isolated from the PBMCs. Methods for isolating T cells (all T cells) from PBMCs are known in the art and described in the present Examples.

[0156] The activation assay may involve preparing the required number of T cells for example in experimental media, such as a T cell medium. The required number of T cells may be prepared at a concentration of 1.0×10^6 cells/ml. T cells may then be stimulated using a suitable T cell activation reagent that provides the signals required for T cell activation. For example, the T cell activation reagent may be a reagent comprising CD3 and CD28, such as beads comprising CD3 and CD28. Isolated T cells may be incubated overnight with the T cell activation reagent to activate the T cells. Following this, the activated T cells may be washed to separate the T cells from the T cell activation reagent and resuspended in T cell medium at a suitable concentration, such as 2.0×10^6 cells/ml. Activated T cells may then be added to plates coated with anti-human CD3 antibody.

[0157] The cells (e.g. HEK.hPD-L1 cells) may be plated at, e.g. 2×10^5 cells per well on to anti-CD3 antibody-coated tissue culture plates in T cell culture medium. After, e.g. 4 hours of incubation, all T cell culture medium may be removed and replaced with 100µl T cell culture medium containing T cells, e.g. at a concentration of 5.0×10^5 cells/ml resulting in 5.0×10^4 cells/well.

[0158] A suitable dilution of each test antibody molecule may be prepared and added to the wells. The T cells may then be incubated at 37°C, 5% CO_2 for 24 hours with the test antibody.

[0159] Supernatants may be collected and assayed to determine the concentration of IL-2 in the supernatant. Methods for determining the concentration of IL-2 in a solution are known in the art and described in the present examples. The concentration of human IL-2 may be plotted versus the log concentration of the antibody molecule. The resulting curves may be fitted using the log (agonist) versus response equation.

[0160] The antibody molecule may be conjugated to a bioactive molecule or a detectable label. In this case, the antibody molecule may be referred to as a conjugate. Such conjugates find application in the treatment of diseases as described herein.

[0161] For example, the bioactive molecule may be an immune system modulator, such as a cytokine, preferably a human cytokine. For example, the cytokine may be a cytokine which stimulates T cell activation and/or proliferation. Examples of cytokines for conjugation to the antibody molecule include IL-2, IL-10, IL-12, IL-15, IL-21, GM-CSF and IFN-γ.

[0162] Alternatively, the bioactive molecule may be a ligand trap, such as a ligand trap of a

cytokine, e.g. of TGF-beta or IL-6.

[0163] Alternatively, the bioactive molecule may be a therapeutic radioisotope.

[0164] Radioimmunotherapy is used in cancer treatment, for example. Therapeutic radioisotopes suitable for radioimmunotherapy are known in the art and include yttrium-90, iodine-131, bismuth-213, astatine-211, lutetium 177, rhenium-188, copper-67, actinium-225, and iodine-125 and terbium-161.

[0165] Suitable detectable labels which may be conjugated to antibody molecules are known in the art and include radioisotopes such as iodine-125, iodine-131, yttrium-90, indium-111 and technetium-99; fluorochromes, such as fluorescein, rhodamine, phycoerythrin, Texas Red and cyanine dye derivatives for example,Cy7 and Alexa750; chromogenic dyes, such as diaminobenzidine; latex beads; enzyme labels such as horseradish peroxidase; phosphor or laser dyes with spectrally isolated absorption or emission characteristics; and chemical moieties, such as biotin, which may be detected via binding to a specific cognate detectable moiety, e.g. labelled avidin.

[0166] The antibody molecule may be conjugated to the bioactive molecule or detectable label by means of any suitable covalent or non-covalent linkage, such as a disulphide or peptide bond. Where the bioactive molecule is a cytokine, the cytokine may be joined to the antibody molecule by means of a peptide linker. Suitable peptide linkers are known in the art and may be 5 to 25, 5 to 20, 5 to 15, 10 to 25, 10 to 20, or 10 to 15 amino acids in length.

[0167] In some embodiments, the bioactive molecule may be conjugated to the antibody molecule by a cleavable linker. The linker may allow release of the bioactive molecule from the antibody molecule at a site of therapy. Linkers may include amide bonds (e.g. peptidic linkers), disulphide bonds or hydrazones. Peptide linkers for example may be cleaved by site specific proteases, disulphide bonds may be cleaved by the reducing environment of the cytosol and hydrazones may be cleaved by acid-mediated hydrolysis.

[0168] The invention also provides an isolated nucleic acid molecule or molecules encoding an antibody molecule of the invention. The skilled person would have no difficulty in preparing such nucleic acid molecules using methods well-known in the art.

[0169] The nucleic acid molecule or molecules may, for example, comprise the sequence set forth in SEQ ID NO: **82, 91,** or **116,** which encode the CH3 domains of **FS22-053-008, FS22-053-017,** and **FS22-172-003,** respectively. Preferably, the nucleic acid molecule or molecules comprise the sequence set forth in SEQ ID NO: **116** or **82,** which encode the CH3 domain of **FS22-172-003** or **FS22-053-008,** respectively. More preferably, the nucleic acid molecule or molecules comprise the sequence set forth in SEQ ID NO: **116,** which encodes the CH3 domain of **FS22-172-003.**

[0170] The nucleic acid molecule or molecules may encode the VH domain and/or VL domain,

preferably the VH domain and VL domain of antibody **E12v2, E05v2,** or **G12v2,** preferably **E12v2** or **E05v2,** more preferably **E12v2.** The VH and VL domain sequences of these antibodies are described herein.

[0171] For example, the nucleic acid molecule(s) may comprise:

1. (i) the VH domain nucleic acid sequence of antibody **E12v2** set forth in SEQ ID NO: **13,** and/or the VL domain nucleic acid sequence of antibody **E12v2** set forth in SEQ ID NO: **15; or**
2. (ii) the VH domain nucleic acid sequence of antibody **E05v2** set forth in SEQ ID NO: **24,** and/or the VL domain nucleic acid sequence of antibody **E05v2** set forth in SEQ ID NO: **26;** or
3. (iii) the VH domain nucleic acid sequence of antibody **G12v2** set forth in SEQ ID NO: **24,** and/or the VL domain nucleic acid sequence of antibody **G12v2** set forth in SEQ ID NO: **31.**

[0172] The nucleic acid molecule or molecules may encode the heavy chain and/or light chain, preferably the heavy chain and light chain of antibody **FS22-172-003-AA/E12v2, FS22-172-003-AA/E05v2, FS22-172-003-AA/G12v2, FS22-053-008-AA/E12v2, or FS22-053-008-AA/E05v2,** preferably antibody **FS22-172-003-AA/E12v2.** The heavy chain and light chain sequences of these antibodies are described herein.

[0173] For example, the nucleic acid molecule(s) may comprise:

1. (i) the heavy chain nucleic acid sequence of antibody **FS22-172-003-AA/E12v2** set forth in SEQ ID NO: **32** or **135,** and/or the light chain nucleic acid sequence of antibody **FS22-172-003-AA/E12v2** set forth in SEQ ID NO: **39** or **136;** or
2. (ii) the heavy chain nucleic acid sequence of antibody **FS22-172-003-AA/E05v2** set forth in SEQ ID NO: **138,** and/or the light chain nucleic acid sequence of antibody **FS22-172-003-AA/E05v2** set forth in SEQ ID NO: **139;**
3. (iii) the heavy chain nucleic acid sequence of antibody **FS22-172-003-AA/G12v2** set forth in SEQ ID NO: **141,** and/or the light chain nucleic acid sequence of antibody **FS22-172-003-AA/G12v2** set forth in SEQ ID NO: **142;**
4. (iv) the heavy chain nucleic acid sequence of antibody **FS22-053-008-AA/E12v2** set forth in SEQ ID NO: **144,** and/or the light chain nucleic acid sequence of antibody **FS22-053-008-AA/E12v2** set forth in SEQ ID NO: **145;** or
5. (v) the heavy chain nucleic acid sequence of antibody **FS22-053-008-AA/E05v2** set forth in SEQ ID NO: **147,** and/or the light chain nucleic acid sequence of antibody **FS22-053-008-AA/E05v2** set forth in SEQ ID NO: **148.**

[0174] Where the nucleic acid encodes the VH and VL domain, or heavy and light chain, of an

antibody molecule of the invention, the two domains or chains may be encoded on two separate nucleic acid molecules.

[0175] An isolated nucleic acid molecule may be used to express an antibody molecule of the invention. The nucleic acid will generally be provided in the form of a recombinant vector for expression. Another aspect of the invention thus provides a vector comprising a nucleic acid as described above. Suitable vectors can be chosen or constructed, containing appropriate regulatory sequences, including promoter sequences, terminator fragments, polyadenylation sequences, enhancer sequences, marker genes and other sequences as appropriate.

[0176] Preferably, the vector contains appropriate regulatory sequences to drive the expression of the nucleic acid in a host cell. Vectors may be plasmids, viral e.g. phage, or phagemid, as appropriate.

[0177] A nucleic acid molecule or vector as described herein may be introduced into a host cell. Techniques for the introduction of nucleic acid or vectors into host cells are well established in the art and any suitable technique may be employed. A range of host cells suitable for the production of recombinant antibody molecules are known in the art, and include bacterial, yeast, insect or mammalian host cells. A preferred host cell is a mammalian cell, such as a CHO, NS0, or HEK cell, for example a HEK293 cell.

[0178] Another aspect of the invention provides a method of producing an antibody molecule of the invention comprising expressing a nucleic acid encoding the antibody molecule in a host cell and optionally isolating and/or purifying the antibody molecule thus produced. Methods for culturing host cells are well-known in the art. The method may further comprise isolating and/or purifying the antibody molecule. Techniques for the purification of recombinant antibody molecules are well-known in the art and include, for example HPLC, FPLC or affinity chromatography, e.g. using Protein A or Protein L. In some embodiments, purification may be performed using an affinity tag on antibody molecule. The method may also comprise formulating the antibody molecule into a pharmaceutical composition, optionally with a pharmaceutically acceptable excipient or other substance as described below.

[0179] PD-L1 is known to be expressed on many cancer cells and is expressed on cell of the immune system. CD137 is expressed on cells of the immune system, including T cells, in particular $CD8^+$ T cells, B cells, NK cells and tumour-infiltrating lymphocytes (TILs). CD137 is expressed at a lower level on $CD4^+$ T cells than $CD8^+$ T cells but has also been shown to be involved in inducing proliferation and activation of some subsets of $CD4^+$ T cells.

[0180] CD137 activation has been shown to play a role in enhancing proliferation, survival and the cytotoxic effector function of $CD8^+$ T cells, as well as $CD8^+$ T cell differentiation and maintenance of memory $CD8^+$ T cells. Activation of CD137 has also been demonstrated to enhance NK cell-mediated ADCC, as well as B cell proliferation, survival and cytokine production.

[0181] As described in detail herein, the present inventors have demonstrated that antibody molecules of the invention are capable of simultaneously binding to PD-L1 and CD137 in order to induce agonism of CD137. In this way, the antibody molecule drives agonism autonomously, based on the expression of the PD-L1 and CD137, and without the need for additional crosslinking agents. Since PD-L1 is expressed on many cancer cells and CD137 is expressed on immune cells, where it has a known role in enhancing the proliferation and survival of immune cells, it is expected that antibody molecules of the invention will be able to enhance an immune response at locations where PD-L1 is expressed, e.g. in the tumour microenvironment. Furthermore, the present inventors have shown that the use of an antibody molecule having these properties, is effective in suppressing tumour growth in syngeneic mouse models of cancer, and that such antibody molecules are more effective than the administration of two binding molecules which bind PD-L1 and CD137, respectively.

[0182] The antibody molecules as described herein may thus be useful for therapeutic applications, in particular in the treatment of cancer.

[0183] An antibody molecule as described herein may be used in a method of treatment of the human or animal body. Related aspects of the invention provide;

1. (i) an antibody molecule described herein for use as a medicament,
2. (ii) an antibody molecule described herein for use in a method of treatment of a disease or disorder,
3. (iii) the use of an antibody molecule described herein in the manufacture of a medicament for use in the treatment of a disease or disorder; and,
4. (iv) a method of treating a disease or disorder in an individual, wherein the method comprises administering to the individual a therapeutically effective amount of an antibody molecule as described herein.

[0184] The individual may be a patient, preferably a human patient.

[0185] Treatment may be any treatment or therapy in which some desired therapeutic effect is achieved, for example, the inhibition or delay of the progress of the condition, and includes a reduction in the rate of progress, a halt in the rate of progress, amelioration of the condition, cure or remission (whether partial or total) of the condition, preventing, ameliorating, delaying, abating or arresting one or more symptoms and/or signs of the condition or prolonging survival of an individual or patient beyond that expected in the absence of treatment.

[0186] Treatment as a prophylactic measure (i.e. prophylaxis) is also included. For example, an individual susceptible to or at risk of the occurrence or re-occurrence of a disease such as cancer may be treated as described herein. Such treatment may prevent or delay the occurrence or re-occurrence of the disease in the individual.

[0187] A method of treatment as described may be comprise administering at least one further treatment to the individual in addition to the antibody molecule. The antibody molecule described herein may thus be administered to an individual alone or in combination with one or more other treatments. Where the antibody molecule is administered to the individual in combination with another treatment, the additional treatment may be administered to the individual concurrently with, sequentially to, or separately from the administration of the antibody molecule. Where the additional treatment is administered concurrently with the antibody molecule, the antibody molecule and additional treatment may be administered to the individual as a combined preparation. For example, the additional therapy may be a known therapy or therapeutic agent for the disease to be treated.

[0188] Whilst an antibody molecule may be administered alone, antibody molecules will usually be administered in the form of a pharmaceutical composition, which may comprise at least one component in addition to the antibody molecule. Another aspect of the invention therefore provides a pharmaceutical composition comprising an antibody molecule as described herein. A method comprising formulating an antibody molecule into a pharmaceutical composition is also provided.

[0189] Pharmaceutical compositions may comprise, in addition to the antibody molecule, a pharmaceutically acceptable excipient, carrier, buffer, stabilizer or other materials well known to those skilled in the art. The term "pharmaceutically acceptable" as used herein pertains to compounds, materials, compositions, and/or dosage forms which are, within the scope of sound medical judgement, suitable for use in contact with the tissues of a subject (e.g., human) without excessive toxicity, irritation, allergic response, or other problem or complication, commensurate with a reasonable benefit/risk ratio. Each carrier, excipient, etc. must also be "acceptable" in the sense of being compatible with the other ingredients of the formulation. The precise nature of the carrier or other material will depend on the route of administration, which may be by infusion, injection or any other suitable route, as discussed below.

[0190] For parenteral, for example subcutaneous or intravenous administration, e.g. by injection, the pharmaceutical composition comprising the antibody molecule may be in the form of a parenterally acceptable aqueous solution which is pyrogen-free and has suitable pH, isotonicity and stability. Those of relevant skill in the art are well able to prepare suitable solutions using, for example, isotonic vehicles, such as Sodium Chloride Injection, Ringer's Injection, Lactated Ringer's Injection. Preservatives, stabilizers, buffers, antioxidants and/or other additives may be employed as required including buffers such as phosphate, citrate and other organic acids; antioxidants, such as ascorbic acid and methionine; preservatives (such as octadecyldimethylbenzyl ammonium chloride; hexamethonium chloride; benzalkonium chloride; benzethonium chloride; phenol, butyl or benzyl alcohol; alkyl parabens, such as methyl or propyl paraben; catechol; resorcinol; cyclohexanol; 3'-pentanol; and m-cresol); low molecular weight polypeptides; proteins, such as serum albumin, gelatin or immunoglobulins; hydrophilic polymers, such as polyvinylpyrrolidone; amino acids, such as glycine, glutamine, asparagines, histidine, arginine, or lysine; monosaccharides, disaccharides and other carbohydrates including glucose, mannose or dextrins; chelating agents, such as EDTA;

sugars, such as sucrose, mannitol, trehalose or sorbitol; salt-forming counter-ions, such as sodium; metal complexes (e.g. Zn-protein complexes); and/or nonionic surfactants, such as TWEEN™, PLURONICS™ or polyethylene glycol (PEG).

[0191] In some embodiments, antibody molecules may be provided in a lyophilised form for reconstitution prior to administration. For example, lyophilised antibody molecules may be re-constituted in sterile water and mixed with saline prior to administration to an individual.

[0192] Administration may be in a "therapeutically effective amount", this being sufficient to show benefit to an individual. The actual amount administered, and rate and time-course of administration, will depend on the nature and severity of what is being treated, the particular individual being treated, the clinical condition of the individual, the cause of the disorder, the site of delivery of the composition, the type of antibody molecule, the method of administration, the scheduling of administration and other factors known to medical practitioners. Prescription of treatment, e.g. decisions on dosage etc., is within the responsibility of general practitioners and other medical doctors, and may depend on the severity of the symptoms and/or progression of a disease being treated. Appropriate doses of antibody molecules are well known in the art (Ledermann et al. (1991) Int. J. Cancer 47: 659-664; and Bagshawe et al. (1991) Antibody, Immunoconjugates and Radiopharmaceuticals 4: 915-922). Specific dosages indicated herein, or in the Physician's Desk Reference (2003) as appropriate for an antibody molecule being administered, may be used. A therapeutically effective amount or suitable dose of an antibody molecule can be determined by comparing *in vitro* activity and *in vivo* activity in an animal model. Methods for extrapolation of effective dosages in mice and other test animals to humans are known. The precise dose will depend upon a number of factors, including whether the size and location of the area to be treated, and the precise nature of the antibody molecule.

[0193] A typical antibody dose is in the range 100 µg to 1 g for systemic applications, and 1 µg to 1 mg for topical applications. An initial higher loading dose, followed by one or more lower doses, may be administered. This is a dose for a single treatment of an adult individual, which may be proportionally adjusted for children and infants, and also adjusted for other antibody formats in proportion to molecular weight.

[0194] Treatments may be repeated at daily, twice-weekly, weekly or monthly intervals, at the discretion of the physician. The treatment schedule for an individual may be dependent on the pharmacokinetic and pharmacodynamic properties of the antibody composition, the route of administration and the nature of the condition being treated.

[0195] Treatment may be periodic, and the period between administrations may be about two weeks or more, e.g. about three weeks or more, about four weeks or more, about once a month or more, about five weeks or more, or about six weeks or more. For example, treatment may be every two to four weeks or every four to eight weeks. Suitable formulations and routes of administration are described above.

[0196] In a preferred embodiment, an antibody molecule as described herein may be for use in a method of treating cancer.

[0197] Cancer may be characterised by the abnormal proliferation of malignant cancer cells. Where a particular type of cancer, such as breast cancer, is referred to, this refers to an abnormal proliferation of malignant cells of the relevant tissue, such as breast tissue. A secondary cancer which is located in the breast but is the result of abnormal proliferation of malignant cells of another tissue, such as ovarian tissue, is not a breast cancer as referred to herein but an ovarian cancer.

[0198] The cancer may be a primary or a secondary cancer. Thus, an antibody molecule as described herein may be for use in a method of treating cancer in an individual, wherein the cancer is a primary tumour and/or a tumour metastasis.

[0199] A tumour of a cancer to be treated using an antibody molecule as described herein may comprise TILs that express CD137, e.g. on their cell surface. In one embodiment, the tumour may have been determined to comprise TILs that express CD137. Methods for determining the expression of an antigen on a cell surface are known in the art and include, for example, flow cytometry.

[0200] For example, the cancer to be treated using an antibody molecule as described herein may be selected from the group consisting of leukaemias, such as acute myeloid leukaemia (AML), chronic myeloid leukaemia (CML), acute lymphoblastic leukaemia (ALL) and chronic lymphocytic leukaemia (CLL); lymphomas, such as Hodgkin lymphoma, non-Hodgkin lymphoma and multiple myeloma; and solid cancers, such as sarcomas (e.g. soft tissue sarcomas), skin cancer (e.g. Merkel cell carcinoma), melanoma, bladder cancer (e.g. urothelial carcinoma), brain cancer (e.g. glioblastoma multiforme), breast cancer, uterine/endometrial cancer, ovarian cancer (e.g. ovarian serous cystadenoma), prostate cancer, lung cancer (e.g. non-small cell lung carcinoma (NSCLC) and small cell lung cancer (SCLC), colorectal cancer (e.g. colorectal adenocarcinoma), cervical cancer (e.g. cervical squamous cell cancer and cervical adenocarcinoma), liver cancer (e.g. hepatocellular carcinoma), head and neck cancer (e.g. head and neck squamous-cell carcinoma), oesophageal cancer, pancreatic cancer, renal cancer (e.g. renal cell cancer), adrenal cancer, stomach cancer (e.g. stomach adenocarcinoma), testicular cancer, cancer of the gall bladder and biliary tracts (e.g. cholangiocarcinoma), thyroid cancer, thymus cancer, bone cancer, and cerebral cancer.

[0201] In a preferred embodiment, the cancer to be treated using an antibody molecule as described herein is a solid cancer.

[0202] More preferably, the cancer to be treated using an antibody molecule as described herein is a solid cancer selected from the group consisting of melanoma, bladder cancer, brain cancer, breast cancer, ovarian cancer, lung cancer, colorectal cancer, cervical cancer, liver cancer, head and neck cancer, pancreatic cancer, renal cancer, stomach cancer and Gastrointestinal Stromal tumours (GISTs).

[0203] In a further preferred embodiment, the cancer to be treated using an antibody molecule as described herein may be a cancer which is responsive to treatment with one or more check-point inhibitors, such as an antibody which binds PD-1, PD-L1 or CTLA4. Such tumours are thought to have higher TIL levels and/or higher tumour mutational burden than tumours which are not responsive to check-point inhibitor therapy. Such tumours are also referred to as warm or hot tumours.

[0204] Examples of such tumours include head and neck squamous-cell carcinoma (HNSCC), melanoma, lung cancer (such as squamous lung cancer, lung adenocarcinoma, non-small cell lung carcinoma [NSCLC], or small-cell lung carcinoma [SCLC]), prostate cancer, cervical cancer (such as cervical squamous cell carcinoma or endocervical andenocarcinoma), bladder cancer, breast cancer, thyroid cancer, kidney cancer, colorectal cancer (MSI or MSS; e.g. colorectal adenocarcinoma), oesophageal cancer, non-Hodgkin's lymphoma (NHL), gastric cancer, endometrial cancer, pancreatic cancer, ovarian cancer, hepatocellular carcinoma, mesothelioma, urothelial cancer, Merkel cell carcinoma, and stomach adenocarcinoma. In a preferred embodiment, the cancer is HNSCC. The cancer may further be a cancer which has not previously been treated with a chemotherapeutic or radiotherapeutic agent, i.e. the individual to be treated may be a cancer patient which has not received treatment with a chemotherapeutic or radiotherapeutic agent for the cancer in question.

[0205] Alternatively, the cancer to be treated using an antibody molecule as described herein may be a cancer, such as pancreatic cancer or prostate cancer which is not responsive to treatment with one or more check-point inhibitors, such as an antibody which binds PD-1, PD-L1 or CTLA4. An individual treated with an antibody of the invention may thus be a cancer patient, such as a pancreatic cancer or prostate cancer patient, with a previous inadequate response to one or more check-point inhibitors, such as an anti-PD-L1 or anti-PD-1 antibody.

[0206] Tumours which are not responsive to treatment with one or more check-point inhibitors are also referred to as cold tumours. Without wishing to be bound by theory, it is thought that treatment of a cancer, which is not responsive to treatment with one or more check-point inhibitors alone, with chemotherapy, radiotherapy, an immunotherapeutic agent, such as an immunostimulatory agent, or an anti-tumour vaccine will result in cancer cell death which in turn will result in an increase in TILs in the tumour and higher expression of immunosuppressive receptors, which in turn will make the cancer responsive to treatment with check-point inhibitors, i.e. turn a cold tumour into a warm tumour. Thus, the antibody molecule of the invention may be for use in a method of treating cancer in an individual, wherein the cancer is not responsive, or refractory, to treatment with one or more check-point inhibitors alone, and wherein the method comprises administering the antibody molecule to the individual in combination with a chemotherapeutic, radiotherapeutic, or immunostimulatory agent, or an anti-cancer vaccine. A method of treating a cancer in an individual, wherein the cancer is not responsive, or refractory, to treatment with one or more check-point inhibitors alone, and wherein the method comprises administering the antibody molecule to the individual in combination with a chemotherapeutic, radiotherapeutic, or immunostimulatory agent, or an

anti-cancer vaccine is also contemplated.

[0207] In the context of cancer, treatment may include inhibiting cancer growth, including complete cancer remission, and/or inhibiting cancer metastasis, as well as inhibiting cancer recurrence. Cancer growth generally refers to any one of a number of indices that indicate change within the cancer to a more developed form. Thus, indices for measuring an inhibition of cancer growth include a decrease in cancer cell survival, a decrease in tumour volume or morphology (for example, as determined using computed tomographic (CT), sonography, or other imaging method), a delayed tumour growth, a destruction of tumour vasculature, improved performance in delayed hypersensitivity skin test, an increase in the activity of anti-cancer immune cells or other anti-cancer immune responses, and a decrease in levels of tumour-specific antigens. Activating or enhancing immune responses to cancerous tumours in an individual may improve the capacity of the individual to resist cancer growth, in particular growth of a cancer already present in the subject and/or to decrease the propensity for cancer growth in the individual.

[0208] In the context of cancer treatment, an antibody molecule as described herein may be administered to an individual in combination with another anti-cancer therapy or therapeutic agent, such as an anti-cancer therapy or therapeutic agent which has been shown to be suitable, or potentially suitable, for the treatment of the cancer in question. For example, the antibody molecule may be administered to the individual in combination with a chemotherapeutic agent, radiotherapy, a radionuclide, an immunotherapeutic agent, an anti-tumour vaccine, an oncolytic virus, an adoptive cell transfer (ACT) therapy, such as adoptive NK cell therapy or therapy with chimeric antigen receptor (CAR) T-cells, autologous TILs or gamma/delta T cells, or an agent for hormone therapy.

[0209] Without wishing to be bound by theory, it is thought that the antibody molecule described herein may act as an adjuvant in anti-cancer therapy. Specifically, it is thought that administration of the antibody molecule to an in individual in combination with chemotherapy or radiotherapy, for example, will trigger a greater immune response against the cancer than is achieved with chemotherapy or radiotherapy alone.

[0210] One or more chemotherapeutic agents for administration in combination with an antibody molecule as described herein may be selected from the group consisting of: taxanes, cytotoxic antibiotics, tyrosine kinase inhibitors, PARP inhibitors, B-Raf enzyme inhibitors, MEK inhibitors, c-MET inhibitors, VEGFR inhibitors, PDGFR inhibitors, alkylating agents, platinum analogues, nucleoside analogues, antifolates, thalidomide derivatives, antineoplastic chemotherapeutic agents and others. Taxanes include docetaxel, paclitaxel and nab-paclitaxel; cytotoxic antibiotics include actinomycin, bleomycin, and anthracyclines such as doxorubicin, mitoxantrone and valrubicin; tyrosine kinase inhibitors include erlotinib, gefitinib, axitinib, PLX3397, imatinib, cobemitinib and trametinib; PARP inhibitors include piraparib; B-Raf enzyme inhibitors include vemurafenib and dabrafenib; alkylating agents include dacarbazine, cyclophosphamide and temozolomide; platinum analogues include carboplatin, cisplatin and oxaliplatin; nucleoside analogues include azacitidine, capecitabine, fludarabine, fluorouracil

and gemcitabine and ; antifolates include methotrexate and pemetrexed. Other chemotherapeutic agents suitable for use in the present invention include defactinib, entinostat, eribulin, irinotecan and vinblastine.

[0211] Preferred therapeutic agents for administration with an antibody molecule as described herein are doxorubicin, mitoxantrone, cyclophosphamide, cisplatin, and oxaliplatin.

[0212] A radiotherapy for administration in combination with an antibody molecule as described herein may be external beam radiotherapy or brachytherapy.

[0213] Radionuclides for administration with an antibody molecule as described herein may be selected from the group consisting of: yttrium-90, iodine-131, bismuth-213, astatine-211, lutetium 177, rhenium-188, copper-67, actinium-225, iodine-125 and terbium-161.

[0214] An immunotherapeutic agent for administration in combination with an antibody molecule as described herein may be a therapeutic antibody molecule, nucleotide, cytokine, or cytokine-based therapy. For example, the therapeutic antibody molecule may bind to an immune regulatory molecule, e.g. an inhibitory checkpoint molecule or an immune costimulatory molecule, a receptor of the innate immune system, or a tumour antigen, e.g. a cell surface tumour antigen or a soluble tumour antigen. Examples of immune regulatory molecules to which the therapeutic antibody molecule may bind include CTLA-4, LAG-3, TIGIT, TIM-3, VISTA, PD-L1, PD-1, CD47, CD73, CSF-1R, KIR, CD40, HVEM, IL-10 and CSF-1. Examples of receptors of the innate immune system to which the therapeutic antibody molecule may bind include TLR4, TLR7, TLR9, RIG-I-like receptors (e.g. RIG-I and MDA-5), and STING. Examples of tumour antigens to which the therapeutic antibody molecule may bind include HER2, EGFW, CD20 and TGF-beta.

[0215] The nucleotide for administration in combination with an antibody molecule as described herein may be an siRNA.

[0216] The cytokines or cytokine-based therapy may be selected from the group consisting of: IL-2, prodrug of conjugated IL-2, GM-CSF, IL-7, IL-12, IL-9, IL-15, IL-18, IL-21, and type I interferon.

[0217] Anti-tumour vaccines for the treatment of cancer have both been implemented in the clinic and discussed in detail within scientific literature (such as Rosenberg, S. 2000 Development of Cancer Vaccines). This mainly involves strategies to prompt the immune system to respond to various cellular markers expressed by autologous or allogenic cancer cells by using those cells as a vaccination method, both with or without granulocyte-macrophage colony-stimulating factor (GM-CSF). GM-CSF provokes a strong response in antigen presentation and works particularly well when employed with said strategies.

[0218] The features disclosed in the foregoing description, or in the following claims, or in the accompanying drawings, expressed in their specific forms or in terms of a means for

performing the disclosed function, or a method or process for obtaining the disclosed results, as appropriate, may, separately, or in any combination of such features, be utilised for realising the invention in diverse forms thereof.

[0219] While the invention has been described in conjunction with the exemplary embodiments described above, many equivalent modifications and variations will be apparent to those skilled in the art when given this disclosure. Accordingly, the exemplary embodiments of the invention set forth above are considered to be illustrative and not limiting.

[0220] For the avoidance of any doubt, any theoretical explanations provided herein are provided for the purposes of improving the understanding of a reader. The inventors do not wish to be bound by any of these theoretical explanations.

[0221] Any section headings used herein are for organizational purposes only and are not to be construed as limiting the subject matter described.

[0222] Throughout this specification, including the claims which follow, unless the context requires otherwise, the word "comprise" and "include", and variations such as "comprises", "comprising", and "including" will be understood to imply the inclusion of a stated integer or step or group of integers or steps but not the exclusion of any other integer or step or group of integers or steps.

[0223] The references to the methods of treatment by therapy or surgery of this description are to be interpreted as references to compounds, pharmaceutical compositions and medicaments of the present invention for use in those methods.

[0224] It must be noted that, as used in the specification and the appended claims, the singular forms "a," "an," and "the" include plural referents unless the context clearly dictates otherwise. Ranges may be expressed herein as from "about" one particular value, and/or to "about" another particular value. When such a range is expressed, another embodiment includes from the one particular value and/or to the other particular value. Similarly, when values are expressed as approximations, by the use of the antecedent "about," it will be understood that the particular value forms another embodiment. The term "about" in relation to a numerical value is optional and means for example +/- 10%.

Examples

Example 1: Antigen selection and characterisation

[0225] The selection and screening methods used to identify mAb^2 that are capable of binding PD-L1 and CD137 and agonising CD137 required the use of various PD-L1 and CD137

antigens. The production of these antigens is described in more detail below.

1.1 Recombinant CD 137 antigens

[0226] Tumour necrosis factor receptor superfamily (TNFRSF) members, such as CD137, are known for their tendency to form multimers which cluster together when bound to their cognate ligands (Croft, M. 2003). This propensity to aggregate for their functionality makes it challenging to produce soluble recombinant proteins that do not aggregate in solution for use in *in vitro* selections such as phage and yeast display and for characterisation of selected proteins.

[0227] Several commercially available recombinant antigens were tested and the majority found to be unsuitable for use in these selections due to the levels of aggregates present. Of those tested only the biotinylated, human secreted CD137, hFc-fusion protein (BPS Biosciences, catalogue no. 71171), designated 'hCD137-hFc-Avi-BPS' hereinafter, had sufficiently low aggregation to be suitable and was used in selections, though with limited success (see **Example 2).**

[0228] As the majority of commercially available antigens were deemed unsuitable, the following recombinant dimeric and monomeric CD137 antigens (see **Table 1),** were produced in-house for use in selections:

Table 1: CD137 Antigens

Type	Designation	Species	Soluble or cell	Biotinylated	Antigen Format
Recombinant	mCD137-mFc-Avi	Mouse	Soluble	Yes	Dimer
Recombinant	mCD137-Avi-His	Mouse	Soluble	Yes	Monomer
Recombinant	hCD137-mFc-Avi	Human	Soluble	Yes	Dimer
Recombinant	hCD137-Avi-His	Human	Soluble	Yes	Monomer
Recombinant	cCD137-mFc-Avi	Cyno	Soluble	Yes	Dimer

[0229] Monomeric antigens were produced by cloning DNA encoding the extracellular domain of the human (SEQ ID NO: 186) or mouse CD137 (SEQ ID NO: 188) along with an Avi sequence and six C-terminal histidine residues into modified pFUSE vectors (Invivogen cat no pfuse-mg2afc2) using EcoRI-HF and BamHI-HF restriction enzymes. The vectors were transfected into HEK293-6E cells (National Research Council of Canada), and expressed CD137 was purified using HisTrap™ excel nickel column (GE LifeSciences 29048586) and

size-exclusion chromatography (SEC) to ensure antigen was a single species and did not contain aggregates.

[0230] To produce the dimeric antigens, DNA constructs encoding the extracellular domain of the human, mouse or cynomolgus CD137 fused with the mIgG2a Fc domain along with an Avi sequence were cloned into modified pFUSE vectors and transfected into HEK293-6E cells. Recombinant CD137 was purified using MabSelect SuRe™ protein A column (GE Healthcare, 11003494) and size-exclusion chromatography (SEC) to ensure antigen was a single species and did not contain aggregates.

[0231] Each of the dimeric and monomeric antigens were biotinylated using a BirA biotin-biotin protein ligase reaction kit (Avidity LLC, BirA500) to produce monomeric CD137 antigens labelled with a single biotin molecule and dimeric CD137 antigens labelled with two biotin molecules, one per each of the two monomers. 3 mg of antigen was mixed with 7.8 µl BirA enzyme mix to a molar ratio of enzyme to substrate of 1:50. Additives were then added in accordance with the manufacturer's recommendations (142 µl Biomix A, 142 µl Biomix B, 142 µ Biotin) and the reaction mix was incubated for two hours at room temperature. To maintain the integrity of the biotinylated protein, the reaction mix was immediately buffer exchanged to DPBS (Life Technologies 14190-169) using Amicon 30 µm filters (Merck Millipore UFC503096).

[0232] Proteins were further purified by SEC to ensure removal of the BirA enzyme and production of a final high quality monodispersed protein preparation with no high molecular weight aggregates. In more detail, materials from the same production lot were mixed together and analysed for stability and purity by size-exclusion high-performance liquid chromatography (SE-HPLC), SDS polyacrylamide gel electrophoresis (SDS-PAGE), and size-exclusion chromatography with multi-angle light scattering (SEC-MALS). Complete biotinylation of the proteins was confirmed in a streptavidin-shifting SDS-PAGE gel. The recombinant human and mouse antigens were confirmed to bind anti-CD137 positive-control antibodies (20H4.9 (US Patent No. 7288638)) and Lob12.3 (University of Southampton), respectively) *in vitro* by surface-plasmon resonance (SPR) and to DO11.10 cells expressing human and mouse CD137 ligand by flow cytometry. Cells were incubated with the CD137 antigens for 1 hour, and then a fluorescently-labelled anti mouse Fc fragment antibody was used to detect cell binding. The recombinant cyno antigen was confirmed to bind to DO11.10 cells (National Jewish Health) expressing cyno CD137 ligand by flow cytometry as described above. To ensure as high a purity as possible for the materials used in selection protocols, thorough protein characterisation of the antigens was performed to ensure the presence of protein aggregates did not exceed 2%.

1.2 Cell-expressed CD137 antigens

[0233] DO11.10 cells (National Jewish Health) expressing full-length mouse CD137 (SEQ ID NO: 187) or human CD137 (SEQ ID NO: 185), designated 'DO11.10.mCD137' and

'DO11.10.hCD137' respectively, were produced in order to present the antigen in a membrane-bound conformation, most similar to its natural form, for selections and further characterisation of selected Fcabs, as listed in **Table 2.**

[0234] Lentiviral transduction was used to generate these DO11.10 cells over-expressing human or mouse CD137 receptors using the Lenti-X HTX Packaging System (Clontech, catalogue no. 631249). Lenti-X expression vector (pLVX) (Clontech, catalogue no. 631253) containing cDNA encoding the human CD137 (SEQ ID NO: 185) or encoding the mouse CD137 (SEQ ID NO: 187) was co-transfected with a Lenti-X HTX Packaging Mix into the Lenti-X 293T Cell Line (Clontech, catalogue no. 632180) to generate virus. The DO11.10 cell line was then transduced with these lentiviral vectors.

[0235] Expression of human CD137 or mouse CD137 on these cells was confirmed by binding of 20H4.9 and Lob12.3 anti-CD137 positive control antibodies, respectively, to the cells by flow cytometry. Cells were incubated with the human or mouse positive control antibodies for 1 hour and then a fluorescently-labelled anti-human Fc detection antibody (Stratech Scientific Ltd, catalogue no. 109-546-098-JIR) was used to detect cell binding.

[0236] DO11.10 cells expressing cynomolgus CD137 (SEQ ID NO: 189), designated 'DO11.10.cCD137', were also generated using the same lentiviral transduction methodology and used to test cross-reactivity of anti-human CD137 Fcabs with cynomolgus CD137. Expression of cynomolgus CD137 was confirmed by binding of an anti-CD137 positive control antibody (MOR7480.1, US 2012/0237498 A1) to the cells by flow cytometry as described earlier.

Table 2: Cell-expressed CD137

Type	Designation	Species	Presentation
Cell	DO11.10.hCD137	Human	Cell-expressed
Cell	DO11.10.mCD137	Mouse	Cell-expressed
Cell	DO11.10.cCD137	Cyno	Cell-expressed

1.3 $CD4^+$ and Fc tagged mouse and human PD-L1

[0237] Human and mouse PD-L1 antigens with fusion proteins were generated for use in antibody selections and screening. Antigens were expressed with either a C-terminal His tag as well as either a monomeric rat $CD4^+$, domains 3 and 4 (rCD4) tag (Brown and Barclay, 1994), a dimeric human IgG1 Fc domain or, for human PD-L1 only, an Avi tag (resulting in hPD-L1-rCD4-His (SEQ ID NO: 195), hPD-L1-Fc-His (SEQ ID NO: 196), mPD-L1-rCD4-His (SEQ ID NO: 197), mPD-L1-Fc-His (SEQ ID NO: 198) and hPD-L1-His-Avi (SEQ ID NO: 199). The production of antigens in different formats enabled the elimination of tag binders during sequential rounds of antibody phage display panning. Expression plasmids encoding the

antigens were transfected into HEK293 cells as described by Chapple *et al.,* 2006. Supernatants were harvested 5 days after transfection and the secreted antigens were purified by Ni-NTA sepharose affinity chromatography (Schofield *et al.,* 2007). rCD4 and Fc-containing PD-L1 antigens were biotinylated using EZ-link Sulfo-NHS-Biotin reagent (Thermo Fisher Scientific, product code 21326) following the manufacturer's recommendations. The biotinylation reaction product was gel filtered and the monomeric fraction was collected. The monomeric fraction was used for all solution-phase phage-display selections. The average number of biotins per molecule was 1 to 3 biotins per PD-L1 monomer as determined using Fluorescence Biotin Quantitation kit (Thermo Fisher Scientific, product code 46610).

Example 2: Selection and characterisation of anti-human CD137 Fcabs

2.1 Naive selection of anti-human CD 137 Fcabs

[0238] In order to select Fcabs that bind to human CD137, yeast and phage display selection campaigns were employed, to maximise the diversity of Fcabs identified. Both cell surface displayed human CD137 and recombinant dimeric human CD137 and were used to provide a variety of antigen formats, in order to exert avidity-driven selection pressure against dimeric or multimeric CD137 proteins. Obtaining an Fcab which bound avidly to CD137 complexes rather than with high affinity to monomeric CD137 was deemed beneficial because such Fcab would preferentially target activated and primed T cells only, where upregulation of CD137 occurs after T cell stimulation. Without wishing to be bound by theory, it was hypothesised that T cells with very low or negligible levels of CD137 membrane expression would be more likely to have CD137 in monomeric state, unlike activated T cells with highly upregulated CD137 where most of the protein would be in dimeric, trimeric, or higher multimeric states. As a result of the avidity-driven selections, the Fcab would preferentially bind activated T cells and not bind well to naive T cells that display only monomeric CD137. By selecting an avid CD137 Fcab potential off-targeted T cell activation would be reduced, with associated reduced toxicity.

[0239] Six naive phage libraries displaying the CH3 domain of human IgG1 were used for selections by phage display. All six libraries comprised randomised AB loops (comprising residues at positions 14-18 according to IMGT numbering) and randomised EF loops (comprising residues at positions 92-101 according to IMGT numbering). One of the libraries comprised clones with an insertion of either two or four amino acids (encoded by two or four NNK codons) at position 101 in the EF loop (inserted residues are at positions 101.4 - 101.1 according to IMGT numbering).

[0240] 3230 phage clones were screened by phage ELISA for binding to dimeric recombinant hCD137 antigen and recombinant Fc was used as a negative control. 1140 phage clones were screened by phage FACS for specific binding to DO11.10.hCD137 cells. Individual hits were then sequenced and the resulting 76 unique sequences were assigned an Fcab clone identifier

and subcloned into a pTT5 expression vector (National Research Council of Canada) containing a HeID1.3 IgG1 heavy chain expression cassette for the purpose of expressing the Fcab clones in mAb^2 format (see **Example 3.2).**

[0241] Four naive yeast libraries displaying CH1 to CH3 domains of human IgG1 were used for selection by yeast display. All four libraries comprised randomised AB loops (comprising residues at positions 14 to 18 according to IMGT numbering) and randomised EF loops (comprising residues at positions 92 to 101 according to IMGT numbering) in the CH3 domain. Two of the libraries further comprised an insertion of five amino acid residues at position 16 in the AB loop of the CH3 domain (residues at positions 16.5 to 16.1 according to IMGT numbering).

[0242] 2784 yeast single clones identified from library selections were screened for antigen binding using a flow cytometry antigen binding assay that involved incubating the cells with biotinylated recombinant dimeric human antigen or mouse Fc fragment to discriminate against yeast clones binding to the Fc portion of the recombinant hCD137 antigen. Selections were repeated with varying antigen concentrations and conditions, such as increasing induction temperature, decreasing the selection stringency or reducing the number of rounds in order to increase the number of hits. Hit sequencing revealed considerably low output diversity, with only 9 Fcab clones having unique sequences identified: FS22-053, FS22-172, FS22-173, FS22-174, FS22-175, FS22-176, FS22-177, FS22-178 and FS22-179.

2.2 Preparation of anti-human CD137 Fcabs in "mock" mAb^2 format

[0243] "Mock" mAb^2 antibodies consisting of IgG1 molecules comprising the 76 anti-human CD137 Fcab clones isolated from phage and 9 clones isolated from yeast selections were produced to allow characterisation of the Fcabs in a mAb^2 format. The mock mAb^2 were prepared by substituting part of the CH3 domain Fcabs comprising the AB, CD and EF loops, for the corresponding region of the CH3 domain of the anti-hen egg lysozyme antibody HeID1.3. Generation of the HeID1.3 antibody is described in Tello *et al.* 1993. The heavy and light chain sequences of antibody HeID1.3 are shown in SEQ ID NO: **191** and **159,** respectively. The mock mAb^2 molecules were produced by transient expression in HEK293-6E cells. To assess the amount of protein produced, IgG protein content was quantified by BioLayer Interferometry using the Octet QKe platform with Protein A quantitation biosensors from PALL (18-5021). Proteins were purified by protein A affinity chromatography using mAb SelectSure columns. 53 phage-derived CD137 mAb^2 proteins presented measurements below the detection threshold and therefore determined to be unsuitable for further analysis. 32 mAb^2 were purified using mAb Select SuRe protein A columns (GE Healthcare, 11003494).

[0244] A selection of these mAb^2were then tested for binding to human recombinant antigen (biotinylated hCD137-mFc-Avi) using BioLayer Interferometry (BLI) using the Octet QKe

platform. 12 mAb^2 did not bind and 19 bound CD137-coated sensors (FS22-007, FS22-033, FS22-042, FS22-049, FS22-050, FS22-052, FS22-053, FS22-054, FS22-169, FS22-172, FS22-173, FS22-174, FS22-179, FS22-180, FS22-181, FS22-183, FS22-187, FS22-194, FS22-195).

***2.3 Activity of selected anti-CD 137 mock mAb^2 in a human NF-$_K$B reporter* assay**

[0245] Multimerisation and clustering is required for TNFR signalling (Bitra *et al.,* 2017). CD137 clusters and activates the NF-κB signalling pathway when it interacts with its cognate ligand, CD137L. Agonist molecules mimic the ligand in driving clustering and activation of CD137, thereby activating the NF-κB signalling pathway. It is known that some agonistic antibodies can inherently cause CD137 clustering upon binding for example, urelumab, whereas as others require additional crosslinking of the antibody itself to induce CD137 clustering, such as utomilumab (Fisher *et al,* 2012). Fc gamma receptors on effector cells are known to induce such crosslinking *in vivo,* though this is inefficient and may occur away from the site of therapeutic interest. Since dose limiting toxicities have been associated with urelumab but not utolimumab, it was decided to select for anti-CD137 binding Fcabs which did not have the ability to inherently agonise, but to select only those that required additional crosslinking in order to induce CD137 clustering. Therefore, an assay that can detect the activation of the NF-κB signalling pathway in a cell upon clustering of CD137 expressed on the cell surface by crosslinked antibodies, but that showed little activity when the antibodies were not crosslinked, was developed. This assay was then used to test the agonistic functional activity of 27 anti-CD137 Fcab clones in mock mAb^2 format, and 6 anti-CD137 Fcab clones in anti-CD20 mAb^2 format, irrespective of whether the Fcabs were found to bind recombinant antigen by BLI or not.

[0246] This can be measured by activation of the NF-κB signalling pathway in the assay. Protein L was used as a crosslinking agent to drive cross linking of the mock mAb^2 via the Fab portions in the assay and NF-κB activation was measured.

[0247] cDNA encoding human CD137 (SEQ ID NO: 185) was subcloned into pMSCV-neomycin vector (Takara Clontech, Cat. 634401) using EcoRI-HF and XhoI restriction enzymes. RetroPack PT67 cell line (Clontech, Cat. 631510) was used to produce retroviral particles following the manufacturer's protocol. This retro virus was subsequently used to transduce HEK.FRT.luc cells that were previously generated by transducing a Flp-In T-REx 293 HEK cell line (Life Technologies, R780-07) with Qiagen Cignal Lenti NFkB Reporter (luc) (Qiagen, cat no 336851) lentivirus containing a NF-κB-sensitive promoter controlling the expression of luciferase. These HEK.FRT.luc.hCD137 cells were used to screen the mock mAb^2 containing the CD137 binders identified in selections.

[0248] A 2 μM dilution of each mock mAb^2 was prepared in DPBS (Life Technologies,

14190169) and further diluted 1:3 in reporter cell medium (DMEM (Gibco, Cat. 61965-026); 10% FCS (Gibco, Cat. 10270-106); 1x PennStrep (Gibco, Cat. 15140-122); Blasticidin 15µg/ml (Melford Laboratories Ltd. Cat. B1105); Puromycin 5µg/ml (Life technologies, Cat. A11113803); Zeocin 100µg/ml (InvivoGen, Cat. 11006-33-0); Geneticin 500µg/ml (Life Technologies, Cat. 10131-027). Protein L (Life Technologies, 21189), was used as an artificial crosslinking agent and was mixed with the mAb^2 molecules in a 1:4 molar ratio. After a 24-hour incubation, cells were treated with 100µl Promega Bio-Gio™ luciferase assay reagent (Promega cat no G7941) according to manufacturer's instructions and luminescence was measured with an integration time of 0.5 seconds on a plate reader with the Gen5 Software, BioTek. Luminescence values are a measure of the luciferase produced in response to the activation of the NF-κB signalling pathway by the clustering of CD137 induced by crosslinked Fcabs. The luminescence values were plotted versus the log concentration of Fcab and the resulting curves were fitted using the log (agonist) vs response equation in GraphPad Prism.

[0249] Hits were identified by having at least a 10-fold increase in luciferase signal when crosslinked with protein L as compared to when not crosslinked. These clones were determined to be capable of inducing CD137 clustering and subsequent activation of downstream signalling pathways. Of all clones tested, two were able to induce this 10-fold increase in luciferase on crosslinking, FS22-053 and FS22-172, though an EC_{50} could not be determined for either. Both were selected for further characterisation in a DO11.10 T cell activation assay. Surprisingly, activity was not observed for the remaining clones in crosslinked conditions despite binding to CD137 target by BLI, perhaps indicating they were binding at an irrelevant epitope on CD137, or that the affinity of such clones was not sufficient to bind CD137 strongly enough to initiate the NF-κB signalling cascade. Overall, while more than 30 Fcabs were tested, only two Fcabs (FS22-053 and FS22-172) were identified from the naive selections which exhibited the desired function in the NF-κB reporter assay when crosslinked and had little activity when not crosslinked.

***2.4 Activity of the selected anti-CD 137 mock mAb^2 in a DO11.10 T cell activation* assay**

[0250] CD137 clustering via agonist molecules on activated T cells elicits T cell activation and downstream signalling resulting in, but not limited to, IL-2 production. Since FS22-053 and FS22-172 were identified as having activity in the NF-κB reporter assay, their ability to activate CD137 was tested in a T cell activation assay. A DO11.10 T cell activation assay using DO11.10 T cells engineered to overexpress human CD137 was developed and T cell activation was assessed by measuring IL-2 release.

[0251] DO11.10 T cells (National Jewish Health) were transduced with a lentiviral vector designed to overexpress mouse or human CD137 as described earlier. As well as FS22-053 and FS22-172, the following clones were tested in this DO11.10 T cell activation assay: FS22-007, FS22-033, FS22-042, FS22-049, FS22-050, FS22-052, FS22-054, (all in "mock" HeID1.3 mAb^2 format). Dilutions of mAb^2 or 20H4.9 positive control mAb either with or without

recombinant Protein L (Life Technologies, 21189) crosslinker were prepared and added to DO11.10.hCD137 cells in a 96 well round bottom plate that had been coated overnight with 0.1 µg/ml anti-CD3 antibody (clone 17A2, BioLegend, 100208). After an 18-hour incubation, supernatants were collected and assayed with mouse IL-2 ELISA kit (eBioscience, 88-7024-86) following the manufacturer's instructions. Plates were read at 450 nm using the plate reader with the Gens Software, BioTek. Absorbance values of 570 nm were subtracted from those of 450 nm (Correction). The standard curve for calculation of cytokine concentration was based on four parameter logistic curve fit (Gens Software, BioTek). The concentration of mIL-2 was plotted vs the log concentration of mAb^2 or benchmark mAb and the resulting curves were fitted using the log (agonist) vs response equation in GraphPad Prism.

[0252] Clones FS22-053 and FS22-172 showed significantly enhanced activity when crosslinked with Protein L in this assay. FS22-053 had an activity of 126 nM when not crosslinked and an activity of 21 nM when crosslinked (an improvement of 6-fold), while FS22-172 had an activity of 950 nM when not crosslinked and an activity of 44nM when crosslinked (an improvement of 22-fold). As a result, both clones were selected for affinity maturation.

[0253] Example 2.4 shows that FS22-053 and FS22-172 could drive clustering and activation of CD137 on the surface of DO11.10 T cells when crosslinked by Protein L in the mAb^2 formats tested.

Example 3: Affinity maturation of anti-human CD137 Fcabs and subsequent characterisation

[0254] As previously discussed, two clones were selected for affinity maturation based on their functional characteristics in the NF-κB reporter assay, DO11.10 T cell activation assays FS22-053 and FS22-172).

3.1 Affinity maturation of FS22-053 and FS22-172

[0255] Four yeast displayed libraries were constructed from the FS22-053 and FS22-172 Fcab clones. Seven residues (at positions 15-16.1 according to IMGT) were randomised using ELLA primers in the AB loop of the CH3 domain of each clone to make libraries FS22-053 AB and FS22-172 AB. Five residues (at positions 92-94 and 97-98 according to IMGT) were randomised using ELLA primers in the EF loop of the CH3 domain resulting in libraries FS22-053 EF and FS22-172 EF.

[0256] For libraries FS22-053 AB and FS22-053 EF, and FS22-172 AB and FS22-172 EF, three or four selection rounds were performed on the yeast libraries to select for affinity matured clones using either dimeric hCD137-mFc-Avi antigen or monomeric hCD137-Avi-His antigen. Monomeric antigen was used in alternation with dimeric antigens to ensure clones

retained affinity to the antigen and did not bind exclusively through avidity. The use of monomeric or dimeric antigen, as well as the concentration used was determined empirically during each round by flow cytometry, determined by whether enrichment against the monomeric or dimeric antigen was observed in the previous round. Whenever possible, a sorting gate above the parental was used to isolate affinity matured clones compared to the parental molecule. Selection pressure was increased up to 1nM of dimeric antigen. During each selection round, individual clones were spotted on agar plates to assess the progress of the selection. Each clone was grown and induced individually and next its binding and structural parameters were determined by flow cytometry using biotinylated dimeric antigen as well as anti-CH2 structural markers as described earlier. This screening cascade was followed to allow the determination of selection success based on a sample of clones from the selection output and to allow for early screening of individual clones that could be subsequently produced as soluble proteins.

[0257] 1152 yeast single clones in total were screened for binding to biotinylated recombinant antigen in an antigen binding flow cytometry as described earlier. Selections on the FS22-053 EF library resulted in enrichment of 138 unique loop sequences. Likewise, 30 unique loop sequences were isolated from the FS22-172 AB library. Libraries FS22-053 AB and FS22-172 EF did not contain any clones which showed any binding improvement over the parental clones. Sequence analysis across the best-binding clones from the FS22-053 EF and FS22-172 AB libraries revealed a conserved PPY sequence pattern in the AB loops.

[0258] The presence of a conserved PPY motif may promote the formation of an extended binding region by introduction of a more rigid or exposed loop based upon the limited flexibility of proline residues. Alternatively, the PPY sequence may represent a specific conserved motif involved in binding for these clones as Proline rich sequences have been demonstrated to bind to aromatic sequences in SH3 domain proteins. Further, since the PPY conserved sequence has been selected for independently in two separate lineages of Fcabs, it may be important for epitope binding on CD137. Additionally, a conserved LE or LD sequence pattern in the EF loops of the CH3 domain of the clones of both the FS22-053 and FS22-172 lineages, which suggests this amino acid motif in the EF loop is required for improved binding.

[0259] In order to assess the progress of the selections and whether it would be necessary to recombine mutated AB and EF loops between affinity matured clones, the top five unique clones from the FS22-053 EF library (FS22-053-008, FS22-053-009, FS22-053-010, FS22-053-011, FS22-053-012) ranked by presenting specific binding to 10 nM dimeric human antigen (higher than 30% APC positive cells in a flow cytometry binding assay), and the top six unique clones from the FS22-172 AB library (FS22-172-001, FS22-172-002, FS22-172-003, FS22-172-004, FS22-172- 005, FS22-172-006, all showing above 10% APC positive cells when screened with 10 nM dimeric human antigen in the same assay) were produced as mock mAb^2 (HelD1.3) and model mAb^2 (PD-L1) to assess functional and kinetic improvement of the randomised loops.

3.2 Construction of anti-human CD 137 Fcabs in "mock" and "model" mAb^2 format

[0260] 16 affinity matured clones derived from the parental FS22-053 clone (FS22-053-001 to FS22-053-016), and 6 affinity matured clones derived from the parental FS22-172 clones (FS22-172-001 to FS22-172-006) were prepared in "mock" and "model" mAb^2 format. Clones FS22-053-001 to FS22-053-007 were not further pursued as they did not express in mAb^2 format at a level that allowed downstream purification for further testing and characterisation.

[0261] "Mock" mAb^2 antibodies comprising the anti-human CD137 Fcabs in HeID1.3 were prepared for further characterisation of the affinity matured Fcabs in mAb^2 format. These mAb^2 were prepared as described in **Example 2.2.**

[0262] "Model" mAb^2 were also produced comprising the anti-human CD137 Fcabs and also a PD-L1 binding Fab region (clone YW243.55.S70 from US 8,217,149 B2). These were prepared in a similar manner to the method described in **Example 2.2** by substitution of part of the CH3 of the anti-PD-L1 binding antibody containing the AB, CD and EF loops with the corresponding region of the Fcab. These PD-L1 model mAb^2 comprised a LALA mutation in the CH2 domain (AA). The introduction of the LALA mutation in the CH2 domain of human IgG1 is known to reduce Fc y receptor binding (Bruhns, P., *et al.* (2009) and Hezareh M., *et al.* (2001)).

[0263] The CD137/HeID1.3 "mock" and CD137-AA/PD-L1 "model" mAb^2 were produced by transient expression in HEK293-6E cells and purified using mAb Select SuRe protein A columns.

***3.3 Activity of human Fcabs in mock mAb^2 format in human NF-$_K$B Reporter Cell* assay**

[0264] The functional activity of the affinity-matured anti-human CD137 Fcabs in mock mAb^2 (HeID1.3) format listed was tested in the same NF-κB luciferase assay described in **Example 2.3.** Luminescence was measured with an integration time of 0.5 seconds in a plate reader with the Gen5 Software, BioTek. As expected, none of the Fcabs showed activity without Protein L crosslinking (-XL). All affinity matured CD137 Fcabs showed a vast improvement over parental CD137 Fcabs for which, while positive in this assay, calculation of an EC_{50} value was not possible (see **Example 2.3**). FS22-053-008 and FS22-172-003 showed the best activity from each family with the lowest EC_{50} (26.34 nM and 32.64 nM, respectively) when crosslinked with Protein L (+XL).

3.4 Activity of affinity matured human Fcabs in model mAb^2 format in human DO11.10 T cell activation assay

[0265] The functional activity of the affinity matured human Fcabs in model mAb^2 (PD-L1 LALA) format was tested in a DO11.10 T cell activation assay, similar to the assay as described in **Example 2.4.**

[0266] HEK.mPD-L1 cells were produced by subcloning cDNA encoding mouse PD-L1 (SEQ ID NO: 187) into pcDNA5FRT vector (Life Technologies) using KpnI and NotI restriction sites and transforming the vectors into the Flp-In T-REx 293 cell line (Life Technologies, R780-07) using Lipofectamine 2000 (Life Technologies, 11668-019). Cells were grown in DMEM containing 10% FBS, 100 µg/ml Hygromycin B (Melford Laboratories Ltd, Z2475) and 15 µg/ml Blasticidin (Melford Laboratories Ltd, B1105) for 3-4 weeks until colonies of stably transformed cells had formed. These colonies were amplified in the presence of 1 µg/ml Doxycyclin (Sigma Aldrich, D9891) and tested for expression of PD-L1 using PE conjugated anti-mouse PD-L1 (MIH5) antibody (BD Biosciences, 558091).

[0267] Cells were detached using cell dissociation buffer, washed once with PBS and 2×10^5 cells were plated in wells of a 96-well plate and then incubated with antibody diluted 1:20 in PBS for 1 hour at 4 °C. Cells were washed once in PBS and then measured on an Accuri C6 cytometer (BD Biosciences) and the data was analysed using FlowJoX. Expression of mouse PD-L1 was again confirmed.

[0268] The 15 clones produced in **Example 3.2** in CD137/PD-L1 mAb^2 were tested in this DO11.10 T cell activation assay. Dilutions of mAb^2 or positive control mAb were prepared and added to either DO11.10.hCD137 (7.5×10^3 cells per well) and HEK.mPD-L1 cells (2×10^4 cells per well) or to DO11.10.hCD137 (7.5×10^3 cells per well) and HEK cells that were not transduced to express mPD-L1 (2×10^4 cells per well) in a 96 well flat bottom plate that had been coated overnight with 0.1 µg/ml anti-CD3 antibody (clone 17A2, BioLegend, 100208). After an 18-hour incubation, supernatants were collected and assayed with mouse IL-2 ELISA kit (eBioscience, 88-7024-86) following the manufacturer's instructions. Plates were read at 450 nm using the plate reader with the Gens Software, BioTek. Absorbance values of 570 nm were subtracted from those of 450 nm (Correction). The standard curve for calculation of cytokine concentration was based on four parameter logistic curve fit (Gens Software, BioTek). The concentration of mIL-2 was plotted vs the log concentration of mAb^2 or benchmark mAb and the resulting curves were fitted using the log (agonist) vs response equation in GraphPad Prism. T cell activation was detected by measuring the release of mIL-2.

[0269] No T cell activity was observed without crosslinking by binding to PD-L1 expressing cells. Upon crosslinking, all mAb^2 had potent T cell activity as seen by the release of high levels of mIL-2 and sub-nanmolar EC_{50} values. All clones other than FS22-053-009 and FS22-172-005, had an EC_{50} of less than 0.3 nM so were as good as, if not better than the positive control (anti-human CD137 mAb, G1-AA/20H4.9). The lowest E_{max}, which is a measure of maximum T cell activation, and might be relevant to greater T cell anti-tumour activity *in vivo,* observed was

7758 pg/ml which was higher than the positive control (anti-human CD137 mAb, G1-AA/20H4.9).

3.5 Primary human CD8$^+$ T cell activation assay

[0270] The ability of the Fcabs to activate CD137 on T cells overexpressing CD137 was shown in **Example 3.3.** To test the activity of the Fcabs on cells which have not been engineered to overexpress CD137, a primary human T cell assay was needed. Activated cytotoxic CD8$^+$ T cells are responsible for directly killing cancer cells and express CD137 on their cell surface (Ye *et al,* 2014). Clustering of CD137 is known to be essential to induce downstream signalling and further CD8$^+$ T cell activation. A CD8$^+$ T cell activation assay was therefore used to assess the ability of Fcabs (in mAb^2 format as detailed below) to drive clustering and subsequent downstream signalling of CD137. CD8$^+$ T cell activation was determined by the release of hIL-2.

[0271] To isolate T cells, peripheral blood mononuclear cells (PBMCs) were collected from leucocyte depletion cones, a by-product of platelet donations. Briefly, leucocyte cone contents were flushed with PBS and overlaid on a Ficoll (Sigma-Aldrich, 1440-02) gradient. PBMCs were collected by centrifugation and the cells that did not cross the Ficoll gradient were recovered. PBMCs were further washed with PBS and remaining red blood cells were lysed through the addition of 10 ml 1X red blood cell lysis buffer (eBioscience, 00-4300-54) according to the manufacturer's instructions. CD8$^+$ T cells were isolated from the PBMCs present in the eluant using the CD8$^+$ T cell isolation kit II (Miltenyi Biotec Ltd, 130-096-495) according to the manufacturer's instructions.

[0272] Incubation with an anti-CD3 antibody was used as a first signal to drive initial activation of the T cells. 96-well flat bottom tissue culture plates were coated with 8 µg/ml anti-CD3 antibody (Clone UCHT1, R&D Systems, MAB100-SP) in PBS overnight at 4°C. The plates were then washed 3 times with 200 µl PBS.

[0273] For cell-based crosslinking of affinity matured human CD137 Fcabs in PD-L1 model mAb^2 format, HEK293 cells overexpressing human PD-L1 (HEK.hPD-L1) were produced essentially as described in **Example 5.3** but by subcloning cDNA encoding the human PD-L1 sequence (SEQ ID NO: 185) instead of mouse PD-L1. HEK.hPD-L1 cells were plated at 2 × 10^5 cells per well on to anti-CD3 antibody-coated (8µg/ml) 96 well flat bottom plates in 100µl T cell culture medium (RPMI medium (Life Technologies, 61870-044) with 10% FBS (Life Technologies), 1X Penicillin Streptomycin (Life Technologies, 15140122), 1mM Sodium Pyruvate (Gibco, 11360-070), 10mM Hepes (Sigma-Aldrich, H0887), 2mM L-Glutamine (Sigma-Aldrich, G7513) and 50µM 2-mercaptoethanol (Gibco, M6250)). Once HEK.hPD-L1 cells or HEK cells that were not transduced to express hPD-L1 had adhered after 4 hours incubation, all T cell culture medium was removed and replaced with 100µl T cell culture

medium containing T cells at a concentration of 5.0×10^5 cells/ml resulting in 5.0×10^4 cells/well.

[0274] mAb^2 were diluted in T cell medium at a 2X final concentration starting at 500nM and a 1:3 titration was carried out. 100µl of mAb^2 titration was added to the cells for a total assay volume of 200µl and 1X concentration of antibody.

[0275] Positive control anti-CD137 antibody (G1-AA/20H4.9) and negative control isotype IgG antibody (G1-AA/HeID1.3) were each diluted in T cell medium at a 2X final concentration starting at 500nM containing 500nM crosslinking agent (anti-human CH2, produced in house (Jefferis *et al.,* 1985 and Jefferis *et al.,* 1992) (mG1/MK1A6)) and a 1:3 titration was carried out. 100µl of diluted positive control antibody/crosslinker mix or negative control IgG antibody/crosslinker mix was added to the cells for a total of 200µl assay volume and 1X concentration of antibody.

[0276] The assay was incubated at 37°C, 5% CO_2 for 72 hours. Supernatants were collected and assayed with human IL-2 ELISA Ready-SET-Go! kit (eBioscience, Cat. 88-7025-88) following the manufacturer's instructions. Plates were read at 450 nm using the plate reader with the Gen5 Software, BioTek. Absorbance values of 630 nm were subtracted from those of 450 nm (Correction). The standard curve for calculation of cytokine concentration was based on a four-parameter logistic curve fit (Gen5 Software, BioTek). The concentration of human IL-2 (hIL-2) was plotted vs the log concentration of antibody and the resulting curves were fitted using the log (agonist) vs response equation in GraphPad Prism.

[0277] The positive control anti-human CD137 mAb, 20H4.9, shows an increase in hIL-2 release with an EC_{50} of 0.5nM when crosslinked with the anti-hCH2 antibody (mG1/MK1A6). All clones had activity in the assay, the majority displaying good potency with sub-nanomolar EC_{50}s. mAb^2 containing Fcabs FS22-053-007, FS22-053-008, FS22-053-010, FS22-053-011, FS22-053-012, FS22-172-003, FS22-172-004, FS22-172-005 elicited the greatest T cell response with the lowest EC_{50}s in the range of 0.19 - to 0.49 nM. A subset of the mAb^2 (containing Fcabs FS22-053-008, FS22-053-011, FS22-053-014, FS22-173-003 and FS22-172-004) were also tested without crosslinking by PD-L1 expressed on HEK cells and showed no activity in this assay, as expected. This confirms activity seen in the NF-kB assay and DO11.10 T cell activation assay.

3.6 Specificity determination of anti-human CD 137 Fcabs by Surface Plasmon Resonance (SPR)

[0278] The specificity of the anti-human CD137 Fcabs for human CD137 compared to other related TNFSFR family members was tested. 8 of the Fcabs were tested in mock mAb^2 (HeID1.3) format and measured by SPR in a Biacore T200 (GE Healthcare) by testing for

binding to other human TNFRSF receptors: CD40, OX40 and GITR. Amine coupling (amine coupling kit, GE Healthcare, BR-1000-50) was used to coat human CD40, GITR and OX40 to approximately 1000 RU in Biacore CM5 chips (GE Healthcare, cat no 29149603). Dilutions of anti-human CD137 Fcabs in mock mAb^2 format (FS22-053-008/HelD1.3, FS22-053-009/HelD1.3, FS22-053-010/HelD1.3, FS22-053-011/HelD1.3, FS22-053-012/HelD1.3, FS22-053-014/HelD1.3, FS22-172-003/HelD1.3, FS22-172-004/HelD1.3) starting at 1 µM were prepared in HBS-EP+ buffer (BR100669) and injected for 3 min at 30 µl/min and then allowed to dissociate in buffer for 4 min. The chip was regenerated by injection of 10 mM glycine pH 2.5 for 12 s at 30 µl/min. Antibodies specific to the different TNFRSF members were used as positive controls to verify Biacore chip coating. Data was double reference subtracted and analysed using BIAevaluation 3.2 software. The Fcabs did not bind to any of the TNFRSF receptors tested, demonstrating their specificity for CD137. As a result, it is not expected that the Fcabs, or mAb^2 comprising the antigen-binding sites from these Fcabs, will elicit off-target binding to anything other than CD137.

3.7 Binding affinity of anti-human CD137 Fcabs in mock mAb^2 format for human, cynomolgus and mouse CD 137 by SPR and generation of FS22-053-017

[0279] The affinity of the anti-human CD137 Fcabs (FS22-053-008, FS22-053-011, FS22-053-014, FS22-172-004, FS22-172-004) in a mock mAb^2 format (see **Example 3.2**) for human, cynomolgus (cyno) and mouse CD137 was measured by SPR, to determine whether the Fcabs may be useful for testing in animal studies. An anti-human Fab capture antibody was immobilised on all four flow cells of a CM5 series S chip (GE Healthcare #BR-1005-30) to an average surface density of 6000 RU following the manufacturer's recommendations (GE Healthcare, human Fab capture Kit, #28958325). Immobilization at 25°C and 10 µl/min flow rate achieved an average final response of 6000 RUs. Each mAb^2 was captured to approximately 150 RU by injecting a 3 µg/ml solution of mAb^2 diluted in HBS-EP+ buffer (GE Healthcare #BR1006-69) for 60 seconds at 30 µl/min. Then different concentrations of human, cyno or mouse CD137 antigen (unbiotinylated human, cyno or mouse CD137-mFc-Avi or human CD137-Avi-His) in HBS-EP+ buffer were flowed over the chip for 3 min at 60 µl/min and then allowed to dissociate for 10 minutes. After each antigen concentration the chip was regenerated by infecting 10mM glycine pH 2.1 at a flow rate of 30 µl/min for 30 seconds. Buffer HBS-EP+ was injected before the highest concentration of antigen and after the lowest concentration of antigen for reference subtraction, and one of the concentrations at random was repeated twice. The binding kinetics were fit with a 1:1 Langmuir model to generate equilibrium binding constants (K_D) for each sample. Data analysis was performed with BiaEvaluation software version 3.2. The results are shown in **Table 3.**

[0280] Analysis of the results revealed an improved binding for both human and cynomolgus CD137 by all affinity matured clones, compared to the respective parent molecules. The binding affinity for the monomeric human CD137 antigens was weaker (by at least 100-fold)

than for the dimeric human and cyno Fc-fusion antigens. As discussed in **Example 2.1,** the Fcabs were selected to preferentially bind to dimeric over monomeric forms of CD137 and this data confirms that the selection strategy was successful. This kinetic behaviour makes them less likely to bind to monomeric CD137 expressed at minimal levels on unstimulated T cells to result in reduced risk of liver or systemic toxicities associated with some anti-CD137 monoclonal antibody therapies.

[0281] The data also shows that the anti-human CD137 Fcabs bound to cynomolgus dimeric CD137 with comparable affinity to human dimeric CD137.

Table 3

Fcab	**Human dimeric CD137 K_D (nM)**	**Cynomolgus dimeric CD137 K_D (nM)**	**Human monomeric CD137 K_D fold difference relative to human dimeric K_D**	**Mouse dimeric CD137 K_D (nM)**
FS22-053	38	34	N/A	N/A
FS22-053-008	4.2	0.9	170-fold	N/A
FS22-053-011	5.5	1.3	>200-fold	N/A
FS22-053-014	3.2	0.9	100-fold	24
FS22-172	52	203	N/A	N/A
FS22-172-003	1.5	1.3	>200-fold	N/A
FS22-172-004	4.3	3.5	>200-fold	N/A
N/A - not applicable as low signal did not allow K_D determination				

[0282] The ability of the Fcabs in a mock mAb^2 format to bind to mouse dimeric CD137 was also tested. None of the clones showed strong binding to the mouse antigen (as shown in the table where N/A indicates that no K_D could be calculated) except for clone FS22-053-014 which was surprisingly found to have a K_D of 24 nM for the mouse antigen. This was unexpected since mouse CD137 and human CD137 share less than 57% sequence homology.

[0283] Sequence analysis of FS22-053-014 revealed a potential sequence liability that could result in a post-translational aspartate isomerisation at position 98 in the EF loop of its CH3 domain. The aspartate (D) at position 98 was mutated to glutamate (E) by site-directed mutagenesis using the QuickChange II mutagenesis kit (Agilent, catalogue no. 200523) according to the manufacturer's recommendations, which yielded clone FS22-053-017.

[0284] Experiments were then carried out to confirm that this mutation did not negatively affect

the binding affinity or functional activity of the FS22-053-017 clone as compared to the FS22-053-014 clone.

[0285] The equilibrium dissociation constant (K_D) of Fcab clone FS22-053-017 was compared to that of clone FS22-053-014 by SPR on a Biacore T200 system using the human CD137-mFc-Avi antigen and mouse PD-L1-mFc-Avi, respectively. The results showed very similar kinetic profiles to human antigen for both Fcab clones, thereby evidencing that mutating the aspartate at position 98 to a glutamate did not have a negative effect on binding to the human antigen. The results also showed that FS22-053-017 showed a 2-fold decrease in binding strength to the mouse CD137 antigen.

[0286] Fcab clone FS22-053-017 was sub-cloned and expressed as a HeID1.3 "mock" mAb^2 (see **Example 2.2)** and then compared to the FS22-053-014 clone, also in HeID1.3 mAb^2 format, in a human CD137 DO11.10 T cell activation assay as described in **Example 2.4.** G1-AA/20H4.9 was used as an anti-CD137 positive control and G1-AA/HeID1.3 as an IgG control. The mAb^2 were tested either without Protein L crosslinking or were crosslinked in a 1:4 ratio with Protein L.

[0287] The results showed that both FS22-053-17 Fcab in mock mAb^2 format and FS22-053-014 Fcab in mock mAb^2 format had comparable activity when crosslinked by Protein L in the same DO11.10 T cell activation assay. Therefore, the mutagenesis carried out did not negatively impact functional activity. Both clones in mock mAb^2 format had no activity without crosslinking.

3.8 Summary of affinity maturation and characterisation of anti-human CD137 Fcabs

[0288] In summary, affinity matured anti-CD137 Fcabs were generated and prepared in a mAb^2 format, which were then characterised. mAb^2 containing these CD137 antigen-binding domains in the CH3 domain showed high levels of activity in a human NF-κB Reporter Cell assay and this activity was shown to be crosslink dependent. mAb^2 containing the antigen-binding domain from the FS22-053-008 and FS22-172-003 Fcabs showed the best activity in this assay.

[0289] Additionally, it was shown that when the mAb^2 were prepared from these Fcabs, such that they contained the CD137 antigen-binding domain and a PD-L1 binding Fab region as well as the LALA mutation in their CH2 domain to reduce or abrogate binding to Fcy receptors, then the mAb^2 had potent T cell activity in a human DO11.10 T cell activation assay and this activity was shown to be dependent on crosslinking by binding to PD-L1 expressing cells. The mAb^2 were also shown to have crosslink-dependent activity in a primary human $CD8^+$ T cell

activation assay, providing further evidence that the mAb^2 containing these affinity matured CD137 antigen-binding domains are able to effectively induce agonism of CD137 and that this agonistic activity is conditional on crosslinking.

[0290] The mAb^2 containing the anti-human CD137 antigen-binding domain were also shown to be specific for CD137 and did not bind to other TNFRSF members. The mAb^2 were shown to preferentially bind human dimeric CD137 antigen over monomeric human CD137 antigen. Finally, these mAb^2 were shown to bind dimeric cynomolgus CD137 with comparable affinity to dimeric human CD137.

[0291] One Fcab clone, FS22-053-014, was surprisingly found to also be able to bind mouse CD137. Sequence analysis of the FS22-053-014 revealed a potential sequence liability, which was corrected by side directed mutagenesis to produce the FS22-053-017 clone. Characterisation of the FS22-053-017 revealed that it retained similar binding properties and showed similar functional activity in a human CD137 DO11.10 T cell activation assay as FS22-053-014.

[0292] Having demonstrated that mAb^2 containing the anti-human CD137 antigen-binding domain require crosslinking in order to cluster and activate CD137, the next aim was to prepare a mAb^2 that binds human PD-L1 in addition to CD137. It was hypothesised that binding of the mAb^2 to human PD-L1 via the Fab arms would cause crosslinking of the antibody molecules, which in turn would lead to clustering and activation of CD137 and that this activation would be dependent on the presence of human PD-L1 expression.

[0293] In order to prepare mAb^2 that bind human PD-L1 in addition to CD137, it was first necessary to generate mAbs that were able to bind PD-L1. The generation of these mAbs is described below.

Example 4: Isolation of naive anti-PD-L1 mAb 280 02 G02

4.1 Selections

[0294] The "IONTAS 1" human antibody phage display library (IONTAS Ltd.) was employed to select for anti-PD-L1 clones. The antibody genes used to construct the IONTAS 1 library were derived from human lymphocytes (42 buffy coat donations) and one tonsil tissue sample. Both the buffy coats and tonsil tissue were obtained under Local Research Ethical Committee approval.

[0295] Three rounds of solid phase selections were performed with the IONTAS 1 antibody phage display library using antigen that was directly coated onto polystyrene Nunc tubes as

described by Schofield *et al,* 2007. The first, second and third selection rounds employed human PD-L1-Fc-His, mouse PD-L1-rCD4-His and human PD-L1-Fc-His, respectively (see **Example 1.3** for antigen details).

[0296] The selected variable heavy (VH) anti-PD-L1 antibody population was shuffled with a naïve variable light (VL) antibody population as described by Dyson *et al.,* 2011, and this shuffled, rescued, antibody-phage-display population was employed in solution phase selections. Briefly, panning was performed with human PD-L1-rCD4-His (10 nM), human PD-L1-rCD4-His (200 pM) and mouse PD-L1-rCD4-His (10 nM) at rounds 1, 2 and 3, respectively, and this resulted in an output anti-PD-L1 scFv population termed "Selection 280". This scFv population contained human and mouse anti-PD-L1 binding scFvs, as determined by a phage polyclonal ELISA performed as described by Dyson *et al.,* 2011, and displayed minimal cross-reactivity with human PD-1 or with rCD4 or Fc tags.

4.2 Screening: ELISA, recombinant blocking assay, *cell-based blocking* assay

4.2.1 Monoclonal scFv ELISA

[0297] The Selection 280 scFv population from **Example 4.1** was screened by ELISA to identify the clones which bound best to human PD-L1. The scFv population was subcloned into the soluble scFv vector pSANG10 and *E.coli* cultures containing soluble scFvs were prepared as described (Martin *et al.,* 2006; Studier, 2005). Soluble scFv were then used in a monoclonal ELISA with immobilised human PD-L1-rCD4-His as described by Schofield *et al.,* 2007. Nunc Maxisorp plates (Thermo Fisher Scientific, 437111) were coated with human PD-L1-rCD4-His (5 µg/ml, PBS) overnight, blocked with 2% MPBS for 1 hour and the *E. coli* culture supernatant (1:2 dilution with 2x 2% MPBS) was added and scFv were allowed to bind for 1 hour at room temperature. Bound scFv were detected with anti-FLAG M2 antibody (Sigma, F1804) labelled with europium. A total of 470 clones were screened and this resulted in the identification of 346 anti-PD-L1 clones with a binding signal for PD-L1 at least 10-fold above background compared with "empty" blocked wells containing no antigens. The 192 best anti-human PD-L1 clones assessed by primary ELISA signal were selected for further analysis.

4.2.2 Screening scFv in ELISA-based PD-L1/PD-1 blocking assay

[0298] To identify clones that blocked the interaction between PD-L1 and PD-1, an ELISA was performed to screen for blocking scFvs. Briefly, nunc maxisorp plates (437111, Thermo Fisher Scientific) were coated with anti-rCD4 (domains 3 and 4) antibody (MCA1022, OX-68, Bio-Rad) overnight, blocked with 3% MPBS and incubated with human PD-1-rCD4-His (5 µg/ml in 3% MPBS) for 1 hour at room temperature. Human PD-L1-Fc-His (50 µl, 0.2 nM), was pre-mixed with *E. coli* culture supernatant containing scFv. The Nunc 96-well plates were washed 3 times

with PBS, 0.1% Tween™-20 (PBS-T) and 3 times with PBS, then the human PD-L1-Fc-His / scFv mix was added and incubated for 1 hour at room temperature. The plates were washed and bound human PD-L1-Fc-His was detected using goat-anti-Fc-biotin (Jackson ImmunoResearch, 109-065-098, Laboratories, 0.1 µg/ml, 3% MPBS) and Streptavidin-Europium (Perkin Elmer, 1244-360) followed by DELFIA enhancement solution (Perkin Elmer, 4001-0010). Of 192 clones screened, 183 displayed at least 90% blocking activity compared with the medium control. The 183 anti-PD-L1 scFv clones identified were screened further for mouse PD-L1 cross-reactivity in a primary ELISA, as described in **Example 4.2.1** above, but using immobilised mouse PD-L1-rCD4-His instead of human PD-L1. This identified 50 mouse cross-reactive anti-PD-L1 clones, which were candidates for conversion to IgG1 format.

4.2.3 Conversion of blocking anti-PD-L1 scFv clones to IgG1 format

[0299] The anti-PD-L1 scFv clones which blocked the interaction between PD-L1 and PD-1 were converted to IgG1 format by sub-cloning the VL and VH genes into the IgG1 expression plasmid pINT3-IgG1 and expressed in HEK293 at 4 ml scale as described by Chapple *et al.,* 2006. The antibodies were batch affinity purified with Protein A sepharose beads (PC-A100) and Proteus "1-step batch" midi-spin columns (Generon, GEN-1SB08) according to the manufacturer's instructions. Dialysis of the purified antibodies was performed with GeBAflex maxi tubes, with an 8 kDa cut-off (Generon, D045). If necessary, the antibodies were concentrated to 2 µM by ultrafiltration.

***4.2.4 Screening for PD-L1-PD-1 blocking activity in Jurkat-NFA T reporter co-culture* assay**

[0300] The functional activity of the purified anti-PD-L1 mAbs was then assessed in a co-culture reporter assay screen. This screen was performed using the GloResponse NFAT-luc2/PD-1 stable Jurkat cell line (Promega, CS187102) and Thaw-and-Use PD-L1 cells (Promega, CS178103) in accordance with the manufacturer's instructions. The PD-L1 cells were plated in HAM'S-F12 medium containing 10% FBS. The next day media was removed and in parallel PD-1 Jurkat reporter cells (Promega, CS187102) were resuspended in assay medium (90% RPMI1640, 1% FBS). To the plate containing adhered PD-L1 cells was added 40 µl of assay media containing different antibodies at a 2x concentration (200 nM) followed by 40 µl of the PD-1 cell mix. The plate was incubated for 6 hours at 37oC, 5% CO2. BioGlo reagent (Promega, G7940, 80 µl) was added to each well and the luciferase output was read using a BMG pherastar plate reader. This identified antibody G1/280_02_G02 as capable of blocking the interaction of PD-L1 with PD-1 in a co-culture assay, as determined by increased luciferase activity compared to controls with no antibody. This activity was confirmed in a dose-response co-culture assay (doubling concentration range: 200 to 1.56 nM) resulting in a calculated half maximal effective concentration (EC50) of 4.2 nM.

4.3 Sequence optimisation

[0301] Preliminary analysis of the sequence of the G1/280_02_G02 antibody resulted in the identification of a potential deamidation site in the VH-CDR2, specifically an NG motif at Kabat positions 54 to 55. As deamidation at this site could potentially affect binding, variant clones were produced in which the NG motif was changed to either NA, NS, SG or GG. These modifications did not result in any significant reduction in affinity for recombinant PD-L1 or potency in PD-L1 blocking activity, and the variant clone containing the NS modification, designated G1/280_02_G02_NS, was chosen for use in a light-chain shuffle.

4.4 Summary naïve selections

[0302] Phage selections strategies identified more than 50 anti-human PD-L1 binding clones with potent *in vitro* PD-1/PD-L1 blocking activity as well as mouse PD-L1 cross-reactivity. In particular, G1/280_02_G02 showed potent activation in a cell-based PD-L1 reporter assay and was therefore selected for further optimisation.

Example 5: Generating and characterising kappa light chain-containing anti-PD-L1 clones

[0303] The G1/280_02_G02_NS antibody possesses a lambda light chain. As most monoclonal antibodies used in a clinical context have kappa light chains (Jain *et al.,* 2017), it was sought, by the use of a chain-shuffling campaign, to generate clones comprising the heavy chain of the G1/280_02_G02_NS antibody but paired with kappa light chains, which retained affinity for human PD-L1 and mouse cross-reactivity. The IONTAS™ kappa-light-chain library in the phage display plasmid pIONTAS-1 (kappa-library) was used to prepare a light-chain-shuffled library of scFv clones comprising the heavy chain of the G1/280_02_G02_NS antibody coupled with light chain variants.

5.1 Phage selections and screening strategy

[0304] A number of phage-display solution selections were performed in three rounds using biotinylated human PD-L1-rCD4-His and mouse PD-L1-rCD4-His antigens (see **Example 1.3** for antigen details). The selections were performed by decreasing the antigen concentrations in every round (varying from 100 to 0.02 nM) and for each round of selection a "no-antigen" control was used.

[0305] Six selection outputs were selected for screening, two from round 2 (nos. 871 and 872) and four from round 3 (nos. 887, 890, 891 and 894) using the soluble scFv expression system

as described in section 1.3.1. A total of 1692 soluble scFv clones were screened for binding to immobilised antigen in ELISA (hu-PD-L1-rCD4-His antigen coated at 3 µg/mL in Dulbecco PBS, 50 µl, onto Maxisorb plates) using the assay described in **Example 4.2.1** above employing DELFIA enhancement solution.

[0306] Of the 1692 clones screened, 1029 clones yielded a signal of more than 2000 RFU in the DELFIA assay, giving a success rate of around 61%. The top 736 clones were then selected and analysed using a secondary assay (affinity ranking) employing three concentrations of hPD-L1-rCD4-His antigen (1.0 nM, 0.2 nM, and 0.04 nM). From the 736 clones screened, the 48 clones which showed the greatest signal were selected for cloning and expression in IgG1 format. Clones were expressed in Expi293F™ (Fisher Scientific cat. no. 13479756) cells at 800 µl scale, and the culture supernatants were harvested on the 5th day post transfection for further screening in IgG1 format.

5.2 SPR screening

[0307] All 48 antibodies were ranked by affinity using SPR (Biacore T200 instrument). For ranking, diluted supernatants (1:10 in running buffer made of 1X PBS and 0.002% Tween™-20) were immobilised onto a Protein-A chip (GE healthcare, product code: 29127556) and human PD-L1-rCD4-Hiswas flowed over the prepared surface at 50 nM concentration. The association (k_a) and dissociation (k_d) rate constants generated using this single injection were used to determine the dissociation constant (K_D). The K_D values of the clones were compared with that of clone G1/280_02_G02_NS in Ig1 format (G1/280_02_G02_NS). Ten clones of unique sequence were identified that showed higher affinity for human PD-L1 than clone G1/280_02_G02_NS and were therefore subjected to full kinetic analysis together with clone G1/280_02_G02_NS.

[0308] Briefly, SPR experiments were performed using a BIAcore T200 instrument. Antibodies from diluted culture supernatant were captured on a Protein A chip (GE Healthcare, 29127556) over FC2 at a flow rate of 10 µl/min, with 60 seconds contact time. Typically, this resulted in 500-800 RU of antibody captured. Doubling dilutions of PD-L1-rCD4-His were injected from 50 nM at a flow rate of 30 µl/min, (Concentration range: 50 nM-0.05 nM) over FC1 and FC2. Association was measured over 180 seconds, and dissociation was measured over 300 seconds. All measurements were performed at 25°C in PBS, pH 7.4, 0.05 % Tween™-20. Kinetic parameters were determined by reference cell subtraction and fitting the sensogram experimental data assuming a 1:1 interaction using the BIAevaluation software (GE, BR-1005-97). The resulting data was fitted using BIAevaluation software and corresponding k_a, k_d, and K_D values were calculated. Out of the ten clones tested, four antibodies, designated "G1/887_04_E12", "894_08_A05", "G1/894_08_E05" and "G1/887_04_G12", exhibited sub-nanomolar K_D values, which were lower than the K_D for G1/280_02_G02_NS. The affinity data obtained under the described screening conditions showed that the kappa light chain shuffle

described in **Example 5.1** allowed the heavy chain of the G1/280_02_G02_NS antibody to be paired not only with a lambda light chain but also with kappa light chains to produce antibodies with good, and in fact improved, affinity for recombinant human PD-L1.

5.3 Characterisation of kappa clones in IgG1 format

5.3.1 Cell based PD-1 / PD-L1 blocking assay

[0309] The ability of the anti-PD-L1 clones containing a kappa light chain, G1/887_04_E12, G1/894_08_E05 and G1/887_04_G12, to block the interaction between PD-1 and PD-L1 was assessed in a bioluminescent cell-based assay using a PD-1/PD-L1 Blockade Bioassay product (Promega, J1250/J1255) in accordance with the manufacturer's recommendations. The blocking activity was compared to the G1/280_02_G02_NS clone.

[0310] Briefly, all antibodies were purified as described in **Example 4.2.3** and tested at 3-fold dilutions from 100 nM to 35 pM (eight concentrations) in duplicates. All clones tested were shown to be potent inhibitors of the PD-1/PD-L1 interaction, with the three kappa light chain-containing clones G1/887_04_E12, G1/894_08_E05 and G1/884_04_G12 exhibiting even better IC_{50} values than the lambda light chain-containing clone G1/280_02_G02_NS.

5.3.2 Affinities

[0311] The binding of the anti-PD-L1 mAbs G1/887_04_E12, G1/887_04_G12 and G1/894_08_E05 to recombinant human (biotinylated hPD-L1-Avi-His, Aero Biosystems, PD1-H82E5), cynomolgus (cPD-L1-His, Acro Biosystems, PD1-C52H4) and mouse PD-L1 (mPD-L1-His, Acro Biosystems, PD1-M5220) was then measured by SPR using a Biacore T200 processing unit (GE Healthcare). Affinities were compared to the 280_02_G02_NS clone in IgG1 format (G1-AA/280_02_G02_NS; the "AA" in this clone name denotes that this clone also contained the "LALA" mutation in the CH2 domain).

[0312] Briefly, the anti-PD-L1 mAbs, diluted in HBS-EP buffer (GE Healthcare, BR100188) at 2 µg/ml, were injected individually on flows cell 2, 3 and 4 of a Protein A chip (GE Healthcare, 29127556) at 30 µl/min to achieve a final response of approximately 110 RU. The recombinant human, cynomolgus and mouse PD-L1-His antigens, diluted in HBS-EP buffer, were injected on flow cell 1, 2, 3 or 4 as appropriate at a concentration range of 81 nM to 0.037 nM with 3-fold dilutions for 4 min at 75 µl/min and then allowed to dissociate in buffer for 10 min. Regeneration was achieved by injecting 10 mM glycine-HCL pH1.5 (GE Healthcare, Human Antibody Capture Kit, BR00356) for 30 sec at a rate of 30 µl/min. Subtracted data (flow cell 2 - flow cell 1, flow cell 3 - flow cell 1, or flow cell 4 - flow cell 1) were analysed using BIAevaluation 3.2 Software (GE Healthcare) to identify binding using the model 1:1 binding with mass

transfer, with refractive index (RI) constant 0. To determine the affinities of the mouse PD-L1 binding curves, the Rmax of the corresponding human binding profiles was used.

[0313] The binding data demonstrated that the G1-AA/280_02_G02_NS clone and the G1/894_08_E05, G1/887_04_E12 and G1/887_04_G12 clones bound to human and cynomolgus PD-L1 with low single-digit nanomolar or subnanomolar affinities and were fully human/cynomolgus cross-reactive. In comparison to the G1-AA/280_02_G02_NS clone, the binding affinities of the G1/894_08_E05, G1/887_04_E12 and G1/887_04_G12 clones were about 1.8 to 4.8 fold higher for human and 2.7 to 4.7 fold higher for cynomolgus PD-L1. The affinities of the clones for recombinant mouse PD-L1 were lower, with K_D values ranging from 38 to 225 nM, with the highest affinity being observed for the G1/887_04_E12 clone. These data show that the heavy chain of the G1-AA/280_02_G02_NS antibody can be paired with both lambda and kappa light chains to produce antibodies with good (and in the case of kappa light chain pairing, sub-nanomolar) affinities for recombinant human and cynomolgus PD-L1, as well as some, albeit lower, affinity for recombinant mouse PD-L1.

5.3.3 Binding of anti-PD-L1 mAbs to cell expressed PD-L1

[0314] The anti-human PD-L1 mAbs, G1/894_08_E05, G1/887_04_E12 and G1/887_04_G12 were then tested for binding to HEK293 cells expressing human PD-L1 (HEK.hPD-L1 cells) using flow cytometry. Non-specific binding was also assessed by testing binding to HEK293 parental cells lacking human PD-L1 (Flp-In T-Rex 293 cell line, Life Technologies, R780-07).

[0315] cNDA encoding human PD-L1 (SEQ ID NO: 185) was subcloned into pcDNA™5/FRT vector (ThermoFisher Scientific Cat. No. V601020) using KpnI and NotI restriction sites and the vector was then transformed into Flp-In T-REx 293 cell line (Life Technologies, R780-07) using Lipofectamine 2000 (Life Technologies, 11668-019). Cells were grown in DMEM containing 10% FBS, 100 µg/ml Hygromycin B (Melford Laboratories Ltd, Z2475) and 15 µg/ml Blasticidin (Melford Laboratories Ltd, B1105) for 3-4 weeks until colonies of stably transformed cells had formed. These colonies were amplified in the presence of 1 µg/ml doxycyclin (Sigma Aldrich, D9891) and tested for expression of PD-L1 using PE-conjugated anti-human PD-L1 (MIH1) antibody (BD Biosciences, 557924). Cells were detached using cell dissociation buffer, washed once with PBS, plated at 2×10^5 cells in wells of a 96-well plate and then incubated with antibody diluted 1:20 in PBS for 1 hour at 4 °C, before being washed again in PBS and measured using an Accuri C6 cytometer (BD Biosciences). The data was analysed using FlowJoX software. Expression of human PD-L1 was detected in the cell line.

[0316] The G1/894_08_E05, G1/887_04_E12 and G1/887_04_G12 clones were found to bind to cell surface human PD-L1 with EC_{50} values in the range of 0.26 - 0.29 nM. No binding to parental HEK293 cells was observed showing the specificity of the binding. Therefore, all mAb clones tested bound specifically to PD-L1, with no non-specific binding observed.

5.3.4 Activity of anti-PD-L1 mAbs in Mixed Lymphocyte Reaction assay

[0317] The activity of the anti-PD-L1 mAbs was tested in a Mixed Lymphocyte Reaction (MLR) assay. A MLR assay measures the cellular immune response that occurs between two allogeneic lymphocyte populations (same species but genetically distinct). The assay uses $CD4^+$ T cells from one donor and monocyte derived dendritic cells (iDCs) from another donor. As the immune cells contain physiological levels of immune checkpoint regulators, the MLR assay can be used to confirm that T cell activation is enhanced by the mAb in a human system.

Generation of expanded $CD4^+$ T cells

[0318] PBMCs were isolated from leukocyte cones by Ficoll gradient separation. $CD4^+$ T cells were isolated using a Human $CD4^+$ T Cell Isolation Kit (Miltenyi Biotec Ltd, 130-096-533) according to the manufacturer's instructions. Human T-Activator CD3/CD28 Dynabeads (Life Technologies, 11131D) were resuspended by vortexing. Beads were transferred to a sterile 15ml tube and 10ml RPMI (Life Technologies, 61870044) with 10% FBS (Life Technologies, 10270106) and 1x Penicillin Streptomycin (Life Technologies, 15140122) was added to wash the Dynabeads. The supernatant was discarded. The required amount of $CD4^+$ T cells at 1.0 $\times 10^6$ cells/ml in RPMI with 10% FBS and 1x Penicillin Streptomycin Solution and 50 IU/ml recombinant human IL-2 (Peprotech, 200-02-50µg) with 3:1 bead to cell ratio was transferred to a T75 flask (Greiner Bio-one, 690195) and incubated at 37°C + 5% CO_2. After 3 days the cells were gently resuspended and counted. The cell density was maintained between 0.8-1 × 10^6 cells/ml by adding fresh media (RPMI-10% FBS + Penicillin Streptomycin Solution 1X + 50IU/ml rhuIL-2) as needed. On day 7 or 8, the CD3/28 beads were removed and $CD4^+$ T cells were rested overnight at 1 × 10^6 cells/ml fresh media RPMI-10% FBS + Penicillin Streptomycin Solution 1X with reduced 10IU/ml rhuIL-2. The cells were stored frozen until required.

Differentiation of iDCs

[0319] Untouched monocytes were isolated from human PBMCs using a Human Pan Monocyte Isolation Kit, (Miltenyi Biotec Ltd, 130-096-537) following the manufacturer's instructions. Monocytes were differentiated to iDCs using Human Mo-DC Differentiation Medium (Miltenyi Biotec Ltd, 130-094-812) following the manufacturer's instructions.

[0320] Expanded T cells were thawed one day before the experiment, washed with AIM V Medium (Gibco, 12055-091) and incubated at 37 °C, 5% CO_2 in AIM V Medium overnight. The anti-human PD-L1 mAbs, G1/894_08_E05, G1/887_04_E12 and G1/887_04_G12 were diluted

at 4x the final concentration in triplicate in 50 µl AIM V Medium in 96 well round bottom plates (VWR, 734-1797). An anti-FITC antibody, designated 4420 (Bedzyk *et al.,* 1989 and Bedzyk *et al.,* 1990), containing the LALA mutation was included as negative control. A 3-fold dilution series starting from 30 nM to 0.002 nM was tested. Both 1×10^4 iDC cells suspended in 50 µl AIM V Medium and 1×10^5 expanded $CD4^+$ T cells suspended in 100 µl AIM V Medium were added to the antibody dilutions and incubated for 5 days at 37°C + 5% CO_2. The following controls were included: $CD4^+$ T cells alone, iDC alone, $CD4^+$ T cells + iDCs, and AIM V Medium only. Supernatants were harvested, samples were diluted (1:25) and interferon gamma (IFN-γ) concentrations measured using Human IFN gamma ELISA Ready-SET-Go! Kit (Life Technologies, 88-7316-77). Plates were read at 450 nm using the plate reader with the Gen5 Software, BioTek. Absorbance values of 630 nm were subtracted from those of 450 nm (Correction). The standard curve for calculation of cytokine concentration was based on a four parameter logistic curve fit (Gen5 Software, BioTek). The concentration of human IFN-γ was plotted vs the log concentration of antibody and the resulting curves were fitted using the log (agonist) vs response equation in GraphPad Prism.

[0321] The anti-human PD-L1 mAbs, G1/894_8_E05, G1/887_4_E12 and G1/887_4_G12, showed potent activity in the MLR assay with EC_{50} values of less than 0.030 nM and a maximum level of IFN-γ (E_{max}) of greater than 10000 pg/ml. The EC_{50} indicates the concentration of mAb at which half of the response is achieved, whereas the E_{max} is an absolute value that indicates the maximum concentration of IFN-γ achieved in the assay. No activity was observed with the negative control G1-AA/4420 mAb as expected.

5.4 Activity of anti-PD-L 1 mAbs in a mouse DO11.10 T cell activation assay

[0322] As the anti-human PD-L1 mAbs G1/887_04_E12, G1/887_4_G12 and G1/894_08_E05 were shown to be weakly cross-reactive to mouse PD-L1 (see **Example 5.3.2)** their functional activity towards mouse PD-L1 was examined in an interleukin-2 (IL-2) release assay based on the DO11.10 OVA T-lymphocyte and LK35.2 B-lymphocyte hybridoma cell lines. IL-2 release is a marker of T cell activation. T cells expressing endogenous murine PD-1 were transfected with empty vector (pLVX). B-cells were transfected with a mouse PD-L1 construct.

5.4.1 Production of T cell lines with an empty vector

[0323] Lentiviral transduction methodology was used to generate DO11.10 cells (National Jewish Health) containing the empty lentiviral vector pLVX using the Lenti-X HTX Packaging System (Clontech, 631249). Lenti-X expression vector (pLVX) (Cat. No 631253) was co-transfected with a Lenti-X HTX Packaging Mix into the Lenti-X 293T Cell Line (Cat. No 632180) to generate virus. The DO11.10 cell line was transduced using the lentiviral particles produced with the Lenti-X HTX Packaging System.

5.4.2 Production of antigen presenting cells over-expressing PD-L1

[0324] Lentiviral transduction methodology was used to generate LK35.2 B cell lymphoma cells (ATCC, HB-98) over-expressing mouse PD-L1 using the Lenti-X HTX Packaging System (Cat. No 631249). Lenti-X expression vector (pLVX) (Cat. No. 631253) containing, cDNA encoding mouse PD-L1 (SEQ ID NO: 187), was co-transfected with a Lenti-X HTX Packaging Mix into the Lenti-X 293T Cell Line (Cat. No. 632180) to generate virus. The LK35.2 cell line was transduced using the lentiviral vectors produced with the Lenti-X HTX Packaging System.

5.4.3 Mouse DO11.10 T cell activation assay

[0325] Dilutions of the anti-PD-L1 mAbs G1/887_04_E12, G1/887_4_G12 and G1/894_08_E05 or the anti-FITC negative control mAb (G1-AA/4420) were prepared in experimental media (DMEM (Gibco, 61965-026), 10% FBS (Gibco, 10270-106), 1 mM Sodium Pyruvate (Gibco, 11360-070)). The mAbs were mixed 1:1 with 4×10^5/ml LK35.2 mPD-L1 cells in experimental media in presence of 2.46 µM OVA peptide (H-ISQAVHAAHAEINEAGR-OH (SEQ ID NO: 192) (Pepscan)) (100 µL LK35.2 mPD-L1 cells (B cell hybridoma transduced with a lentiviral vector containing mPD-L1 to overexpress mouse PD-L1)/mAb mix per well in 96-round bottom plate) and incubated at 37°C, 5% CO_2 for 1 hour. 2×10^5 DO11.10 pLVX cells (DO11.10 T cell hybridoma transduced with an empty lentiviral vector)/ml in 100 µl volume experimental media were added to 100 µl of the LK35.2 mPD-L1/(mAbs) mix. The cells were then mixed before being incubated at 37°C, 5% CO_2 for 24 hours. Supernatants were collected and assayed with mouse IL-2 ELISA kit (eBioscience, 88-7024-88 or R&D systems, SM2000) following the manufacturer's instructions. Plates were read at 450 nm using the plate reader with the Gen5 Software, BioTek. Absorbance values of 570 nm were subtracted from those of 450 nm (Correction). The standard curve for calculation of cytokine concentration was based on a four parameter logistic curve fit (Gen5 Software, BioTek). The concentration of mouse IL-2 was plotted vs the log concentration of mAb and the resulting curves were fitted using the log (agonist) vs response equation in GraphPad Prism.

[0326] The anti-human PD-L1 mAbs showed significant activity in the mouse T cell activation assay with potencies (EC_{50}) in the range of 1-4.4 nM. No activity was observed with the negative control mAb as expected. Of the three clones tested, G1/887_04_E12, which showed the highest affinity for recombinant mouse PD-L1, was also the most potent clone in the T cell activation assay. The differences in potency were smaller than the measured affinities which is likely due to the high overexpression of mouse PD-L1 on the LK35.2 cells in this assay.

5.5 Summary for characterisation kappa clones in IgG1 format

[0327] The anti-PD-L1 mAbs G1/894_08_E05, G1/887_04_E12, and G1/887_04_G12, containing the selected kappa light chains demonstrated cynomolgus and mouse PD-L1 cross-reactivity, showed specific binding to cell surface-expressed PD-L1, and showed even higher affinity for recombinant human and cynomolgus PD-L1 than the lambda light chain-containing clone G1/280_02_G02. The anti-PD-L1 mAbs G1/894_08_E05, G1/887_04_E12, and G1/887_04_G12 were shown to be potent activators of human T cells *in vitro* and to have functional mouse cross-reactivity.

Example 6: Sequence optimisation of the PD-L1 mAbs

6.1 Identification and removal of potential protein deamidation sites

[0328] Analysis of the sequence of the G1/280_02_G02_NS clone resulted in the identification of the sequence NSNT in the H-CDR2 loop (at Kabat positions 54-57) as a potential deamidation site, which if deamidated could affect binding. The heavy chain of this clone was retained in all kappa light chain-containing clones obtained by the chain shuffling campaign described in **Example 5,** so this potential deamidation site was also present in clones G1/887_04_E12, G1/894_08_A05, G1/894_08_E05 and G1/887_4_G12. Using specific primers closest to germline sequence, the NSNT sequence was changed in the four kappa light chain-containing clones by site-directed mutagenesis to either GGST, SGGT or SGNA to produce the variant clones identified. At the same time as removing this potential deamidation site, the role of the proline residue at Kabat position 28 in the VH region of the G1/887_04_E12 clone, which was unintentionally introduced into the sequence of this antibody during the kappa light chain shuffle, was also investigated by reverting it back to a threonine residue as contained in the G1/280_02_G02_NS clone. The parent and resulting variant clones (all in IgG1 format) were transfected at 0.8 ml scale, and culture supernatants harvested five days after transfections were used to determine the affinities of the clones for human and cynomolgus PD-L1-rCD4-His by SPR. Cyno PD-L1-rCD4-His was generated as described in **Example 1.3.** With the exception of the variant clones derived from the G1/887_04_E12 clone, all variant clones retained their sub-nanomolar affinities for human and cynomolgus PD-L1 as compared to their respective parent clone.

[0329] The modified clones derived from the G1/894_08_A05, G1/894_08_E05 and G1/887_04_G12 parent clones all showed sub-nanomolar affinities for human and cynomolgus PD-L1 comparable to those of their respective parent clone, indicating that the GGST, SGGT and SGNA substitutions were well tolerated. The much reduced affinities of the G1/929_01_A01, G1/929_01_A02 and G1/929_01_A03 clones compared to their parent (G1/887_04_E12) were considered likely to be due to the removal of the proline in the VH region at Kabat position 28 rather than to the presence of the GGST, SGGT and SGNA substitutions in H-CDR2. It was surprising that this proline residue in the G1/887_04_E12 clone appeared to be important for its affinity for PD-L1. The variants derived from the three parent

clones G1/887_04_E12, G1/894_08_E05 and G1/887_04_G12 which contained the SGGT substitution in their H-CDR2 (positions 54-57), namely clones G1/929_01_A02, G1/929_01_A08 and G1/929_01_A11, were selected for further characterisation on the basis that this SGGT substitution was closest to germline sequence.

[0330] Using site-directed mutagenesis, the potential deamidation site (NSNT at Kabat position 54 to 57) in the H-CDR2 loop of the G1/280_02_G02_NS clone was also modified to SGGT. Additionally, a further potential deamidation site (NS motif) identified at Kabat positions 31 to 32 in the CDR1 of the lambda light chain of this clone was modified to NY by mutating serine 32 (Kabat numbering) to a tyrosine, as tyrosine is found at this position in several germline sequences, such as IGLV2-8-01, IGLV2-8-02, IGLV2-8-03, IGLV2-11-01, IGLV2-11-02, IGLV2-11-03 and IGLV2-14-01, IGLV2-14-02, IGLV2-14-03, IGLV2-14-04. The combination of these modifications yielded the lambda light chain-containing clone G1/lam-G02v3, which was also selected for further characterisation.

Example 7: Characterisation of mAbs

7.1 Cloning and production of clones in mAb format

[0331] The threonine residue at Kabat position 28 in the VH region of the G1/929_01_A02 "SGGT" variant clone identified in **Example 6** was mutated to a proline, as is present at the same position in its parent clone G1/887_04_E12, with a view to improving its affinity for human and cynomolgus PD-L1. Transient expression in HEK293-6E cells and purification using mAb Select SuRe protein A columns was used to produce this modified variant clone and the other three "SGGT" variant clones (G1/929_01_A08, G1/929_01_A11 and G1/lam-G02v3) identified in **Example 6** in IgG1 format and with the LALA mutation to enable testing of their functional activity in the absence of effector function. The resulting mAbs were designated G1-AA/E12v2, G1-AA/E05v2, G1-AA/G12v2 and G1-AA/lamG02v3(called either G1-AA/lamG02v3 or G1-AA/lambdav3). The heavy and light chain sequences respectively are shown in SEQ ID NO: 16 and SEQ ID NO: 17 for G1-AA/E12v2, SEQ ID NO: 27 and SEQ ID NO: 28 for G1-AA/E05v2, SEQ ID NO: 27 and SEQ ID NO: 33 for G1-AA/G12v2 and SEQ ID NO: 27 and SEQ ID NO: 44 for G1-AA/lam-G02v3.

7.2 Affinities of mAb for human and cynomolgus PD-L1

[0332] To determine whether the further sequence modifications present in G1-AA/lam-G02v3 (namely, NSNT to SGGT in the VH-CDR2, NS to NY in the VL-CDR1, and the LALA mutation) and the kappa light chain-containing mAb G1-AA/E12v2, G1-AA/E05v2, and G1-AA/G12v2 (namely, the LALA mutation and, in the G1-AA/E12v2 only, threonine to proline at Kabat position 28 in the VH region) had affected binding kinetics, the affinities of these anti-PD-L1

mAb for human and cynomolgus PD-L1 were determined as described in **Example 5.3.2.** The mAbs G1-AA/lam-G02v3, G1-AA/E05v2, G1-AA/E12v2 and G1-AA/G12v2 exhibited affinities for human and cynomolgus PD-L1 similar to those observed in **Example 5.3** for mAbs G1-AA/280_02_G02_NS, G1/894_08_E05, G1/887_04_E12 and G1/887_04_G12, demonstrating that the binding affinities of the mAbs and mAb^2 tested were not affected by the modification of the potential deamidation sites or the introduction of the LALA mutation. The G1-AA/E12v2 mAb showed the lowest K_D value of all four mAbs tested (0.21 nM for human PD-L1, and 0.37 nM for cynomolgus PD-L1). The results are shown in **Table 4.**

[0333] The VH of G1-AA/E12v2 mAb differs from G1/929_01_A02 region **(Example 6)** by one residue, E12v2 has a proline at Kabat position 28 whereas G1/929_01_A02 has a threonine at this position. G1/929_01_A02 had a greater than 10-fold lower affinity for both human and cynomolgus PD-L1 when compared to G1-AA/E12v2, this data demonstrates the importance of the proline residue at position 28 in the VH of clone E12v2 (Kabat nomenclature) for its affinity for human and cynomolgus PD-L1.

Table 4

Clone	Human PD-L1-His K_D (nM)	Cyno PD-L1-His K_D (nM)
G1-AA/lam-G02v3	1.34	2.45
G1-AA/E05v2	0.50	0.89
G1-AA/E12v2	0.21	0.37
G1-AA/G12v2	0.44	0.75

7.3 Activity of anti-human PD-L1 mAbs in MLR

[0334] The anti-PD-L1 mAbs, G1-AA/E05v2, G1-AA/E12v2 and G1-AA/G05v2 were tested in a Mixed Lymphocyte Reaction (MLR) assay as described in **Example 5.3.4.** G1-AA/4420 was used as a negative control. The resulting data are shown in **Table 5.** The mAbs G1-AA/E05v2, G1-AA/E12v2 and G1-AA/G12v2 showed potent activity in the MLR assay with EC_{50} values of less than 0.054 nM and a maximum level of IFN-γ (E_{max}) of greater than 600 pg/ml **(Table 5).** The EC_{50} and especially the E_{max} values were significantly different from those described in **Example 5.3.4.** This difference is believed to be due to donor variability, as the response depends on the allogenic reaction between T cells from one donor and the monocyte derived dendritic cells from another donor. The potency of the anti-human PD-L1 mAbs was consistent with the data described in **Example 5.3.4,** as was the ranking of the clones by order of potency. No activity was observed for the negative control G1-AA/4420 mAb as expected.

Table 5

Clone	Functional activity in MLR Assay	
	EC_{50} (nM)	E_{max} (pg/ml)
G1-AA/E05v2	0.047	632
G1-AA/E12v2	0.054	666
G1-AA/G12v2	0.040	686
G1-AA/4420 negative control	No activity	

7.4 Expression, purification and analytical characterisation of anti-PD-L1 mAbs

[0335] The mAbs G1-AA/E05v2, G1-AA/E12v2 and G1-AA/G12v2 were produced at lab-scale and characterised by the standard analytical methods of SEC and Differential Scanning Calorimetry (DSC).

7.4.1 Lab scale expression and purification of anti-PD-L1 mAbs

[0336] DNA sequences encoding the mAbs G1-AA/E05v2, G1-AA/E12v2 and G1-AA/G12v2 were transfected into HEK293 6E (National Research Council Canada) cells using PEIpro (Polyplus, France). After 5 days, cell culture fluids were harvested, and purified on MabSelect Protein-A pre-packed columns using AKTAxpress instrument (both GE Healthcare, Uppsala, Sweden). Equilibration of the columns was carried out in 50mM Tris, 250 mM NaCl at pH 7.0 followed by loading with harvested cell culture fluid. The resin was washed using 50mM Tris, 250 mM NaCl at pH 7.0 and this was followed by eluting the mAb using buffer at pH of less than 3.5.

7.4.2 Analysis by SE-UPLC

[0337] Post-purification SE-UPLC was performed within 24 hours of purification (material was stored at 4°C) using an Acquity H-Class Bio UPLC (Waters Corp. UK) to measure the percentage of monomer. An Acquity UPLC BEH200 SEC 1.7mm column (4.6 × 150mm) was used, the mobile phase consisted of 250mM sodium phosphate, 100 mM L-Arginine at pH 6.8. Quantification of monomer, low molecular and high molecular weight species was performed using Empower software (Waters Corp. UK).

7.4.3 Thermostability

[0338] The melting temperature (T_m) of G1-AA/E05v2, G1-AA/E12v2 and G1-AA/G12v2 was

measured using a Microcal VP-capillary differential scanning calorimeter (DSC). G1-AA/lam-G02v3 was included to assess the difference between the kappa and lambda light chain-containing mAbs. Samples were measured in sample buffer at a concentration of 0.2 mg/ml. The scan rate was set at 60°C/hr and data were collected between 35°C and 100°C. Data analysis was performed with Origin 7.0 software. As the DSC peaks of the Fab and CH3 were overlapping, one value was reported.

Table 6

mAb	Monomer purity post-Protein A %	Tm of Fab/CH3
G1-AA/E05v2	99.48 ± 0.01 %	80.4-82.8°C
G1-AA/E12v2	98.85 ± 0.07%	81.4-84.1°C
G1-AA/G12v2	99.83 ± 0.11%	78.1-81.3°C
G1-AA/lam-G02v3	99.75 ± 0.25%	68.1°C

[0339] A summary of the results is shown in **Table 6.** The three mAbs: G1-AA/E05v2, G1-AA/E12v2 and G1-AA/G12v2 showed favourable analytical characterisation parameters; monomer purity post-protein A was greater than 98% and the thermal stability of the Fab transition (Tm) was found to be at the higher end of transitions typically reported for IgG1, with G1-AA/E12v2 appearing to be the most thermally stable (Fab/CH3 T_M= 81.484.1°C). The lambda light chain mAb, G1-AA/lamG02v3, had a lower Tm than the three kappa light chain-containing mAbs.

Example 8: Production and characterisation of anti-human CD137/PD-L1 mAb^2

8.1 Production of anti-human CD137/PD-L1 mAb^2

[0340] CD137/PD-L1 mAb^2 antibodies consisting of IgG1 molecules comprising the 3 anti-human CD137 Fcab clones FS22-053-008, FS22-053-017 and FS22-172-003 (see **Example 3)** were produced to allow characterisation of the Fcabs in a mAb^2 format. The CD137/PD-L1 mAb^2 were prepared by substituting part of the CH3 domain Fcabs comprising the AB, CD and EF loops, for the corresponding region of the CH3 domain of one of three anti-PD-L1 binding antibodies (G1-AA/E05v2, G1-AA/E12v2, G1-AA/G12v2; see **Example 7.1).** All resulting mAb^2 contained the LALA mutation. The CD137/PD-L1 mAb^2 were expressed transiently using PElpro (Polyplus, France) in HEK293 6E (NRCC, Canada) cells. After 5 days, cell culture fluids were harvested, and purified on MabSelect Protein-A pre-packed columns using AKTAxpress instrument (both GE Healthcare, Uppsala, Sweden). Equilibration of the columns was carried out in 50mM Tris-HCl, 250 mM NaCl, pH 7.0 followed by loading with harvested cell culture fluid. The resin was then subjected to wash in 50mM Tris-HCl, 250 mM NaCl, pH 7.0 followed

eluting the mAb^2 using buffer at pH <3.5.

[0341] To assess the amount of protein produced, IgG protein content was quantified by BioLayer Interferometry using the Octet QKe (ForteBio) platform with Protein A quantitation biosensors from PALL (18-5021). Proteins were purified by Protein A affinity chromatography using mAb SelectSure columns. Nine mAb^2 were purified using mAb Select SuRe Protein A columns (GE Healthcare, 11003494). The results are shown in **Table 7.**

Table 7

CD137/PD-L1 mAb^2				
CD137 Fcab	**PD-L1 Fab**	**mAb^2**	**Titre in HEK transient expression (mg/L)**	**Yield (Protein A)**
FS22-053-008-AA	E05v2	FS22-053-008-AA/E05v2	88	69%
FS22-053-008-AA	E12v2	FS22-053-008-AA/E12v2	113	74 %
FS22-053-008-AA	G12v2	FS22-053-008-AA/G12v2	108	88%
FS22-053-017-AA	E05v2	FS22-053-017-AA/E05v2	61	88%
FS22-053-017-AA	E12v2	FS22-053-017-AA/E 12v2	198	65%
FS22-053-017-AA	G12v2	FS22-053-017-AA/G12v2	89	81 %
FS22-172-003-AA	E05v2	FS22-172-003-AA/E05v2	127	82 %
FS22-172-003-AA	E12v2	FS22-172-003-AA/E12v2	260	76 %
FS22-172-003-AA	G12v2	FS22-172-003-AA/G12v2	229	69 %

[0342] All 9 CD137/PD-L1 mAb^2 antibodies were produced by transient expression in HEK 293 6E and obtained titres and protein A purification yields within typical range expected at the lab scale. FS22-172-003-AA-lam/G02v3 was also expressed and purified for further testing.

8.2 Biophysical characterisation of mAb^2 by size exclusion chromatography (SEC) and SDS-PAGE

8.2. 1 Analysis by SE-HPLC

[0343] Post-purification SE-HPLC was performed on an Agilent 1100 series HPLC (Agilent, UK), fitted with a TSK-GEL SUPERSW3000 4.6 mm ID × 30.0 cm column (Tosoh Bioscience) using 20 mM sodium phosphate, 200 mM sodium chloride, pH 6.8 as a mobile phase. Quantification of % monomer was performed using Chemstation software (Agilent, UK).

8.2.2 Analysis by CE-SDS

[0344] CE-SDS analysis was performed on a 2100 Bioanalyzer Capillary Electrophoresis System (Agilent, UK), according to manufacturer's instructions. For reducing conditions, DTT was added and samples were denatured at 70° C for 5 minutes.

Table 8

mAb^2	**Reduced CE-SDS Sum of % heavy chain + % light chain**	**SEC-HPLC % monomer**
FS22-053-008-AA/E05v2	99.7 %	99.6 %
FS22-053-008-AA/E12v2	99.8 %	98.9 %
FS22-053-008-AA/G12V2	Not tested	62.6 %
FS22-053-017-AA/E05v2	99.8 %	99.5 %
FS22-053-017-AA/E12v2	99.7 %	99.6 %
FS22-053-017-AA/G12V2	99.0 %	99.6 %
FS22-172-003-AA/E05v2	99.2 %	99.1 %
FS22-172-003-AA/E12v2	99.7 %	97.9%
FS22-172-003-AA/G12v2	99.6 %	99.3 %

[0345] A summary of analytical results is shown in **Table 8.** All mAb^2, except FS22-053-008-AA/G12v2, showed high purity post purification using Protein A; low level of soluble aggregation and fragmentation as showed by % monomer post protein A > 95% and a high purity by reduced CE-SDS (> 95 %, sum of % heavy chain and % light chain). FS22-053-008-AA/G12v2 displayed aggregation post Protein A purification and as a result it was not progressed any further.

Example 9: Characterisation of mAb^2 binding

9.1 Binding affinity of anti-human CD 137/PD-L1 mAb^2 for human and cynomolgus PD-L1 by SPR

[0346] Binding of the anti-human CD137/PD-L1 mAb^2, FS22-172-003-AA/lam-G02v3, FS22-172-003-AA/E05v2, FS22-053-008-AA/E05v2, FS22-172-003-AA/E12v2, FS22-053-008-AA/E12v2 and FS22-172-003-AA/G12v2 to recombinant human and cynomolgus PD-L1 antigens was then measured by SPR using a Biacore T200 processing unit (GE Healthcare).

[0347] Briefly, the anti-human CD137/PD-L1 mAb^2, diluted in HBS-EP buffer (GE Healthcare, BR100188) at 2 µg/ml, were injected individually on flows cell 2, 3 and 4 of a Protein A chip (GE Healthcare, 29127556) at 30 µl/min to achieve a final response of approximately 110 RU. Two different recombinant human PD-L1 antigens were used i.e. hPD-L1-His-Avi (see **Example 1.3** for antigen details) and biotinylated hPD-L1-Avi-His (Acrobiosystems, PD-1-H82E5). Human and cynomolgus PD-L1-His (Acrobiosystems, PD-1-C52H4) antigens, diluted in HBS-EP buffer, were injected on flow cell 1, 2, 3 or 4 as appropriate at a concentration range of 81 nM to 0.037 nM with 3-fold dilutions for 4 min at 75 µl/min and then allowed to dissociate in buffer for 10 min. Regeneration was achieved by injecting 10 mM glycine-HCL pH1.5 (GE Healthcare, Human Antibody Capture Kit, BR00356) for 30 sec at a rate of 30 µl/min. Subtracted data (flow cell 2 - flow cell 1, flow cell 3 - flow cell 1, or flow cell 4 - flow cell 1) were analysed using BIAevaluation 3.2 Software (GE Healthcare) to identify binding using the model 1:1 binding with mass transfer, with refractive index (RI) constant 0.

Table 9

Clone	Human PD-L1-His K_D (nM)	Cynomolgus PD-L1-His K_D (nM)
FS22-172-003-AA/lam-G02v3	1.54	1.91
FS22-172-003-AA/E05v2	0.50	0.59
FS22-172-003-AA/E12v2	0.19	0.36
FS22-172-003-AA/G12v2	0.49	0.53
FS22-053-008-AA/E05v2	0.47	0.58
FS22-053-008-AA/E12v2	0.19	0.25

[0348] The binding data demonstrated that each of the anti-human CD137/PD-L1 mAb^2 bound to human and cynomolgus PD-L1 with low to subnanomolar affinities and so were human/cynomolgus cross-reactive **(Table 9).** All mAb^2 clones bound to human and cynomolgus PD-L1 equally well with equivalent KD values for each antigen.

9.2 Binding affinity of anti-human CD 137/PD-L1 mAb^2 for human and cynomolgus CD137 by SPR

[0349] The binding of the anti-human CD137/PD-L1 mAb^2 to recombinant dimeric human and cynomolgus CD137 antigens was also measured by SPR using a Biacore T200 processing unit (GE Healthcare).

[0350] Briefly, 20 µg/ml anti-human Fab antibody (GE Healthcare, Human Fab Capture kit 28958325) was coated on flow cells 1, 2, 3 and 4 of a Biacore sensor S chip CM5 (GE Healthcare, BR100530) achieving a final response of approximately 5000 RU. The mAb^2 clones, diluted in HBS-EP buffer (GE Healthcare, BR100188) at 2-5 µg/ml, were injected individually on flows cell 2, 3 and 4 at 30 µl/min to achieve a response of approximately 70 RU (200 RU for FS22-172-003-AA/E12v2). The recombinant dimeric antigens, human CD137-mFc-Avi or cynomolgus CD137-mFc-Avi (see **Example 1.1** for antigen details) diluted in HBS-EP buffer, were injected on flow cell 1, 2, 3 or 4 as appropriate at a concentration range of 81 nM to 0.037 nM with 3-fold dilutions for 4 minutes at 70 µl/min and then allowed to dissociate in buffer for 10 minutes. Regeneration was achieved by injecting 10 mM glycine pH 2.1 (GE Healthcare, Human Fab Capture kit 28958325) for 60 seconds at a rate of 30 µl/min. Data analysis was performed as described in **Example 9.1.**

Table 10

mAb^2 clone	**Human CD137-mFc-Avi K_D (nM)**	**Cyno CD137-mFc-Avi K_D (nM)**
FS22-172-003-AA/Iam-G02v3	1.3	2.2
FS22-172-003-AA/E05v2	1.5	1.0
FS22-172-003-AA/E12v2	0.7	0.8
FS22-172-003-AA/G12v2	2.2	1.8
FS22-053-008-AA/E05v2	2.8	1.1
FS22-053-008-AA/E12v2	2.6	0.6

[0351] The binding data demonstrated that the anti-human CD137/PD-L1 mAb^2 clones bound to dimeric human and cynomolgus CD137 with low nanomolar affinities and were fully human/cynomolgus cross-reactive **(Table 10).** As expected, these results were similar to the binding data reported for these Fcab clones in "mock" mAb^2 format **(Table 3, Example 3.7).** The highest affinity for dimeric CD137 was observed for FS22-172-003-AA/E12v2, which affinity was subsequently also tested against monomeric CD137-His-Avi using the same method as described above. No binding of FS22-172-003-AA/E12v2 to monomeric CD137 up to 81 nM was detected, illustrating that the Fcab binding regions of the anti-human CD137/PD-

L1 mAb^2 have a low affinity for monomeric CD137. These results are similar to those also observed for the FS22-053-008 CD137 Fcabs showing that the conversion of the Fcab to a mAb^2 format resulted in little change in binding to CD137.

9.3 Specificity determination of anti-human CD137/PD-L1 mAb^2 by SPR

9.3.1 Specificity for human PD-L1

[0352] To analyse specificity of the anti-human CD137/PD-L1 mAb^2, the binding of six mAb^2 (FS22-172-003-AA/lam-G02v3, FS22-172-003-AA/E05v2, FS22-053-008-AA/E05v2, FS22-172-003-AA/E12v2, FS22-053-008-AA/E12v2 and FS22-172-003-AA/G12v2) to other T cell targets was tested using SPR. The aim was to demonstrate specificity by showing no binding of the mAb^2 to the antigens PD-L2, CD80, PD-1, and B7-H3 at a concentration of 1 µM.

[0353] Flow cells on CM5 chips were immobilised with approximately 1000 RU of either human PD-L2-Fc (R&D Biosystems, 1224-PL), CD80-Fc (R&D Biosystems, 140-B1), PD-1-His (R&D Biosystems, 8986-PD), B7-H3-His (F-star in-house production, SEQ ID NO: 193), PD-L1-Fc (R&D Biosystems, 156-B7) and PD-L1-His (Acrobiosystems, PD-1-H83F3). Flow cell 1 was left for blank immobilisation. The mAb^2 were diluted to 1 µM and 1 nM in 1x HBS-EP buffer (GE Healthcare, product code BR100188), allowed to flow over the chip for 3 min and then allowed to dissociate for 4 min. A 30-seconds injection of 10 mM glycine pH 1.5 was used for regeneration. Positive control antibodies were injected at 50-100 nM to demonstrate the coating of each antigen. Binding levels were determined at the end of the association phase and compared.

[0354] All mAb^2 tested showed a high level of specificity with less than 10 RU of mAb^2 binding to the four antigens detected at 1 µM compared to a range of 105 to 570 RU of binding response detected at 1 nM for binding to either human PD-L1-Fc or PD-L1-His. These results demonstrated the high level of specificity of the anti-human CD137/PD-L1 mAb^2 for PD-L1 with no binding to the other T cell targets listed.

9.3.2 Specificity for human CD137

[0355] It is expected that the specificity of the CD137 Fcab binding moiety is retained in the CD137/PD-L1 mAb^2 when compared to CD137/HelD1.3 mAb^2 (see **Example 3.6).** The specificity of FS22-172-003-AA/E12v2 for TNFR family members, OX40, GITR, CD40 and DR6 (R&D Biosystems) was analysed by SPR similarly as described in **Example 9.3.1.** At a concentration of 1 µM, FS22-172-003-AA/E12v2 bound with less than 7 RU to human OX40,

GITR, CD40 and DR6 compared to 278 RU to human CD137-mFc. This result demonstrates the high level of specificity of the FS22-172-003-AA/E12v2 mAb^2 for CD137.

9.4 Simultaneous binding of anti-human CD137/PD-L1 mAb^2 to human PD-L1 and human CD137 by SPR

[0356] The ability of the FS22-172-003-AA/E12v2 mAb^2 to bind simultaneously to human CD137 and human PD-L1-His Avi (see **Example 1.3** for antigen details) was tested by SPR on a Biacore T200. G1/S70 was used as control. Human PD-L1 His, diluted to 10 µg/ml in sodium acetate buffer pH 5.0 (GE Healthcare, 18-1069), was immobilised on a CM5 Sensor S chip (GE Healthcare, BR100530) to a surface density of approximately 1100 RU. One flow cell was activated and deactivated without any protein immobilised for background subtraction. The antibodies, diluted to 5 µg/ml in HBS-EP buffer, were captured at a flow rate of 30 µl/min to achieve a density of about 200-300 RU. Binding of human CD137-mFc-Avi was tested at 0 and 100 nM for 5 min at 30 µl/min, followed by a dissociation step of 2.5 min. The sensor chip was regenerated after each cycle with 20 mM NaOH for 60 seconds at a flow rate of 30 µl/min. FS22-172-003-AA/E12v2 was able to bind simultaneously to both human PD-L1 and human CD137, whereas the control G1/S70 only bound to human PD-L1.

9.5 Binding affinity of anti-human CD137/PD-L1 mAb^2 to cell surface expressed human or cynomolgus PD-L1 by flow cytometry

[0357] To assess binding of the anti-human CD137/PD-L1 mAb^2 to cell surface human and cynomolgus PD-L1, HEK293 cells overexpressing human PD-L1 were generated. HEK293 cells overexpressing human PD-L1 (HEK.hPD-L1) were produced as described in Example **5.3.3.** HEK293 cells overexpressing cynomolgus PD-L1 (HEK.cPD-L1) were also produced as described in **Example 5.3.3,** except the cDNA encoding cynomolgus PD-L1 (SEQ ID NO: 189) was subcloned into the pcDNA™5/FRT vector instead of the human PD-L1 sequence.

[0358] The anti-human CD137/PD-L1 mAb^2, FS22-172-003-AA/E12v2, was then tested for binding to HEK293 cells expressing human or cynomolgus PD-L1 using flow cytometry. Non-specific binding was also assessed by testing binding to HEK293 parental cells lacking human PD-L1 (Flp-In T-Rex 293 cell line, Life Technologies, R780-07). Binding affinities were compared with a positive control antibody G1-AA/E12v2 (SEQ ID NO: 16 and 17 for the heavy chain and light chain, respectively), the variable domains of which were cloned and expressed in the human IgG1 format comprising the LALA mutation in the CH2 domain (G1-AA format).

[0359] HEK293, HEK.hPD-L1 and HEK.cPD-L1 suspensions were prepared in FACS buffer (DPBS (Gibco, 14190-094) containing 0.5% BSA (Sigma, A7906)) and seeded at 1×10^5

cell/well in 100 µl in round bottomed 96-well plates (VWR, 734-1797). Cells were washed once in FACS buffer. mAb^2 FS22-172-003-AA/E12v2, mock mAb^2 FS22-172-003-AA/HeID1.3, mAb G1-AA/E12v2 and negative control mAb G1-AA/4420 were diluted (400 nM - 0.005 nM, 5-fold dilutions) in 100 µl FACS buffer. The washed cells were resuspended in the diluted antibody mixture, incubated at 4°C for 30 minutes, and then washed once in FACS buffer. 100 µl/well of secondary antibody (goat anti-human IgG Alexa Fluor 647 labelled antibody, Invitrogen, A21445) diluted 1:1000 in FACS buffer was then added, incubated for 20 mins at 4°C, and the cells washed again with FACS buffer and resuspended in 100 µl of PBS containing 7AAD (1:1000, Biotium, 40043) before being analysed using a Canto II flow cytometer (BD Bioscience). Dead cells were excluded and the fluorescence in the APC channel (638nm 660/20) was measured. The geometric mean fluorescence intensity (GMFI) values were plotted vs the log concentration of antibody and the resulting curves were fitted using the log (agonist) vs response equation in GraphPad Prism.

[0360] The FS22-172-003-AA/E12v2 mAb^2 and G1-AA/E12v2 antibody were found to bind to cell surface human PD-L1 with EC_{50} values in the range of 3.1 - 3.7 nM and cell surface cynomolgus PD-L1 with EC_{50} values in the range 0.6 - 0.7 nM (see **Table 11)** No binding to HEK293 cells lacking PD-L1 overexpression was observed showing the specificity of the binding. Therefore, FS22-172-003-AA/E12v2 mAb^2 tested bound specifically to PD-L1, with no non-specific binding observed. These results show that the specificity to human and cyno PD-L1 observed for the PD-L1 mAb (see **Example 5.3.3)** is retained.

Table 11

		FS22-172-003-AA/E12v2 EC_{50} (nM)	**G1-AA/E12v2 EC_{50} (nM)**
Human PD-L1	EC_{50} (nM)	3.7 ± 0.4	3.1
Cynomolgus PD-L1	EC_{50} (nM)	0.7 ± 0.3	0.6 ± 0.3

9.6 Binding affinity of anti-human CD 137/PD-L1 mAb^2 to cell surface expressed human or cynomolgus CD 137 by flow cytometry

[0361] DO11.10 cells (National Jewish Health) expressing full-length human (SEQ ID NO: 185) or cynomolgus CD137 (SEQ ID NO: 189), designated 'DO11.10.hCD137' and 'DO11.10.cCD137' respectively, were produced in order to present the antigen in a membrane-bound conformation, most similar to its natural form, for further characterisation of selected anti-human CD137/PD-L1 mAb^2. Details of the DO11.10.hCD137 and DO11.10.cCD137 cell production and confirmation of expression are described in **Example 1.2.**

[0362] The anti-human CD137/PD-L1 mAb^2 FS22-172-003-AA/E12v2 was tested for binding to cells expressing human or cynomolgus CD137 (DO11.10.hCD137 or DO11.10.cCD137) using flow cytometry. Non-specific binding was also assessed by testing binding to DO11.10 cells lacking CD137 expression. The variable domains of MOR7480.1 (US Patent No. 2012/0237498) were cloned and expressed in human IgG1 format comprising the LALA mutation in the CH2 domain (G1-AA format) and this was used as a positive control.

[0363] Briefly, DO11.10, DO11.10.hCD137 or DO11.10.cCD137 suspensions were prepared in FACS buffer (DPBS containing (Gibco, 14190-094) containing 0.5% BSA (Sigma, A7906)) and seeded at 1×10^5 cell/well in 100 µl in round bottomed 96-well plates (VWR, 734-1797). Cells were washed once in FACS buffer and mAb^2 FS22-172-003-AA/E12v2, mock mAb^2 FS22-172-003-AA/HelD1.3, antibody G1-AA/MOR7480.1 and negative control mAb G1-AA/4420 were diluted (400 nM - 0.005 nM, 5-fold dilutions) in 100 µl FACS buffer. The washed cells were resuspended in the diluted antibody mixture, incubated at 4°C for 30 minutes, and then washed once in FACS buffer. 100 µl/well of secondary antibody (goat anti-human IgG Alexa Fluor 647 labelled antibody, Invitrogen, A21445) diluted 1:1000 in FACS buffer was then added, the cells/antibody mixture was incubated for 20 mins at 4°C, and the cells were then washed again with FACS buffer and resuspended in 100 µl of PBS containing 7AAD (1:1000, Biotium, 40043) before being analysed using a Canto II flow cytometer (BD Bioscience). Dead cells were excluded and the fluorescence in the APC channel (638nm 660/20) was measured. The geometric mean fluorescence intensity (GMFI) values were plotted vs the log concentration of antibody and the resulting curves were fitted using the log (agonist) vs response equation in GraphPad Prism.

[0364] The results are shown in **Table 12.** FS22-172-003-AA/E12v2 mAb^2 and FS22-172-003-AA/HelD1.3 mock mAb^2 were found to bind to cell surface-expressed human and cyno CD137 receptors with EC_{50} values in the range of 4.8 - 9.1 nM, and the positive control mAb was found to bind to human and cyno CD137 receptors with an EC_{50} value of 1.45 nM and 4.4nM respectively. No binding to DO11.10 or HEK293 cells which did not overexpress CD137 was observed confirming the specificity of binding by the mAb^2.

Table 12

Antigen	**FS22-172-003-AA/ E12v2 (EC_{50} (nM))**	**FS22-172-003-AA/ HelD1.3 (EC_{50} (nM))**	**G1-AA/MOR7480.1 (EC_{50} (nM))**
Human CD137	6.2 ± 1.95	6.25 ± 2.03	1.48 ± 0.4
Cynomolgus CD137	7.39 ± 6.07	9.09 ± 6.93	2.6 ± 1.85

9.7 Binding affinity of anti-human CD137/PD-L1 mAb^2 to endogenously expressed CD137 and PD-L1 on activated primary human T cells

[0365] The affinity of the anti-human CD137/PD-L1 mAb^2 for endogenously expressed CD137 and PD-L1 on activated primary human T cells was determined using flow cytometry. To isolate T cells, peripheral blood mononuclear cells (PBMCs) were isolated from leucocyte depletion cones, a by-product of platelet donations. Briefly, leucocyte cone contents were flushed with PBS and overlaid on a Ficoll (Sigma-Aldrich, 1440-02) gradient. PBMCs were isolated by centrifugation and the cells that did not cross the Ficoll gradient were recovered. PBMCs were further washed with PBS and remaining red blood cells were lysed through the addition of 10 ml 1X red blood cell lysis buffer (eBioscience, 00-4300-54) according to the manufacturer's instructions. Pan T cells were isolated from the PBMCs present in the eluent using the Pan T Cell Isolation kit II (Miltenyi Biotec Ltd, 130-095-130) according to the manufacturer's instructions. CD137 is rapidly expressed to high levels on activated $CD8^+$ T cells and also on activated $CD4^+$ T cells with lower levels (Xue-Zhong Yu *et al,* 2013), therefore Pan T cells were stimulated for 24 hours using Dynabeads™ Human T-Activator CD3/CD28 beads (Thermo, 11132D) according to manufacturer's instructions. Human T-Activator beads were washed from the T cells using a DynaMagTM-15 Magnet (Thermo, 12301D) following manufacturer's instructions before being using a cell binding assay to test for binding of FS22-172-003-AA/E12v2 mAb^2, FS22-172-003-AA/HelD1.3 mock mAb^2, G1-AA/E12v2 positive control anti-human PD-L1 antibody, G1-AA/MOR7480.1 positive control anti-human CD137 antibody, G1-AA/4420 negative control antibody.

[0366] Stimulated pan human T cell suspensions were prepared in FACS buffer ((DPBS (Gibco, 14190-094) containing 0.5% BSA (Sigma, A7906)) and seeded at 1×10^5 cell/well in 100 µl in round bottomed 96-well plates (VWR, 734-1797). Cells were washed once in FACS buffer and mAb^2 FS22-172-003-AA/E12v2, mock mAb^2 FS22-172-003-AA/HelD1.3, positive control antibody G1-AA/E12v2, positive control antibody G1-AA/20H4.9, and negative control antibody G1-AA/4420 were diluted (80 nM - 0.005 nM, 5-fold dilutions) in 100 µl FACS buffer. The washed cells were resuspended in the diluted antibody mixture containing anti-human $CD4^+$ FITC labelled antibody (BD Biosciences, 550628) and anti-human $CD8^+$ eFluor450 labelled antibody (Invitrogen, 48-0087-42) to differentiate between $CD4^+$ and $CD8^+$ T cells, incubated at 4°C for 30 minutes, and then washed once in FACS buffer. 100 µl/well of secondary antibody (goat anti-human IgG Alexa Fluor 647 labelled antibody, Invitrogen, A21445) diluted 1:1000 in FACS buffer was then added, the cells/antibody mixture was incubated for 20 mins at 4°C, and the cells were then washed again with FACS buffer and resuspended in 100 µl of PBS containing 7AAD (1:1000, Biotium, 40043) before being analysed using a Canto II flow cytometer (BD Bioscience). Dead cells were excluded and the fluorescence in the APC channel (638nm 660/20) was measured to show test antibody binding. The geometric Mean Fluorescence Intensity (GMFI) values were plotted vs the log concentration of antibody and the resulting curves were fitted using the log (agonist) vs response equation in GraphPad Prism.

[0367] The FS22-172-003-AA/E12v2 mAb^2 was found to bind to stimulated human primary $CD4^+$ T cells and $CD8^+$ T cells as shown by the MFI values in **Figure 2.** The PD-L1 positive control antibody G1-AA/E12v2 bound with similar MFI values as the mAb^2 to both $CD4^+$ and $CD8^+$ T cells, confirming that PD-L1 was expressed on the cells.

[0368] G1-AA/MOR7480.1, the CD137 positive control was found to bind to the same cells described above though the MFI was much lower than observed for either FS22-172-003-AA/E12v2 or G1-AA/E12v2. This is likely due to there being a lower level of CD137 expression on the cells, compared to PD-L1 expression. Further, the MFI value was higher for binding of G1-AA/MOR7480.1 to $CD8^+$ T cells than on $CD4^+$ T cells. As described earlier it is expected to observe lower CD137 expression on stimulated $CD4^+$ T cells than on $CD8^+$ T cells (Xue-Zhong Yu *et al,* 2013) which accounts for the low binding level of CD137 positive control antibody MOR7480.1 on $CD4^+$ T cells as opposed to $CD8^+$ T cells. This low CD137 expression seen on primary T cells, particularly on $CD4^+$ T cells, also likely accounts for seeing no or little binding of the Fcab in mock mAb^2 format (FS22-172-003-AA/HelD1.3).

9.8 Binding of anti-human CD137/PD-L1 mAb^2 to FcRn by SPR

[0369] The neonatal Fc receptor (FcRn) binding is critical for antibody recycling (Martins *et al.,* 2016). The binding of FS22-172-003-AA/lam-G02v3, FS22-172-003-AA/E12v2 and FS22-053-008-AA/E12v2 mAb^2 to human and mouse FcRn was measured by SPR using BIAcore T200 (GE Healthcare). G1-AA/HelD1.3 was included as an isotype control IgG control lacking mutations in the CH3 domain.

[0370] Briefly, mAb^2 were individually coated on flow cell 2, 3 and 4 of Series S Sensor Chip CM5 (GE Healthcare, BR100530) to achieve a response of approximately 1000 RU. Flow cell 1 was activated/deactivated but left blank as a reference. Human FcRn (Aero Biosystems, FCM-H5286) or mouse FcRn (R&D systems, 9114-Fc) was dialysed and diluted in MHBS-EP^+B pH 6.0 or pH 7.4 buffer (10 mM MES, FortéBio, 18-5026; 1x HBS-EP, GE Healthcare, BR100669; 0.1 mg/ml BSA, Sigma, A7906) and injected on flow cell 1, 2, 3 and 4 at 2000-3000 nM with 2-fold dilutions for 1 min at 80 µl/min and then allowed to dissociate in buffer for 3 min. Regeneration was not required. Subtracted data (flow cell 2 - flow cell 1, flow cell 3 - flow cell 1, or flow cell 4 - flow cell 1) was analysed using Biacore T200 Evaluation Software 2.0 to identify binding using the model steady state affinity. The binding data are shown in **Table 13** and demonstrated that FS22-172-003-AA/lam-G02v3, FS22-172-003-AA/E12v2 and FS22-053-008-AA/E12v2 mAb^2 bound to human or mouse FcRn at pH 6.0 with similar affinities as the control antibody G1-AA/HelD1.3. No binding was observed with human or mouse FcRn at pH7.4. This data showed that FcRn binding was retained by the mAb^2.

Table 13

	Human FcRn K_D (M)		Mouse FcRn K_D (M)	
	pH 6.0	**pH 7.4**	**pH 6.0**	**pH 7.4**
FS22-172-003-AA/Iam-G02v3	1.22×10^{-6}	No binding	1.67×10^{-7}	No binding
FS22-172-003-AA/E12v2	1.12×10^{-6}	No binding	1.58×10^{-7}	No binding
FS22-053-008-AA/E12v2	9.98×10^{-7}	No binding	1.77×10^{-7}	No binding
G1-AA/HeID1.3	1.23×10^{-6}	No binding	1.60×10^{-1}	No binding

9.9 Binding of anti-human CD137/PD-L1 mAb^2 to cells expressing Fcγ receptors by flow cytometry

[0371] Agonistic antibodies targeting TNFRSF members require crosslinking via Fcγ receptors to drive target clustering and activation to achieve *in vivo* activity (Li *et al,* 2013). However, in order to circumnavigate potential off-target effects such as systemic CD137 activation due to crosslinking by Fcγ receptor binding and to decrease the possibility of inducing ADCC of immune cells, for example T cells, that express both targets, it was decided to decrease the Fcγ receptor binding ability of the anti-human CD137/PD-L1 mAb^2 by introduction of a LALA mutation in the CH2 domain (see **Example 3.2** for details on the LALA format). Cell binding by flow cytometry to CHO cells over-expressing only FcγRIIA (ECACC Cat No: 15042905), FcγRIIA (ECACC Cat No: 15042903), FcγRIIIA (ECACC Cat No: 15042902), FcγRIIIA (ECACC Cat No: 15042901), or FcγRIIB (ECACC Cat No: 15042907) was used to confirm that the presence of the LALA mutation in the CH2 domain of the anti-human CD137/PD-L1 mAb^2 had reduced its binding affinity for the previously mentioned Fcγ receptors.

[0372] Briefly, CHO.FcγRIIA.131H, CHO.FcγRIIA.131E, CHO.FcγRIIIA.158F, CHO.FcγRIIIA.158V, CHO.FcγRIIB, or CHO.WT suspensions were prepared in FACS buffer (DPBS containing (Gibco, 14190-094) containing 0.5% BSA (Sigma, A7906)) and seeded at 1×10^5 cell/well in 100 µl in round bottomed 96-well plates (VWR, 734-1797). Cells were washed once in FACS buffer and mAb^2 FS22-172-003-AA/E12v2, positive control for Fcγ receptor binding antibody G1/4420 and negative control for Fcγ receptor antibody G1-AA/4420 were diluted (500 nM-0.03 nM, 4-fold dilutions) in 100 µl FACS buffer. The washed cells were resuspended in the diluted antibody mixture, incubated at 4°C for 30 minutes, and then washed once in FACS buffer. 100 µl/well of secondary antibody (goat anti-human IgG Alexa Fluor 488 labelled antibody, Stratech Scientific Ltd, 109-545-098-JIR) diluted 1:1000 in FACS buffer was then added, the cells/antibody mixture was incubated for 20 mins at 4°C, and the cells were then washed again with FACS buffer and resuspended in 100 µl of PBS containing 7AAD (1:1000, Biotium, 40043) before being analysed using a CytoFLEX flow cytometer (Beckman Coulter). Dead cells were excluded and the fluorescence in the FITC channel (488nm 525/40) was measured. The geometric mean fluorescence intensity (GMFI) values

were plotted vs the log concentration of antibody and the resulting curves were fitted using the log (agonist) vs response equation in GraphPad Prism.

[0373] The FS22-172-003-AA/E12v2 mAb^2 showed no binding (or bound below the level of the negative control antibody G1-AA/4420) to all the Fcy receptor expressing cells tested **(Figure 3** (A) FcgRIIA 131H, (B) FcgRIIA 131E, (C) FcgRIIB, (D) FcgRIIIA 158F, (E) FcgRIIIA 158V). This indicates that the LALA mutation decreases binding to FcyRIIA, FcyRIIIA, or FγgRIIB which would also decrease mAb^2 crosslinking via these receptors *in vivo.*

Example 10: Characterisation of mAb^2 function

***10.1 Activity of anti-human CD137/PD-L1 mAb^2 in a human primary $CD8^+$ T cell* assay**

[0374] The human primary T cell assay described in **Example 3.5** was used to test the activity of the mAb^2.

[0375] For cell-based crosslinking of anti-human CD137/PD-L1 mAb^2, HEK293 cells overexpressing hPD-L1 (HEK.hPD-L1) were produced essentially as described in **Example 3.5.** HEK.hPD-L1 cells have been engineered to express a high level of human PD-L1 and were used alongside MDA-MB-231 cells which express a medium level of human PD-L1 as well as SKBR3 cells which express a low level of human PD-L1 **(Table 14)** as quantified by Antibody Binding Capacity beads (Quantum Simply Cellular, Bans Laboratories, Inc. cat no. 816A) following manufacturer's instructions.

Table 14

Cell line	Antibody Binding Capacity
HEK WT	7463 (± 971)
HEK.hPD-L1	702000 (± 58000)
MDA-MB-231	137369 (± 2429)
SKBR3	14734 (± 239)

[0376] The $CD8^+$ T cells were isolated and activated using an anti-CD3 antibody as described in **Example 3.5.** HEK.hPD-L1 cells were plated at 2×10^5 cells per well on to anti-CD3 antibody-coated (8µg/ml) 96 well flat bottom plates in 100µl T cell culture medium (RPMI medium (Life Technologies, 61870-044) with 10% FBS (Life Technologies), 1X Penicillin Streptomycin (Life Technologies, 15140122), 1mM Sodium Pyruvate (Gibco, 11360-070), and 50µM 2-mercaptoethanol (Gibco, M6250)). Once HEK.hPD-L1 cells or HEK cells that were not transduced to express hPD-L1 used as controls had adhered after 4 hours incubation, all T cell

culture medium was removed and replaced with 100µl T cell culture medium containing T cells at a concentration of 5.0×10^5 cells/ml resulting in 5.0×10^4 cells/well.

[0377] For cell-based crosslinking with lower more physiological levels of PD-L1 expression, the human breast adenocarcinoma cell line, MDA-MB-231 (ATCC HTB-26), was used with the same methodology as described for HEK.hPD-L1 cell-based crosslinking.

[0378] mAb^2 were diluted in T cell medium at a 2X final concentration starting at 50nM and a 1:5 titration was carried out. 100µl of mAb^2 titration was added to the cells for a total assay volume of 200µl and 1X concentration of antibody.

[0379] Positive control anti-CD137 antibody (G1-AA/20H4.9) was diluted in T cell medium at a 2X final concentration starting at 50nM containing 50nM crosslinking agent (the anti-human CH2 antibody (mG1/MK1A6)) and a 1:5 titration was carried out. 100µl of diluted positive control antibody/crosslinker mix was added to the cells for a total of 200µl assay volume and 1X concentration of antibody.

[0380] The assay was incubated at 37°C, 5% CO_2 for 72 hours. Supernatants were collected and assayed with human IL-2 ELISA Ready-SET-Go! kit (eBioscience, Cat. 88-7025-88) following the manufacturer's instructions. Plates were read at 450 nm using the plate reader with the Gen5 Software, BioTek. Absorbance values of 630 nm were subtracted from those of 450 nm (Correction). The standard curve for calculation of cytokine concentration was based on a four-parameter logistic curve fit (Gen5 Software, BioTek). The concentration of human IL-2 (hIL-2) was plotted vs the log concentration of antibody and the resulting curves were fitted using the log (agonist) vs response equation in GraphPad Prism.

[0381] **Table 15** shows the EC_{50} values and maximum response of IL-2 release observed in the T cell activation assay in the presence of the anti-human CD137/PD-L1 mAb^2 tested with cell-based crosslinking. The positive control anti-human CD137 mAb, 20H4.9, shows an increase in hIL-2 release with an EC_{50} of 0.21 to 0.31 nM when crosslinked with anti-hCH2 antibody in either assay. All clones had activity in the assays, each displaying potency with sub-nanomolar EC_{50}s. mAb^2 containing Fcab FS22-172-003 elicited the greatest T cell response with EC_{50}s in the range of 0.19 to 0.31 nM in the HEK.hPD-L1 based assay and 0.01 - 0.02 nM in the MDA-MB-231 based assay. A subset of the mAb^2 (containing Fcabs FS22-053-008, FS22-053-011, FS22-053-014, FS22-173-003 and FS22-172-004) were also tested without crosslinking by PD-L1 expressed on HEK cells and showed no activity in this assay, as expected. **Figure 4** and **Figure 5** shows representative plots of IL-2 release for the T cell activation assay for mAb^2 listed in **Table 15.**

[0382] The FS22-053 and FS22-172 Fcab lineage was also tested in this assay using the lowest PD-L1 expressing human breast adenocarcinoma cell-line, SK-BR-3 (ATCC HTB-30).

As expected the lower PD-L1 expression resulted in lower $CD8^+$ T cell activation in line with the previous two assays (data not shown).

Table 15

	EC_{50} (nM) Donor 171115A		EC_{50} (nM) Donor 171115B	
mAb^2	**HEK.hPD-L1 XL**	**MDA-MB-231 XL**	**HEK.hPD-L1 XL**	**MDA-MB-231 XL**
FS22-053-008-AA/E05v2	0.16	0.01	0.11	0.02
FS22-053-008-AA/E12v2	0.10	0.01	0.11	0.02
FS22-053-008-AA/G12v2	0.13	0.02	0.12	0.02
FS22-053-017-AA/E05v2	0.15	0.01	0.12	0.01
FS22-053-017-AA/E12v2	0.11	0.01	0.12	0.01
FS22-053-017-AA/G12v2	0.10	0.01	0.20	0.01
FS22-172-003-AA/E05v2	0.27	0.02	0.19	0.02
FS22-172-003-AA/E12v2	0.24	0.02	0.31	0.02
FS22-172-003-AA/G12v2	0.21	0.02	0.22	0.01
G1-AA/20H4.9	0.21	0.31	0.29	0.28

[0383] The results showed that the mAb^2 could bind to cells expressing different levels of PD-L1. Binding to the cell-expressed PD-L1 resulted in crosslinking of the mAb^2 such that they were able to bind to, cluster and activate CD137 on T cells, as measured by IL-2 production. The level of activation observed related to the level of crosslinking by binding PD-L1, where the mAb^2 bound to cells expressing higher levels of hPD-L1 (HEK.hPD-L1) there was greater activation, whereas lower levels of PD-L1 expression elicited less activation.

***10.2 Activity* of *an anti-human CD137/PD-L1* mAb^2 *crosslinked with different populations of HEK.hPD-L1 cells in a human primary* $CD8^+$ *T cell activation* assay**

[0384] As the expression level of PD-L1 by different cell lines was observed to impact activation of CD137, it was decided to explore further the impact of PD-L1 expression on the

functional activity of the mAb^2 tested. A similar assay to that described in **Example 10.1** was performed, where the ratio of HEK.hPD-L1 to HEK.WT cells was varied in order to modulate the level of human PD-L1 expression in a population based approach.

[0385] HEK.hPD-L1 cells and HEK cells that were not transduced to express hPD-L1 (HEK.WT) were plated in different ratios to provide the percentage of HEK.hPD-L1 cells of the total HEK cells present listed in **Figure 6** (100%, 50%, 25%, 12.5%, 6.5% or 0%).HEK cells were plated at 2×10^5 total HEK cells per well onto anti-CD3 antibody-coated (8µg/ml) 96 well flat bottom plates in 100µl T cell culture medium (RPMI medium (Life Technologies, 61870-044) with 10% FBS (Life Technologies), 1X Penicillin Streptomycin (Life Technologies, 15140122), 1mM Sodium Pyruvate (Gibco, 11360-070), and 50µM 2-mercaptoethanol (Gibco, M6250)). Once all HEK cells had adhered after 4 hours incubation, all T cell culture medium was removed and replaced with 100µl T cell culture medium containing T cells at a concentration of 5.0×10^5 cells/ml resulting in 5.0×10^4 cells/well.

[0386] The assay was run with anti-human CD137/PD-L1 mAb2 FS22-172-003-AA/E12v2 but otherwise followed the protocol described in **Example 10.1.** The anti-CD137 positive control antibody G1-AA/20H4.9 was included with additional crosslinking via an anti-CH2 antibody. Antibody G1-AA/4420 was used as a negative control.

[0387] The results in **Figure 6** show that as the population of HEK.hPD-L1 cells increased, activity of the mAb^2 also increased, as illustrated by an increase in the maximum hIL-2 concentration observed. Where 100% of the HEK cell population present were HEK.hPD-L1, maximal crosslinking was achieved and the highest maximum hIL-2 concentration was observed. The positive control antibody G1-AA/20H4.9 also reached a similar maximum hIL-2 concentration when maximally artificially crosslinked by an anti-CH2 antibody.

[0388] The data supports the observation that the amount of PD-L1 present in the system (represented by testing cell lines expressing different levels of PD-L1 on their cell surface or by modulating the number of cells in a population which display PD-L1) controls the crosslinking of the mAb^2 and thereby dictates the level of CD137 agonism induced by the mAb^2. However, even where only low levels of PD-L1 are present, the mAb^2 was still capable of agonising CD137. The mAb^2 is therefore expected to have activity where PD-L1 is expressed in a system, and activated T cells that express CD137 are present. As the level of PD-L1 in the system increases, the agonism exerted is also expected to increase. In contrast to the mAb^2 which was still capable of inducing CD137 agonism in the presence of low levels of CD137, CD137/PD-L1 molecules which bind CD137 monovalently are expected to have low efficiency in the presence of low PD-L1 levels, as molecules bound to PD-L1 are likely to be too far apart to drive clustering of CD137, which is not expected to be an issue where the molecule can bind CD137 bivalently, as is the case in the mAb^2 of the invention.

10.3 Activity of anti-human CD137/PD-L1* mAb^2 *in a human primary mixed lymphocyte

***reaction* assay**

[0389] The activity of the anti-human CD137/PD-L1 mAb^2 was tested in a Mixed Lymphocyte Reaction (MLR) assay (see **Example 5.3.4).** The MLR assay used $CD4^+$ T cells from one donor and monocyte derived dendritic cells (iDCs) from another donor. As the immune cells contain physiological levels of immune checkpoint regulators, the MLR assay can be used to confirm that T cell activation is enhanced by the mAb^2 in a human system.

[0390] Expanded $CD4^+$ T cells and iDC were generated as described in **Example 5.3.4.**

[0391] Expanded T cells were thawed one day before the experiment, washed with AIM V Medium (Gibco, 12055-091) and incubated at 37 °C, 5% CO2 in AIM V Medium overnight. The anti-CD137 and anti-PD-L1 antibodies and anti-human CD137/PD-L1 mAb^2 listed in **Table 16** were diluted 4x the final concentration in triplicate in 50µl AIMV Medium in 96 well round bottom plates (VWR, 734-1797). An anti-Cytomegalovirus (CMV) gH glycoprotein antibody, designated MSL109 (described in WO1994/016730 A1), containing the LALA mutation was included as negative control. A 3-fold dilution series starting from 30 nM to 0.002 nM was tested. 1x104 iDC cells suspended in 50 µl AIM V Medium and 1x105 expanded $CD4^+$ T cells suspended in 100 µl AIM V Medium were both added to the antibody dilutions and incubated for 5 days at 37°C + 5% CO2. The following negative controls were included: $CD4^+$ T cells alone, iDC alone, $CD4^+$ T cells + iDCs, and AIM V Medium only. Supernatants were harvested, samples were diluted (1:25) and interferon gamma (IFN-γ) concentrations measured using Human IFN gamma ELISA Ready-SET-Go! Kit (Life Technologies, 88-7316-77). Plates were read at 450 nm using the plate reader with the Gen5 Software, BioTek. Absorbance values of 630 nm were subtracted from those of 450 nm (Correction). The standard curve for calculation of cytokine concentration was based on a four-parameter logistic curve fit (Gen5 Software, BioTek). The concentration of human IFN-γ was plotted vs the log concentration of antibody and the resulting curves were fitted using the log (agonist) vs response equation in GraphPad Prism.

[0392] The anti-human PD-L1 antibody G1/S70, showed potent activity in the MLR assay with an EC_{50} value of 0.06 nM and a maximum level of IFN-γ (E_{max}) of 1135 pg/ml **(Table 16,** representative **Figure 7A** and **7B).** The EC_{50} indicates the concentration of mAb at which half of the agonistic response is achieved, whereas the E_{max} is an absolute value that indicates the maximum concentration of IFN-γ achieved in the assay. No activity was observed with the negative control G1-AA/MSL109 antibody, as expected. The positive anti-human CD137 antibody control G1-AA/20H4.9, when crosslinked with anti-hCH2 antibody, did not elicit any activity, indicating that CD137 expression may be low and that PD-L1 blockade overwhelms CD137 signalling in this assay because PD-L1 blockade is very strong. Surprisingly, all anti-human CD137/PD-L1 mAb^2 tested in this assay showed very potent EC_{50} values of less than

0.04 nM and high E_{max} values in the range of 2626 to 3327 pg/ml. This indicates that the mAb^2 have increased potency in this assay above that of either of the PD-L1 and CD137 monoclonal antibodies.

Table 16

Molecule(s)	Type	EC50 (nM)	E_{max} (pg/ml)
FS22-172-003-AA/E05v2	mAb^2	0.03	2654
FS22-172-003-AA/E12v2	mAb^2	0.02	2626
FS22-053-008-AA/E05v2	mAb^2	0.02	2797
FS22-053-008-AA/E12v2	mAb^2	0.04	3128
FS22-053-017-AA/E 12v2	mAb^2	0.04	3327
G1-AA/20H4.9 + anti-human CH2	CD137 mAb	N/A	N/A
G1/S70	PD-L1 mAb	0.06	1135
G1-AA/MSL109	Isotype	N/A	N/A
$CD4^+$ T cells alone	Cell control	N/A	N/A
iDC alone	Cell control	N/A	N/A
$CD4^+$ T cells + iDC alone	Cell control	N/A	N/A
N/A - not applicable as low signal did not allow EC_{50} determination			

[0393] Following the same protocol described above, the activity of the anti-human CD137/PD-L1 mAb^2 FS22-172-003-AA/E12v2 was tested again in an MLR but this time against each component part (the anti-human FS22-172-003 Fcab in mock mAb^2 format and the anti-PD-L1 antibody G1-AA/E12v2), as well as the combination of the two.

[0394] The anti-human PD-L1 component antibody G1-AA/E12v2, showed potent activity in the MLR assay with an EC_{50} value of 0.08 nM and a maximum level of IFN-γ (E_{max}) of 12421 pg/ml **(Table 17;** representative **Figure 7C).** No activity was observed with the negative control G1-AA/4420 antibody, as expected, and no activity was observed with the anti-human Fcab FS22-173-003 in mock mAb^2 format. The positive anti-human CD137 antibody control, G1-AA/20H4.9, when crosslinked with anti-hCH2 antibody, did not elicit any activity, indicating that CD137 expression may be low and that PD-L1 blockade overwhelms the CD137 signalling in this assay because PD-L1 blockade is very strong as seen above. As expected, the anti-human CD137/PD-L1 FS22-172-003-AA/E12v2 mAb^2 showed a very potent EC_{50} value of 0.07 nM and a high E_{max} value of 17874 pg/ml. This indicates that the mAb^2 has increased potency in this assay above that of either of the anti-PD-L1 and anti-CD137 monoclonal antibodies alone or both in combination. The data also shows that the mAb^2 had greater potency than the combination of two antibodies comprising the Fcab and Fab binding sites of the mAb^2,

respectively.

Table 17

Molecule(s)	Type	EC_{50} (nM)	E_{max} (pg/ml)
FS22-172-003-AA/E12v2	mAb^2	0.07	17874
FS22-172-003-AA/HelD1.3	mAb^2	N/A	3574
G1-AA/E12v2	PD-L1 mAb	0.08	12421
FS22-172-003-AA/HelD1.3 + G1-AA/E12v2	Component Combination	0.06	12301
G1-AA/20H4.9 + anti-human CH2	CD137 mAb	1.9	4307
G1-AA/E12v2 + G1-AA/20H4.9 + anti-human CH2	mAb Combination	0.14	17525
G1-AA/4420	Isotype	N/A	N/A
$CD4^+$ T cells alone	Cell control	N/A	N/A
iDC alone	Cell control	N/A	N/A
$CD4^+$ T cells + iDC alone	Cell control	N/A	N/A
N/A - not applicable as low signal did not allow EC_{50} determination			

***10.4 Activity of anti-human CD137/PD-L1* mAb^2 *in an antigen recall T cell activation* assay**

[0395] The activity of anti-human CD137/PD-L1 mAb^2 was tested in an antigen recall T cell activation assay by measuring the immune response to two distinct peptide pools containing physiologically relevant antigens. One pool comprised MHC class I-restricted peptides from Cytomegalovirus, Epstein-Barr virus, and Influenza virus (CEF) which test $CD8^+$ T cell activation and the second pool comprised MHC class II-restricted peptides from Cytomegalovirus, Epstein-Barr virus, Influenza virus, and Tetanus toxin (CEFT), which tested $CD4^+$ T cell activation. As human PBMCs from a single donor were used, and as the immune cells contained physiological levels of immune checkpoint regulators and were stimulated by antigen presentation rather than T cell receptor crosslinking by anti-CD3 antibody, the results of the assay confirm that antigen-driven T cell activation is enhanced by the mAb^2 in a human system.

[0396] Cryopreserved peripheral blood mononuclear cells (PBMCs) were thawed and counted and 1.9×10^5 cells were seeded per well in to a 96 well flat bottom plate in 200 µl Roswell Park Memorial Institute (RPMI) media containing 10% fetal bovine serum (FBS) + 1 ng/ml IL-2 + 5

ng/ml IL-7 and either 1 µg/ml CEF peptide pool (Thinkpeptides, cat no. PX-CEF-G) or 1 µg/ml CEFT peptide pool (Thinkpeptides, cat no. PX-CEFT-G). Cells were incubated at 37°C with 5% CO_2 for 3 days. After 3 days, media was replenished by the addition of 22.5 µl fresh RPMI containing 10% FBS and maintaining 1 ng/ml IL-2 and 1 ng/ml IL-7. Cells were incubated at 37°C with 5% CO_2 for a further 4 days.

[0397] Cells were collected and pooled together and then distributed across 96 well round bottom plates at 1×10^5 cells per well in 150 µl RPMI containing 10% FBS + 1 ng/ml IL-2 + 5 ng/ml IL-7 and either 1 µg/ml CEF peptide pool or 1 µg/ml CEFT peptide pool. mAb^2 were diluted in the same media as cells were seeded in and added to the cells.

[0398] Each of the positive control anti-CD137 antibody (G1-AA/20H4.9) and positive control anti-PD-L1 antibody (G1-AA/E12v2) were diluted in the same media as cells were seeded in, at a 2X final concentration starting at 400 nM containing 400 nM crosslinking agent (the anti-human CH2 antibody (MK1A6)) and a 1:5 titration was carried out. 50 µl of diluted either positive control antibody/crosslinker mix was added to the cells for a total of 200µl assay volume and 1X concentration of antibody.

[0399] The assay was incubated at 37°C, 5% CO_2 for 72 hours. Supernatants were collected and assayed with an MSD U-PLEX kit (Meso Scale Discovery, cat no. K15067L-2) following the manufacturer's instructions. Plates were read on a MESO QuickPlex SQ 120 electrochemiluminescence plate reader instrument using a sample dilution of 1:5. A standard curve for the calculation of cytokine concentration was calculated using the MSD Discovery Workbench 4.0 software and the concentration of cytokine in the supernatant was fitted using the log (agonist) vs response equation in GraphPad Prism.

[0400] As shown in **Table 18** and **Table 19,** the anti-human PD-L1 antibody G1-AA/E12v2, showed activity for both $CD4^+$ and $CD8^+$ T cell activation with an EC_{50} value of 0.06 nM and 0.04 nM respectively (E_{max} of 65840 pg/ml and 86613 pg/ml respectively). The EC_{50} indicates the concentration of mAb at which half of the agonistic response is achieved, whereas the E_{max} is an absolute value that indicates the maximum concentration of IFN-γ achieved in the assay. The positive anti-human CD137 antibody control G1-AA/20H4.9, when crosslinked with anti-hCH2 antibody, showed activity for $CD8^+$ T cell activation, with an EC_{50} value of 0.33 nM and an E_{max} value of 116204 pg/ml, but did not elicit any activity for $CD4^+$ T cell activation, indicating that CD137 expression may be higher on $CD8^+$ T cells compared to $CD4^+$ T cells. No activity was observed with the negative control G1-AA/4420 antibody, as expected. Surprisingly, the mAb^2 showed activation in both $CD4^+$ T cell activation and $CD8^+$ T cell activation assays with EC_{50} values of 0.08 nM and 0.03 nM respectively. The mAb^2 could bind PBMC-expressed PD-L1 and had equivalent PD-L1 activity on both cell types. Further, binding to the PBMC-expressed PD-L1 resulted in crosslinking of the mAb^2 such that they were able to bind to, cluster and activate CD137 on both T cell subtypes, as measured by IFN-γ release.

The maximum concentration of IFN-γ released by T cells treated with mAb^2 was higher than any of the positive control antibodies with E_{max} values of 86680 pg/ml and 188242 pg/ml for $CD4^+$ T cell activation and $CD8^+$ T cell activation respectively. This indicates the mAb^2 has increased activity in this assay above that of either of the PD-L1 and CD137 monoclonal antibodies.

Table 18 - CEFT peptide pool antigen recall assay values ($CD4^+$ T cell activation)

Molecule(s)	**Type**	**EC_{50} (nM)**	**E_{max} (pg/ml)**
FS22-172-003-AA/E12v2	mAb^2	0.08	86680
G1-AA/20H4.9 + anti-human CH2	CD137 mAb	N/A	12965
G1-AA/E12v2	PD-L1 mAb	0.06	65840
G1-AA/4420	Isotype	N/A	N/A
N/A - not applicable as low signal did not allow EC_{50} determination			

Table 19 - CEF peptide pool antigen recall assay values ($CD8^+$ T cell activation)

Molecule(s)	**Type**	**EC_{50} (nM)**	**E_{max} (pg/ml)**
FS22-172-003-AA/E12v2	mAb^2	0.03	188242
G1-AA/20H4.9 + anti-human CH2	CD137 mAb	0.33	116204
G1-AA/E12v2	PD-L1 mAb	0.04	86613
G1-AA/4420	Isotype	N/A	N/A
N/A - not applicable as low signal did not allow EC_{50} determination			

***10.5 Activity of anti-human CD137/PD-L1* mAb^2 *in a PD-L1 blockade mouse DO11.10 T cell activation* assay**

[0401] The activity of FS22-172-003-AA/E12v2was tested in a mouse DO11.10 T cell activation assay to investigate PD-L1 checkpoint blockade activity. The functional activity towards human PD-L1 was examined in an IL-2 release assay using DO11.10 OVA T cell and LK35.2 B cell hybridoma cells as described in **Example 5.4.**

[0402] Results are shown **Table 20.** The anti-human CD137/PD-L1 mAb^2 showed potent activity in the mouse DO11.10 T cell activation assay with an EC_{50} value of 1.27 nM, which confirms that FS22-172-003-AA/E12v2 can bind PD-L1 and block the interaction of PD-L1 with PD-1. Its activity was similar to that of the positive control anti-human PD-L1 antibodies G1-AA/E12v2 and G1-AA/S70, indicating that no loss of anti-human PD-L1 activity occurred when G1-AA/E12v2 was incorporated in to the FS22-172-003-AA/E12v2 mAb^2 molecule.

Table 20 - DO11.10 T cell activation assay values (mouse IL-2 release)

Molecule(s)	Type	EC_{50} (nM)	E_{max} (pg/ml)
FS22-172-003-AA/E12v2	mAb^2	1.27	424
G1-AA/E12v2	PD-L1 mAb	1.19	480
G1-AA/S70	PD-L1 mAb	1.4	498
G1-AA/HelD1.3	Human IgG1 isotype control mAb	N/A	N/A
N/A - not applicable as low signal did not allow EC_{50} determination			

Example 11: Functional cross reactivity of anti-human CD137/PD-L1 mAb^2 in cynomolqus functional assays

***11.1 Activity of anti-human CD137/PD-L1* mAb^2 *in a cynomolgus DO11.10 T cell activation* assay**

[0403] CD137 clustering via agonist molecules on activated T cells elicits T cell activation and downstream signalling resulting in, but not limited to, IL-2 production. The ability of anti-human CD137/PD-L1 mAb^2 to activate DO11.10 cells expressing cynomolgus CD137 was tested in a T cell activation assay. A DO11.10 T cell activation assay using DO11.10 T cells engineered to overexpress cynomolgus CD137 was developed and T cell activation was assessed by measuring IL-2 release.

[0404] DO11.10 cells (National Jewish Health) expressing full-length cynomolgus CD137 (SEQ ID NO: 189) designated 'DO11.10.cCD137', were produced and expression of cynomolgus CD137 confirmed as described in **Example 1.2.**

[0405] The following anti-human CD137/PD-L1 mAb^2 were tested in this DO11.10 T cell activation assay: FS22-172-003-AA/lamG02v3, FS22-053-008-AA/E05v2, FS22-053-008-AA/E12v2, FS22-053-008-AA/G12v2, FS22-053-017-AA/E05v2, FS22-053-017-AA/E12v2, FS22-053-017-AA/G12v2, FS22-172-003-AA/E05v2, FS22-172-003-AA/E12v2, FS22-172-003-AA//G12v2. Dilutions of mAb^2 or G1-AA/MOR7480.1 positive control mAb either with or without anti-hCH2 antibody (mG1/MK1A6) crosslinker were prepared and added to DO11.10.cCD137 cells in a 96 well round bottom plate that had been coated overnight with 0.1 µg/ml anti-CD3 antibody (clone 17A2, BioLegend, 100208) and had been seeded with 2×10^5 HEK.cyPD-L1 cells to be used as cell-based crosslinking cells, which overexpress cynomolgus PD-L1. Cells over expressing cynomolgus PD-L1 were made as described in **Example 5.3.3,** using the

cynomolgus PD-L1 as described in **Example 9.5.** After an 18-hour incubation, supernatants were collected and assayed with mouse IL-2 ELISA kit (eBioscience, 88-7024-86) following the manufacturer's instructions. Plates were read at 450 nm using the plate reader with the Gens Software, BioTek. Absorbance values of 570 nm were subtracted from those of 450 nm (Correction). The standard curve for calculation of cytokine concentration was based on four parameter logistic curve fit (Gens Software, BioTek). The concentration of mIL-2 was plotted vs the log concentration of mAb^2 or benchmark mAb and the resulting curves were fitted using the log (agonist) vs response equation in GraphPad Prism.

[0406] All anti-human CD137/PD-L1 mAb^2 tested in this assay showed activity in the presence of HEK cells overexpressing cynomolgus PD-L1 to crosslink the mAb^2, indicating that all mAb^2 are able to bind both cynomolgus PD-L1 and bind and cluster cynomolgus CD137 eliciting DO11.10 T cell activation as readout by IL-2 production (see **Table 21** and **Figure** 8). All anti-human CD137/PD-L1 mAb^2 showed similar activity with EC50 values in the range of 0.06 to 0.11 nM and E_{max} values in the range of 8060 to 12300 pg/ml IL-2 only when crosslinked via cell-expressed cynomolgus PD-L1. In the absence of cynomolgus PD-L1, when the assay was carried out using HEK cells that do not express cynomolgus PD-L1, there was no activity as a result of no crosslinking. The positive control CD137 antibody G1-AA/MOR7480.1 which has been shown to be cynomolgus cross-reactive (Fisher *et al,* 2012) shows activity in this assay, when crosslinked with anti-CH2 however all anti-human CD137/PD-L1 mAb^2 are better both in terms of lower EC_{50} values and higher E_{max} values indicating cross-reactivity and better activity in a cynomolgus CD137 expressing system.

Table 21

Molecule	**Type**	**EC_{50} (nM) (crosslinked)**	**E_{max} (pg/ml) (crosslinked)**
FS22-172-003-AA-lam/GO2v3	mAb^2	0.08	12304
FS22-053-008-AA/E05V2	mAb^2	0.06	8057
FS22-053-008-AA/E12V2	mAb^2	0.08	9010
FS22-053-008-AA/G12V2	mAb^2	0.07	9656
FS22-053-017-AA/E05V2	mAb^2	0.10	9021
FS22-053-017-AA/E12V2	mAb^2	0.11	9362
FS22-053-017-AA/G12V2	mAb^2	0.08	8933
FS22-172-003-AA/E05V2	mAb^2	0.08	10520

Molecule	Type	EC_{50} (nM) (crosslinked)	E_{max} (pg/ml) (crosslinked)
FS22-172-003-AA/E12V2	mAb^2	0.06	11291
FS22-172-003-AA/G12V2	mAb^2	0.06	11216
G1-AA/MOR7480.1	CD137 mAb	0.71	5705

***11.2 Activity of anti-human CD137/PD-L1* mAb^2 *in a cynomolgus primary mixed leukocyte reaction* assay**

[0407] The activity of the anti-human CD137/PD-L1 mAb^2 was tested in a cynomolgus Mixed Lymphocyte Reaction (MLR) assay. Similar to the human MLR assay described in **Example 10.3** this assay measures a cellular immune assay response that occurs between two allogeneic lymphocyte populations (same species but genetically distinct). The assay uses $CD4^+$ T cells from one cynomolgus individual and $CD14^+$ monocytes from another individual. As the immune cells contain physiological levels of immune checkpoint regulators, the MLR assay can be used to confirm that T cell activation is enhanced by the mAb^2 in a cynomolgus system.

Isolation of $CD4^+$ T cells

[0408] PBMCs were isolated from cynomolgus monkey blood samples by Ficoll gradient separation. $CD4^+$ T cells were isolated using a Non-human primate $CD4^+$ isolation kit (Miltenyi Biotec Ltd, 130-091-102) according to the manufacturer's instructions. The cells were used fresh in the MLR assay.

Isolation of $CD14^+$ monocytes

[0409] Untouched monocytes were isolated from cynomolgus PBMCs using a Non-human primate CD14 isolation kit, (Miltenyi Biotec Ltd, 130-091-097) following the manufacturer's instructions. Monocytes were used fresh in the MLR assay.

MLR assay

[0410] The anti-human CD137/PD-L1 mAb^2 FS22-172-003-AA/E12v2 and anti-human PD-L1 antibody G1-AA/E12v2 and isotype control antibody G1-AA/4420 were diluted 4x the final concentration in triplicate in 50µl AIM V Medium in 96 well round bottom plates (VWR, 734-1797). An anti-hen egg lysozyme (HEL) antibody, designated HelD1.3 (described in **Example 2.2),** containing the LALA mutation was included as negative control. A 4-fold dilution series starting from 300 nM to 0.02 nM was tested. 7.5×10^4 monocyte cells suspended in 50 µl AIM V Medium and 7.5×10^5 $CD4^+$ T cells suspended in 100 µl AIM V Medium were both added to the antibody dilutions and incubated for 6 days at 37°C + 5% CO2. The following negative controls were included: $CD4^+$ T cells alone, $CD14^+$ monocytes alone, $CD4^+$ T cells + iDCs, and AIM V Medium only. Supernatants were harvested on day 2 and interleukin 2 (IL-2) concentrations were measured using a MILLIPLEX MAP Non-Human Primate Cytokine Magnetic Bead Panel (Merck Millipore, cat no. PRCYTOMAG-40K-01), supernatants were also harvested on day 6 and interferon gamma (IFN-y) concentrations measured using the same kit. Samples analysed on Bio Plex 200 machines, from Bio-Rad.

[0411] Both anti-human CD137/PD-L1 mAb^2 showed activity in this assay indicating that the mAb^2 are capable of binding cynomolgus PD-L1 and subsequently bind and cluster cynomolgus CD137 at expression levels endogenous to freshly isolated cynomolgus immune cells resulting in cytokine release as a result of T cell activation (see **Figure 9).**

***11.3 Activity of anti-human CD137/PD-L1* mAb^2 *in a cynomolgus primary PBMC* assay**

[0412] The activity of anti-human CD137/PD-L1 mAb^2 was tested in a cynomolgus primary PBMC assay. This assay measures a cellular immune assay response that occurs in a mixed population of PBMCs that have been stimulated with anti-CD3 mAb. The assay uses whole PBMCs from one cynomolgus individual and, as the immune cells contain physiological levels of immune checkpoint regulators, the PBMC assay can be used to confirm that T cell activation is enhanced by the mAb^2 in a cynomolgus system.

[0413] The experiment was performed essentially as described in **Example 3.5** with the following deviations: the positive control anti-CD137 antibody (G1-AA/MOR7480.1) was diluted in the same media as cells were seeded in, at a 2X final concentration starting at 40 nM containing 40 nM crosslinking agent (the anti-human CH2 antibody (MK1A6) and a 1:4 titration was carried out. The mAb^2 (FS22-172-003-AA/E12v2) and the negative control antibody (G1-AA/HelD1.3) were diluted in the same manner without the crosslinking agent. 100 µl of diluted antibody/crosslinker mix was added to the cells for a total of 200µl assay volume and 1X concentration of antibody. The assay was incubated at 37°C with 5% CO_2 for 3 days. Supernatants were collected and assayed with an MSD V-Plex Proinflammatory Panel 1 (NHP) kit (Meso Scale Discovery, cat no. K15056D-2) following the manufacturer's instructions. Plates were read on a MESO QuickPlex SQ 120 electrochemiluminescence plate reader instrument. A

standard curve for the calculation of cytokine concentration was calculated using the MSD Discovery Workbench 4.0 software and the concentration of cytokine in the supernatant was fitted using the log (agonist) vs response equation in GraphPad Prism.

[0414] **Figure 28A** shows a representative plot of IFN-γ release from T cell activation in the cynomolgus PBMC assay and **Figure 28B** shows a representative plot of IFN-γ release from T cell activation in the human PBMC assay.

[0415] The anti-human CD137 antibody G1-AA/MOR7480.1 when crosslinked with anti-hCH2 antibody, showed activity in both PBMC assays. No activity was observed with the negative control G1-AA/HelD1.3 antibody, as expected. Surprisingly, the mAb^2 showed similar activation in both PBMC assays with EC_{50} values of 0.08 nM and 0.03 nM respectively. The EC_{50} indicates the concentration of mAb at which half of the agonistic response is achieved. Therefore, the mAb^2 could bind to the PBMC-expressed PD-L1 resulted in crosslinking of the mAb^2 such that they were able to bind to, cluster and activate CD137 on both species' T cells, as measured by IFN-γ release. The maximum concentration of IFN-γ released by T cells treated with mAb^2 was higher than any of the positive control antibodies, indicating that the mAb^2 has increased activity in this assay above that of anti-CD137 monoclonal antibodies.

Example 12: Production of an anti-mouse CD137 Fcab

[0416] To test the activity of mAb^2 containing a CD137 antigen-binding region in *in vivo* mouse models, because of the risk of not being able to obtain mouse human cross-reactive Fcabs due to the low sequence homology between the mouse and human CD137 sequences, Fcabs which specifically bound to mouse CD137 were generated and characterised. After mouse CD137-binding Fcabs were generated, surprisingly, FS22-053-14 was subsequently found to be able to be mouse and human cross-reactive.

12.1 Naïve selection of anti-mouse CD137 Fcabs

[0417] In order to select Fcabs that bind to human CD137, yeast and phage display selection campaigns were employed, similar to that previously described for selection of Fcabs binding to human CD137 (see **Example 2.1).** Recombinant mouse dimeric CD137 or cells expressing full-length mouse CD137 used as antigens (see **Example 1).**

[0418] In-house mCD137-mFc-Avi antigen and DO11.10 cells expressing mCD137 (DO11.10.mCD137) were used in selections using the six phage libraries. All round 3 recombinant antigen outputs (576 clones) and all round 3 cell selection outputs (576 clones) were screened by phage ELISA and for cell binding to DO11.10.mCD137 cells. 34 Fcab clone hits were subcloned and produced as HelD1.3 mAb^2 as described in **Example 2.2.**

[0419] The four naive yeast libraries displaying CH1 to CH3 domains of human IgG1 previously used for selection of Fcabs binding to human CD137 were used for selections of Fcabs binding to mouse CD137. A total of 53 separate rounds of selections were performed to identify anti-mouse CD137 binders. In-house-produced, recombinant, dimeric, biotinylated mouse CD137 (mCD137-mFc-Avi) antigen was used to select binders from the yeast naive libraries.

12.2 Characterisation of anti-mouse CD137 Fcabs from naïve selections

[0420] The specificity of the anti-mouse CD137 Fcabs for mouse CD137 was tested in HeID1.3 "mock" mAb^2 format and measured by BLI in an Octet QKe system by testing for binding of the Fcabs to other mouse TNFRSF receptors (CD40, OX40, GITR). Streptavidin biosensors (PALL ForteBio 18-5021) to coat 10 ng/µl mouse CD40, GITR, OX40 receptors (all obtained from R&D Systems and biotinylated using an EZ-Link Sulfo-NHS-SS-Biotin kit from Thermoscientific #21328). Anti-mouse CD137 Fcabs in mock mAb^2 format were diluted 1:1 in kinetic buffer (PALL 18-1092) to a final concentration of at least 1µM. Antigen-coated sensors were dipped into the mAb^2 solutions for 180 seconds followed by 180 seconds in 1 × kinetic buffer. Antibodies for each of the TNFRSF receptors were used as positive controls. The Fcab clones FS22m-055, FS22m-063, FS22m-066, FS22m-075, FS22m-135, FS22m-055, FS22m-063, FS22m-066 did not bind to any of the TNFRSF receptors tested, thus demonstrating their specificity for mouse CD137.

[0421] HEK.FRT.luc cells expressing the mouse CD137 sequence (SEQ ID NO: 187) were produced following the same methodology as previously described in **Example 2.3.** The mAb^2 containing the anti-mouse CD137 Fcabs previously selected were screened using this cell line, HEK.FRT.luc.mCD137, according to the method described in **Example 2.3.** 56 mAb^2 were tested of which 29 were positive for NF-κB activity. Lob12.3 containing a human IgG1 Fc with a LALA mutation (G1-AA/Lob12.3), was used as a positive control anti-mouse CD137 mAb and showed an increase in luminescence confirming the assay's validity. HeID1.3, also containing a human IgG1 Fc with a LALA mutation, was used as a negative control human IgG isotype to rule out interference from the human IgG mock Fab in this assay. EC_{50}s were calculated where possible and mAb^2 which did not reach a plateau in activity were disregarded in favour of mAb^2 which showed classic sigmoidal activity kinetics. mAb^2 were ranked in order of EC_{50} and fold-change in activity upon Protein L crosslinking. FS22m-063 was selected based on it having the best EC_{50} upon crosslinking (1.44nM) and highest fold-change in activity upon crosslinking (27-fold).

***12.3 Activity* of *FS22m-063, FS22-053-014 and FS22-053-017 Fcabs in mock* mAb^2 *format in mouse CD137 DO11.10 T cell activation* assay**

[0422] The FS22-053-017 clone (in HeID1.3 mock mAb^2 format) was also compared against the murine CD137 binding Fcab clone FS22m-063 (also in HeID1.3 mock mAb^2 format), as well as the parental FS22-053-014 clone (in HeID1.3 mock mAb^2 format), in a mouse CD137 DO11.10 T cell activation assay as described in **Example 2.4.** The mAb^2 molecules were crosslinked with Protein L at a 4:1 molar ratio (mAb^2:Protein L). The results are shown in **Table 22.**

[0423] As expected, all of the molecules tested showed activity as measured by IL-2 release when crosslinked by Protein L but had no activity when not crosslinked. FS22m-063 which was selected to bind to mouse CD137 had the best activity in the assay, with an EC_{50} of 0.39nM when crosslinked. Both FS22-053-14 and FS22-053-017 had activity in the assay, indicating that function was not lost due to mutagenesis, though FS22-053-017 had a slight loss in activity with an EC_{50} which was approximately 8-fold worse than FS22-053-14 when cross linked by Protein L. **Figure 10** shows that the affinity-matured human and murine cross-reactive CD137 Fcabs FS22-053-014 and FS22-053-017, and anti-mouse CD137 Fcab FS22m-063, in HeID1.3 mock mAb^2 format activate CD137 when crosslinked with Protein L leading to a release of mIL-2 in a DO11.10 T cell activation assay.

Table 22

Fcab clone (in HeID1.3 mAb^2 format) or mAb	**IL-2 release with or without Protein L crosslinking**		
	No XL	**+XL E_{max} (IL-2 pg/ml)**	**+XL EC_{50} (nM)**
FS22-053-014	N/A	28071	2.04
FS22-053-017	N/A	41042	16.74
FS22m-063	N/A	24175	0.39
G1-AA/Lob12.3 + Protein L	N/A	21332	2.26
N/A - not applicable as low signal did not allow EC_{50} determination			

Example 13: *In vitro* characterisation of anti-mouse CD137/PD-L1 mAb^2

[0424] To test the activity of mAb^2 containing a CD137 antigen-binding region in *in vivo* mouse models, FS22m-063 was chosen as the Fcab which showed the best activity in the T cell activation assay as described in **Example 12.3.**

13.1 Construction, expression and purification of anti-mouse CD137/PD-L1 mAb^2

[0425] Anti-mouse CD137/PD-L1 mAb^2 were produced comprising the anti-mouse CD137 Fcab FS22m-063 and also a PD-L1 binding Fab region (clone YW243.55.S70 from US 8,217,149 B2). They were prepared similarly to the method described in **Example 3.2** by substitution of part of the CH3 of the anti-PD-L1 binding antibody containing the AB, CD and EF loops with the corresponding region of the Fcab. These PD-L1 model mAb^2 comprised a LALA mutation in the CH2 domain (AA). The introduction of the LALA mutation in the CH2 domain of human IgG1 is known to reduce Fc y receptor binding (Bruhns, P., *et al.* (2009) and Hezareh M., *et al.* (2001)).

[0426] FS22m-063-AA/PD-L1 mAb^2 were produced by transient expression in HEK293-6E cells and purified using mAb Select SuRe protein A columns.

***13.2 Activity of anti-mouse CD137/PD-L1* mAb^2 *in a mouse primary OT-1 T cell activation* assay**

[0427] To test the activity of the anti-mouse CD137/PD-L1 mAb^2 on cells which have not been engineered to overexpress CD137, a mouse primary T cell assay was needed. Activated cytotoxic $CD8^+$ T cells are responsible for directly killing cancer cells and express CD137 on their cell surface (Ye *et al,* 2014). Clustering of CD137 is known to be essential to induce downstream signalling and further $CD8^+$ T cell activation. A $CD8^+$ T cell activation assay was therefore used to assess the ability of mAb^2 to drive clustering and subsequent downstream signalling of CD137. Whilst attempts were made to mirror the human $CD8^+$ T cell activation assay identically, murine $CD8^+$ T cells isolated from naive C57BL/6 or Balb/c spleens did not show the activation potential required for such an assay. Therefore, an alternative antigen-specific $CD8^+$ T cell activation assay was developed. $CD8^+$ T cell activation was achieved by antigen stimulation of genetically modified OT-1 T cells, isolated from C57BL/6 OT-1 mice (Jackson Laboratory, Cat no. 003831) having a T cell receptor specific for ovalbumin peptide 257-264, and was determined by the release of IL-2.

[0428] To isolate $CD8^+$ T cells, splenocytes were isolated from fresh OT-1 mouse spleens. Briefly, each spleen from a C57BU6 OT-1 mouse was collected and stored in PBS before being transferred to a well of a 6-well tissue culture plate and mechanically disrupted with 2 needles. The disrupted spleen was passed through a 70µm cell strainer and the strainer was rinsed with PBS. The cell suspension was then pelleted by centrifugation, the supernatant removed, and red blood cells were lysed through the addition of 10 ml 1X red blood cell lysis buffer (eBioscience, 00-4300-54) according to the manufacturer's instructions. Splenocytes were plated for T cell activation medium (IMDM, 5%FCS, 50µM 2-Mercapto Ethanol, 1X Penstrep) containing 10nM SIINFEKL peptide (SEQ ID NO: 194) InvivoGen, cat no. vac-sin) in 6-well

plates at 10×10^6 cells per well. Plates were incubated for 48 hours at 37'C with 5% CO2. After 48 hours $CD8^+$ T cells were isolated by using a $CD8^+$ T cell Isolation Kit (Miltenyi Biotec, 130-104-075) following manufacturer's instructions. Isolated and activated $CD8^+$ T cells were plated in medium (IMDM, 5% FCS, 50µM 2-Mercapto Ethanol, 1X Penstrep) supplemented with 30U/ml IL-2 (Peprotech, AF-200-02) and kept at less than 1×10^6 per ml at each daily split for 3 further days. After the three days of expansion cells were then used in the following assay.

[0429] Incubation with B16.F10 cells, which were cultured in the presence of IFN-γ to induce expression of PD-L1, and that were then pulsed with SIINFEKL peptide was used as a first signal to drive initial activation of the OT-1 T cells and were subsequently used to assess the efficacy of anti-mouse CD137/PD-L1 mAb^2 FS22m-063-AA/S70.

Briefly, B16.F10 cells were first cultured in the presence of 20 ng/ml murine IFN-γ

[0430] (Peprotech, cat no. AF-315-05-100LIG) to induce PD-L1 expression. These cells were then incubated with 500nM SIINFEKL peptide for one hour at 37°C before being seeded at 1.5 × 10^4 cells per well in 100 µl media in a flat bottom 96-well plate. 2 × 10^4 OT-1 cells per well were added to the B16.F10 cells in 50µl media. Test antibodies (FS22m-063-AA/S70, G1-AA/S70, G1-AA/Lob12.3, FS22m-063-AA/HelD1.3) were prepared in a 1:4 titration starting at 160nM (4X final concentration) and 50µl of antibody mix was added to each well accordingly resulting in a final assay volume of 200µl. The assay was incubated for 3 days at 37°C with 5% CO_2. After 3 days, supernatants were harvested and an ELISA for mIFN-γ (eBioscience, cat no. 88-7314-88) was performed according to manufacturer's instructions.

[0431] As seen in **Figure 11** and in **Table 23,** the anti-mouse CD137/PD-L1 mAb^2 has the highest potency with an EC_{50} value of 0.003 nM. This assay indicates that the mAb^2 has strong potency as a result of clustering of CD137 leading to increased agonism and $CD8^+$ T cell activation.

Table 23

Molecule	Type	EC_{50} (nM)	E_{max} (pg/ml)
FS22m-063-AA/S70	mAb^2	0.003	23886
G1-AA/S70 + G1-AA/Lob12.3 + anti-hCH2	Positive control mAb combination	0.02	24703
G1-AA/S70	PD-L1 mAb	0.02	19477
G1-AA/Lob12.3 + anti-hCH2	CD137 mAb	0.36	17833
FS22m-063-AA/HelD1.3	Mock mAb^2	n/a	3854
N/A means - not applicable as low signal did not allow EC_{50} determination			

[0432] Having shown activity *in vitro* and activity superior to positive antibody controls, it was desirable to then test the anti-mouse CD137/PD-L1 mAb^2 in a suitable *in vivo* syngeneic mouse tumour model.

Example 14: *In vivo* characterisation of anti-mouse CD137/PD-L1 mAb^2

14.1 Activity of anti-mouse CD137/PD-L1* mAb^2 *in a CT26 syngeneic mouse tumour model

[0433] Having shown that the FS22m-063 Fcab is capable of driving clustering and activation of CD137 *in vitro,* it was desirable to test its ability to activate CD137 *in vivo.*

Preparation of FS22m-063 Fcab in mAb^2 format for *in vivo* testing in mice

[0434] A mAb^2 comprising the anti-mouse CD137 Fcab, FS22m-063, and a Fab region specific for PD-L1 using similar methodology to the model mAb^2 produced in **Example 3.2** was prepared and tested for *in vivo* anti-tumour activity in a CT26 syngeneic mouse tumour model.

Controls: G1/Lob12.3, G1-AA/Lob12.3, G1/S70, G1-AA/4420.

[0435] Control antibodies for the *in vivo* experiments were produced by joining the variable heavy region of the anti-PD-L1 antibody S70 (clone YW243.55.S70 from US 8,217,149 B2) to the human IgG1 (G1m17) constant region containing the LALA mutation, and the variable light region from the S70 antibody was joined to the human constant region (Lm1) via human kappa J- region. The anti-mouse CD137 antibody Lob12.3 (Taraban *et al.,* 2002) in human IgG1 format with and without the LALA mutation in the constant region was used as an anti-mouse CD137 positive control antibody. The mAb^2 was generated by replacing the CH3 domain of the reformatted construct described above with FS22m-063 and was designated 'FS22m-063-AA/S70'.

[0436] Syngeneic mouse models are accepted as appropriate murine systems for testing the anti-tumour effect of inhibiting therapeutic targets and have been used extensively to validate development of human therapeutics. The CT26 syngeneic tumour model was used in this experiment as CT26 tumours are known to be highly immunogenic (Lechner *et al,* 2013) and partially respond to anti-CD137 antibody monotherapy (Kim *et al,* 2008) and express PD-L1

(Kleinovink *et al.,* 2017).

[0437] Balb/c female mice (Charles River) aged 8-10 weeks and weighing 20-25 g each were rested for one week prior to the study start. All animals were micro-chipped and given a unique identifier. Each cohort had 12 mice. The CT26 colon carcinoma cell line (S. Rosenberg, NIH) was initially expanded, stored, and then pre-screened by IDEXX Bioresearch for pathogens using the IMPACT I protocol and shown to be pathogen-free.

[0438] Each animal received 0.1×10^6 cells injected subcutaneously in the left flank in 100µl DMEM. 7 days following tumour cell inoculation, mice which did not have tumours at this point were removed from the study.

[0439] The FS22m-063-AA/S70 mAb^2 and control antibodies (G1/Lob12.3, G1-AA/Lob12.3 (anti-CD137 positive controls), G1/S70 (positive control anti-PD-L1), G1-AA/4420 (isotype control)) were injected intraperitoneally into mice at 20µg per mouse (a final concentration of ~1 mg/kg) in DPBS + 1mM arginine + 0.05 Tween 80. Each mouse received the mAb^2 molecule or the control antibody or a combination of two control antibodies by 200 µl intraperitoneal (IP) injection on days 7, 9, and 11 following tumour inoculation. Accurate measurements of tumours were taken, any drug dosing due on the day in question was performed, and the mice were put under close observation for the remainder of the study. Tumour volume measurements were taken with callipers to determine the longest axis and the shortest axis of the tumour. The following formula was used to calculate the tumour volume:
$L \times (S^2) / 2$
Where L = longest axis; S= shortest axis

[0440] As shown in **Figure 12,** the FS22m-063-AA/S70 mAb^2 showed significant tumour growth inhibition compared to mice treated with some of the control antibodies. Statistical significance was shown pairwise for growth rates over the full time of study using the Mixed Model analysis comparing all groups. None of the mice showed signed of overt toxicity and all treatments were well tolerated indicating that a bispecific targeting CD137 and PD-L1 does not induce significant toxicity.

[0441] All animals containing tumours measuring equal or below $62.5mm^3$ were counted as fully responding animals (see **Table 24). 28%** of the animals treated with G1/Lob12.3 (anti-CD137 positive control without LALA mutation) were deemed to be tumour free at the end of the study, while 7% of the animals treated with G1-AA/Lob12.3 (anti-CD137 positive control with the LALA mutation) and 0% of FS22m-063-AA/S70 (anti-mouse CD137 Fcab FS22m-063 in a model PD-L1 mAb^2 format) treated mice were deemed tumour free. FS22m-063-AA/S70 induces significant tumour growth inhibition, in a CT26 syngeneic tumour model compared to IgG control treated mice. No animals treated with G1-AA/4420 (IgG control) or G1/S70 (PD-L1 positive control) were tumour free by the end of the study. The graphs in **Figure 17** show the tumour growth measurements in mm^3 for each animal over time.

Table 24: Number and percentage of tumour-free mice by study end in the CT26

syngeneic tumour study.

Compound	Tumour-free mice by study end
G1-AA/4420	0/13 (0%
G1-AA/Lob12.3	1/14 (7%)
G1/S70	0/14 (0%)
G1/Lob12.3	4/14 (28%)
G1-AA/Lob12.3 + G1/S70	1/14 (7%)
FS22m-063-AA/S70	0/14 (0%)

[0442] The study shows that in mice with a fully functioning immune system, in a CT26 syngeneic mouse tumour model, CD137 agonism, presumably as a result of crosslinking via PD-L1, leads to a reduction in tumour growth, presumably through increased cytotoxic activity of $CD8^+$ T cells in the tumour.

[0443] Survival analysis **(Figure 18** and **Table 25)** showed that the FS22m-063-AA/S70 induced a significant survival benefit compared to isotype control (G1-AA/4420). **Table 25** shows a summary of median survival in days for each group and pairwise statistical analyses (Log-rank) in CT26 syngeneic tumour model grown subcutaneously in Balb/c mice treated with G1-AA/4420 (IgG control), the combination of G1/S70 plus G1-AA/Lob12.3 and FS22m-063-AA/S70 (the anti-mouse CD137 Fcab FS22m-063 in a model PD-L1 mAb^2 format). FS22m-063-AA/S70 resulted in significantly increased survival compared to IgG control treated mice. FS22m-063-AA/S70 showed no significant survival benefit over the combination of G1/S70 + G1-AA/Lob12.3.

Table 25: Median survival times for animals treated with each compound.

Compound	Median Survival (Days)	p-values Log-rank	
FS22m-063-AA/S70	30.5		
G1/S70 + G1-AA/Lob12.3	27	0.2235	Ns
G1-AA/4420	26	0.0058	**

[0444] Having shown that in mice with a fully functioning immune system, in a CT26 syngeneic mouse tumour model, CD137 agonism, presumably as a result of crosslinking via PD-L1, leads to a reduction in tumour growth, presumably through increased cytotoxic activity of $CD8^+$ T cells in the tumour, the study was repeated with the following deviations.

The FS22m-063-AA/S70 mAb^2 and control antibodies G1-AA/Lob12.3 (positive control anti-CD137), G1/S70 (positive control anti-PD-L1), G1-AA/HelD1.3 (isotype control)) were injected intraperitoneally into mice at 200µg per mouse (a final concentration of ~10 mg/kg) in DPBS + 1mM arginine + 0.05 Tween 80. Each mouse received the mAb^2 molecule or the control

antibody or a combination of two control antibodies by 200 µl intraperitoneal (IP) injection on days 7, 9, and 11 following tumour inoculation.

[0445] Treatment with FS22m-063-AA/S70 resulted in significant tumour growth inhibition (shown as tumour volume mean in **Figure 19)** compared to the control antibodies.

[0446] Survival analysis **(Figure 20** and **Table 26)** showed that the FS22m-063-AA/S70 induced a significant survival benefit compared to isotype control (G1-AA/HeID1.3) and G1/S70. There was no significant survival benefit over G1-AA/Lob12.3.

[0447] Table 26 shows a summary of median survival in days for each group and pairwise statistical analyses (Log-rank) in CT26 syngeneic tumour model grown subcutaneously in Balb/c mice treated with G1-AA/HeID1.3 (IgG control), G1/S70 (anti-PD-L1 positive control), G1-AA/Lob12.3 (anti-CD137 positive control) and FS22m-063-AA/S70 (anti-mouse CD137 Fcab FS22m-063 in a model PD-L1 mAb^2 format). FS22m-063-AA/S70 induced significant survival in a CT26 syngeneic tumour model compared to IgG control treated mice and CD137 positive control treated mice.

Table 26: Summary of median survival in days for each group and pairwise statistical analyses (Log-rank) in CT26 syngeneic tumour model.

Compound	Median Survival (Days)	p-values Log-rank	
FS22m-063-AA/S70	48.5		
G1/S70	23.5	0.0057	**
G1-AA/Lob12.3	28	0.131	Ns
G1-AA/HeID1.3	27	0.0149	*

14.2 Dose-response activity of anti-mouse CD137/PD-L1* mAb^2 *in a CT26 syngeneic mouse tumour model

Dose-response anti-tumour activity

[0448] The anti-mouse CD137/PD-L1 mAb^2 FS22m-063-AA/S70 showed anti-tumour activity in the CT26 syngeneic tumour model at a dose of 20µg per mouse (-1mg//kg) dosed three times every two days (q2dx3). To investigate the optimum dose of FS22m-063-AA/S70 mAb^2 *in vivo,* a range of doses (2, 6, 20 and 200 µg/mouse, equivalent to approximately 0.1, 0.3, 1, and 10 mg/kg) were tested in the CT26 model at a q2dx3 dosing schedule as described above starting 7 days after tumour cell inoculation. The negative control antibody G1-AA/4420 was included at a dose of 200µg per mouse (~10 mg/kg) with the same scheduling. The positive control

antibody G1/Lob12.3 was included at a sub-optimal dose of 20µg per mouse (~1 mg/kg) with the same scheduling.

[0449] Following the same protocol as described in **Example 14.1,** Balb/c female mice (Charles River) aged 8-10 weeks and weighing 20-25 g each were rested for one week prior to the study start. All animals were micro-chipped and given a unique identifier. Each cohort had 12 mice. The CT26 colon carcinoma cell line (ATCC CRL-2638) was initially expanded, stored, and then pre-screened by IDEXX Bioresearch for pathogens using the IMPACT I protocol and shown to be pathogen-free. Each animal received 0.1×10^5 cells injected subcutaneously in the left flank in 100µl DMEM. 7 days following tumour cell inoculation, mice which did not have tumours at this point were removed from the study.

[0450] On study day 7, the FS22m-063-AA/S70 mAb^2 was injected intraperitoneally into mice at a final concentration according the dose range described above. Control antibodies (G1/Lob12.3 (CD137 positive control antibody), G1-AA/4420 (isotype control)) were injected intraperitoneally into mice at a final concentration of 20µg per mouse (~1 mg/kg) and 200µg per mouse (~10 mg/kg) respectively in DPBS + 1mM arginine + 0.05 Tween 80. Each mouse received the mAb^2 molecule or the control antibody by 200 µl intraperitoneal (IP) injection on days 7, 9, and 11 following tumour inoculation (q2dx3). Accurate measurements of tumours were taken, any drug dosing due on the day in question was performed, and the mice were put under close observation for the remainder of the study. Tumour volume measurements were taken with callipers to determine the longest axis and the shortest axis of the tumour as described in **Example 14.1.**

[0451] As shown in **Figure 13A,** the FS22m-063-AA/S70 mAb^2 showed significant tumour growth inhibition compared to mice treated with the isotype control (G1-AA/4420) when dosed at ~0.3 mg/kg up to ~10 mg/kg Statistical significance was shown using the Mixed Model analysis comparing all groups Survival analysis, **Figure 13B** and **Table 27,** shows that FS22m-63-AA/S70 mAb^2 induces a statistically significant survival benefit compared to isotype control in CT26 syngeneic model when dosed at levels above 0.3 mg/kg. Statistical significance performed using log rank (Mantel Cox) test. * $P \leq 0.05$; ** $P \leq 0.01$; *** $P \leq 0.001$; **** $P \leq 0.0001$. None of the mice showed signed of overt toxicity and all treatments were well tolerated.

Table 27

Treatment	Median Survival (days)	Statistical significance (log rank test)			
		FS22m-063-AA/S70			
		10mg/kg	1mg/kg	0.3mg/kg	0.1mg/kg
FS22m-063-AA/S70 10mg/kg	39				
FS22m-063-AA/S70 1 mg/kg	29	ns			

Treatment	Median Survival (days)	Statistical significance (log rank test)			
		FS22m-063-AA/S70			
		10mg/kg	1mg/kg	0.3mg/kg	0.1mg/kg
FS22m-063-AA/S70 0.3mg/kg	24	***	*		
FS22m-063-AA/S70 0.1 mg/kg	21	****	***	**	
G1-AA/4420 10mg/kg	21	****	**	*	ns
NS means not significant					

[0452] The study shows that in mice with a fully functioning immune system, in a CT26 syngeneic mouse tumour model, CD137 agonism, presumably as a result of crosslinking via PD-L1, leads to a dose dependent reduction in tumour growth and a dose dependent increase in survival, presumably through increased cytotoxic activity of $CD8^+$ T cells in the tumour.

14.3 Dose-response mechanism of action

[0453] The mechanism of action of the anti-mouse CD137/PD-L1 mAb^2 was assessed in the same CT26 tumour-bearing mouse model as described in **Example 14.2.** Blood, spleen and tumour tissue from CT26 tumour-bearing treated with FS22m-063-AA/S70 at four different doses (2, 6, 20 and 200 µg/mouse, equivalent to approximately 0.1, 0.3, 1, 10 mg/kg) as well as negative control antibody G1-AA/4420 was tested for T cell activation and proliferation markers known to be downstream effects of CD137 agonism (Fisher *et al.,* 2012).

[0454] Following the same study protocol as described in this example at day 9 (48 hours after first dose), day 11 (48 hours after second dose) and at day 15 (96 hours after third and final dose) blood was collected in to EDTA-containing tubes by cardiac puncture, and spleen and tumour tissue was collected by dissection. Spleen and tumour tissue was disaggregated to single cell suspension by standard mechanical and enzymatic methods. Red blood cells were lysed once in red blood cell lysis buffer (eBioscience, cat no. 00-4300-54) according to manufacturer's instructions.

[0455] Red blood cells of the uncoagulated blood were lysed twice in red blood cell lysis buffer (eBioscience cat no 00-4300-54) according to manufacturer's instructions.

[0456] All samples were then treated the same. Cells were then washed once with PBS and samples stained with fixable viability dye (Invitrogen, cat no. 65-0865-14) at 1:3000 dilution in PBS following manufacturer's instructions. The cells were stained for flow cytometry for cell surface markers with an antibody staining panel (all but Ki67 and FoxP3 antibodies) **(Table 28** below) in the presence of Fc block (eBioscience cat no 14-0161-86 at 1:50) for 30 minutes at

4°C. The cells were then fixed and permeabilized with the eBioscience Foxp3 staining kit (eBioscience cat no 00-5523-00) according to manufacturer's instructions. Cells were resuspended in 100 µl permeabilization buffer with Ki67 and Foxp3 antibodies in the presence of Fc block (all in 1:100 dilution) and incubated 30 minutes in the dark at room temperature. Cells were then washed once with permeabilization buffer and resuspended in 200 µl PBS + 0.5% BSA. The cells were then analysed in a BD Fortessa flow cytometer. Data was analysed with FlowJoX, Excel and GraphPad Prism. The data plotted represents the T cell abundance and proliferation observed over time for $CD4^+$ and $CD8^+$ T cell subpopulations. The data is presented as the percentage of the parental population according to the population description in the Y axis.

[0457] As shown in **Figure 14B** the $CD8^+$:$CD4^+$ percentage ratio increases in favour of $CD8^+$ T cells, both in the tumour and the periphery in line with an increased dose of anti-mouse CD137/PD-L1 mAb^2, indicating that the treatment causes a shift in the balance of the two T cell subpopulations likely to be as a result of increase $CD8^+$ T cell numbers. By day 15, the proliferation marker on $CD8^+$ T cells is increased in line with treatment dose level with highest proliferation seen at the highest dose level. This would indicate that $CD8^+$ T cells are proliferated which is a sign of activation and would account for the increased $CD8^+$ T cell numbers resulting in an increased $CD8^+$:$CD4^+$ T cell ratio.

[0458] Overall, this study has shown that increasing the dose level of anti-mouse CD137/PD-L1 results in more $CD8^+$ T cells in the tumour. The main role of $CD8^+$ T cells (often also called cytotoxic lymphocytes) is the killing of infected or malignant cells via 3 main mechanisms: 1) release of cytokines e.g. TNFα and IFN-γ, 2) production and release of cytotoxic granules and 3) expression of FasL. The presence of more $CD8^+$ T cells in the tumour following treatment with anti-mouse CD137/PD-L1 presumably results in cytotoxic activity via these mechanisms against the tumour, resulting in tumour control.

Table 28

Target	Antibody Clone	Fluorophore	Company	Cat no.
CD45	30-F11	AF700	eBioscience	56-0451-82
CD3	145-2C11	PECy7	eBioscience	25-0031-82
$CD4^+$	RM4-5	BUV395	BD Biosciences	740208
$CD8^+$	53-6.7	BUV737	BD Biosciences	564297
FoxP3	Fjk-16S	PerCP-Cy5.5	Invitrogen	45-5773-82
CD44	IM7	BV650	BioLegend	103049
CD62L	MEL-14	Bv421	BioLegend	104435
CD69	H1.2F3	Bv510	BioLegend	104532
Ki67	16A8	647	BioLegend	652407
PD-L1	10F.9G2	Bv785	BioLegend	124331

Target	Antibody Clone	Fluorophore	Company	Cat no.
IgG	MK1A6	FITC	Bio-Rad	MCA647F
Viability	n/a	780	Invitrogen	65-0865-14
n/a means not applicable				

14.4 Activity of anti-mouse CD137/PD-L1* mAb^2 *in a MC38 syngeneic mouse tumour model

[0459] Syngeneic mouse models are accepted as appropriate murine systems for testing the anti-tumour effect of inhibiting therapeutic targets and have been used extensively to validate development of human therapeutics. The MC38 syngeneic tumour model was used in this experiment as MC38 tumours are known to be highly immunogenic and respond to anti-CD137 antibody monotherapy (Kocak *et al,* 2006) and express PD-L1 (Juneja *et al,* 2017).

[0460] C57BL/6 female mice (The Jackson Laboratory) aged 9-10 weeks and weighing 18 to 24 g each were rested for one week prior to the study start. All animals were micro-chipped and given a unique identifier. Each cohort had 12 mice. The MC38 colon carcinoma cell line (National Cancer Institute, USA) was initially expanded, stored, and then pre-screened for pathogens and shown to be pathogen-free. Each animal received 1×10^6 cells injected subcutaneously in the right flank in 100µl in serum-free culture medium (Dulbecco's Modified Eagle Medium). 7 days following tumour cell inoculation, mice which did not have tumours at this point were removed from the study.

[0461] The FS22m-063-AA/S70 mAb^2 and control antibodies (G1-AA/Lob12.3 (CD137 positive control), G1-AA/S70 (positive control PD-L1), G1-AA/4420 (isotype control)) were injected intraperitoneally into mice at a fixed concentration of 20 µg per dose in DPBS + 1mM arginine + 0.05 Tween 80. Each mouse received the mAb^2 molecule or the control antibody by 200 µl intraperitoneal (IP) injection on days 7, 9, and 11 following tumour inoculations. Accurate measurements of tumours were taken, any drug dosing due on the day in question was performed, and the mice were put under close observation for the remainder of the study. Tumour volume measurements were taken with callipers to determine the longest axis and the shortest axis of the tumour. The following formula was used to calculate the tumour volume:
$L \times (S^2) / 2$
Where L = longest axis; S= shortest axis

[0462] As shown in **Figure 15,** the FS22m-063-AA/S70 mAb^2 showed significant tumour growth inhibition compared to mice treated with any of the control antibodies. Statistical significance was shown pairwise for growth rates over the full time of study using a Mixed Model analysis comparing all groups. As shown in **Table 29,** unexpectedly all mice treated with

FS22m-063-AA/S70 mAb^{2}were tumour free at the end of the study, compared to only 4 of 12 mice treated with a combination of anti-PD-L1 and anti-CD137 antibodies (G1-AA/S70 + G1-AA/Lob12.3) or the PD-L1 or CD137 antibodies alone. The graphs in **Figure 21** show the tumour growth measurements in mm^3 for each animal over time.

Table 29

Group	% Tumour Free Mice	Number Tumour Free Mice
G1-AA/Lob12.3	16%	2/12
G1-AA/4420	0%	0/12
G1-AA/S70	16%	2/12
G1-AA/S70 + G1-AA/Lob12.3	33%	4/12
FS22m-063-AA/S70	100%	12/12

[0463] The study shows that in mice with a fully functioning immune system, in a second syngeneic tumour model, MC38, which shows suboptimal response to 1 mg/kg of PD-L1 mAb, surprisingly, 1 mg/kg of CD137/PD-L1 mAb^2 induces complete tumour regression in 100 % of treated mice.

[0464] Survival analysis **(Figure 22** and **Table 30)** shows the summary of median survival in days for each treatment group treated with 3 doses of G1-AA/4420 (isotype control), G1-AA/S70 (anti-PD-L1 positive control), G1-AA/Lob12.3 (anti-CD137 positive control), the combination of G1-AA/S70 plus G1-AA/Lob12.3, and FS22m-063-AA/S70 (the anti-mouse CD137 Fcab FS22m-063 in a model PD-L1 mAb^2 format). **Table 30** also shows pairwise statistical analyses (Log-rank). FS22m-063-AA/S70 induces full survival in a MC38 syngeneic tumour model, with 100% survival of the animals at the end of the study (labelled 'undefined'), compared to the IgG control treated mice.

Table 30: Median survival in MC38 tumour model

Compound	Median Survival (Days)	p-values Log-rank	
FS22m-063-AA/S70	undefined		
G1-AA/S70 + G1-AA/Lob12.3	33.5	0.0006	***
G1-AA/Lob12.3	25	0.0001	***
G1-AA/S70	28	<0.0001	****
G1-AA/4420	20	<0.0001	****

14.5 Activity of anti-mouse CD137/PD-L1 mAb^2 *in a B16.F10 syngeneic mouse tumour model*

[0465] The B16.F10 syngeneic tumour model was used to test the anti-tumour activity of the

anti-mouse CD137/PD-L1 mAb^2 (FS22m-063-AA/S70) *in vivo.* This model is seen as more challenging to treat with therapeutic antibodies (Baird, J. R., *et al,* 2013). Antibody G1-AA/4420 was used as an isotype control in the study. The B16.F10 syngeneic tumour model has not been previously shown to be sensitive to CD137 agonist antibodies. However, tumour infiltrating lymphocytes (TILs) isolated from B16.F10 tumours express CD137 (Curran. M., *etal,* 2013).

[0466] C57BL/6 female mice (Charles River) aged 8-10 weeks and weighing 20-25 g each were acclimatised for one week prior to the study start. All animals were micro-chipped and given a unique identifier. Each cohort had 10 mice. The B16.F10 melanoma cell line (ATCC cat no CRL-6475) was initially expanded, stored, and then pre-screened by IDEXXX Bioresearch for pathogens using the IMPACT I protocol and shown to be pathogen free. B16.F10 cells were thawed from -150°C storage and added to 20 ml DMEM (Gibco, 61965-026) with 10% FCS (Gibco, 10270-106) in a T175 tissue culture flask. Each animal received 1×10^6 cells injected subcutaneously in the left flank.

[0467] 20 µg of each antibody was injected into mice (~1 mg/kg) in 200 µl PBS. Each mouse received the antibodies by intraperitoneal (IP) injection every 2 days for 3 doses starting on day 7 post tumour cell inoculation. Tumour volumes were determined by measuring using callipers (as described in **Example 14.1)** and any drug dosing due on the day in question was performed, and the mice were subjected to close observation for the remainder of the trial. Tumour volumes were calculated as described in **Example 14.1.**

[0468] The trial was halted when humane endpoints were reached based on tumour volume and condition. Statistical analysis of growth rates was carried out pairwise over the full time of the study using the Mixed Model analysis.

[0469] There was significant slowing of tumour growth rate for the anti-mouse CD137/PD-L1 mAb^2 compared to isotype control antibody G1-AA/4420 **(Figure 16).** FS22m-063-AA/S70 induced partial tumour growth inhibition in a B16.F10 syngeneic tumour model compared to IgG control treated mice. The graphs in **Figure 23** show the tumour growth measurements in mm^3 for each animal over time.

[0470] Survival analysis **(Table** 31) shows the summary of median survival in days for each group and pairwise statistical analyses (Log-rank) in the B16.F10 syngeneic tumour model grown subcutaneously in C57BL/6 mice treated with G1-AA/4420 (isotype control) and the anti-mouse CD137/PD-L1 mAb^2 FS22m-063-AA/S70. FS22m-063-AA/S70 induced increased survival in a B16.F10 syngeneic tumour model compared to IgG control treated mice.

Table 31: Median survival in the B16.F10 syngeneic tumour model

Compound	Median Survival (Days)	p-values Log-rank
FS22m-063-AA/S70	23.5	n/a
G1-AA/4420	19	n/a

[0471] This study showed that in mice with a fully functioning immune system, in a notoriously difficult to treat B16.F10 syngeneic mouse tumour model, CD137 agonism, presumably as a result of crosslinking via PD-L1, leads to a reduction in tumour growth, presumably through increased cytotoxic activity of $CD8^+$ T cells in the tumour.

14.6 Liver pharmacology of anti-mouse CD 137/PD-L1* mAb^2 *in CT26 syngeneic mouse tumour bearing model

[0472] Anti-CD137 mAb treatment of solid tumour patients with urelumab in investigational clinical trials has resulted in severe treatment related immune events which have been shown to be related to the dose of urelumab administered. The effects of these immune events manifested in the liver as severe hepatoxicity (Segal, N. H., *et al,* 2017).

[0473] Preclinical mechanistic work undertaken in mice wherein animals were dosed using CD137 agonistic tool antibodies has shown similar hepatotoxicity. These studies showed a requirement for T cells and CD137 in the resultant hepatotoxicity (Niu, L., *et* al 2007 and Dubrot J, *et al.* 2010). Although poorly understood, the interplay between the myeloid and T cell compartments has also been shown to be important in initiating the inflammatory cascade leading to liver damage and hepatotoxicity (Bartkowiak, T *et al.,* 2018). Therefore, these animal models have translational relevance for the clinic in predicting the risk of hepatoxicity in human patients following administration of other CD137 agonists and specifically a CD137/PD-L1 mAb^2.

[0474] Mice from the CT26 syngeneic tumour study described in **Example 14.1** showed no overt signs of toxicity following repeated dosing with FS22m-063-AA/S70 mAb^2 which has CD137 agonist capacity upon PD-L1 crosslinking. To determine whether in these animals the immune activation observed as a result of treatment with ~1 mg/kg FS22m-063-AA/S70 mAb^2 (which correlated with anti-tumour immune activity) correlated with hepatotoxicity, liver samples were taken at necropsy for histological assessment. FS22m-063-AA/S70 mAb^2 and control mice were necropsied 4, 7 and 14 days after the last administration (three mice per group per timepoint) and liver samples were formalin fixed and paraffin embedded. Sections of liver were then cut and subjected to histopathological evaluation via hematoxilin and eosin staining and scoring of parameters of liver inflammation and damage by a certified pathologist. The methods for tissue preparation and histopathological staining by hematoxilin and eosin are highly standardised and well known within the art.

[0475] A scoring system was used to assess liver pathology in the hematoxilin and eosin stained sections. Liver was scored for pathology corresponding to hepatocellular necrosis, portal tract inflammation, degenerative hepatocytes and increased mitoses. The frequency of

mice showing minimal, slight, moderate and marked effects within each group are shown in **Table 32.**

[0476] FS22m-063-AA/S70 mAb^2 treated animals have minimal liver pathology. Specifically:

- minimal to slight hepatocellular necrosis with mixed lymphocyte infiltrate in the parenchyma
- minimal to slight mixed inflammatory cells in periportal tracts
- minimal degenerative hepatocytes
- minimal to marked increased mitoses

Table 32: Liver findings

Liver	G1/4420 (Isotype control)			FS22m-063-AA/S70		
	D4	D7	D14	D4	D7	D14
Hepatocellular necrosis, degeneration with mixed inflammatory cells (parenchymal)						
Minimal	3	3	3	2	2	3
Slight	0	0	0	1	1	0
Mixed inflammatory cells (+/- SCN) in portal tracts						
Minimal	1	0	0	1	3	3
Slight	0	0	0	1	0	0
Degenerative hepatocyte						
Minimal	0	0	0	0	0	0
Increased mitoses						
Minimal	1	1	1	2	2	3
Slight	1	0	1	1	0	0
Moderate	0	0	0	0	0	0
Marked	0	0	0	0	0	0

[0477] These findings are not deemed to represent severe hepatoxicity, as observed with other examples of anti-CD137 agonist antibodies.

[0478] Given the relevance of preclinical studies in mice for risk assessment of severe hepatoxicity in human patients treated with CD137 agonist agents, these results indicate that a mAb^2 agonising CD137 via crosslinking mediated through PD-L1 binding has a low risk of inducing hepatoxicity in human patients treated at therapeutic doses.

14.7 Tumour and peripheral receptor occupancy and pharmacodynamic effects of anti-

mouse CD137/PD-L1* mAb^2 *in a CT26 syngeneic mouse tumour model

[0479] In **Example 14.3,** the anti-mouse CD137-PD-L1 mAb^2 FS22m-063-AA/S70 showed the ability to increase CD8$^+$ T cells in the tumour after multiple doses. To investigate the extent of target binding on T cells, PD-L1 blockade and the effect FS22m-063-AA/S70 has on T cell proliferation, a single-dose pharmacodynamic study was run in the same CT26 syngeneic tumour model as described in **Example 14.1.**

[0480] Antibody G1-AA/4420 was used as a control. Anti-mouse CD137/PD-L1 mAb^2 and control antibodies for the *in vivo* experiments were produced as described in **Example 14.1.**

[0481] Following the same protocol as described in **Example 14.1,** Balb/c female mice (Charles River) aged 8-10 weeks and weighing 20-25g each were rested for one week prior to the study start. All animals were micro-chipped and given a unique identifier. This study comprised 3 dosing groups, receiving either control antibody or mAb^2 at one of two doses over 8 time points (2h, 6h, 24h, 48h, 72h, 96h, 120h, 192h). Each dosing cohort had 64 mice (8 mice per timepoint). The CT26 colon carcinoma cell line (S. Rosenberg, NIH) was initially expanded, stored, and then pre-screened by IDEXX Bioresearch for pathogens using the IMPACT I protocol and shown to be pathogen-free. Each animal received 1×10^5 cells injected subcutaneously in the left flank in 100µl DMEM. 7 days following tumour cell inoculation, mice which did not have tumours at this point were removed from the study.

[0482] Each mouse received the test sample via a 100 µl intravenous (IV) injection on day 11 following tumour inoculation. In the groups receiving mAb^2, FS22m-063-AA/S70 mAb^2 was injected intravenously into mice at either 20µg or 200µg per mouse (a final concentration of ~1 mg/kg and ~10 mg/kg respectively) and in the group receiving control antibody G1-AA/4420 (isotype control) was injected intravenously into mice at 200µg per mouse (a final concentration of ~10 mg/kg) in DPBS + 1mM arginine + 0.05 Tween 80.

[0483] The tumour and peripheral blood receptor engagement and pharmacodynamic response as a result of dosing with the anti-mouse CD137/PD-L1 mAb^2 was assessed. Tumour tissue and blood from CT26 tumour-bearing mice treated with FS22m-063-AA/S70 (anti-mCD137/PD-L1 mAb^2) at each of the doses, as well as negative control antibody G1-AA/4420, was tested for anti-mouse CD137/PD-L1 mAb^2-bound positive T cells, T cell proliferation, and free PD-L1 not bound by anti-mouse CD137/PD-L1 mAb^2. Total CD137 expression was also assessed.

[0484] Blood (100µl) was collected in to EDTA coated capillaries by tail vein bleeding and were lysed twice in red blood cell lysis buffer (eBioscience cat no 00-4300-54) according to manufacturer's instructions.

[0485] Tumour tissue was collected by dissection and was disaggregated to single cell suspension by standard mechanical and enzymatic methods. Any red blood cells remaining in the disaggregated tumour tissue were lysed once in red blood cell lysis buffer (eBioscience, cat no. 00-4300-54) according to manufacturer's instructions.

[0486] Cells were washed once with PBS and samples stained with fixable viability dye (Invitrogen, cat no. 65-0865-14) at 1:3000 dilution in PBS following manufacturer's instructions. The cells were stained for cell surface markers for flow cytometry with an antibody staining panel (all but Ki67 and FoxP3 antibodies) **(Table 33** below) in the presence of Fc block (eBioscience cat no 14-0161-86 at 1:50) for 30 minutes at 4°C. The cells were then fixed and permeabilized with the eBioscience Foxp3 staining kit (eBioscience cat no 00-5523-00) according to manufacturer's instructions. Cells were resuspended in 100 µl permeabilization buffer with Ki67 and Foxp3 antibodies in the presence of Fc block and incubated for 30 minutes in the dark at room temperature. Cells were then washed once with permeabilization buffer and resuspended in 200 µl PBS + 0.5% BSA. The cells were then analysed in a BD Fortessa flow cytometer. Data was analysed with FlowJoX, Excel and GraphPad Prism.

[0487] Figure 24 shows the percentage of $CD4^+$ and $CD8^+$ T cells isolated from either blood or tumours that were positive for anti-IgG antibody bound to the mCD137/PD-L1 mAb^2 in the sample. As shown in **Figure 24,** the T cells were positive for bound anti-mCD137/PD-L1 mAb^2 as soon as 2 hours after intravenous administration. There was a dose-dependent correlation in the longevity of binding, with anti-mCD137/PD-L1 mAb^2 no longer detected after 96hr on T cells isolated from blood and tumour after administration of a 1mg/kg dose, whereas anti-mCD137/PD-L1 mAb^2 was still detected between 120hr and 192h after administration of 10mg/kg dose. As expected, minimal background staining was observed for the control antibody. Populations of T cells isolated from tumour that were positive for anti-mCD137/PD-L1 mAb^2 were larger at the outset compared to T cells isolated from blood. This could indicate that the levels of target expression, either CD137 or PD-L1, were higher on T cells isolated from the tumour, such that the anti-mCD137/PD-L1 was more efficiently targeted to the tumour compared to T cells in the blood.

[0488] Figure 25 shows Ki67 detection as a marker for T cell proliferation on $CD4^+$ and $CD8^+$ T cells isolated from blood and tumours. As indicated in **Figure 25,** when compared to control antibody, the anti-mCD137/PD-L1 mAb^2 resulted in increases in the frequency of Ki67 positive peripheral blood T cells indicating a pharmacodynamic (PD) response, i.e. that both targets are or have been at some point engaged resulting in the activation of T cells as seen by a proliferative response, at both dose levels tested. Since tumour infiltrating T cells are exposed to an inflammatory environment, the T cell populations isolated from the tumours exhibited a higher frequency of Ki67 positive proliferative T cells. In contrast, the base line frequency of Ki67 positive T cells was much lower in the blood. Both $CD4^+$ and $CD8^+$ T cells appeared to respond to anti-mCD137/PD-L1 treatment, indicating that CD137 on both cell types was

engaged by mAb^2 and clustered together by binding PD-L1 leading to CD137 signalling and T cell activation resulting in increased proliferation. The effect appeared stronger for $CD8^+$ T cells which is in line with $CD8^+$ T cells expressing higher levels of CD137 than $CD4^+$ T cells. The data suggest that maximum effect is achieved at 1 mg/kg, although the duration of the response appears greater at 10 mg/kg, which could be related to a more prolonged receptor occupancy and therefore longer target engagement at the higher dose level. The more prolonged the receptor occupancy, the greater the PD response. In the tumour, T cells are already highly proliferative, and a dose-correlated increase in magnitude of proliferation on both $CD4^+$ and $CD8^+$ T cells over time was observed.

[0489] Samples from the control antibody G1-AA/4420 treated mice were spiked with 100nM anti-mCD137/PD-L1 mAb^2 and acted as control for 100% PD-L1 receptor engagement. This was shown by the lack of binding from a competing anti-mPD-L1 antibody (clone 10F.9G2, see **Table 33).** Samples from tumours and blood of mice treated with anti-mCD137/PD-L1 showed near complete PD-L1 blockade at the 10mg/kg dose for the full length of the study, as shown in **Figure 26** represented by 100% PD-L1 receptor occupancy. In samples from mice treated with 1mg/kg anti-mCD137/PD-L1, the PD-L1 receptor engagement decreased after approximately 72h on T cells present in blood and tumours, with PD-L1 receptor engagement on T cells present in blood decreased much faster than in T cells present in tumours. This data indicates a tumour-specific blockade of PD-L1 having both the advantage of inhibiting the PD-1/PD-L1 axis and retaining the anti-mCD137/PD-L1 mAb^2 in the tumour for longer than in the blood, which is expected to allow the full effect of the drug to persist in the tumour, whilst at the same time limiting off target effects in the periphery.

[0490] Overall, this study showed that increasing the dose of anti-mouse CD137/PD-L1 resulted in activation and proliferation of $CD8^+$ and $CD4^+$ T cells in the tumour as measured by the number of cells to which the mAb^2 bound, PD-L1 receptor engagement by the mAb^2 and increased expression of Ki67 as a marker of proliferation. Activated and proliferating $CD8^+$ and $CD4^+$ cells were also observed in the peripheral blood, acting as a further marker of anti-mouse CD137/PD-L1 induced activity. This dose-dependent T-cell activation supports the tumour growth inhibition previously observed in **Example 14** upon administration of anti-mouse CD137/PD-L1.

[0491] The main role of $CD8^+$ T cells (often also called cytotoxic lymphocytes) is the killing of infected or malignant cells via 3 main mechanisms: 1) release of cytokines (e.g. TNFα and IFN-γ), 2) production and release of cytotoxic granules and 3) expression of Fas ligand. The presence of more $CD8^+$ T cells in the tumour following treatment with anti-mouse CD137/PD-L1 is expected to result in cytotoxic activity via these mechanisms against the tumour, resulting in tumour control. Whilst $CD8^+$ T cells are the overriding cytotoxic T cell that account for tumour cell killing, $CD4^+$ T cells play a pivotal role in adaptive immunity by recognising peptides presented by MHC class II molecules, becoming activated and producing IFN-γ and TNFα

which both mediate protection from tumours (Zanetti, 2015, JI, 2015).

Table 33

Target	Antibody Clone	Fluorophore	Company	Cat no.
CD45	30-F11	AF700	eBioscience	56-0451-82
CD3	145-2C11	BUV737	BD Biosciences	564618
CD4	RM4-5	Bv786	BD Biosciences	563727
CD8	53-6.7	BUV395	BD Biosciences	563786
FoxP3	Fjk-16S	PerCP-Cy5.5	Invitrogen	45-5773-82
CD4+4	IM7	BV650	BioLegend	103049
CD62L	MEL-14	Bv421	BioLegend	104435
CD137	17B5	PE	BioLegend	106105
Ki67	16A8	PE-Cy7	BioLegend	652426
PD-L1	10F.9G2	Bv605	BioLegend	124321
IgG	MK1A6	FITC	Bio-Rad	MCA647F
Viability	n/a	e780	Invitrogen	65-0865-14
n/a means not applicable				

Example 15: Anti-human CD137/PD-L1 mAb^2 pharmacokinetics in mouse

[0492] In order to determine the pharmacokinetics of anti-CD137/PD-L1 mAb^2 in mice, C57BL/6 female mice (see **Example 14.4)** but without MC38 tumours, i.e. tumour-free mice, were administered 100µl anti-CD137/PD-L1 mAb^2 at 4 doses (25mg/kg, 10mg/kg, 3mg/kg and 1mg/kg) and monitored for 384 hours.

[0493] Microsampling of around 20µl of whole blood was performed at 2, 6, 24, 48, 96, and 384 hours, and processed to isolate approximately 5µl of serum. The amount of anti-CD137/PD-L1 mAb^2 present at each time point was determined using the Gyrolab xPlore system by Gyros Protein Technologies. A sandwich assay was performed using a Gyrolab Bioaffy 1000 CD (Product Number P0004253) with biotinylated goat anti-human IgG-(heavy and light chain) monkey adsorbed antibody (Cambridge Bioscience product number A80-319B) as capture antibody and goat anti-Human IgG-AlexaFluor® 647 (Cambridge Bioscience product number 2040-31) as detection antibody. A standard curve generated in the range of 8000-0.07 ng/ml was used to determine sample concentration, with samples undergoing dilution in Rexxip AN buffer as required (Gyros product number P0004994). Other buffers were used as per the manufacturer's recommendations. The average sample concentration from individual mice per time point (three mice per time point) was plotted **(Figure 27).**

[0494] Figure 27 shows the pharmacokinetics of anti-CD137/PD-L1 mAb^2, demonstrating that the mAb^2 has comparable terminal clearance to a standard human IgG in mice (Bergman *et al,* 1998).

Example 16: Pharmacokinetic/Pharmacodynamic response to and tolerability of anti-human CD137/PD-L1 mAb^2 in cynomolgus monkeys

[0495] A preliminary dose range finding study was conducted to evaluate the pharmacokinetic/pharmacodynamic (PK/PD) response to and tolerability of anti-human CD137/PD-L2 mAb^2 in cynomolgus monkeys. Briefly, the FS22-172-003-AA/E12v2 mAb^2 was administered to cynomolgus monkeys via intravenous (IV) infusion as a single dose or as repeat doses. Standard toxicology parameters such as body weight, food consumption, clinical observations, haematology and blood chemistry were assessed for the evaluation of tolerability over the duration of the study.

[0496] The FS22-172-003-AA/E12v2 mAb^2 had a terminal half-life of approximately 6 days and was generally well tolerated up to 30 mg/kg dosed weekly as determined by clinical chemistry and histopathology results). Increased serum sPD-L1 levels (an indication of direct target engagement and cell activation) were observed in all animals on day 1, with peak achieved at 168 hours post end of infusion, following which the levels declined in line with the decline in the systemic levels of the FS22-172-003-AA/E12v2 mAb^2.

[0497] Consistent with the findings of the study to assess the PD response of the anti-mouse CD137/PD-L1 mAb^2 in a syngeneic mouse tumour model (Example 15), a drug-related increase in cell proliferation and activation was also observed in CD4$^+$ and CD8$^+$ Central Memory and Effector Memory T cells, which was measured by an increased expression of Ki67. Similar kinetics were observed for NK cells and a moderate but transient increase in the relative percentage and absolute counts of CD4$^+$ regulatory T cells (CD4$^+$ FoxP3$^+$).

[0498] Taken together these results strongly indicate that the anti-human FS22-172-003-AA/E12v2 mAb^2 has potent *in vivo* pharmacological activity in the cynomolgus monkey and is well tolerated up 30mg/kg. Furthermore, the PK/PD data generated is in line with the surrogate molecule (FS22m-063-AA/S70) data, strengthening the rationale for the use of FS22-172-003-AA/E12v2 mAb^2 in the clinical setting.

Sequence Listing

[0499]

CDR amino acid sequences of E12v2 mAb (Kabat)

VH CDR1 - SYGIS (SEQ ID NO: 1)

VH CDR2 - WISAYSGGTNYAQKLQG (SEQ ID NO: 2)

VH CDR3 - DLFPTIFGVSYYYY (SEQ ID NO: 3)

VL CDR1 - RASQSIGNRLA (SEQ ID NO: 4)

VL CDR2 - EASTSET (SEQ ID NO: 5)

VL CDR3 - QQSYSTPYT (SEQ ID NO: 6)

CDR amino acid sequences of E12v2 (IMGT)

VH CDR1 - GYPFTSYG (SEQ ID NO: 7)

VH CDR2 - ISAYSGGT (SEQ ID NO: 8)

VH CDR3 - ARDLFPTIFGVSYYYY (SEQ ID NO: 9)

VL CDR1 - QSIGNR (SEQ ID NO: 10)

VL CDR2 - EAS (SEQ ID NO: 11)

VL CDR3 - QQSYSTPYT (SEQ ID NO: 6)

VH domain amino acid sequence of E12v2 mAb (SEQ ID NO: 12)

IMGT CDRs (bold italics); Kabat CDRs (italics and underlined).

*EVQLVQSGAEVKRPGASVKVSCKAS**GYPFTSYG**ISWVRQAPGQGLEWMG**WISAYSGGT**NYAQKLQ*
*GRVTMTTDTSTSTAYMELRSLRSDDTAVYYC**ARDLFPTIFGVSYYYY**WGQGTLVTVSS*

VH domain nucleic acid sequence of E12v2 mAb (SEQ ID NO: 13)

GAAGTGCAGCTGGTGCAGTCCGGAGCCGAAGTCAAGAGGCCTGGAGCGTCCGTGAAGGTGTCC
TGCAAAGCCTCAGGATACCCCTTCACTTCGTACGGGATTTCCTGGGTCCGCCAAGCACCGGGTC
AAGGCTTGGAGTGGATGGGATGGATCAGCGCGTATTCCGGGGGAACCAACTACGCTCAAAAGC
TGCAGGGTCGCGTGACCATGACCACCGATACCTCCACCTCAACGGCCTACATGGAACTGAGATC
TCTGCGGAGCGACGACACTGCCGTGTACTACTGTGCCCGGGACCTGTTCCCCACTATCTTCGGA
GTGTCGTACTACTACTACTGGGGCCAGGGGACTCTCGTGACCGTGTCGAGC

VL domain amino acid sequence of E12v2 mAb (SEQ ID NO: 14)

IMGT CDRs (bold italics); Kabat CDRs (italics and underlined).

*DIQMTQSPSTLSASVRDRVIITC**RAS**QSIGNR**LA**WYQHKPGKAPKLLIY**EAS**TSET**GVPSRFSGSGSG*
*TDFTLTISSLQPEDFATYYC**QQSYSTPYT**FGQGTKLEIK*

VL domain nucleic acid sequence of E12v2 mAb (SEQ ID NO: 15)

GACATCCAGATGACGCAGAGCCCGTCTACCCTGTCCGCCTCCGTGAGAGATCGCGTGATCATCA
CCTGTCGGGCCAGCCAGTCCATCGGAAACCGCTTGGCGTGGTACCAGCACAAGCCTGGGAAGG
CTCCGAAGCTGCTCATCTACGAAGCCTCGACTTCGGAGACTGGTGTCCCTAGCCGGTTCAGCGG
ATCGGGATCAGGGACCGATTTCACTCTGACCATTTCCTCCCTGCAACCCGAGGACTTCGCCACC
TACTACTGCCAACAGTCATATTCCACCCCGTACACCTTCGGACAAGGCACCAAGCTCGAAATCAA
G

Heavy chain amino acid sequence of G1-AA/E12v2 mAb (with LALA) (SEQ ID NO: 16)

VH domain (italics); IMGT CDRs (bold and italics); Kabat CDRs (italics and underlined); LALA mutation (bold and underlined)

*EVQLVQSGAEVKRPGASVKVSCKAS**GYPFTSYG**ISWVRQAPGQGLEWMG**WISAYSGGT**NYAQKLQ*
*GRVTMTTDTSTSTAYMELRSLRSDDTAVYYC**ARDLFPTIFGVSYYYY**WGQGTLVTVSS*ASTKGPSVF

PLAPSSKSTSGGTAALGCLVKDYFPEPVTVSWNSGALTSGVHTFPAVLQSSGLYSLSSVVTVPSSSL
GTQTYICNVNHKPSNTKVDKKVEPKSCDKTHTCPPCPAPE**AA**GGPSVFLFPPKPKDTLMISRTPEVT
CVVVDVSHEDPEVKFNWYVDGVEVHNAKTKPREEQYNSTYRVVSVLTVLHQDWLNGKEYKCKVSN
KALPAPIEKTISKAKGQPREPQVYTLPPSRDELTKNQVSLTCLVKGFYPSDIAVEWESNGQPENNYKT
TPPVLDSDGSFFLYSKLTVDKSRWQQGNVFSCSVMHEALHNHYTQKSLSLSPG

Light chain amino acid sequence of G1-AA/E12v2 mAb (SEQ ID NO: 17)

VH domain (italics); IMGT CDRs (bold and italics); Kabat CDRs (italics and underlined)

*DIQMTQSPSTLSASVRDRVIITC**RAS**QSIGNR**LA**WYQHKPGKAPKLLIY**EAS**TSET*GVPSRFSGSGSG
*TDFTLTISSLQPEDFATYYC**QQSYSTPYT**FGQGTKLEI*KRTVAAPSVFIFPPSDEQLKSGTASVVCLLN
NFYPREAKVQWKVDNALQSGNSQESVTEQDSKDSTYSLSSTLTLSKADYEKHKVYACEVTHQGLSS
PVTKSFNRGEC

CDR amino acid sequences of E05v2 mAb (Kabat)

VH CDR1 - SYGIS (SEQ ID NO: 1)

VH CDR2 - WISAYSGGTNYAQKLQG (SEQ ID NO: 2)

VH CDR3 - DLFPTIFGVSYYYY (SEQ ID NO: 3)

VL CDR1 - RASQSISGRLA (SEQ ID NO: 18)

VL CDR2 - EASNLES (SEQ ID NO: 19)

VL CDR3 - QQSYSTPRVT (SEQ ID NO: 20)

CDR amino acid sequences of E05v2 (IMGT)

VH CDR1 - GYTFTSYG (SEQ ID NO: 21)

VH CDR2 - ISAYSGGT (SEQ ID NO: 8)

VH CDR3 - ARDLFPTIFGVSYYYY (SEQ ID NO: 9)

VL CDR1 - QSISGR (SEQ ID NO: 22)

VL CDR2 - EAS (SEQ ID NO: **11)**

VL CDR3 - QQSYSTPRVT (SEQ ID NO: **20)**

VH domain amino acid sequence of E05v2 mAb (SEQ ID NO: **23)**

IMGT CDRs (bold and italics); Kabat CDRs (italics and underlined)

*EVQLVQSGAEVKRPGASVKVSCKAS**GYTFTSYG**ISWVRQAPGQGLEWMG**WISAYSGGT**NYAQKLQ*
*GRVTMTTDTSTSTAYMELRSLRSDDTAVYYC**ARDLFPTIFGVSYYYY**WGQGTLVTVSS*

VH domain nucleic acid sequence of E05v2 mAb (SEQ ID NO: 24)

GAAGTGCAGCTGGTGCAGTCCGGAGCCGAAGTCAAGAGGCCTGGAGCGTCCGTGAAGGTGTCC

TGCAAAGCCTCAGGATACACCTTCACTTCGTACGGGATTTCCTGGGTCCGCCAAGCACCGGGTC
AAGGCTTGGAGTGGATGGGATGGATCAGCGCGTATTCCGGGGGAACCAACTACGCTCAAAAGC
TGCAGGGTCGCGTGACCATGACCACCGATACCTCCACCTCAACGGCCTACATGGAACTGAGATC
TCTGCGGAGCGACGACACTGCCGTGTACTACTGTGCCCGGGACCTGTTCCCCACTATCTTCGGA
GTGTCGTACTACTACTACTGGGGCCAGGGGACTCTCGTGACCGTGTCGAGC

VL domain amino acid sequence of E05v2 mAb (SEQ ID NO: **25)**

IMGT CDRs (bold and italics); Kabat CDRs (italics and underlined)
*DIQMTQSPSTLSASVGDRVTITCRAS**QSISGR**LAWYQQKPGKAPNLLIY**EAS**NLESGVPSRFSGSGS*
*GTEFTLTISSLQPEDFATYYC**QQSYSTPRVT**FGQGTKVEIK*

VL domain nucleic acid sequence of E05v2 mAb (SEQ ID NO: 26)

GACATTCAGATGACCCAATCCCCGTCCACGCTGAGCGCCTCCGTCGGTGATCGCGTGACAATCA
CTTGTCGGGCGTCGCAGTCCATCTCTGGAAGGCTCGCCTGGTACCAGCAGAAGCCTGGAAAGG
CTCCCAACCTCCTTATCTACGAAGCCAGCAACCTGGAGTCCGGAGTGCCTAGCCGGTTCAGCGG

ATCAGGGTCCGGTACCGAGTTCACCCTGACCATTTCCTCGCTCCAACCTGAGGACTTCGCCACC
TACTACTGCCAACAGTCCTATTCAACTCCGCGCGTGACCTTCGGCCAGGGCACTAAGGTCGAAA
TCAAA

Heavy chain amino acid sequence of G1-AA/E05v2 mAb (with LALA) (SEQ ID NO: **27)**
VH domain (italics); IMGT CDRs (bold and italics); Kabat CDRs (italics and underlined); LALA mutation (bold and underlined)
*EVQLVQSGAEVKRPGASVKVSCKAS**GYTFTSYG**ISWVRQAPGQGLEWMG**WISAYSGGT**NYAQKLQ*
*GRVTMTTDTSTSTAYMELRSLRSDDTAVYYC**ARDLFPTIFGVSYYYY**WGQGTLVTVSSASTKGPSVF*
PLAPSSKSTSGGTAALGCLVKDYFPEPVTVSWNSGALTSGVHTFPAVLQSSGLYSLSSVVTVPSSSL
*GTQTYICNVNHKPSNTKVDKKVEPKSCDKTHTCPPCPAPE**AA**GGPSVFLFPPKPKDTLMISRTPEVT*
CVVVDVSHEDPEVKFNWYVDGVEVHNAKTKPREEQYNSTYRVVSVLTVLHQDWLNGKEYKCKVSN
KALPAPIEKTISKAKGQPREPQVYTLPPSRDELTKNQVSLTCLVKGFYPSDIAVEWESNGQPENNYKT
TPPVLDSDGSFFLYSKLTVDKSRWQQGNVFSCSVMHEALHNHYTQKSLSLSPG

Light chain amino acid sequence of G1-AA/E05v2 mAb and FS22-172-003-AA/E05v2 and FS22-053-008-AA/E05v2 mAb[2] (SEQ ID NO: 28)
VH domain (italics); IMGT CDRs (bold and italics); Kabat CDRs (italics and underlined)
*DIQMTQSPSTLSASVGDRVTITCRAS**QSISGR**LAWYQQKPGKAPNLLIY**EAS**NLESGVPSRFSGSGS*
*GTEFTLTISSLQPEDFATYYC**QQSYSTPRVT**FGQGTKVEIK*RTVAAPSVFIFPPSDEQLKSGTASVVCL
LNNFYPREAKVQWKVDNALQSGNSQESVTEQDSKDSTYSLSSTLTLSKADYEKHKVYACEVTHQGL
SSPVTKSFNRGEC

CDR amino acid sequences of G12v2 mAb (Kabat)

VH CDR1 - SYGIS (SEQ ID NO: **1)**

VH CDR2 - WISAYSGGTNYAQKLQG (SEQ ID NO: **2)**

VH CDR3 - DLFPTIFGVSYYYY (SEQ ID NO: **3)**

VL CDR1 - RASQSISGRLA (SEQ ID NO: **18)**

VL CDR2 - EASNLES (SEQ ID NO: **19)**

VL CDR3 - QQSYSWPRT (SEQ ID NO: **29)**

CDR amino acid sequences of G12v2 (IMGT)

VH CDR1 - GYTFTSYG (SEQ ID NO: **21)**

VH CDR2 - ISAYSGGT (SEQ ID NO: **8)**

VH CDR3 - ARDLFPTIFGVSYYYY (SEQ ID NO: **9)**

VL CDR1 - QSISGR (SEQ ID NO: **22)**

VL CDR2 - EAS (SEQ ID NO: **11)**

VL CDR3 - QQSYSWPRT (SEQ ID NO: **29)**

VH domain amino acid sequence of G12v2 mAb (SEQ ID NO: **23)**

IMGT CDRs (bold and italics); Kabat CDRs (italics and underlined)

*EVQLVQSGAEVKRPGASVKVSCKAS**GYTFTSYG**ISWVRQAPGQGLEWMG**WISAYSGGT**NYAQKLQ*
*GRVTMTTDTSTSTAYMELRSLRSDDTAVYYC**ARDLFPTIFGVSYYYY**WGQGTLVTVSS*

VH domain nucleic acid sequence of G12v2 mAb (SEQ ID NO: **24)**

GAAGTGCAGCTGGTGCAGTCCGGAGCCGAAGTCAAGAGGCCTGGAGCGTCCGTGAAGGTGTCC
TGCAAAGCCTCAGGATACACCTTCACTTCGTACGGGATTTCCTGGGTCCGCCAAGCACCGGGTC
AAGGCTTGGAGTGGATGGGATGGATCAGCGCGTATTCCGGGGGAACCAACTACGCTCAAAAGC
TGCAGGGTCGCGTGACCATGACCACCGATACCTCCACCTCAACGGCCTACATGGAACTGAGATC

TCTGCGGAGCGACGACACTGCCGTGTACTACTGTGCCCGGGACCTGTTCCCCACTATCTTCGGA
GTGTCGTACTACTACTACTGGGGCCAGGGGACTCTCGTGACCGTGTCGAGC

VL domain amino acid sequence of G12v2 mAb (SEQ ID NO: 30)

IMGT CDRs (bold and italics); Kabat CDRs (italics and underlined)

*DIQMTQSPSTLSASVGDRVTITC**RAS**QSISGR**LAWYQQKPGKAPNLLIY**EAS**NLES**GVPSRFSGSGS*
*GTEFTLTISSLQPEDFATYYC**QQSYSWPRT**FGQGTKVEIK*

VL domain nucleic acid sequence of G12v2 mAb (SEQ ID NO: **31)**

GACATTCAGATGACCCAGTCCCCGAGCACGCTGTCCGCAAGCGTGGGGGACAGAGTGACCATC
ACTTGCCGCGCCTCACAATCCATCAGCGGACGCTTGGCCTGGTACCAGCAGAAGCCCGGAAAG
GCCCCAAACCTTCTGATCTACGAAGCCTCGAACCTGGAGTCAGGCGTCCCTTCGCGGTTCTCTG
GCTCCGGTTCCGGAACTGAGTTCACCCTCACCATCTCGTCCCTGCAACCGGAAGATTTCGCCAC
CTACTACTGCCAACAGTCGTACTCCTGGCCCCGGACATTCGGACAGGGAACCAAAGTCGAGATT
AAG

Heavy chain amino acid sequence of G1-AA/G12v2 mAb (with LALA) (SEQ ID NO: 27)

VH domain (italics); IMGT CDRs (bold and italics); Kabat CDRs (italics and underlined); LALA mutation (bold and underlined)

*EVQLVQSGAEVKRPGASVKVSCKAS**GYTFTSYG**ISWVRQAPGQGLEWMG**WISAYSGGT**NYAQKLQ*
*GRVTMTTDTSTSTAYMELRSLRSDDTAVYYC**ARDLFPTIFGVSYYYY**WGQGTLVTVSS*ASTKGPSVF
PLAPSSKSTSGGTAALGCLVKDYFPEPVTVSWNSGALTSGVHTFPAVLQSSGLYSLSSVVTVPSSSL
GTQTYICNVNHKPSNTKVDKKVEPKSCDKTHTCPPCPAPE**AA**GGPSVFLFPPKPKDTLMISRTPEVT
CVVVDVSHEDPEVKFNWYVDGVEVHNAKTKPREEQYNSTYRVVSVLTVLHQDWLNGKEYKCKVSN
KALPAPIEKTISKAKGQPREPQVYTLPPSRDELTKNQVSLTCLVKGFYPSDIAVEWESNGQPENNYKT
TPPVLDSDGSFFLYSKLTVDKSRWQQGNVFSCSVMHEALHNHYTQKSLSLSPG

Light chain amino acid sequence of G1-AA/G12v2 mAb and FS22-172-003-AA/G12v2 and FS22-053-008-AA/G12v2 mAb[2] (SEQ ID NO: 33)

VH domain (italics); IMGT CDRs (bold and italics); Kabat CDRs (italics and underlined)
DIQMTQSPSTLSASVGDRVTITC<u>*RAS***QSISGR***LAWYQQKPGKAPNLLIY***EAS***NLES*</u>*GVPSRFSGSGS GTEFTLTISSLQPEDFATYYC*<u>***QQSYSWPRT***</u>*FGQGTKVEIK*RTVAAPSVFIFPPSDEQLKSGTASVVCL LNNFYPREAKVQWKVDNALQSGNSQESVTEQDSKDSTYSLSSTLTLSKADYEKHKVYACEVTHQGL SSPVTKSFNRGEC

<u>CDR amino acid sequences of lambdav3/lam-G02v3 mAb (Kabat)</u>

VH CDR1 - SYGIS (SEQ ID NO: **1)**

VH CDR2 - WISAYSGGTNYAQKLQG (SEQ ID NO: **2)**

VH CDR3 - DLFPTIFGVSYYYY (SEQ ID NO: **3)**

VL CDR1 - TGTSSDVGGYNYVS (SEQ ID NO: **34)**

VL CDR2 - EVTNRPS (SEQ ID NO: 35)

VL CDR3 - SSFKRGSTLVV (SEQ ID NO: 36)

<u>CDR amino acid sequences of lambdav3/lam-G02v3 (IMGT)</u>

VH CDR1 - GYTFTSYG (SEQ ID NO: 21)

VH CDR2 - ISAYSGGT (SEQ ID NO: 8)

VH CDR3 - ARDLFPTIFGVSYYYY (SEQ ID NO: 9)

VL CDR1 - SSDVGGYNY (SEQ ID NO: 37)

VL CDR2 - EVT (SEQ ID NO: **38)**

VL CDR3 - SSFKRGSTLVV (SEQ ID NO: **36)**

<u>VH domain amino acid sequence of lambdav3/lam-G02v3 mAb (SEQ ID NO: **23)**</u>
IMGT CDRs (bold and italics); Kabat CDRs (italics and underlined)
*EVQLVQSGAEVKRPGASVKVSCKAS***GYTFT***<u>SYG</u>**<u>*IS*</u>***WVRQAPGQGLEWMG***<u>*WI***SAYSGGT***NYAQKLQ*</u>
<u>*G*</u>*RVTMTTDTSTSTAYMELRSLRSDDTAVYYC****ARDLFPTIFGVSYYYY****WGQGTLVTVSS*

<u>VH domain nucleic acid sequence of lambdav3/lam-G02v3 mAb (SEQ ID NO: 24)</u>
GAAGTGCAGCTGGTGCAGTCCGGAGCCGAAGTCAAGAGGCCTGGAGCGTCCGTGAAGGTGTCC
TGCAAAGCCTCAGGATACACCTTCACTTCGTACGGGATTTCCTGGGTCCGCCAAGCACCGGGTC
AAGGCTTGGAGTGGATGGGATGGATCAGCGCGTATTCCGGGGGAACCAACTACGCTCAAAAGC
TGCAGGGTCGCGTGACCATGACCACCGATACCTCCACCTCAACGGCCTACATGGAACTGAGATC
TCTGCGGAGCGACGACACTGCCGTGTACTACTGTGCCCGGGACCTGTTCCCCACTATCTTCGGA
GTGTCGTACTACTACTACTGGGGCCAGGGGACTCTCGTGACCGTGTCGAGC

<u>VL domain amino acid sequence of lambdav3/lam-G02v3 mAb (SEQ ID NO: **41)**</u>
IMGT CDRs (bold and italics); Kabat CDRs (italics and underlined)
QSALTQPASVSGSPGQSITISC<u>*TGT***SSDVGGYNY***VSWYQQFPGKAPKLMIF***EVT***NRPS*</u>*GVSDRFSGS KSDNTASLTISGLQAEDEAEYYC*<u>***SSFKRGSTLVV***</u>*FGGGTKLTVL*

<u>VL domain nucleic acid sequence of lambdav3/lam-G02v3 mAb (SEQ ID NO: **42)**</u>
CAGTCGGCCCTTACTCAACCCGCGTCAGTCTCCGGTAGCCCCGGACAGTCCATCACGATTTCGT

GCACCGGAACCAGCAGCGATGTCGGGGGATACAACTACGTGTCCTGGTACCAGCAGTTCCCGG
GAAAGGCCCCTAAGCTGATGATCTTCGAAGTCACTAACAGACCTTCCGGAGTGTCGGACCGGTT
CTCCGGCTCCAAGTCCGACAACACTGCGAGCCTGACCATCTCGGGCCTGCAAGCCGAGGACGA
AGCCGAGTACTACTGTAGCTCATTCAAGCGCGGTTCCACCCTCGTGGTGTTCGGCGGTGGCACT
AAGCTCACCGTGCTGGGA

Heavy chain amino acid sequence of G1-AA/lambdav3/lam-G02v3 mAb (with LALA) (SEQ ID NO: 27) VH domain (italics); IMGT CDRs (bold and italics); Kabat CDRs (italics and underlined); LALA mutation (bold and underlined)

*EVQLVQSGAEVKRPGASVKVSCKAS**GYTFTSYG**ISWVRQAPGQGLEWMG**WISAYSGGT**NYAQKLQ*
*GRVTMTTDTSTSTAYMELRSLRSDDTAVYYC**ARDLFPTIFGVSYYYY**WGQGTLVTVSS*ASTKGPSVF
PLAPSSKSTSGGTAALGCLVKDYFPEPVTVSWNSGALTSGVHTFPAVLQSSGLYSLSSVVTVPSSSL
GTQTYICNVNHKPSNTKVDKKVEPKSCDKTHTCPPCPAPE**AA**GGPSVFLFPPKPKDTLMISRTPEVT
CVVVDVSHEDPEVKFNWYVDGVEVHNAKTKPREEQYNSTYRVVSVLTVLHQDWLNGKEYKCKVSN
KALPAPIEKTISKAKGQPREPQVYTLPPSRDELTKNQVSLTCLVKGFYPSDIAVEWESNGQPENNYKT
TPPVLDSDGSFFLYSKLTVDKSRWQQGNVFSCSVMHEALHNHYTQKSLSLSPG

Light chain amino acid sequence of G1-AA/lambdav3/lam-G02v3 mAb (SEQ ID NO: 44)

VL domain (italics); IMGT CDRs (bold and italics); Kabat CDRs (italics and underlined)

*QSALTQPASVSGSPGQSITISCTGT**SSDVGGYNY**VSWYQQFPGKAPKLMIF**EVT**NRPSGVSDRFSGS*
*KSDNTASLTISGLQAEDEAEYYC**SSFKRGSTLVV**FGGGTKLTVL*GQPAAAPSVTLFPPSSEELQANKA
TLVCLISDFYPGAVTVAWKADSSPVKAGVETTTPSKQSNNKYAASSYLSLTPEQWKSHRSYSCQVTH
EGSTVEKTVAPTECS

Alternative definition of HCDR1 (IMGT) (SEQ ID NO: 45)

GYX_1FTSYG

where X_1 is P or T

Alternative definition of LCDR1 (Kabat) (SEQ ID NO: 46)

$RASQSIX_2X_3RLA$

where X_2 is S or G, X_3 is N or G

Alternative definition of LCDR2 (Kabat) (SEQ ID NO: 47)

$EASX_4X_5EX_6$

Where X_4 is T or N; X_5 is S or L; X_6 is T or S

Alternative definition of LCDR3 (Kabat) (SEQ ID NO: 48)

$QQSYSX_7PX_8X_9T$

Where X_7 is T or W; X_8 is absent or R; X_9 is Y, R, or V

Alternative definition of LCDR1 (IMGT) (SEQ ID NO: 49)

$QSIX_{10}X_{11}R$

Where X_{10} is G or S; X_{11} is N or G

Alternative definition of LCDR3 (IMGT) (SEQ ID NO: 50)

$QQSYSX_{12}X_{13}X_{14}X_{15}T$

Where X_{12} is absent or T; X_{13} is T, W, or P; X_{14} is P or R; X_{15} is Y or R

HFW amino acid sequences IgG1 (Kabat)

HFW1 - EVQLVQSGAEVKRPGASVKVSCKASGYX$_{16}$FT (SEQ ID NO: **51)**
Where X$_{16}$ is P or T

HFW2 - WVRQAPGQGLEWMG (SEQ ID NO: **52)**

HFW3 - RVTMTTDTSTSTAYMELRSLRSDDTAVYYCAR (SEQ ID NO: **53)**

HFW4 - WGQGTLVTVSS (SEQ ID NO: **54)**

HFW amino acid sequences of IgG1 (IMGT)

HFW1 - EVQLVQSGAEVKRPGASVKVSCKAS (SEQ ID NO: **55)**

HFW2 - ISWVRQAPGQGLEWMGW (SEQ ID NO: **56)**

HFW3 - NYAQKLQGRVTMTTDTSTSTAYMELRSLRSDDTAVYYC (SEQ ID NO: **57)**

HFW4 - WGQGTLVTVSS (SEQ ID NO: **54)**

LFW amino acid sequences of kappa light chain (Kabat)

LFW1 - DIQMTQSPSTLSASVRDRVIITC (SEQ ID NO: **58)**

LFW2 - WYQHKPGKAPKLLIY (SEQ ID NO: **59)**

LFW3 - GVPSRFSGSGSGTDFTLTISSLQPEDFATYYC (SEQ ID NO: **60)**

LFW4 - FGQGTKLEIK (SEQ ID NO: **61)**

LFW amino acid sequences of kappa light chain (IMGT)

LFW1 - DIQMTQSPSTLSASVRDRVIITCRAS (SEQ ID NO: **62)**

LFW2 - LAWYQHKPGKAPKLLIY (SEQ ID NO: **63)**

LFW3 - TSETGVPSRFSGSGSGTDFTLTISSLQPEDFATYYC (SEQ ID NO: **64)**

LFW4 - FGQGTKLEIK (SEQ ID NO: **61)**

LFW amino acid sequences of lambda light chain (Kabat)

LFW1 - QSALTQPASVSGSPGQSITISC (SEQ ID NO: **65)**

LFW2 - WYQQFPGKAPKLMIF (SEQ ID NO: **66)**

LFW3 - GVSDRFSGSKSDNTASLTISGLQAEDEAEYYC (SEQ ID NO: **67)**

LFW4 - FGGGTKLTVL (SEQ ID NO: **68)**

LFW amino acid sequences of lambda light chain (IMGT)

LFW1 - QSALTQPASVSGSPGQSITISCTGT (SEQ ID NO: **69)**

LFW2 - VSWYQQFPGKAPKLMIF (SEQ ID NO: **70)**

LFW3 - NRPSGVSDRFSGSKSDNTASLTISGLQAEDEAEYYC (SEQ ID NO: **71)**

LFW4 - FGGGTKLTVL (SEQ ID NO: **68)**

Amino acid sequences of WT CH3 domain structural loops

WT AB loop - RDELTKNQ (SEQ ID NO: 72)

WT CD loop - SNGQPENNY (SEQ ID NO: 73)

WT EF loop - DKSRWQQGNV (SEQ ID NO: 74)

Amino acid sequence of WT CH3 domain (SEQ ID NO: 75)
AB, CD and EF loops underlined
GQPREPQVYTLPPSRDELTKNQVSLTCLVKGFYPSDIAVEWESNGQPENNYKTTPPVLDSDGSFFLY
SKLTVDKSRWQQGNVFSCSVMHEALHNHYTQKSLSLSPG

Amino acid sequence of the CH2 domain (SEQ ID NO: 76)
APELLGGPSVFLFPPKPKDTLMISRTPEVTCVVVDVSHEDPEVKFNWYVDGVEVHNAKTKPREEQYN
STYRVVSVLTVLHQDWLNGKEYKCKVSNKALPAPIEKTISKAK

Amino acid sequence of the CH2 domain with LALA mutation (SEQ ID NO: 77)
LALA mutation underlined
APEAAGGPSVFLFPPKPKDTLMISRTPEVTCVVVDVSHEDPEVKFNWYVDGVEVHNAKTKPREEQY
NSTYRVVSVLTVLHQDWLNGKEYKCKVSNKALPAPIEKTISKAK

Amino acid sequence of the CH2 domain with LALA mutation and P114A mutation (SEQ ID NO: 176) LALA mutation underlined; P114A mutation bold and underlined
APEAAGGPSVFLFPPKPKDTLMISRTPEVTCVVVDVSHEDPEVKFNWYVDGVEVHNAKTKPREEQY
NSTYRVVSVLTVLHQDWLNGKEYKCKVSNKALAAPIEKTISKAK

Amino acid sequence of PPY motif (SEQ ID NO: 78)
PPY

Amino acid sequences of FS22-053-008 CH3 domain structural loop sequences

FS22-053-008 first sequence - NPPYLFS (SEQ ID NO: 79)

FS22-053-008 second sequence - DYWRWLE (SEQ ID NO: 80)

Amino acid sequence of FS22-053-008 CH3 domain (SEQ ID NO: 81)
First and second sequences underlined
GQPREPQVYTLPPSRDELNPPYLFSNQVSLTCLVKGFYPSDIAVEWESNGQPENNYKTTPPVLDSDG
SFFLYSKLTVDYWRWLEGNVFSCSVMHEALHNHYTQKSLSLSPG

Nucleic acid sequence of FS22-053-008 CH3 domain (SEQ ID NO: 82)
GGACAGCCTCGAGAACCACAGGTGTACACCCTGCCCCCATCCCGGGATGAGCTGAACCCGCCG
TACCTGTTCTCTAACCAGGTCAGCCTGACCTGCCTGGTCAAAGGCTTCTATCCCAGCGACATCG
CCGTGGAGTGGGAGAGCAATGGGCAGCCGGAGAACAACTACAAGACCACGCCTCCCGTACTGG
ACTCCGACGGCTCCTTCTTCCTCTACAGCAAGCTCACCGTGGATTACTGGAGGTGGCTGGAAGG

GAACGTCTTCTCATGCTCCGTGATGCATGAGGCGCTGCACAACCACTACACTCAGAAGAGCTTG
TCCCTGTCGCCCGGT

Amino acid sequences of FS22-053-009 CH3 domain structural loop sequences

FS22-053-009 first sequence - NPPYLFS (SEQ ID NO: 79)

FS22-053-009 second sequence - EHTRWLD (SEQ ID NO: 83)

Amino acid sequence of FS22-053-009 CH3 domain (SEQ ID NO: 84)

First and second sequences underlined

GQPREPQVYTLPPSRDELNPPYLFSNQVSLTCLVKGFYPSDIAVEWESNGQPENNYKTTPPVLDSDG
SFFLYSKLTVEHTRWLDGNVFSCSVMHEALHNHYTQKSLSLSPG

Nucleic acid sequence of FS22-053-009 CH3 domain (SEQ ID NO: 85)

GGCCAGCCTCGAGAACCACAGGTGTACACCCTGCCCCCATCCCGGGATGAGCTGAACCCGCCG
TACCTGTTCTCTAACCAGGTCAGCCTGACCTGCCTGGTCAAAGGCTTCTATCCCAGCGACATCG
CCGTGGAGTGGGAGAGCAATGGGCAGCCGGAGAACAACTACAAGACCACGCCTCCCGTGCTGG
ACTCCGACGGCTCCTTCTTCCTCTACAGCAAGCTCACCGTGGAACATACTAGGTGGCTGGATGG
GAACGTCTTCTCATGCTCCGTGATGCATGAGGCTCTGCACAACCACTACACACAGAAGAGCCTC
TCCCTGTCTCCGGGT

Amino acid sequences of Fcab FS22-053-011 CH3 domain structural loop sequences

FS22-053-011 first sequence - NPPYLFS (SEQ ID NO: 79)

FS22-053-011 second sequence - DYWRWTD (SEQ ID NO: 86)

Amino acid sequence of Fcab FS22-053-011 CH3 domain (SEQ ID NO: 87)

First and second sequences underlined

GQPREPQVYTLPPSRDELNPPYLFSNQVSLTCLVKGFYPSDIAVEWESNGQPENNYKTTPPVLDSDG
SFFLYSKLTVDYWRWTDGNVFSCSVMHEALHNHYTQKSLSLSPG

Nucleic acid sequence of Fcab FS22-053-011 CH3 domain (SEQ ID NO: 88)

GGCCAGCCTCGAGAACCACAGGTGTACACCCTGCCCCCATCCCGGGATGAGCTGAACCCGCCG
TACCTGTTCTCTAACCAGGTCAGCCTGACCTGCCTGGTCAAAGGCTTCTATCCCAGCGACATCG
CCGTGGAGTGGGAGAGCAATGGGCAGCCGGAGAACAACTACAAGACCACGCCTCCCGTGCTGG
ACTCCGACGGCTCCTTCTTCCTCTACAGCAAGCTCACCGTGGATTACTGGAGGTGGACTGATGG
GAACGTCTTCTCATGCTCCGTGATGCATGAGGCTCTGCACAACCACTACACACAGAAGAGCCTC
TCCCTGTCTCCGGGT

Amino acid sequences of Fcab FS22-053-017 CH3 domain structural loop sequences

FS22-053-017 first sequence - NPPYLFS (SEQ ID NO: 79)

FS22-053-017 second sequence - YHWRWLE (SEQ ID NO: 89)

Amino acid sequence of Fcab FS22-053-017 CH3 domain (SEQ ID NO: 90)

First and second sequences underlined

GQPREPQVYTLPPSRDELNPPYLFSNQVSLTCLVKGFYPSDIAVEWESNGQPENNYKTTPPVLDSDG
SFFLYSKLTVYHWRWLEGNVFSCSVMHEALHNHYTQKSLSLSPG

Nucleic acid sequence of Fcab FS22-053-017 CH3 domain (SEQ ID NO: 91)

GGACAGCCTCGAGAACCACAGGTGTACACTCTGCCCCCTTCACGCGACGAACTCAATCCGCCCT
ACCTGTTCTCCAACCAAGTCTCCCTGACCTGTCTTGTGAAGGGTTTCTACCCATCCGATATCGCC

GTGGAGTGGGAGAGCAACGGACAGCCGGAGAACAACTATAAGACTACCCCGCCTGTGCTGGAC

TCGGACGGCAGCTTCTTCTTGTACTCCAAACTGACCGTGTACCACTGGCGGTGGCTGGAAGGGA
ACGTGTTTAGCTGCTCCGTCATGCATGAAGCCCTGCACAACCACTACACCCAGAAGTCCCTCTC
GCTCTCTCCGGGT

Amino acid sequences of Fcab FS22-053-014 CH3 domain structural loop sequences

FS22-053-014 first sequence - NPPYLFS (SEQ ID NO: 79)

FS22-053-014 second sequence - YHWRWLD (SEQ ID NO: 92)

Amino acid sequence of Fcab FS22-053-014 CH3 domain (SEQ ID NO: 93)

First and second sequences underlined

GQPREPQVYTLPPSRDELNPPYLFSNQVSLTCLVKGFYPSDIAVEWESNGQPENNYKTTPPVLDSDG
SFFLYSKLTVYHWRWLDGNVFSCSVMHEALHNHYTQKSLSLSPG

Nucleic acid sequence of Fcab FS22-053-014 CH3 domain (SEQ ID NO: 94)

GGACAGCCTCGAGAGCCTCAAGTGTACACCCTGCCCCCATCCCGGGATGAGCTGAACCCGCCG
TACCTGTTCTCTAACCAGGTCAGCCTGACCTGCCTGGTCAAAGGCTTCTATCCCAGCGACATCG
CCGTGGAGTGGGAGAGCAATGGGCAGCCGGAGAACAACTACAAGACCACGCCTCCCGTGCTGG
ACTCCGACGGCTCCTTCTTCCTCTACAGCAAGCTCACCGTGTACCATTGGAGGTGGCTGGATGG
GAACGTCTTCTCATGCTCCGTGATGCATGAGGCGCTGCACAACCACTACACTCAGAAGAGCTTG
TCCCTGTCGCCCGGA

Amino acid sequences of Fcab FS22-053-010 CH3 domain structural loop sequences

FS22-053-010 first sequence - NPPYLFS (SEQ ID NO: 79)

FS22-053-010 second sequence - DYMRWLD (SEQ ID NO: 95)

Amino acid sequence of Fcab FS22-053-010 CH3 domain (SEQ ID NO: 96)

First and second sequences underlined

GQPREPQVYTLPPSRDELNPPYLFSNQVSLTCLVKGFYPSDIAVEWESNGQPENNYKTTPPVLDSDG
SFFLYSKLTVDYMRWLDGNVFSCSVMHEALHNHYTQKSLSLSPG

Nucleic acid sequence of Fcab FS22-053-010 CH3 domain (SEQ ID NO: 97)

GGCCAGCCTCGAGAACCACAGGTGTACACCCTGCCCCCATCCCGGGATGAGCTGAACCCGCCG
TACCTGTTCTCTAACCAGGTCAGCCTGACCTGCCTGGTCAAAGGCTTCTATCCCAGCGACATCG
CCGTGGAGTGGGAGAGCAATGGGCAGCCGGAGAACAACTACAAGACCACGCCTCCCGTGCTGG
ACTCCGACGGCTCCTTCTTCCTCTACAGCAAGCTCACCGTGGATTACATGAGGTGGCTGGATGG
GAACGTCTTCTCATGCTCCGTGATGCATGAGGCTCTGCACAACCACTACACACAGAAGAGCCTC
TCCCTGTCTCCGGGT

Amino acid sequences of Fcab FS22-053-012 CH3 domain structural loop sequences

FS22-053-012 first sequence - NPPYLFS (SEQ ID NO: 79)

FS22-053-012 second sequence - DHMRWLE (SEQ ID NO: 98)

Amino acid sequence of Fcab FS22-053-012 CH3 domain (SEQ ID NO: 99)

First and second sequences underlined

GQPREPQVYTLPPSRDELNPPYLFSNQVSLTCLVKGFYPSDIAVEWESNGQPENNYKTTPPVLDSDG
SFFLYSKLTVDHMRWLEGNVFSCSVMHEALHNHYTQKSLSLSPG

Nucleic acid sequence of Fcab FS22-053-012 CH3 domain (SEQ ID NO: 100)

GGCCAGCCTCGAGAACCACAGGTGTACACCCTGCCCCCATCCCGGGATGAGCTGAACCCGCCG
TACCTGTTCTCTAACCAGGTCAGCCTGACCTGCCTGGTCAAAGGCTTCTATCCCAGCGACATCG

CCGTGGAGTGGGAGAGCAATGGGCAGCCGGAGAACAACTACAAGACCACGCCTCCCGTGCTGG
ACTCCGACGGCTCCTTCTTCCTCTACAGCAAGCTCACCGTGGATCATATGAGGTGGCTGGAAGG
GAACGTCTTCTCATGCTCCGTGATGCATGAGGCTCTGCACAACCACTACACACAGAAGAGCCTC
TCCCTGTCTCCGGGT

Amino acid sequences of Fcab FS22-053-013 CH3 domain structural loop sequences

FS22-053-013 first sequence - NPPYLFS (SEQ ID NO: 79)

FS22-053-013 second sequence - GYERWLE (SEQ ID NO: 101)

Amino acid sequence of Fcab FS22-053-013 CH3 domain (SEQ ID NO: 102)

First and second sequences underlined

GQPREPQVYTLPPSRDELNPPYLFSNQVSLTCLVKGFYPSDIAVEWESNGQPENNYKTTPPVLDSDG
SFFLYSKLTVGYERWLEGNVFSCSVMHEALHNHYTQKSLSLSPG

Nucleic acid sequence of Fcab FS22-053-013 CH3 domain (SEQ ID NO: 103)

GGCCAGCCTCGAGAACCACAGGTGTACACCCTGCCCCCATCCCGGGATGAGCTGAACCCGCCG
TACCTGTTCTCTAACCAGGTCAGCCTGACCTGCCTGGTCAAAGGCTTCTATCCCAGCGACATCG
CCGTGGAGTGGGAGAGCAATGGGCAGCCGGAGAACAACTACAAGACCACGCCTCCCGTGCTGG
ACTCCGACGGCTCCTTCTTCCTCTACAGCAAGCTCACCGTGGGTTACGAAAGGTGGCTGGAAGG
GAACGTCTTCTCATGCTCCGTGATGCATGAGGCTCTGCACAACCACTACACACAGAAGAGCCTC
TCCCTGTCTCCGGGT

Amino acid sequences of Fcab FS22-053-015 CH3 domain structural loop sequences

FS22-053-015 first sequence - NPPYLFS (SEQ ID NO: 79)

FS22-053-015 second sequence - DHWRWLQ (SEQ ID NO: 104)

Amino acid sequence of Fcab FS22-053-015 CH3 domain (SEQ ID NO: 105)

First and second sequences underlined

GQPREPQVYTLPPSRDELNPPYLFSNQVSLTCLVKGFYPSDIAVEWESNGQPENNYKTTPPVLDSDG
SFFLYSKLTVDHWRWLQGNVFSCSVMHEALHNHYTQKSLSLSPG

Nucleic acid sequence of Fcab FS22-053-015 CH3 domain (SEQ ID NO: 106)

GGCCAGCCTCGAGAACCACAGGTGTACACCCTGCCCCCATCCCGGGATGAGCTGAACCCGCCG
TACCTGTTCTCTAACCAGGTCAGCCTGACCTGCCTGGTCAAAGGCTTCTATCCCAGCGACATCG
CCGTGGAGTGGGAGAGCAATGGGCAGCCGGAGAACAACTACAAGACCACGCCTCCCGTGTTGG
ACTCCGACGGCTCCTTCTTCCTCTACAGCAAGCTCACCGTGGATCATTGGAGGTGGCTGCAGGG
GAACGTCTTCTCATGCTCCGTGATGCATGAGGCTCTGCACAACCACTACACACAGAAGAGCCTC
TCCCTGTCTCCGGGT

Amino acid sequences of Fcab FS22-053-016 CH3 domain structural loop sequences

FS22-053-016 first sequence - NPPYLFS (SEQ ID NO: 79)

FS22-053-016 second sequence - DYIRWLN (SEQ ID NO: 107)

Amino acid sequence of Fcab FS22-053-016 CH3 domain (SEQ ID NO: 108)

First and second sequences underlined
GQPREPQVYTLPPSRDELNPPYLFSNQVSLTCLVKGFYPSDIAVEWESNGQPENNYKTTPPVLDSDG
SFFLYSKLTVDYIRWLNGNVFSCSVMHEALHNHYTQKSLSLSPG

Nucleic acid sequence of Fcab FS22-053-016 CH3 domain (SEQ ID NO: 109)
GGCCAGCCTCGAGAACCACAGGTGTACACCCTGCCCCCATCCCGGGATGAGCTGAACCCGCCG
TACCTGTTCTCTAACCAGGTCAGCCTGACCTGCCTGGTCAAAGGCTTCTATCCCAGCGACATCG
CCGTGGAGTGGGAGAGCAATGGGCAGCCGGAGAACAACTACAAGACCACGCCTCCCGTGCTGG
ACTCCGACGGCTCCTTCTTCCTCTACAGCAAGCTCACCGTGGATTACATCAGGTGGCTGAACGG
GAACGTCTTCTCATGCTCCGTGATGCATGAGGCTCTGCACAACCACTACACACAGAAGAGCCTC
TCCCTGTCTCCGGGT

Amino acid sequences of FS22-053 CH3 domain structural loop sequences

FS22-053-008 first sequence - NPPYLFS (SEQ ID NO: 79)

FS22-053-008 second sequence - YYNRWQD (SEQ ID NO: 110)

Amino acid sequences of FS22-053 CH3 domain (SEQ ID NO: 111)
First and second sequences underlined
GQPREPQVYTLPPSRDELNPPYLFSNQVSLTCLVKGFYPSDIAVEWESNGQPENNYKTTPPVLDSDG
SFFLYSKLTVYYNRWQDGNVFSCSVMHEALHNHYTQKSLSLSPG

Nucleic acid sequence of Fcab FS22-053 CH3 domain (SEQ ID NO: 112)
GGCCAGCCTCGAGAACCACAGGTGTACACCCTGCCCCCATCCCGGGATGAGCTGAACCCGCCG
TACCTGTTCTCTAACCAGGTCAGCCTGACCTGCCTGGTCAAAGGCTTCTATCCCAGCGACATCG
CCGTGGAGTGGGAGAGCAATGGGCAGCCGGAGAACAACTACAAGACCACGCCTCCCGTGCTGG
ACTCCGACGGCTCCTTCTTCCTCTACAGCAAGCTCACCGTGTATTATAACAGGTGGCAGGATGG
GAACGTCTTCTCATGCTCCGTGATGCATGAGGCTCTGCACAACCACTACACACAGAAGAGCCTC
TCCCTGTCTCCGGGT

Amino acid sequences of Fcab FS22-172-003 CH3 domain structural loop sequences

FS22-172-003 first sequence - PYIIPPY (SEQ ID NO: 113)

FS22-172-003 second sequence - GADRWLE (SEQ ID NO: 114)

Amino acid sequence of Fcab FS22-172-003 CH3 domain (SEQ ID NO: 115)
First and second sequences underlined
GQPREPQVYTLPPSRDELPYIIPPYNQVSLTCLVKGFYPSDIAVEWESNGQPENNYKTTPPVLDSDGS
FFLYSKLTVGADRWLEGNVFSCSVMHEALHNHYTQKSLSLSPG

Nucleic acid sequence of Fcab FS22-172-003 CH3 domain (SEQ ID NO: 116)
GGACAGCCTCGAGAACCACAGGTGTACACCCTGCCCCCATCCCGGGATGAGCTGCCATACATC
ATCCCACCATACAACCAGGTCAGCCTGACCTGCCTGGTCAAAGGCTTCTATCCCAGCGACATCG
CCGTGGAGTGGGAGAGCAATGGGCAGCCGGAGAACAACTACAAGACCACGCCTCCCGTGCTGG
ACTCCGACGGCTCCTTCTTCCTCTACAGCAAGCTCACCGTGGGCGCAGATAGGTGGCTGGAAG
GGAACGTCTTCTCATGCTCCGTGATGCATGAGGCGCTGCACAACCACTACACTCAGAAGAGCTT
GTCCCTGTCGCCCGGT

Amino acid sequences of Fcab FS22-172-002 CH3 domain structural loop sequences

FS22-172-002 first sequence - PFQMPPY (SEQ ID NO: 117)

FS22-172-002 second sequence - GADRWLE (SEQ ID NO: 114)

Amino acid sequence of Fcab FS22-172-002 CH3 domain (SEQ ID NO: 118)

First and second sequences underlined

GQPREPQVYTLPPSRDELPFQMPPYNQVSLTCLVKGFYPSDIAVEWESNGQPENNYKTTPPVLDSD
GSFFLYSKLTVGADRWLEGNVFSCSVMHEALHNHYTQKSLSLSPG

Nucleic acid sequence of Fcab FS22-172-002 CH3 domain (SEQ ID NO: 119)

GGCCAGCCTCGAGAACCACAGGTGTACACCCTGCCCCCATCCCGGGATGAGCTGCCATTCCAG
ATGCCACCATACAACCAGGTCAGCCTGACCTGCCTGGTCAAAGGCTTCTATCCCAGCGACATCG
CCGTGGAGTGGGAGAGCAATGGGCAGCCGGAGAACAACTACAAGACCACGCCTCCCGTGCTGG
ACTCCGACGGCTCCTTCTTCCTCTACAGCAAGCTCACCGTGGGCGCAGATAGGTGGCTGGAAG
GGAACGTCTTCTCATGCTCCGTGATGCATGAGGCTCTGCACAACCACTACACACAGAAGAGCCT
CTCCCTGTCTCCGGGT

Amino acid sequences of Fcab FS22-172-004 CH3 domain structural loop sequences

FS22-172-004 first sequence - NYIYPPY (SEQ ID NO: 120)

FS22-172-004 second sequence - GADRWLE (SEQ ID NO: 114)

Amino acid sequence of Fcab FS22-172-004 CH3 domain (SEQ ID NO: 121)

First and second sequences underlined

GQPREPQVYTLPPSRDELNYIYPPYNQVSLTCLVKGFYPSDIAVEWESNGQPENNYKTTPPVLDSDG
SFFLYSKLTVGADRWLEGNVFSCSVMHEALHNHYTQKSLSLSPG

Nucleic acid sequence of Fcab FS22-172-004 CH3 domain (SEQ ID NO: 122)

GGACAGCCTCGAGAGCCTCAAGTGTACACCCTGCCCCCATCCCGGGATGAGCTGAACTACATCT
ACCCACCATACAACCAGGTCAGCCTGACCTGCCTGGTCAAAGGCTTCTATCCCAGCGACATCGC
CGTGGAGTGGGAGAGCAATGGGCAGCCGGAGAACAACTACAAGACCACGCCTCCCGTGCTGGA
CTCCGACGGCTCCTTCTTCCTCTACAGCAAGCTCACCGTGGGCGCAGATAGGTGGCTGGAAGG
GAACGTCTTCTCATGCTCCGTGATGCATGAGGCGCTGCACAACCACTACACTCAGAAGAGCTTG
TCCCTGTCGCCCGGA

Amino acid sequences of Fcab FS22-172-001 CH3 domain structural loop sequences

FS22-172-001 first sequence - PFVMPPY (SEQ ID NO: 123)

FS22-172-001 second sequence - GADRWLE (SEQ ID NO: 114)

Amino acid sequence of Fcab FS22-172-001 CH3 domain (SEQ ID NO: 124)

First and second sequences underlined

GQPREPQVYTLPPSRDELPFVMPPYNQVSLTCLVKGFYPSDIAVEWESNGQPENNYKTTPPVLDSD
GSFFLYSKLTVGADRWLEGNVFSCSVMHEALHNHYTQKSLSLSPG

Nucleic acid sequence of Fcab FS22-172-001 CH3 domain (SEQ ID NO: 125)

GGCCAGCCTCGAGAACCACAGGTGTACACCCTGCCCCCATCCCGGGATGAGCTGCCATTCGTT
ATGCCACCATACAACCAGGTCAGCCTGACCTGCCTGGTCAAAGGCTTCTATCCCAGCGACATCG
CCGTGGAGTGGGAGAGCAATGGGCAGCCGGAGAACAACTACAAGACCACGCCTCCCGTGCTGG
ACTCCGACGGCTCCTTCTTCCTCTACAGCAAGCTCACCGTGGGCGCAGATAGGTGGCTGGAAG
GGAACGTCTTCTCATGCTCCGTGATGCATGAGGCTCTGCACAACCACTACACACAGAAGAGCCT
CTCCCTGTCTCCGGGT

Amino acid sequences of Fcab FS22-172-005 CH3 domain structural loop sequences

FS22-172-005 first sequence - QQVYPPY (SEQ ID NO: 126)

FS22-172-005 second sequence - GADRWLE (SEQ ID NO: 114)

Amino acid sequence of Fcab FS22-172-005 CH3 domain (SEQ ID NO: 127)

First and second sequences underlined

GQPREPQVYTLPPSRDELQQVYPPYNQVSLTCLVKGFYPSDIAVEWESNGQPENNYKTTPPVLDSD
GSFFLYSKLTVGADRWLEGNVFSCSVMHEALHNHYTQKSLSLSPG

Nucleic acid sequence of Fcab FS22-172-005 CH3 domain (SEQ ID NO: 128)

GGCCAGCCTCGAGAACCACAGGTGTACACCCTGCCCCCATCCCGGGATGAGCTGCAGCAGGTT
TACCCACCATACAACCAGGTCAGCCTGACCTGCCTGGTCAAAGGCTTCTATCCCAGCGACATCG
CCGTGGAGTGGGAGAGCAATGGGCAGCCGGAGAACAACTACAAGACCACGCCTCCCGTGCTGG
ACTCCGACGGCTCCTTCTTCCTCTACAGCAAGCTCACCGTGGGCGCAGATAGGTGGCTGGAAG
GGAACGTCTTCTCATGCTCCGTGATGCATGAGGCTCTGCACAACCACTACACACAGAAGAGCCT
CTCCCTGTCTCCGGGT

Amino acid sequences of Fcab FS22-172-006 CH3 domain structural loop sequences

FS22-172-006 first sequence - RKYYPPY (SEQ ID NO: 129)

FS22-172-006 second sequence - GADRWLE (SEQ ID NO: 114)

Amino acid sequence of Fcab FS22-172-006 CH3 domain (SEQ ID NO: 130)

First and second sequences underlined

GQPREPQVYTLPPSRDELRKYYPPYNQLSLTCLVKGFYPSDIAVEWESNGQPENNYKTTPPVLDSD
GSFFLYSKLTVGADRWLEGNVFSCSVMHEALHNHYTQKSLSLSPG

Nucleic acid sequence of Fcab FS22-172-006 CH3 domain (SEQ ID NO: 131)

GGCCAGCCTCGAGAACCACAGGTGTACACCCTGCCCCCATCCCGGGATGAGCTGCGTAAATAC
TACCCGCCGTACAACCAGCTCAGCCTGACCTGCCTGGTCAAAGGCTTCTATCCCAGCGACATCG
CCGTGGAGTGGGAGAGCAATGGGCAGCCGGAGAACAACTACAAGACCACGCCTCCCGTGCTGG
ACTCCGACGGCTCCTTCTTCCTCTACAGCAAGCTCACCGTGGGCGCAGATAGGTGGCTGGAAG
GGAACGTCTTCTCATGCTCCGTGATGCATGAGGCTCTGCACAACCACTACACACAGAAGAGCCT
CTCCCTGTCTCCGGGT

Amino acid sequences of Fcab FS22-172 CH3 domain structural loop sequences

FS22-172 first sequence - RKYYPPY (SEQ ID NO: 129)

FS22-172 second sequence - GADRWLE (SEQ ID NO: 114)

Amino acid sequence of Fcab FS22-172 CH3 domain (SEQ ID NO: 132)

First and second sequences underlined

GQPREPQVYTLPPSRDELRKYYPPYNQVSLTCLVKGFYPSDIAVEWESNGQPENNYKTTPPVLDSD
GSFFLYSKLTVGADRWLEGNVFSCSVMHEALHNHYTQKSLSLSPG

Nucleic acid sequence of Fcab FS22-172 CH3 domain (SEQ ID NO: 133)

GGCCAGCCTCGAGAACCACAGGTGTACACCCTGCCCCCATCCCGGGATGAGCTGCGTAAATAC
TACCCGCCGTACAACCAGGTCAGCCTGACCTGCCTGGTCAAAGGCTTCTATCCCAGCGACATCG
CCGTGGAGTGGGAGAGCAATGGGCAGCCGGAGAACAACTACAAGACCACGCCTCCCGTGCTGG
ACTCCGACGGCTCCTTCTTCCTCTACAGCAAGCTCACCGTGGGCGCAGATAGGTGGCTGGAAG
GGAACGTCTTCTCATGCTCCGTGATGCATGAGGCTCTGCACAACCACTACACACAGAAGAGCCT
CTCCCTGTCTCCGGGT

Amino acid sequence of the heavy chain of FS22-172-003-AA/E12v2 mAb^2 with LALA mutation

(SEQ ID NO: 134)

VH domain (italics); LALA mutation (bold underlined)

EVQLVQSGAEVKRPGASVKVSCKASGYPFTSYGISWVRQAPGQGLEWMGWISAYSGGTNYAQKLQ
*GRVTMTTDTSTSTAYMELRSLRSDDTAVYYCARDLFPTIFGVSYYYYWGQGTLVTVSS*ASTKGPSVF
PLAPSSKSTSGGTAALGCLVKDYFPEPVTVSWNSGALTSGVHTFPAVLQSSGLYSLSSVVTVPSSSL
GTQTYICNVNHKPSNTKVDKKVEPKSCDKTHTCPPCPAPE**AA**GGPSVFLFPPKPKDTLMISRTPEVT

CVVVDVSHEDPEVKFNWYVDGVEVHNAKTKPREEQYNSTYRVVSVLTVLHQDWLNGKEYKCKVSN
KALPAPIEKTISKAKGQPREPQVYTLPPSRDELPYIIPPYNQVSLTCLVKGFYPSDIAVEWESNGQPEN
NYKTTPPVLDSDGSFFLYSKLTVGADRWLEGNVFSCSVMHEALHNHYTQKSLSLSPG

Nucleic acid sequence of the heavy chain of FS22-172-003-AA/E12v2 mAb^2 with LALA mutation (SEQ ID NO: 135)

GAAGTTCAGCTGGTTCAGTCTGGCGCCGAAGTGAAAAGACCTGGCGCCTCTGTGAAGGTGTCCT
GCAAGGCTTCTGGCTACCCCTTTACCTCCTACGGCATCTCCTGGGTCCGACAGGCTCCTGGACA
AGGCTTGGAATGGATGGGCTGGATCTCCGCTTATTCCGGCGGCACCAATTACGCCCAGAAACTG
CAGGGCAGAGTGACCATGACCACCGACACCTCTACCTCCACCGCCTACATGGAACTGCGGTCC
CTGAGATCTGACGACACCGCCGTGTACTACTGCGCCAGAGATCTGTTCCCCACCATCTTCGGCG
TGTCCTACTACTACTATTGGGGCCAGGGCACCCTGGTCACCGTGTCCTCTGCTTCTACCAAGGG
ACCCAGCGTGTTCCCTCTGGCTCCTTCCAGCAAGTCTACCTCTGGCGGAACAGCTGCTCTGGGC
TGCCTGGTCAAGGACTACTTTCCTGAGCCTGTGACCGTGTCTTGGAACTCTGGCGCTCTGACAT
CTGGCGTGCACACCTTTCCAGCTGTGCTGCAGTCCTCCGGCCTGTACTCTCTGTCCTCTGTCGT
GACCGTGCCTTCCAGCTCTCTGGGAACCCAGACCTACATCTGCAATGTGAACCACAAGCCTTCC
AACACCAAGGTGGACAAGAAGGTGGAACCCAAGTCCTGCGACAAGACCCACACCTGTCCTCCAT
GTCCTGCTCCAGAAGCTGCTGGCGGCCCTTCCGTGTTTCTGTTCCCTCCAAAGCCTAAGGACAC
CCTGATGATCTCTCGGACCCCTGAAGTGACCTGCGTGGTGGTGGATGTGTCTCACGAGGACCCA
GAAGTGAAGTTCAATTGGTACGTGGACGGCGTGGAAGTGCACAACGCCAAGACCAAGCCTAGA
GAGGAACAGTACAACTCCACCTACAGAGTGGTGTCCGTGCTGACCGTGCTGCACCAGGATTGGC
TGAACGGCAAAGAGTACAAGTGCAAGGTGTCCAACAAGGCCCTGCCTGCTCCTATCGAAAAGAC
CATCTCCAAGGCCAAGGGCCAGCCTAGGGAACCCCAGGTTTACACCTTGCCTCCATCTCGGGAC
GAGCTGCCCTACATCATCCCTCCATACAACCAGGTGTCCCTGACCTGCCTCGTGAAGGGCTTCT
ACCCTTCCGATATCGCCGTGGAATGGGAGAGCAATGGCCAGCCTGAGAACAACTACAAGACAAC
CCCTCCTGTGCTGGACTCCGACGGCTCATTCTTTCTGTACTCCAAGCTGACAGTGGGCGCCGAC
AGATGGCTGGAAGGGAACGTGTTCTCCTGCAGCGTGATGCACGAGGCCCTGCACAATCACTACA
CACAGAAGTCCCTGTCTCTGTCCCCTGGC

Amino acid sequence of the light chain of FS22-172-003-AA/E12v2 and FS22-053-008-AA/E12v2 mAb^2 (SEQ ID NO: 17)

DIQMTQSPSTLSASVRDRVIITCRASQSIGNRLAWYQHKPGKAPKLLIYEASTSETGVPSRFSGSGSG
TDFTLTISSLQPEDFATYYCQQSYSTPYTFGQGTKLEIKRTVAAPSVFIFPPSDEQLKSGTASVVCLLN
NFYPREAKVQWKVDNALQSGNSQESVTEQDSKDSTYSLSSTLTLSKADYEKHKVYACEVTHQGLSS
PVTKSFNRGEC

Nucleic acid sequence of the light chain of FS22-172-003-AA/E12v2 mAb^2 (SEQ ID NO: 136)

GACATCCAGATGACCCAGTCTCCATCCACACTGTCCGCCTCTGTGCGGGACAGAGTGATCATCA
CCTGTAGAGCCAGCCAGTCCATCGGCAACAGACTGGCCTGGTATCAGCACAAGCCTGGCAAGG
CTCCCAAGCTGCTGATCTACGAGGCCTCCACATCTGAGACAGGCGTGCCCTCTAGATTCTCCGG
CTCTGGCTCTGGCACCGACTTTACCCTGACAATCTCCAGCCTGCAGCCTGAGGACTTCGCCACC
TACTACTGCCAGCAGTCCTACAGCACCCCTTACACCTTTGGCCAGGGCACCAAGCTGGAAATCA
AGCGTACGGTGGCCGCTCCCAGCGTGTTCATCTTCCCCCCAAGCGACGAGCAGCTGAAGAGCG
GCACCGCCAGCGTGGTGTGTCTGCTGAACAACTTCTACCCCAGGGAGGCCAAGGTGCAGTGGA
AGGTGGACAACGCCCTGCAGAGCGGCAACAGCCAGGAGAGCGTCACCGAGCAGGACAGCAAG
GACTCCACCTACAGCCTGAGCAGCACCCTGACCCTGAGCAAGGCCGACTACGAGAAGCACAAG
GTGTACGCCTGTGAGGTGACCCACCAGGGCCTGTCCAGCCCCGTGACCAAGAGCTTCAACAGG
GGCGAGTGC

Amino acid sequence of the heavy chain of FS22-172-003-AA/E05v2 mAb^2 with LALA mutation (SEQ ID NO: 137)

VH domain (italics); LALA mutation (bold underlined)

EVQLVQSGAEVKRPGASVKVSCKASGYTFTSYGISWVRQAPGQGLEWMGWISAYSGGTNYAQKLQ
*GRVTMTTDTSTSTAYMELRSLRSDDTAVYYCARDLFPTIFGVSYYYYWGQGTLVTVSS*ASTKGPSVF
PLAPSSKSTSGGTAALGCLVKDYFPEPVTVSWNSGALTSGVHTFPAVLQSSGLYSLSSVVTVPSSSL
GTQTYICNVNHKPSNTKVDKKVEPKSCDKTHTCPPCPAPE**AA**GGPSVFLFPPKPKDTLMISRTPEVT
CVVVDVSHEDPEVKFNWYVDGVEVHNAKTKPREEQYNSTYRVVSVLTVLHQDWLNGKEYKCKVSN
KALPAPIEKTISKAKGQPREPQVYTLPPSRDELPYIIPPYNQVSLTCLVKGFYPSDIAVEWESNGQPEN
NYKTTPPVLDSDGSFFLYSKLTVGADRWLEGNVFSCSVMHEALHNHYTQKSLSLSPG

Nucleic acid sequence of the heavy chain of FS22-172-003-AA/E05v2 mAb^2 with LALA mutation (SEQ ID NO: 138)

GAAGTGCAGCTGGTGCAGTCCGGAGCCGAAGTCAAGAGGCCTGGAGCGTCCGTGAAGGTGTCC
TGCAAAGCCTCAGGATACACCTTCACTTCGTACGGGATTTCCTGGGTCCGCCAAGCACCGGGTC
AAGGCTTGGAGTGGATGGGATGGATCAGCGCGTATTCCGGGGGAACCAACTACGCTCAAAAGC
TGCAGGGTCGCGTGACCATGACCACCGATACCTCCACCTCAACGGCCTACATGGAACTGAGATC
TCTGCGGAGCGACGACACTGCCGTGTACTACTGTGCCCGGGACCTGTTCCCCACTATCTTCGGA
GTGTCGTACTACTACTACTGGGGCCAGGGGACTCTCGTGACCGTGTCGAGCGCTAGCACTAAG
GGCCCGTCGGTGTTCCCGCTGGCCCCATCGTCCAAGAGCACATCAGGGGGTACCGCCGCCCTG
GGCTGCCTTGTGAAGGATTACTTTCCCGAGCCCGTCACAGTGTCCTGGAACAGCGGAGCCCTGA
CCTCCGGAGTGCATACTTTCCCGGCTGTGCTTCAGTCCTCTGGCCTGTACTCATTGTCCTCCGTG
GTCACCGTCCCTTCGTCCTCCCTGGGCACCCAGACCTATATCTGTAATGTCAACCATAAGCCCTC
GAACACCAAGGTCGACAAGAAGGTCGAGCCGAAGTCGTGCGACAAGACTCACACTTGCCCGCC
TTGCCCAGCCCCGGAAGCTGCCGGTGGTCCTTCGGTGTTCCTCTTCCCGCCCAAGCCGAAGGA
TACCCTGATGATCTCACGGACCCCCGAAGTGACCTGTGTGGTGGTGGACGTGTCCCACGAGGA
CCCGGAAGTGAAATTCAATTGGTACGTGGATGGAGTGGAAGTGCACAACGCCAAGACCAAGCCA
CGGGAAGAACAGTACAACTCTACCTACCGCGTGGTGTCCGTGCTCACTGTGCTGCACCAAGACT
GGCTGAACGGGAAGGAGTACAAGTGCAAAGTGTCCAACAAGGCGCTGCCTGCCCCAATTGAGA
AAACTATCTCGAAAGCCAAGGGACAGCCTCGAGAACCACAGGTGTACACCCTGCCCCCATCCCG
GGATGAGCTGCCATACATCATCCCACCATACAACCAGGTCAGCCTGACCTGCCTGGTCAAAGGC
TTCTATCCCAGCGACATCGCCGTGGAGTGGGAGAGCAATGGGCAGCCGGAGAACAACTACAAG
ACCACGCCTCCCGTGCTGGACTCCGACGGCTCCTTCTTCCTCTACAGCAAGCTCACCGTGGGCG
CAGATAGGTGGCTGGAAGGGAACGTCTTCTCATGCTCCGTGATGCATGAGGCGCTGCACAACCA
CTACACTCAGAAGAGCTTGTCCCTGTCGCCCGGT

Nucleic acid sequence of the light chain of FS22-172-003-AA/E05v2 mAb^2 (SEQ ID NO: 139)

GACATTCAGATGACCCAATCCCCGTCCACGCTGAGCGCCTCCGTCGGTGATCGCGTGACAATCA
CTTGTCGGGCGTCGCAGTCCATCTCTGGAAGGCTCGCCTGGTACCAGCAGAAGCCTGGAAAGG
CTCCCAACCTCCTTATCTACGAAGCCAGCAACCTGGAGTCCGGAGTGCCTAGCCGGTTCAGCGG
ATCAGGGTCCGGTACCGAGTTCACCCTGACCATTTCCTCGCTCCAACCTGAGGACTTCGCCACC
TACTACTGCCAACAGTCCTATTCAACTCCGCGCGTGACCTTCGGCCAGGGCACTAAGGTCGAAA
TCAAAAGAACCGTGGCAGCCCCATCGGTGTTTATCTTCCCGCCCTCGGACGAACAGCTGAAGTC
AGGCACTGCTAGCGTGGTCTGTCTCCTGAACAATTTCTACCCGCGCGAAGCTAAGGTCCAGTGG
AAGGTCGACAACGCGCTGCAGTCCGGAAACAGCCAGGAGTCAGTGACCGAGCAGGACTCCAAG
GATTCCACTTATTCCCTGTCCTCCACCCTGACTTTGAGCAAGGCCGACTACGAGAAGCACAAAGT
GTACGCCTGCGAAGTGACCCATCAAGGGCTTTCGTCGCCCGTGACCAAGAGCTTCAACCGGGG
CGAATGC

Amino acid(AA) sequence of the heavy chain of FS22-172-003-AA/G12v2 mAb^2 with LALA mutation (SEQ ID NO: 140)

VH domain (italics); LALA mutation (bold underlined)

EVQLVQSGAEVKRPGASVKVSCKASGYTFTSYGISWVRQAPGQGLEWMGWISAYSGGTNYAQKLQ
*GRVTMTTDTSTSTAYMELRSLRSDDTAVYYCARDLFPTIFGVSYYYYWGQGTLVTVSS*ASTKGPSVF
PLAPSSKSTSGGTAALGCLVKDYFPEPVTVSWNSGALTSGVHTFPAVLQSSGLYSLSSVVTVPSSSL
GTQTYICNVNHKPSNTKVDKKVEPKSCDKTHTCPPCPAPE**AA**GGPSVFLFPPKPKDTLMISRTPEVT

CVVVDVSHEDPEVKFNWYVDGVEVHNAKTKPREEQYNSTYRVVSVLTVLHQDWLNGKEYKCKVSN
KALPAPIEKTISKAKGQPREPQVYTLPPSRDELPYIIPPYNQVSLTCLVKGFYPSDIAVEWESNGQPEN
NYKTTPPVLDSDGSFFLYSKLTVGADRWLEGNVFSCSVMHEALHNHYTQKSLSLSPG

Nucleic acid sequence of the heavy chain of FS22-172-003-AA/G12v2 mAb^2 with LALA mutation (SEQ ID NO: 141)

GAAGTGCAGCTGGTGCAGTCCGGAGCCGAAGTCAAGAGGCCTGGAGCGTCCGTGAAGGTGTCC
TGCAAAGCCTCAGGATACACCTTCACTTCGTACGGGATTTCCTGGGTCCGCCAAGCACCGGGTC
AAGGCTTGGAGTGGATGGGATGGATCAGCGCGTATTCCGGGGGAACCAACTACGCTCAAAAGC
TGCAGGGTCGCGTGACCATGACCACCGATACCTCCACCTCAACGGCCTACATGGAACTGAGATC
TCTGCGGAGCGACGACACTGCCGTGTACTACTGTGCCCGGGACCTGTTCCCCACTATCTTCGGA
GTGTCGTACTACTACTACTGGGGCCAGGGGACTCTCGTGACCGTGTCGAGCGCTAGCACTAAG
GGCCCGTCGGTGTTCCCGCTGGCCCCATCGTCCAAGAGCACATCAGGGGGTACCGCCGCCCTG
GGCTGCCTTGTGAAGGATTACTTTCCCGAGCCCGTCACAGTGTCCTGGAACAGCGGAGCCCTGA
CCTCCGGAGTGCATACTTTCCCGGCTGTGCTTCAGTCCTCTGGCCTGTACTCATTGTCCTCCGTG
GTCACCGTCCCTTCGTCCTCCCTGGGCACCCAGACCTATATCTGTAATGTCAACCATAAGCCCTC
GAACACCAAGGTCGACAAGAAGGTCGAGCCGAAGTCGTGCGACAAGACTCACACTTGCCCGCC
TTGCCCAGCCCCGGAAGCTGCCGGTGGTCCTTCGGTGTTCCTCTTCCCGCCCAAGCCGAAGGA
TACCCTGATGATCTCACGGACCCCCGAAGTGACCTGTGTGGTGGTGGACGTGTCCCACGAGGA
CCCGGAAGTGAAATTCAATTGGTACGTGGATGGAGTGGAAGTGCACAACGCCAAGACCAAGCCA
CGGGAAGAACAGTACAACTCTACCTACCGCGTGGTGTCCGTGCTCACTGTGCTGCACCAAGACT
GGCTGAACGGGAAGGAGTACAAGTGCAAAGTGTCCAACAAGGCGCTGCCTGCCCCAATTGAGA
AAACTATCTCGAAAGCCAAGGGACAGCCTCGAGAACCACAGGTGTACACCCTGCCCCCATCCCG
GGATGAGCTGCCATACATCATCCCACCATACAACCAGGTCAGCCTGACCTGCCTGGTCAAAGGC
TTCTATCCCAGCGACATCGCCGTGGAGTGGGAGAGCAATGGGCAGCCGGAGAACAACTACAAG
ACCACGCCTCCCGTGCTGGACTCCGACGGCTCCTTCTTCCTCTACAGCAAGCTCACCGTGGGCG
CAGATAGGTGGCTGGAAGGGAACGTCTTCTCATGCTCCGTGATGCATGAGGCGCTGCACAACCA
CTACACTCAGAAGAGCTTGTCCCTGTCGCCCGGT

Nucleic acid sequence of the light chain of FS22-172-003-AA/G12v2 mAb^2 (SEQ ID NO: 142)

GACATTCAGATGACCCAGTCCCCGAGCACGCTGTCCGCAAGCGTGGGGGACAGAGTGACCATC
ACTTGCCGCGCCTCACAATCCATCAGCGGACGCTTGGCCTGGTACCAGCAGAAGCCCGGAAAG
GCCCCAAACCTTCTGATCTACGAAGCCTCGAACCTGGAGTCAGGCGTCCCTTCGCGGTTCTCTG
GCTCCGGTTCCGGAACTGAGTTCACCCTCACCATCTCGTCCCTGCAACCGGAAGATTTCGCCAC
CTACTACTGCCAACAGTCGTACTCCTGGCCCCGGACATTCGGACAGGGAACCAAAGTCGAGATT
AAGCGGACTGTGGCGGCTCCTAGCGTGTTCATCTTTCCCCCGTCCGACGAACAGCTGAAGTCCG
GTACCGCTAGCGTGGTCTGTCTCCTGAACAATTTCTACCCGCGCGAAGCTAAGGTCCAGTGGAA
GGTCGACAACGCGCTGCAGTCCGGAAACAGCCAGGAGTCAGTGACCGAGCAGGACTCCAAGGA
TTCCACTTATTCCCTGTCCTCCACCCTGACTTTGAGCAAGGCCGACTACGAGAAGCACAAAGTGT
ACGCCTGCGAAGTGACCCATCAAGGGCTTTCGTCGCCCGTGACCAAGAGCTTCAACCGGGGCG
AATGC

AA sequence of the heavy chain of FS22-053-008-AA/E12v2 mAb^2 with LALA mutation (SEQ ID NO: 143)

VH domain (italics); LALA mutation (bold underlined)

EVQLVQSGAEVKRPGASVKVSCKASGYPFTSYGISWVRQAPGQGLEWMGWISAYSGGTNYAQKLQ
*GRVTMTTDTSTSTAYMELRSLRSDDTAVYYCARDLFPTIFGVSYYYYWGQGTLVTVSS*ASTKGPSVF
PLAPSSKSTSGGTAALGCLVKDYFPEPVTVSWNSGALTSGVHTFPAVLQSSGLYSLSSVVTVPSSSL
GTQTYICNVNHKPSNTKVDKKVEPKSCDKTHTCPPCPAPE**AA**GGPSVFLFPPKPKDTLMISRTPEVT
CVVVDVSHEDPEVKFNWYVDGVEVHNAKTKPREEQYNSTYRVVSVLTVLHQDWLNGKEYKCKVSN
KALPAPIEKTISKAKGQPREPQVYTLPPSRDELNPPYLFSNQVSLTCLVKGFYPSDIAVEWESNGQPE
NNYKTTPPVLDSDGSFFLYSKLTVDYWRWLEGNVFSCSVMHEALHNHYTQKSLSLSPG

Nucleic acid sequence of the heavy chain of FS22-053-008-AA/E12v2 mAb^2 with LALA mutation (SEQ ID NO: 144)

GAAGTGCAGCTGGTGCAGTCCGGAGCCGAAGTCAAGAGGCCTGGAGCGTCCGTGAAGGTGTCC

TGCAAAGCCTCAGGATACCCCTTCACTTCGTACGGGATTTCCTGGGTCCGCCAAGCACCGGGTC
AAGGCTTGGAGTGGATGGGATGGATCAGCGCGTATTCCGGGGGAACCAACTACGCTCAAAAGC
TGCAGGGTCGCGTGACCATGACCACCGATACCTCCACCTCAACGGCCTACATGGAACTGAGATC
TCTGCGGAGCGACGACACTGCCGTGTACTACTGTGCCCGGGACCTGTTCCCCACTATCTTCGGA
GTGTCGTACTACTACTACTGGGGCCAGGGGACTCTCGTGACCGTGTCGAGCGCTAGCACTAAG
GGCCCGTCGGTGTTCCCGCTGGCCCCATCGTCCAAGAGCACATCAGGGGGTACCGCCGCCCTG
GGCTGCCTTGTGAAGGATTACTTTCCCGAGCCCGTCACAGTGTCCTGGAACAGCGGAGCCCTGA
CCTCCGGAGTGCATACTTTCCCGGCTGTGCTTCAGTCCTCTGGCCTGTACTCATTGTCCTCCGTG
GTCACCGTCCCTTCGTCCTCCCTGGGCACCCAGACCTATATCTGTAATGTCAACCATAAGCCCTC
GAACACCAAGGTCGACAAGAAGGTCGAGCCGAAGTCGTGCGACAAGACTCACACTTGCCCGCC
TTGCCCAGCCCCGGAAGCTGCCGGTGGTCCTTCGGTGTTCCTCTTCCCGCCCAAGCCGAAGGA
TACCCTGATGATCTCACGGACCCCCGAAGTGACCTGTGTGGTGGTGGACGTGTCCCACGAGGA
CCCGGAAGTGAAATTCAATTGGTACGTGGATGGAGTGGAAGTGCACAACGCCAAGACCAAGCCA
CGGGAAGAACAGTACAACTCTACCTACCGCGTGGTGTCCGTGCTCACTGTGCTGCACCAAGACT
GGCTGAACGGGAAGGAGTACAAGTGCAAAGTGTCCAACAAGGCGCTGCCTGCCCCAATTGAGA
AAACTATCTCGAAAGCCAAGGGACAGCCTCGAGAACCACAGGTGTACACCCTGCCCCCATCCCG
GGATGAGCTGAACCCGCCGTACCTGTTCTCTAACCAGGTCAGCCTGACCTGCCTGGTCAAAGGC
TTCTATCCCAGCGACATCGCCGTGGAGTGGGAGAGCAATGGGCAGCCGGAGAACAACTACAAG
ACCACGCCTCCCGTACTGGACTCCGACGGCTCCTTCTTCCTCTACAGCAAGCTCACCGTGGATT
ACTGGAGGTGGCTGGAAGGGAACGTCTTCTCATGCTCCGTGATGCATGAGGCGCTGCACAACC
ACTACACTCAGAAGAGCTTGTCCCTGTCGCCCGGT

Nucleic acid sequence of the light chain of FS22-053-008-AA/E12v2 mAb^2 (SEQ ID NO: 145)

GACATCCAGATGACGCAGAGCCCGTCTACCCTGTCCGCCTCCGTGAGAGATCGCGTGATCATCA
CCTGTCGGGCCAGCCAGTCCATCGGAAACCGCTTGGCGTGGTACCAGCACAAGCCTGGGAAGG
CTCCGAAGCTGCTCATCTACGAAGCCTCGACTTCGGAGACTGGTGTCCCTAGCCGGTTCAGCGG
ATCGGGATCAGGGACCGATTTCACTCTGACCATTTCCTCCCTGCAACCCGAGGACTTCGCCACC
TACTACTGCCAACAGTCATATTCCACCCCGTACACCTTCGGACAAGGCACCAAGCTCGAAATCAA
GCGGACTGTCGCCGCACCTTCCGTGTTCATTTTCCCACCCTCCGACGAACAGCTGAAATCGGGT
ACAGCTAGCGTGGTCTGTCTCCTGAACAATTTCTACCCGCGCGAAGCTAAGGTCCAGTGGAAGG
TCGACAACGCGCTGCAGTCCGGAAACAGCCAGGAGTCAGTGACCGAGCAGGACTCCAAGGATT
CCACTTATTCCCTGTCCTCCACCCTGACTTTGAGCAAGGCCGACTACGAGAAGCACAAAGTGTAC
GCCTGCGAAGTGACCCATCAAGGGCTTTCGTCGCCCGTGACCAAGAGCTTCAACCGGGGCGAA
TGC

AA sequence of the heavy chain of FS22-053-008-AA/E05v2 with LALA mutation (SEQ ID NO: 146) VH domain (italics); LALA mutation (bold underlined)

EVQLVQSGAEVKRPGASVKVSCKASGYTFTSYGISWVRQAPGQGLEWMGWISAYSGGTNYAQKLQ
*GRVTMTTDTSTSTAYMELRSLRSDDTAVYYCARDLFPTIFGVSYYYYWGQGTLVTVSS*ASTKGPSVF
PLAPSSKSTSGGTAALGCLVKDYFPEPVTVSWNSGALTSGVHTFPAVLQSSGLYSLSSVVTVPSSSL
GTQTYICNVNHKPSNTKVDKKVEPKSCDKTHTCPPCPAPE**AA**GGPSVFLFPPKPKDTLMISRTPEVT
CVVVDVSHEDPEVKFNWYVDGVEVHNAKTKPREEQYNSTYRVVSVLTVLHQDWLNGKEYKCKVSN
KALPAPIEKTISKAKGQPREPQVYTLPPSRDELNPPYLFSNQVSLTCLVKGFYPSDIAVEWESNGQPE
NNYKTTPPVLDSDGSFFLYSKLTVDYWRWLEGNVFSCSVMHEALHNHYTQKSLSLSPG

Nucleic acid sequence of the heavy chain of FS22-053-008-AA/E05v2 mAb^2 with LALA mutation (SEQ ID NO: 147)

GAAGTGCAGCTGGTGCAGTCCGGAGCCGAAGTCAAGAGGCCTGGAGCGTCCGTGAAGGTGTCC
TGCAAAGCCTCAGGATACACCTTCACTTCGTACGGGATTTCCTGGGTCCGCCAAGCACCGGGTC
AAGGCTTGGAGTGGATGGGATGGATCAGCGCGTATTCCGGGGGAACCAACTACGCTCAAAAGC
TGCAGGGTCGCGTGACCATGACCACCGATACCTCCACCTCAACGGCCTACATGGAACTGAGATC
TCTGCGGAGCGACGACACTGCCGTGTACTACTGTGCCCGGGACCTGTTCCCCACTATCTTCGGA
GTGTCGTACTACTACTACTGGGGCCAGGGGACTCTCGTGACCGTGTCGAGCGCTAGCACTAAG
GGCCCGTCGGTGTTCCCGCTGGCCCCATCGTCCAAGAGCACATCAGGGGGTACCGCCGCCCTG
GGCTGCCTTGTGAAGGATTACTTTCCCGAGCCCGTCACAGTGTCCTGGAACAGCGGAGCCCTGA
CCTCCGGAGTGCATACTTTCCCGGCTGTGCTTCAGTCCTCTGGCCTGTACTCATTGTCCTCCGTG
GTCACCGTCCCTTCGTCCTCCCTGGGCACCCAGACCTATATCTGTAATGTCAACCATAAGCCCTC

GAACACCAAGGTCGACAAGAAGGTCGAGCCGAAGTCGTGCGACAAGACTCACACTTGCCCGCC
TTGCCCAGCCCCGGAAGCTGCCGGTGGTCCTTCGGTGTTCCTCTTCCCGCCCAAGCCGAAGGA
TACCCTGATGATCTCACGGACCCCCGAAGTGACCTGTGTGGTGGTGGACGTGTCCCACGAGGA
CCCGGAAGTGAAATTCAATTGGTACGTGGATGGAGTGGAAGTGCACAACGCCAAGACCAAGCCA
CGGGAAGAACAGTACAACTCTACCTACCGCGTGGTGTCCGTGCTCACTGTGCTGCACCAAGACT
GGCTGAACGGGAAGGAGTACAAGTGCAAAGTGTCCAACAAGGCGCTGCCTGCCCCAATTGAGA
AAACTATCTCGAAAGCCAAGGGACAGCCTCGAGAACCACAGGTGTACACCCTGCCCCCATCCCG
GGATGAGCTGAACCCGCCGTACCTGTTCTCTAACCAGGTCAGCCTGACCTGCCTGGTCAAAGGC
TTCTATCCCAGCGACATCGCCGTGGAGTGGGAGAGCAATGGGCAGCCGGAGAACAACTACAAG
ACCACGCCTCCCGTACTGGACTCCGACGGCTCCTTCTTCCTCTACAGCAAGCTCACCGTGGATT
ACTGGAGGTGGCTGGAAGGGAACGTCTTCTCATGCTCCGTGATGCATGAGGCGCTGCACAACC
ACTACACTCAGAAGAGCTTGTCCCTGTCGCCCGGT

Nucleic acid sequence of the light chain of FS22-053-008-AA/E05v2 mAb^2 (SEQ ID NO: 148)

GACATTCAGATGACCCAATCCCCGTCCACGCTGAGCGCCTCCGTCGGTGATCGCGTGACAATCA
CTTGTCGGGCGTCGCAGTCCATCTCTGGAAGGCTCGCCTGGTACCAGCAGAAGCCTGGAAAGG
CTCCCAACCTCCTTATCTACGAAGCCAGCAACCTGGAGTCCGGAGTGCCTAGCCGGTTCAGCGG
ATCAGGGTCCGGTACCGAGTTCACCCTGACCATTTCCTCGCTCCAACCTGAGGACTTCGCCACC
TACTACTGCCAACAGTCCTATTCAACTCCGCGCGTGACCTTCGGCCAGGGCACTAAGGTCGAAA
TCAAAAGAACCGTGGCAGCCCCATCGGTGTTTATCTTCCCGCCCTCGGACGAACAGCTGAAGTC
AGGCACTGCTAGCGTGGTCTGTCTCCTGAACAATTTCTACCCGCGCGAAGCTAAGGTCCAGTGG
AAGGTCGACAACGCGCTGCAGTCCGGAAACAGCCAGGAGTCAGTGACCGAGCAGGACTCCAAG
GATTCCACTTATTCCCTGTCCTCCACCCTGACTTTGAGCAAGGCCGACTACGAGAAGCACAAAGT
GTACGCCTGCGAAGTGACCCATCAAGGGCTTTCGTCGCCCGTGACCAAGAGCTTCAACCGGGGG
CGAATGC

AA sequence of the heavy chain of FS22-053-008-AA/G12v2 with LALA mutation (SEQ ID NO: 149) VH domain (italics); LALA mutation (bold underlined)

EVQLVQSGAEVKRPGASVKVSCKASGYTFTSYGISWVRQAPGQGLEWMGWISAYSGGTNYAQKLQ
*GRVTMTTDTSTSTAYMELRSLRSDDTAVYYCARDLFPTIFGVSYYYYWGQGTLVTVSS*ASTKGPSVF
PLAPSSKSTSGGTAALGCLVKDYFPEPVTVSWNSGALTSGVHTFPAVLQSSGLYSLSSVVTVPSSSL
GTQTYICNVNHKPSNTKVDKKVEPKSCDKTHTCPPCPAPE**AA**GGPSVFLFPPKPKDTLMISRTPEVT
CVVVDVSHEDPEVKFNWYVDGVEVHNAKTKPREEQYNSTYRVVSVLTVLHQDWLNGKEYKCKVSN
KALPAPIEKTISKAKGQPREPQVYTLPPSRDELNPPYLFSNQVSLTCLVKGFYPSDIAVEWESNGQPE
NNYKTTPPVLDSDGSFFLYSKLTVDYWRWLEGNVFSCSVMHEALHNHYTQKSLSLSPG

Nucleic acid sequence of the heavy chain of FS22-053-008-AA/G12v2 mAb^2 with LALA mutation (SEQ ID NO: 150)

GAAGTGCAGCTGGTGCAGTCCGGAGCCGAAGTCAAGAGGCCTGGAGCGTCCGTGAAGGTGTCC
TGCAAAGCCTCAGGATACACCTTCACTTCGTACGGGATTTCCTGGGTCCGCCAAGCACCGGGTC
AAGGCTTGGAGTGGATGGGATGGATCAGCGCGTATTCCGGGGGAACCAACTACGCTCAAAAGC
TGCAGGGTCGCGTGACCATGACCACCGATACCTCCACCTCAACGGCCTACATGGAACTGAGATC
TCTGCGGAGCGACGACACTGCCGTGTACTACTGTGCCCGGGACCTGTTCCCCACTATCTTCGGA
GTGTCGTACTACTACTACTGGGGCCAGGGGACTCTCGTGACCGTGTCGAGCGCTAGCACTAAG
GGCCCGTCGGTGTTCCCGCTGGCCCCATCGTCCAAGAGCACATCAGGGGGTACCGCCGCCCTG
GGCTGCCTTGTGAAGGATTACTTTCCCGAGCCCGTCACAGTGTCCTGGAACAGCGGAGCCCTGA
CCTCCGGAGTGCATACTTTCCCGGCTGTGCTTCAGTCCTCTGGCCTGTACTCATTGTCCTCCGTG
GTCACCGTCCCTTCGTCCTCCCTGGGCACCCAGACCTATATCTGTAATGTCAACCATAAGCCCTC
GAACACCAAGGTCGACAAGAAGGTCGAGCCGAAGTCGTGCGACAAGACTCACACTTGCCCGCC
TTGCCCAGCCCCGGAAGCTGCCGGTGGTCCTTCGGTGTTCCTCTTCCCGCCCAAGCCGAAGGA
TACCCTGATGATCTCACGGACCCCCGAAGTGACCTGTGTGGTGGTGGACGTGTCCCACGAGGA
CCCGGAAGTGAAATTCAATTGGTACGTGGATGGAGTGGAAGTGCACAACGCCAAGACCAAGCCA
CGGGAAGAACAGTACAACTCTACCTACCGCGTGGTGTCCGTGCTCACTGTGCTGCACCAAGACT
GGCTGAACGGGAAGGAGTACAAGTGCAAAGTGTCCAACAAGGCGCTGCCTGCCCCAATTGAGA
AAACTATCTCGAAAGCCAAGGGACAGCCTCGAGAACCACAGGTGTACACCCTGCCCCCATCCCG
GGATGAGCTGAACCCGCCGTACCTGTTCTCTAACCAGGTCAGCCTGACCTGCCTGGTCAAAGGC

TTCTATCCCAGCGACATCGCCGTGGAGTGGGAGAGCAATGGGCAGCCGGAGAACAACTACAAG
ACCACGCCTCCCGTACTGGACTCCGACGGCTCCTTCTTCCTCTACAGCAAGCTCACCGTGGATT
ACTGGAGGTGGCTGGAAGGGAACGTCTTCTCATGCTCCGTGATGCATGAGGCGCTGCACAACC
ACTACACTCAGAAGAGCTTGTCCCTGTCGCCCGGT

Nucleic acid sequence of the light chain of FS22-053-008-AA/G12v2 mAb[2] (SEQ ID NO: 151)

GACATTCAGATGACCCAGTCCCCGAGCACGCTGTCCGCAAGCGTGGGGGACAGAGTGACCATC
ACTTGCCGCGCCTCACAATCCATCAGCGGACGCTTGGCCTGGTACCAGCAGAAGCCCGGAAAG
GCCCCAAACCTTCTGATCTACGAAGCCTCGAACCTGGAGTCAGGCGTCCCTTCGCGGTTCTCTG
GCTCCGGTTCCGGAACTGAGTTCACCCTCACCATCTCGTCCCTGCAACCGGAAGATTTCGCCAC
CTACTACTGCCAACAGTCGTACTCCTGGCCCCGGACATTCGGACAGGGAACCAAAGTCGAGATT
AAGCGGACTGTGGCGGCTCCTAGCGTGTTCATCTTTCCCCCGTCCGACGAACAGCTGAAGTCCG
GTACCGCTAGCGTGGTCTGTCTCCTGAACAATTTCTACCCGCGCGAAGCTAAGGTCCAGTGGAA
GGTCGACAACGCGCTGCAGTCCGGAAACAGCCAGGAGTCAGTGACCGAGCAGGACTCCAAGGA
TTCCACTTATTCCCTGTCCTCCACCCTGACTTTGAGCAAGGCCGACTACGAGAAGCACAAAGTGT
ACGCCTGCGAAGTGACCCATCAAGGGCTTTCGTCGCCCGTGACCAAGAGCTTCAACCGGGGCG
AATGC

AA sequence of the heavy chain of FS22-053-017AA/E12v2 with LALA mutation (SEQ ID NO: 152) VH domain (italics); LALA mutation (bold underlined)

EVQLVQSGAEVKRPGASVKVSCKASGYPFTSYGISWVRQAPGQGLEWMGWISAYSGGTNYAQKLQ
*GRVTMTTDTSTSTAYMELRSLRSDDTAVYYCARDLFPTIFGVSYYYYWGQGTLVTVSS*ASTKGPSVF

PLAPSSKSTSGGTAALGCLVKDYFPEPVTVSWNSGALTSGVHTFPAVLQSSGLYSLSSVVTVPSSSL
GTQTYICNVNHKPSNTKVDKKVEPKSCDKTHTCPPCPAPE**AA**GGPSVFLFPPKPKDTLMISRTPEVT
CVVVDVSHEDPEVKFNWYVDGVEVHNAKTKPREEQYNSTYRVVSVLTVLHQDWLNGKEYKCKVSN
KALPAPIEKTISKAKGQPREPQVYTLPPSRDELNPPYLFSNQVSLTCLVKGFYPSDIAVEWESNGQPE
NNYKTTPPVLDSDGSFFLYSKLTVYHWRWLEGNVFSCSVMHEALHNHYTQKSLSLSPG

AA sequence of the heavy chain of FS22-053-017AA/E05v2 with LALA mutation (SEQ ID NO: 153) VH domain (italics); LALA mutation (bold underlined)

EVQLVQSGAEVKRPGASVKVSCKASGYTFTSYGISWVRQAPGQGLEWMGWISAYSGGTNYAQKLQ
*GRVTMTTDTSTSTAYMELRSLRSDDTAVYYCARDLFPTIFGVSYYYYWGQGTLVTVSS*ASTKGPSVF
PLAPSSKSTSGGTAALGCLVKDYFPEPVTVSWNSGALTSGVHTFPAVLQSSGLYSLSSVVTVPSSSL
GTQTYICNVNHKPSNTKVDKKVEPKSCDKTHTCPPCPAPE**AA**GGPSVFLFPPKPKDTLMISRTPEVT
CVVVDVSHEDPEVKFNWYVDGVEVHNAKTKPREEQYNSTYRVVSVLTVLHQDWLNGKEYKCKVSN
KALPAPIEKTISKAKGQPREPQVYTLPPSRDELNPPYLFSNQVSLTCLVKGFYPSDIAVEWESNGQPE
NNYKTTPPVLDSDGSFFLYSKLTVYHWRWLEGNVFSCSVMHEALHNHYTQKSLSLSPG

AA sequence of the heavy chain of FS22-053-017AA/G12v2 with LALA mutation (SEQ ID NO: 154) VH domain (italics); LALA mutation (bold underlined)

EVQLVQSGAEVKRPGASVKVSCKASGYTFTSYGISWVRQAPGQGLEWMGWISAYSGGTNYAQKLQ
*GRVTMTTDTSTSTAYMELRSLRSDDTAVYYCARDLFPTIFGVSYYYYWGQGTLVTVSS*ASTKGPSVF
PLAPSSKSTSGGTAALGCLVKDYFPEPVTVSWNSGALTSGVHTFPAVLQSSGLYSLSSVVTVPSSSL
GTQTYICNVNHKPSNTKVDKKVEPKSCDKTHTCPPCPAPE**AA**GGPSVFLFPPKPKDTLMISRTPEVT
CVVVDVSHEDPEVKFNWYVDGVEVHNAKTKPREEQYNSTYRVVSVLTVLHQDWLNGKEYKCKVSN
KALPAPIEKTISKAKGQPREPQVYTLPPSRDELNPPYLFSNQVSLTCLVKGFYPSDIAVEWESNGQPE
NNYKTTPPVLDSDGSFFLYSKLTVYHWRWLEGNVFSCSVMHEALHNHYTQKSLSLSPG

AA sequence of the heavy chain of FS22-172-003AA/lam-G02v3 with LALA mutation (SEQ ID NO: 155)

VH domain (italics); LALA mutation (bold underlined)

EVQLVQSGAEVKRPGASVKVSCKASGYTFTSYGISWVRQAPGQGLEWMGWISAYSGGTNYAQKLQ
*GRVTMTTDTSTSTAYMELRSLRSDDTAVYYCARDLFPTIFGVSYYYYWGQGTLVTVSS*ASTKGPSVF
PLAPSSKSTSGGTAALGCLVKDYFPEPVTVSWNSGALTSGVHTFPAVLQSSGLYSLSSVVTVPSSSL
GTQTYICNVNHKPSNTKVDKKVEPKSCDKTHTCPPCPAPE**AA**GGPSVFLFPPKPKDTLMISRTPEVT
CVVVDVSHEDPEVKFNWYVDGVEVHNAKTKPREEQYNSTYRVVSVLTVLHQDWLNGKEYKCKVSN

KALPAPIEKTISKAKGQPREPQVYTLPPSRDELPYIIPPYNQVSLTCLVKGFYPSDIAVEWESNGQPEN
NYKTTPPVLDSDGSFFLYSKLTVGADRWLEGNVFSCSVMHEALHNHYTQKSLSLSPG

AA sequence of the heavy chain of FS22-172-003AA/S70 with LALA mutation (SEQ ID NO: 156)

VH domain (italics); LALA mutation (bold underlined)

EVQLVESGGGLVQPGGSLRLSCAASGFTFSDSWIHWVRQAPGKGLEWVAWISPYGGSTYYADSVK
*GRFTISADTSKNTAYLQMNSLRAEDTAVYYCARRHWPGGFDYWGQGTLVTVSA*ASTKGPSVFPLAP
SSKSTSGGTAALGCLVKDYFPEPVTVSWNSGALTSGVHTFPAVLQSSGLYSLSSVVTVPSSSLGTQT
YICNVNHKPSNTKVDKKVEPKSCDKTHTCPPCPAPE**AA**GGPSVFLFPPKPKDTLMISRTPEVTCVVV
DVSHEDPEVKFNWYVDGVEVHNAKTKPREEQYNSTYRVVSVLTVLHQDWLNGKEYKCKVSNKALP
APIEKTISKAKGQPREPQVYTLPPSRDELPYIIPPYNQVSLTCLVKGFYPSDIAVEWESNGQPENNYKT
TPPVLDSDGSFFLYSKLTVGADRWLEGNVFSCSVMHEALHNHYTQKSLSLSPG

AA sequence of the light chain of S70 (SEQ ID NO: 157)

VL domain (italics);

DIQMTQSPSSLSASVGDRVTITCRASQDVSTAVAWYQQKPGKAPKLLIYSASFLYSGVPSRFSGSGS
*GTDFTLTISSLQPEDFATYYCQQYLYHPATFGQGTKVEIK*RTVAAPSVFIFPPSDEQLKSGTASVVCLL
NNFYPREAKVQWKVDNALQSGNSQESVTEQDSKDSTYSLSSTLTLSKADYEKHKVYACEVTHQGLS
SPVTKSFNRGEC

AA sequence of the heavy chain of FS22-172-003AA/HeID1.3 with LALA mutation (SEQ ID NO: 158) VH domain (italics); LALA mutation (bold underlined)

QVQLQESGPGLVRPSQTLSLTCTVSGSTFSGYGVNWVRQPPGRGLEWIGMIWGDGNTDYNSALKS
*RVTMLVDTSKNQFSLRLSSVTAADTAVYYCARERDYRLDYWGQGSLVTVSS*ASTKGPSVFPLAPSS
KSTSGGTAALGCLVKDYFPEPVTVSWNSGALTSGVHTFPAVLQSSGLYSLSSVVTVPSSSLGTQTYI
CNVNHKPSNTKVDKKVEPKSCDKTHTCPPCPAPE**AA**GGPSVFLFPPKPKDTLMISRTPEVTCVVVDV
SHEDPEVKFNWYVDGVEVHNAKTKPREEQYNSTYRVVSVLTVLHQDWLNGKEYKCKVSNKALPAPI
EKTISKAKGQPREPQVYTLPPSRDELPYIIPPYNQVSLTCLVKGFYPSDIAVEWESNGQPENNYKTTP
PVLDSDGSFFLYSKLTVGADRWLEGNVFSCSVMHEALHNHYTQKSLSLSPG

AA sequence of the light chain of HeID1.3 (SEQ ID NO: 159)

VL domain (italics)

DIQMTQSPASLSASVGETVTITCRASGNIHNYLAWYQQKQGKSPQLLVYNAKTLADGVPSRFSGSGS
*GTQYSLKINSLQPEDFGSYYCQHFWSTPRTFGGGTKLEIK*RTVAAPSVFIFPPSDEQLKSGTASVVCL
LNNFYPREAKVQWKVDNALQSGNSQESVTEQDSKDSTYSLSSTLTLSKADYEKHKVYACEVTHQGL
SSPVTKSFNRGEC

AA sequence of the heavy chain of FS22m-063AA/S70 with LALA mutation (SEQ ID NO: 160)

VH domain (italics); LALA mutation (bold underlined)

EVQLVESGGGLVQPGGSLRLSCAASGFTFSDSWIHWVRQAPGKGLEWVAWISPYGGSTYYADSVK
*GRFTISADTSKNTAYLQMNSLRAEDTAVYYCARRHWPGGFDYWGQGTLVTVSA*ASTKGPSVFPLAP
SSKSTSGGTAALGCLVKDYFPEPVTVSWNSGALTSGVHTFPAVLQSSGLYSLSSVVTVPSSSLGTQT
YICNVNHKPSNTKVDKKVEPKSCDKTHTCPPCPAPE**AA**GGPSVFLFPPKPKDTLMISRTPEVTCVVV
DVSHEDPEVKFNWYVDGVEVHNAKTKPREEQYNSTYRVVSVLTVLHQDWLNGKEYKCKVSNKALP
APIEKTISKAKGQPREPQVYTLPPSRDEPYWSYVSLTCLVKGFYPSDIAVEWESNGQPENNYKTTPP
VLDSDGSFFLYSKLTVMNYRWELGNVFSCSVMHEALHNHYTQKSLSLSPG

AA sequence of the heavy chain of FS22m-063AA/HeID1.3 with LALA mutation (SEQ ID NO: 161)

VH domain (italics); LALA mutation (bold underlined)

QVQLQESGPGLVRPSQTLSLTCTVSGSTFSGYGVNWVRQPPGRGLEWIGMIWGDGNTDYNSALKS
*RVTMLVDTSKNQFSLRLSSVTAADTAVYYCARERDYRLDYWGQGSLVTVSS*ASTKGPSVFPLAPSS
KSTSGGTAALGCLVKDYFPEPVTVSWNSGALTSGVHTFPAVLQSSGLYSLSSVVTVPSSSLGTQTYI
CNVNHKPSNTKVDKKVEPKSCDKTHTCPPCPAPE**AA**GGPSVFLFPPKPKDTLMISRTPEVTCVVVDV
SHEDPEVKFNWYVDGVEVHNAKTKPREEQYNSTYRVVSVLTVLHQDWLNGKEYKCKVSNKALPAPI

EKTISKAKGQPREPQVYTLPPSRDEPYWSYVSLTCLVKGFYPSDIAVEWESNGQPENNYKTTPPVLD
SDGSFFLYSKLTVMNYRWELGNVFSCSVMHEALHNHYTQKSLSLSPG

AA sequence of the heavy chain of G1-AA/E12v2 with LALA mutation (SEQ ID NO: 162)

VH domain (italics); LALA mutation (bold underlined)

EVQLVQSGAEVKRPGASVKVSCKASGYPFTSYGISWVRQAPGQGLEWMGWISAYSGGTNYAQKLQ
*GRVTMTTDTSTSTAYMELRSLRSDDTAVYYCARDLFPTIFGVSYYYYWGQGTLVTVSS*ASTKGPSVF
PLAPSSKSTSGGTAALGCLVKDYFPEPVTVSWNSGALTSGVHTFPAVLQSSGLYSLSSVVTVPSSSL
GTQTYICNVNHKPSNTKVDKKVEPKSCDKTHTCPPCPAPEAAGGPSVFLFPPKPKDTLMISRTPEVT
CVVVDVSHEDPEVKFNWYVDGVEVHNAKTKPREEQYNSTYRVVSVLTVLHQDWLNGKEYKCKVSN

KALPAPIEKTISKAKGQPREPQVYTLPPSRDELTKNQVSLTCLVKGFYPSDIAVEWESNGQPENNYKT
TPPVLDSDGSFFLYSKLTVDKSRWQQGNVFSCSVMHEALHNHYTQKSLSLSPG

AA sequence of the heavy chain of G1/S70 (SEQ ID NO: 163)

VH domain (italics)

EVQLVESGGGLVQPGGSLRLSCAASGFTFSDSWIHWVRQAPGKGLEWVAWISPYGGSTYYADSVK
*GRFTISADTSKNTAYLQMNSLRAEDTAVYYCARRHWPGGFDYWGQGTLVTVSA*ASTKGPSVFPLAP
SSKSTSGGTAALGCLVKDYFPEPVTVSWNSGALTSGVHTFPAVLQSSGLYSLSSVVTVPSSSLGTQT
YICNVNHKPSNTKVDKKVEPKSCDKTHTCPPCPAPELLGGPSVFLFPPKPKDTLMISRTPEVTCVVVD
VSHEDPEVKFNWYVDGVEVHNAKTKPREEQYNSTYRVVSVLTVLHQDWLNGKEYKCKVSNKALPAP
IEKTISKAKGQPREPQVYTLPPSRDELTKNQVSLTCLVKGFYPSDIAVEWESNGQPENNYKTTPPVLD
SDGSFFLYSKLTVDKSRWQQGNVFSCSVMHEALHNHYTQKSLSLSPGK

AA sequence of the heavy chain of G1-AA/S70 with LALA mutation (SEQ ID NO: 164)

VH domain (italics); LALA mutation (bold underlined)

EVQLVESGGGLVQPGGSLRLSCAASGFTFSDSWIHWVRQAPGKGLEWVAWISPYGGSTYYADSVK
*GRFTISADTSKNTAYLQMNSLRAEDTAVYYCARRHWPGGFDYWGQGTLVTVSA*ASTKGPSVFPLAP
SSKSTSGGTAALGCLVKDYFPEPVTVSWNSGALTSGVHTFPAVLQSSGLYSLSSVVTVPSSSLGTQT
YICNVNHKPSNTKVDKKVEPKSCDKTHTCPPCPAPEAAGGPSVFLFPPKPKDTLMISRTPEVTCVVVD
VSHEDPEVKFNWYVDGVEVHNAKTKPREEQYNSTYRVVSVLTVLHQDWLNGKEYKCKVSNKALPAP
IEKTISKAKGQPREPQVYTLPPSRDELTKNQVSLTCLVKGFYPSDIAVEWESNGQPENNYKTTPPVLD
SDGSFFLYSKLTVDKSRWQQGNVFSCSVMHEALHNHYTQKSLSLSPGK

AA sequence of the heavy chain of G1/4420 (SEQ ID NO: 165)

VH domain (italics)

EVKLDETGGGLVQPGRPMKLSCVASGFTFSDYWMNWVRQSPEKGLEWVAQIRNKPYNYETYYSDS
*VKGRFTISRDDSKSSVYLQMNNLRVEDMGIYYCTGSYYGMDYWGQGTSVTVSS*ASTKGPSVFPLAP
SSKSTSGGTAALGCLVKDYFPEPVTVSWNSGALTSGVHTFPAVLQSSGLYSLSSVVTVPSSSLGTQT
YICNVNHKPSNTKVDKKVEPKSCDKTHTCPPCPAPELLGGPSVFLFPPKPKDTLMISRTPEVTCVVVD
VSHEDPEVKFNWYVDGVEVHNAKTKPREEQYNSTYRVVSVLTVLHQDWLNGKEYKCKVSNKALPAP
IEKTISKAKGQPREPQVYTLPPSRDELTKNQVSLTCLVKGFYPSDIAVEWESNGQPENNYKTTPPVLD
SDGSFFLYSKLTVDKSRWQQGNVFSCSVMHEALHNHYTQKSLSLSPGK

AA sequence of the light chain of 4420 (SEQ ID NO: 166)

VL domain (italics)

DVVMTQTPLSLPVSLGDQASISCRSSQSLVHSNGNTYLRWYLQKPGQSPKVLIYKVSNRFSGVPDRF
*SGSGSGTDFTLKISRVEAEDLGVYFCSQSTHVPWTFGGGTKLEIK*RTVAAPSVFIFPPSDEQLKSGTA
SVVCLLNNFYPREAKVQWKVDNALQSGNSQESVTEQDSKDSTYSLSSTLTLSKADYEKHKVYACEV
THQGLSSPVTKSFNRGEC

AA sequence of the heavy chain of G1-AA/4420 with LALA mutation (SEQ ID NO: 167)

VH domain (italics); LALA mutation (bold underlined)

EVKLDETGGGLVQPGRPMKLSCVASGFTFSDYWMNWVRQSPEKGLEWVAQIRNKPYNYETYYSDS
*VKGRFTISRDDSKSSVYLQMNNLRVEDMGIYYCTGSYYGMDYWGQGTSVTVSS*ASTKGPSVFPLAP
SSKSTSGGTAALGCLVKDYFPEPVTVSWNSGALTSGVHTFPAVLQSSGLYSLSSVVTVPSSSLGTQT

YICNVNHKPSNTKVDKKVEPKSCDKTHTCPPCPAPE**AA**GGPSVFLFPPKPKDTLMISRTPEVTCVVV
DVSHEDPEVKFNWYVDGVEVHNAKTKPREEQYNSTYRVVSVLTVLHQDWLNGKEYKCKVSNKALP
APIEKTISKAKGQPREPQVYTLPPSRDELTKNQVSLTCLVKGFYPSDIAVEWESNGQPENNYKTTPPV
LDSDGSFFLYSKLTVDKSRWQQGNVFSCSVMHEALHNHYTQKSLSLSPGK

AA sequence of the heavy chain of G1-AA/HelD1.3 with LALA mutation (SEQ ID NO: 168)

VH domain (italics); LALA mutation (bold underlined)

QVQLQESGPGLVRPSQTLSLTCTVSGSTFSGYGVNWVRQPPGRGLEWIGMIWGDGNTDYNSALKS
*RVTMLVDTSKNQFSLRLSSVTAADTAVYYCARERDYRLDYWGQGSLVTVSS*ASTKGPSVFPLAPSS
KSTSGGTAALGCLVKDYFPEPVTVSWNSGALTSGVHTFPAVLQSSGLYSLSSVVTVPSSSLGTQTYI
CNVNHKPSNTKVDKKVEPKSCDKTHTCPPCPAPE**AA**GGPSVFLFPPKPKDTLMISRTPEVTCVVVDV
SHEDPEVKFNWYVDGVEVHNAKTKPREEQYNSTYRVVSVLTVLHQDWLNGKEYKCKVSNKALPAPI
EKTISKAKGQPREPQVYTLPPSRDELTKNQVSLTCLVKGFYPSDIAVEWESNGQPENNYKTTPPVLD
SDGSFFLYSKLTVDKSRWQQGNVFSCSVMHEALHNHYTQKSLSLSPGK

AA sequence of the heavy chain of G1-AA/MLS109 with LALA mutation (SEQ ID NO: 169)

VH domain (italics); LALA mutation (bold underlined)

EEQVLESGGGLVKPGGSLRLSCAASGFTFSPYSVFWVRQAPGKGLEWVSSINSDSTYKYYADSVKG
*RFTISRDNAENSIFLQMNSLRAEDTAVYYCARDRSYYAFSSGSLSDYYYGLDVWGQGTTVIVSS*AST
KGPSVFPLAPSSKSTSGGTAALGCLVKDYFPEPVTVSWNSGALTSGVHTFPAVLQSSGLYSLSSVVT
VPSSSLGTQTYICNVNHKPSNTKVDKKVEPKSCDKTHTCPPCPAPE**AA**GGPSVFLFPPKPKDTLMIS
RTPEVTCVVVDVSHEDPEVKFNWYVDGVEVHNAKTKPREEQYNSTYRVVSVLTVLHQDWLNGKEY
KCKVSNKALPAPIEKTISKAKGQPREPQVYTLPPSRDELTKNQVSLTCLVKGFYPSDIAVEWESNGQP
ENNYKTTPPVLDSDGSFFLYSKLTVDKSRWQQGNVFSCSVMHEALHNHYTQKSLSLSPGK

Amino acid sequence of the light chain of MLS109 (SEQ ID NO: 170)

VL domain (italics)

DIVMTQSPLSLSVTPGEPASISCRSSQSLLHTNGYNYLDWYVQKPGQSPQLLIYLASNRASGVPDRFS
*GSGSGTDFTLKISRVETEDVGVYYCMQALQIPRTFGQGTKVEIK*RTVAAPSVFIFPPSDEQLKSGTAS
VVCLLNNFYPREAKVQWKVDNALQSGNSQESVTEQDSKDSTYSLSSTLTLSKADYEKHKVYACEVT
HQGLSSPVTKSFNRGEC

Amino acid sequences of FS22-172-003 CH3 domain AB and EF loops

AB loop - RDELPYIIPPYNQ (SEQ ID NO: 171)

EF loop - GADRWLEGNV (SEQ ID NO: 172)

Amino acid sequences of FS22-53-008 CH3 domain AB and EF loops

AB loop - RDELNPPYLFSNQ (SEQ ID NO: 173)

EF loop - DYWRWLEGNV (SEQ ID NO: 174)

Amino acid sequences of FS22-053-017 CH3 domain AB and EF loops

AB loop - RDELNPPYLFSNQ (SEQ ID NO: 173)

EF loop - YHWRWLEGNV (SEQ ID NO: 175)

Amino acid sequence of the heavy chain of G1/280 02 G02 (SEQ ID NO: 177)

VH domain (italics)

EVQLVQSGAEVKRPGASVKVSCKASGYTFTSYGISWVRQAPGQGLEWMGWISAYNGNTNYAQKLQ
*GRVTMTTDTSTSTAYMELRSLRSDDTAVYYCARDLFPTIFGVSYYYYWGQGTLVTVSS*ASTKGPSVF
PLAPSSKSTSGGTAALGCLVKDYFPEPVTVSWNSGALTSGVHTFPAVLQSSGLYSLSSVVTVPSSSL
GTQTYICNVNHKPSNTKVDKKVEPKSCDKTHTCPPCPAPELLGGPSVFLFPPKPKDTLMISRTPEVTC

GTQTYICNVNHKPSNTKVDKKVEPKSCDKTHTCPPCPAPELLGGPSVFLFPPKPKDTLMISRTPEVTC
VVVDVSHEDPEVKFNWYVDGVEVHNAKTKPREEQYNSTYRVVSVLTVLHQDWLNGKEYKCKVSNK
ALPAPIEKTISKAKGQPREPQVYTLPPSRDELTKNQVSLTCLVKGFYPSDIAVEWESNGQPENNYKTT
PPVLDSDGSFFLYSKLTVDKSRWQQGNVFSCSVMHEALHNHYTQKSLSLSPG

Amino acid sequence of the light chain of G1/280 02 G02 (SEQ ID NO: 178)

VL domain (italics)

QSALTQPASVSGSPGQSITISCTGTSSDVGGYNSVSWYQQFPGKAPKLMIFEVTNRPSGVSDRFSGS
*KSDNTASLTISGLQAEDEAEYYCSSFKRGSTLVVFGGGTKLTVL*GQPAAAPSVTLFPPSSEELQANKA
TLVCLISDFYPGAVTVAWKADSSPVKAGVETTTPSKQSNNKYAASSYLSLTPEQWKSHRSYSCQVTH
EGSTVEKTVAPTECS

Amino acid sequence of human PD-L1 (SEQ ID NO: 179)

Extracellular domain (italics); transmembrane and intracellular domains (bold)

FTVTVPKDLYVVEYGSNMTIECKFPVEKQLDLAALIVYWEMEDKNIIQFVHGEEDLKVQHSSYRQRAR
LLKDQLSLGNAALQITDVKLQDAGVYRCMISYGGADYKRITVKVNAPYNKINQRILVVDPVTSEHELTC
QAEGYPKAEVIWTSSDHQVLSGKTTTTNSKREEKLFNVTSTLRINTTTNEIFYCTFRRLDPEENHTAEL
*VIPELPLAHPPNER***THLVILGAILLCLGVALTFIFRLRKGRMMDVKKCGIQDTNSKKQSDTHLEET**

Amino acid sequence of human PD-L1 extracellular domain (SEQ ID NO: 180)

FTVTVPKDLYVVEYGSNMTIECKFPVEKQLDLAALIVYWEMEDKNIIQFVHGEEDLKVQHSSYRQRAR
LLKDQLSLGNAALQITDVKLQDAGVYRCMISYGGADYKRITVKVNAPYNKINQRILVVDPVTSEHELTC
QAEGYPKAEVIWTSSDHQVLSGKTTTTNSKREEKLFNVTSTLRINTTTNEIFYCTFRRLDPEENHTAEL
VIPELPLAHPPNER

Amino acid sequence of mouse PD-L1 (SEQ ID NO: 181)

Extracellular domain (italics); transmembrane and intracellular domains (bold)

FTITAPKDLYVVEYGSNVTMECRFPVERELDLLALVVYWEKEDEQVIQFVAGEEDLKPQHSNFRGRA
SLPKDQLLKGNAALQITDVKLQDAGVYCCIISYGGADYKRITLKVNAPYRKINQRISVDPATSEHELICQ
AEGYPEAEVIWTNSDHQPVSGKRSVTTSRTEGMLLNVTSSLRVNATANDVFYCTFWRSQPGQNHTA
*ELIIPELPATHPPQNRTH***WVLLGSILLFLIVVSTVLLFLRKQVRMLDVEKCGVEDTSSKNRNDTQFEET**

Amino acid sequence of mouse PD-L1 extracellular domain (SEQ ID NO: 182)

FTITAPKDLYVVEYGSNVTMECRFPVERELDLLALVVYWEKEDEQVIQFVAGEEDLKPQHSNFRGRA
SLPKDQLLKGNAALQITDVKLQDAGVYCCIISYGGADYKRITLKVNAPYRKINQRISVDPATSEHELICQ
AEGYPEAEVIWTNSDHQPVSGKRSVTTSRTEGMLLNVTSSLRVNATANDVFYCTFWRSQPGQNHTA
ELIIPELPATHPPQNRTH

Amino acid sequence of cynomolgus PD-L1 (SEQ ID NO: 183)

Extracellular domain (italics); transmembrane and intracellular domains (bold)

FTVTVPKDLYVVEYGSNMTIECKFPVEKQLDLTSLIVYWEMEDKNIIQFVHGEEDLKVQHSNYRQRAQ
LLKDQLSLGNAALRITDVKLQDAGVYRCMISYGGADYKRITVKVNAPYNKINQRILVVDPVTSEHELTC
QAEGYPKAEVIWTSSDHQVLSGKTTTTNSKREEKLLNVTSTLRINTTANEIFYCIFRRLDPEENHTAEL
*VIPELPLALPPNERTH***LVILGAIFLLLGVALTFIFYLRKGRMMDMKKCGIRVTNSKKQRDTQLEETKG**
PSARFDIPDEIPVIESKPNTLSIVLGTTLTVAMIIVATIFGYRRQKGRLRTLKL

Amino acid sequence of cynomolgus PD-L1 extracellular domain (SEQ ID NO: 184)

FTVTVPKDLYVVEYGSNMTIECKFPVEKQLDLTSLIVYWEMEDKNIIQFVHGEEDLKVQHSNYRQRAQ
LLKDQLSLGNAALRITDVKLQDAGVYRCMISYGGADYKRITVKVNAPYNKINQRILVVDPVTSEHELTC
QAEGYPKAEVIWTSSDHQVLSGKTTTTNSKREEKLLNVTSTLRINTTANEIFYCIFRRLDPEENHTAEL
VIPELPLALPPNERTH

Amino acid sequence of human CD137 (SEQ ID NO: 185)

Extracellular domain (italics); transmembrane and intracellular domains (bold)

LQDPCSNCPAGTFCDNNRNQICSPCPPNSFSSAGGQRTCDICRQCKGVFRTRKECSSTSNAECDCT
PGFHCLGAGCSMCEQDCKQGQELTKKGCKDCCFGTFNDQKRGICRPWTNCSLDGKSVLVNGTKER
*DVVCGPSPADLSPGASSVTPPAPAREPGHSPQ***IISFFLALTSTALLFLLFFLTLRFSVVKRGRKKLLYI**

FKQPFMRPVQTTQEEDGCSCRFPEEEEGGCEL

Amino acid sequence of human CD137 extracellular domain (SEQ ID NO: 186)

LQDPCSNCPAGTFCDNNRNQICSPCPPNSFSSAGGQRTCDICRQCKGVFRTRKECSSTSNAECDCT
PGFHCLGAGCSMCEQDCKQGQELTKKGCKDCCFGTFNDQKRGICRPWTNCSLDGKSVLVNGTKER
DVVCGPSPADLSPGASSVTPPAPAREPGHSPQ

Amino acid sequence of mouse CD137 (SEQ ID NO: 187)

Extracellular domain (italics); transmembrane and intracellular domains (bold)

VQNSCDNCQPGTFCRKYNPVCKSCPPSTFSSIGGQPNCNICRVCAGYFRFKKFCSSTHNAECECIE
GFHCLGPQCTRCEKDCRPGQELTKQGCKTCSLGTFNDQNGTGVCRPWTNCSLDGRSVLKTGTTEK
*DVVCGPPVVSFSPSTTISVTPEGGPGGHSLQVL***TLFLALTSALLLALIFITLLFSVLKWIRKKFPHIFKQ**
PFKKTTGAAQEEDACSCRCPQEEEGGGGGYEL

Amino acid sequence of mouse CD137 extracellular domain (SEQ ID NO: 188)

VQNSCDNCQPGTFCRKYNPVCKSCPPSTFSSIGGQPNCNICRVCAGYFRFKKFCSSTHNAECECIE
GFHCLGPQCTRCEKDCRPGQELTKQGCKTCSLGTFNDQNGTGVCRPWTNCSLDGRSVLKTGTTEK
DVVCGPPVVSFSPSTTISVTPEGGPGGHSLQVL

Amino acid sequence of cynomolgus CD137 (SEQ ID NO: 189)

Extracellular domain (italics); transmembrane and intracellular domains (bold)

LQDLCSNCPAGTFCDNNRSQICSPCPPNSFSSAGGQRTCDICRQCKGVFKTRKECSSTSNAECDCIS
GYHCLGAECSMCEQDCKQGQELTKKGCKDCCFGTFNDQKRGICRPWTNCSLDGKSVLVNGTKERD
*VVCGPSPADLSPGASSATPPAPAREPGHSPQ***IIFFLALTSTVVLFLLFFLVLRFSVVKRSRKKLLYIFK**
QPFMRPVQTTQEEDGCSCRFPEEEEGGCEL

Amino acid sequence of cynomolgus CD137 extracellular domain (SEQ ID NO: 190)

LQDLCSNCPAGTFCDNNRSQICSPCPPNSFSSAGGQRTCDICRQCKGVFKTRKECSSTSNAECDCIS
GYHCLGAECSMCEQDCKQGQELTKKGCKDCCFGTFNDQKRGICRPWTNCSLDGKSVLVNGTKERD
VVCGPSPADLSPGASSATPPAPAREPGHSPQ

Amino acid sequence of the heavy chain of G1/HeID1.3 (SEQ ID NO: 191)

VH domain (italics)

QVQLQESGPGLVRPSQTLSLTCTVSGSTFSGYGVNWVRQPPGRGLEWIGMIWGDGNTDYNSALKS
*RVTMLVDTSKNQFSLRLSSVTAADTAVYYCARERDYRLDYWGQGSLVTVSS*ASTKGPSVFPLAPSS
KSTSGGTAALGCLVKDYFPEPVTVSWNSGALTSGVHTFPAVLQSSGLYSLSSVVTVPSSSLGTQTYI
CNVNHKPSNTKVDKKVEPKSCDKTHTCPPCPAPELLGGPSVFLFPPKPKDTLMISRTPEVTCVVVDV
SHEDPEVKFNWYVDGVEVHNAKTKPREEQYNSTYRVVSVLTVLHQDWLNGKEYKCKVSNKALPAPI
EKTISKAKGQPREPQVYTLPPSRDELTKNQVSLTCLVKGFYPSDIAVEWESNGQPENNYKTTPPVLD
SDGSFFLYSKLTVDKSRWQQGNVFSCSVMHEALHNHYTQKSLSLSPG

OVA peptide (SEQ ID NO: 192)

ISQAVHAAHAEINEAGR

Amino acid sequence of Human B7-H3 extracellular domain (SEQ ID NO: 193)

ILEVQVPEDPVVALVGTDATLCCSFSPEPGFSLAQLNLIWQLTDTKQLVHSFAEGQDQGSAYANRTAL
FPDLLAQGNASLRLQRVRVADEGSFTCFVSIRDFGSAAVSLQVAAPYSKPSMTLEPNKDLRPGDTVTI
TCSSYQGYPEAEVFWQDGQGVPLTGNVTTSQMANEQGLFDVHSILRVVLGANGTYSCLVRNPVLQ
QDAHSSVTITPQRSPTGAVEVQVPEDPVVALVGTDATLRCSFSPEPGFSLAQLNLIWQLTDTKQLVHS
FTEGRDQGSAYANRTALFPDLLAQGNASLRLQRVRVADEGSFTCFVSIRDFGSAAVSLQVAAPYSKP
SMTLEPNKDLRPGDTVTITCSSYRGYPEAEVFWQDGQGVPLTGNVTTSQMANEQGLFDVHSVLRVV
LGANGTYSCLVRNPVLQQDAHGSVTITGQPMT

SIINFEKL peptide (SEQ ID NO: 194)

SIINFEKL

Amino acid sequence of Human PD-L1-rCD4-His (SEQ ID NO: 195)

Signal peptide (underlined); Extracellular domain of PD-L1 (regular font); C-terminal rat $CD4^+$ (domains 3 and 4) (italics); Junction between antigen and C-terminal fusion encoding a NotI restriction site (bold and underlined); C-terminal hexahistidine tag (bold)

MRIFAVFIFMTYWHLLNAFTVTVPKDLYVVEYGSNMTIECKFPVEKQLDLAALIVYWEMEDKNIIQFVH
GEEDLKVQHSSYRQRARLLKDQLSLGNAALQITDVKLQDAGVYRCMISYGGADYKRITVKVNAPYNKI
NQRILVVDPVTSEHELTCQAEGYPKAEVIWTSSDHQVLSGKTTTTNSKREEKLFNVTSTLRINTTTNEI
FYCTFRRLDPEENHTAELVIPELPLAHPPNERT**AAA***TSITAYKSEGESAEFSFPLNLGEESLQGELRW*
KAEKAPSSQSWITFSLKNQKVSVQKSTSNPKFQLSETLPLTLQIPQVSLQFAGSGNLTLTLDRGILYQE
VNLVVMKVTQPDSNTLTCEVMGPTSPKMRLILKQENQEARVSRQEKVIQVQAPEAGVWQCLLSEGE
*EVKMDSKIQVLSKGLN***GSHHHHHH**

Amino acid sequence of Human PD-L1-Fc-His (SEQ ID NO: 196)

Signal peptide (underlined) Extracellular domain of PD-L1 (regular font) Human IgG1 Fc (italics) Junction between antigen and C-terminal fusion encoding a NotI restriction site (bold and underlined) C-terminal hexahistidine tag (bold)

MRIFAVFIFMTYWHLLNAFTVTVPKDLYVVEYGSNMTIECKFPVEKQLDLAALIVYWEMEDKNIIQFVH
GEEDLKVQHSSYRQRARLLKDQLSLGNAALQITDVKLQDAGVYRCMISYGGADYKRITVKVNAPYNKI
NQRILVVDPVTSEHELTCQAEGYPKAEVIWTSSDHQVLSGKTTTTNSKREEKLFNVTSTLRINTTTNEI
FYCTFRRLDPEENHTAELVIPELPLAHPPNERT**AAA***DKTHTCPPCPAPELLGGPSVFLFPPKPKDTLMI*
SRTPEVTCVVVDVSHEDPEVKFNWYVDGVEVHNAKTKPREEQYNSTYRVVSVLTVLHQDWLNGKE
YKCKVSNKALPAPIEKTISKAKGQPREPQVYTLPPSRDELTKNQVSLTCLVKGFYPSDIAVEWESNGQ
*PENNYKTTPPVLDSDGSFFLYSKLTVDKSRWQQGNVFSCSVMHEALHNHYTQKSLSLSPGK***GSHHH**
HHH

Amino acid sequence of Mouse PD-L1-rCD4-His (SEQ ID NO: 197)

Signal peptide (underlined); Extracellular domain of PD-L1 (regular font); C-terminal rat $CD4^+$ (domains 3 and 4) (italics); Junction between antigen and C-terminal fusion encoding a NotI restriction site (bold and underlined); C-terminal hexahistidine tag (bold)

MRIFAGIIFTACCHLLRAFTITAPKDLYVVEYGSNVTMECRFPVERELDLLALVVYWEKEDEQVIQFVA
GEEDLKPQHSNFRGRASLPKDQLLKGNAALQITDVKLQDAGVYCCIISYGGADYKRITLKVNAPYRKIN
QRISVDPATSEHELICQAEGYPEAEVIWTNSDHQPVSGKRSVTTSRTEGMLLNVTSSLRVNATANDV
FYCTFWRSQPGQNHTAELIIPELPATHPPQNRT**AAA***TSITAYKSEGESAEFSFPLNLGEESLQGELRW*
KAEKAPSSQSWITFSLKNQKVSVQKSTSNPKFQLSETLPLTLQIPQVSLQFAGSGNLTLTLDRGILYQE
VNLVVMKVTQPDSNTLTCEVMGPTSPKMRLILKQENQEARVSRQEKVIQVQAPEAGVWQCLLSEGE
*EVKMDSKIQVLSKGLN***GSHHHHHH**

Amino acid sequence of Mouse PD-L1-Fc-His (SEQ ID NO: 198)

Signal peptide (underlined) Extracellular domain of PD-L1 (regular font) Human IgG1 Fc (italics) Junction between antigen and C-terminal fusion encoding a NotI restriction site (bold and underlined) C-terminal hexahistidine tag (bold)

MRIFAGIIFTACCHLLRAFTITAPKDLYVVEYGSNVTMECRFPVERELDLLALVVYWEKEDEQVIQFVA
GEEDLKPQHSNFRGRASLPKDQLLKGNAALQITDVKLQDAGVYCCIISYGGADYKRITLKVNAPYRKIN
QRISVDPATSEHELICQAEGYPEAEVIWTNSDHQPVSGKRSVTTSRTEGMLLNVTSSLRVNATANDV
FYCTFWRSQPGQNHTAELIIPELPATHPPQNRT**AAA***DKTHTCPPCPAPELLGGPSVFLFPPKPKDTL*
MISRTPEVTCVVVDVSHEDPEVKFNWYVDGVEVHNAKTKPREEQYNSTYRVVSVLTVLHQDWLNGK
EYKCKVSNKALPAPIEKTISKAKGQPREPQVYTLPPSRDELTKNQVSLTCLVKGFYPSDIAVEWESNG
*QPENNYKTTPPVLDSDGSFFLYSKLTVDKSRWQQGNVFSCSVMHEALHNHYTQKSLSLSPGK***GSHH**
HHHH

Amino acid sequence of Human PD-L1-His-Avi (SEQ ID NO: 199)

Extracellular domain of PD-L1 (regular font) C-terminal hexahistidine tag (italics) Avi tag (bold)

FTVTVPKDLYVVEYGSNMTIECKFPVEKQLDLAALIVYWEMEDKNIIQFVHGEEDLKVQHSSYRQRAR

LLKDQLSLGNAALQITDVKLQDAGVYRCMISYGGADYKRITVKVNAPYNKINQRILVVDPVTSEHELTC
QAEGYPKAEVIWTSSDHQVLSGKTTTTNSKREEKLFNVTSTLRINTTTNEIFYCTFRRLDPEENHTAEL
VIPELPLAHPPNER*GSHHHHHH*GG**GLNDIFEAQKIEWHE**

Codon-optimised nucleic acid sequences encoding the FS22-172-003-AA/E12v2 heavy chain (SEQ ID NO: 32)

AAGCTTGCCGCCACCATGGAATGGTCCTGGGTGTTCCTGTTCTTCCTGTCCGTGACCACCGGCG
TGCACTCTGAAGTTCAGCTGGTTCAGTCTGGCGCCGAAGTGAAAAGACCTGGCGCCTCTGTGAA
GGTGTCCTGCAAGGCTTCTGGCTACCCCTTTACCTCCTACGGCATCTCCTGGGTCCGACAGGCT
CCTGGACAAGGCTTGGAATGGATGGGCTGGATCTCCGCTTATTCCGGCGGCACCAATTACGCCC
AGAAACTGCAGGGCAGAGTGACCATGACCACCGACACCTCTACCTCCACCGCCTACATGGAACT
GCGGTCCCTGAGATCTGACGACACCGCCGTGTACTACTGCGCCAGAGATCTGTTCCCCACCATC
TTCGGCGTGTCCTACTACTACTATTGGGGCCAGGGCACCCTGGTCACCGTGTCCTCTGCTTCTA
CCAAGGGACCCAGCGTGTTCCCTCTGGCTCCTTCCAGCAAGTCTACCTCTGGCGGAACAGCTGC
TCTGGGCTGCCTGGTCAAGGACTACTTTCCTGAGCCTGTGACCGTGTCTTGGAACTCTGGCGCT
CTGACATCTGGCGTGCACACCTTTCCAGCTGTGCTGCAGTCCTCCGGCCTGTACTCTCTGTCCT
CTGTCGTGACCGTGCCTTCCAGCTCTCTGGGAACCCAGACCTACATCTGCAATGTGAACCACAA
GCCTTCCAACACCAAGGTGGACAAGAAGGTGGAACCCAAGTCCTGCGACAAGACCCACACCTGT
CCTCCATGTCCTGCTCCAGAAGCTGCTGGCGGCCCTTCCGTGTTTCTGTTCCCTCCAAAGCCTA
AGGACACCCTGATGATCTCTCGGACCCCTGAAGTGACCTGCGTGGTGGTGGATGTGTCTCACGA
GGACCCAGAAGTGAAGTTCAATTGGTACGTGGACGGCGTGGAAGTGCACAACGCCAAGACCAA
GCCTAGAGAGGAACAGTACAACTCCACCTACAGAGTGGTGTCCGTGCTGACCGTGCTGCACCAG
GATTGGCTGAACGGCAAAGAGTACAAGTGCAAGGTGTCCAACAAGGCCCTGCCTGCTCCTATCG
AAAAGACCATCTCCAAGGCCAAGGGCCAGCCTAGGGAACCCCAGGTTTACACCTTGCCTCCATC
TCGGGACGAGCTGCCCTACATCATCCCTCCATACAACCAGGTGTCCCTGACCTGCCTCGTGAAG
GGCTTCTACCCTTCCGATATCGCCGTGGAATGGGAGAGCAATGGCCAGCCTGAGAACAACTACA
AGACAACCCCTCCTGTGCTGGACTCCGACGGCTCATTCTTTCTGTACTCCAAGCTGACAGTGGG
CGCCGACAGATGGCTGGAAGGGAACGTGTTCTCCTGCAGCGTGATGCACGAGGCCCTGCACAA
TCACTACACACAGAAGTCCCTGTCTCTGTCCCCTGGCAAG TGATGAATTC

Codon-optimised nucleic acid sequences encoding the FS22-172-003-AA/E12v2 light chain (SEQ ID NO: 39)

AAGCTTGCCGCCACCATGTCTGTGCCTACACAGGTTCTGGGACTGCTGCTGCTGTGGCTGACCG
ACGCCAGATGCGACATCCAGATGACCCAGTCTCCATCCACACTGTCCGCCTCTGTGCGGGACAG
AGTGATCATCACCTGTAGAGCCAGCCAGTCCATCGGCAACAGACTGGCCTGGTATCAGCACAAG
CCTGGCAAGGCTCCCAAGCTGCTGATCTACGAGGCCTCCACATCTGAGACAGGCGTGCCCTCTA
GATTCTCCGGCTCTGGCTCTGGCACCGACTTTACCCTGACAATCTCCAGCCTGCAGCCTGAGGA
CTTCGCCACCTACTACTGCCAGCAGTCCTACAGCACCCCTTACACCTTTGGCCAGGGCACCAAG
CTGGAAATCAAGCGTACGGTGGCCGCTCCCAGCGTGTTCATCTTCCCCCCAAGCGACGAGCAG
CTGAAGAGCGGCACCGCCAGCGTGGTGTGTCTGCTGAACAACTTCTACCCCAGGGAGGCCAAG
GTGCAGTGGAAGGTGGACAACGCCCTGCAGAGCGGCAACAGCCAGGAGAGCGTCACCGAGCA
GGACAGCAAGGACTCCACCTACAGCCTGAGCAGCACCCTGACCCTGAGCAAGGCCGACTACGA
GAAGCACAAGGTGTACGCCTGTGAGGTGACCCACCAGGGCCTGTCCAGCCCCGTGACCAAGAG
CTTCAACAGGGGCGAGTGCTGATGAATTC

References

[0500]

Altschul SF, Gish W, Miller W, Myers EW, Lipman DJ. Basic local alignment search tool. J. Mol. Biol. 215(3), 403-10 (1990).

Altschul SF, Madden TL, Schäffer AA, Zhang J, Zhang Z, Miller W, Lipman DJ. Gapped BLAST and PSI-BLAST: a new generation of protein database search programs. Nucleic Acids Res. 25(17), 3389-402 (1997).

Bagshawe KD, Sharma SK, Springer CJ, Antoniw P, Rogers GT, Burke PJ, Melton R. Antibody-enzyme conjugates can generate cytotoxic drugs from inactive precursors at tumor sites. Antibody, Immunoconjugates and Radiopharmaceuticals 4, 915-922 (1991).

Baird JR et al. Immune-mediated regression of established B16F10 melanoma by intratumoral injection of attenuated Toxoplasma gondii protects against rechallenge. J Immunol. 190(1): 469-478 (2013).

Bartkowiak T, Curran MA. 4-1BB Agonists: Multi-Potent Potentiators of Tumor Immunity. Front Oncol. Jun 8;5, 117 (2015).

Bartkowiak T et al. Activation of 4-1BB on Liver Myeloid Cells Triggers Hepatitis via an Interleukin-27-Dependent Pathway. Clin Cancer Res. 24(5), 1138-51 (2018).

Bergman I, Burckart GJ, Pohl CR, Venkataramanan R, Barmada MA, Griffin JA And Cheung NV. Pharmacokinetics of IgG and IgM Anti-Ganglioside Antibodies in Rats and Monkeys After Intrathecal Administration. The Journal of Pharmacology and Experimental Therapeutics 284(1), 111-115 (1998)

Bitra A, Doukov T, Wang J, Picarda G, Benedict CA, Croft M, Zajonc DM. Crystal structure of murine 4-1BB and its interaction with 4-1BBL support a role for galectin-9 in 4-1BB signaling. J Biol Chem. 293(4):1317-1329 (2017).

Brown MH, Barclay AN. Expression of immunoglobulin and scavenger receptor superfamily domains as chimeric proteins with domains 3 and 4 of CD4 for ligand analysis. Protein Eng. 7(4), 515-21 (1994).

Bruhns P, Iannascoli B, England P, Mancardi DA, Fernandez N, Jorieux S, Daëron M. Specificity and affinity of human Fcgamma receptors and their polymorphic variants for human IgG subclasses. Blood. 113(16):3716-25 (2009).

Chacon JA, Wu RC, Sukhumalchandra P, Molldrem JJ, Sarnaik A, Pilon-Thomas S, Weber J, Hwu P, Radvanyi L. Co-stimulation through 4-1BB/CD137 improves the expansion and function of CD8(+) melanoma tumor-infiltrating lymphocytes for adoptive T-cell therapy. PLoS One. 8(4):e60031 (2013).

Chapple SD, Crofts AM, Shadbolt SP, McCafferty J, Dyson MR. Multiplexed expression and screening for recombinant protein production in mammalian cells. BMC Biotechnol. 6:49 (2006).

Chester C, Ambulkar S, Kohrt HE. 4-1BB agonism: adding the accelerator to cancer immunotherapy. Cancer Immunol Immunother. 65(10):1243-8 (2016).

Chester C, Sanmamed MF, Wang J, Melero I. Immunotherapy targeting 4-1BB: mechanistic

rationale, clinical results, and future strategies. Blood. 131(1):49-57 (2018).

Claus C et al. A novel tumor-targeted 4-1BB agonist and its combination with T-cell bispecific antibodies: an off-the-shelf cancer immunotherapy alternative to CAR T-cells [abstract]. In: Proceedings of the American Association for Cancer Research Annual Meeting 2017. Cancer Res. 77 (2017).

Croft M. Co-stimulatory members of the TNFR family: keys to effective T-cell immunity? Nat Rev Immunol. 3(8):609-20 (2003).

Curran MA, Geiger TL, Montalvo W, Kim M, Reiner SL, Al-Shamkhani A, Sun JC, Allison J. P. Systemic 4-1BB activation induces a novel T cell phenotype driven by high expression of Eomesodermin. J. Exp.Med. 210(4): 743-755 (2013).

Dubrot J et al. Treatment with anti-CD137 mAbs causes intense accumulations of liver T cells without selective antitumor immunotherapeutic effects in this organ. Cancer Immunol Immunother. 59(8):1223-1233 (2010).

Dyson MR, Zheng Y, Zhang C, Colwill K, Pershad K, Kay BK, Pawson T, McCafferty J: Mapping protein interactions by combining antibody affinity maturation and mass spectrometry. Anal. Biochem. 417(1), 25-35 (2011).

Fisher TS et al. Targeting of 4-1BB by monoclonal antibody PF-05082566 enhances T-cell function and promotes anti-tumor activity. Cancer Immunol Immunother. 61(10):1721-33 (2012).

Grosso J, Inzunza D, Wu Q, Simon J, Singh P, Zhang X, Phillips T, Simmons P, Cogswell J. Programmed death-ligand 1 (PD-L1) expression in various tumor types. Journal for Immunotherapy of Cancer. 1(Suppl 1):P53. (2013).

Hasenhindl C, Traxlmayr MW, Wozniak-Knopp G, Jones PC, Stadlmayr G, Rüker F, Obinger C. Stability assessment on a library scale: a rapid method for the evaluation of the commutability and insertion of residues in C-terminal loops of the CH3 domains of IgG1-Fc. Protein Eng. Des. Sel., 26(10), 675-82 (2013).

Hezareh M, Hessell AJ, Jensen RC, van de Winkel JG, Parren PW. Effector function activities of a panel of mutants of a broadly neutralizing antibody against human immunodeficiency virus type 1. J Virol. 75(24):12161-8. (2001).

Hinner MJ, Aiba, RSB., Wiedenmann A, Schlosser C, Allersdorfer A, Matschiner G, Rothe C, Moebius U, Kohrt HE, Olwill SA. Costimulatory T cell engagement via a novel bispecific anti-CD137 /anti-HER2 protein. J. Immunotherapy Cancer 3 (Suppl 2): P187. (2015).

Holliger P, Hudson PJ. Engineered antibody fragments and the rise of single domains. Nat Biotechnol. 23(9):1126-36 (2005).

Hu S, Shively L, Raubitschek A, Sherman M, Williams LE, Wong JY, Shively JE, Wu AM. Minibody: A novel engineered anti-carcinoembryonic antigen antibody fragment (single-chain

Fv-CH3) which exhibits rapid, high-level targeting of xenografts. Cancer Res. 56(13):3055-61 (1996).

Hurtado JC, Kim YJ, Kwon BS. Signals through 4-1BB are costimulatory to previously activated splenic T cells and inhibit activation-induced cell death. J Immunol. 15;158(6):2600-9 (1997).

Idusogie EE, Presta LG, Gazzano-Santoro H, Totpal K, Wong PY, Ultsch M, Meng YG, Mulkerrin MG. Mapping of the C1q binding site on rituxan, a chimeric antibody with a human IgG1 Fc. J Immunol. 164(8), 4178-84 (2000).

Jain T et al. Biophysical properties of the clinical-stage antibody landscape. PNAS 114 (5), 944-949 (2017).

Jefferis R, Reimer CB, Skvaril F, de Lange G, Ling NR, Lowe J, Walker MR, Phillips DJ, Aloisio CH, Wells TW. Evaluation of monoclonal antibodies having specificity for human IgG sub-classes: results of an IUIS/WHO collaborative study. Immunol. Lett. 10(3-4), 223-52 (1985).

Jefferis R, Reimer CB, Skvaril F, de Lange GG, Goodall DM, Bentley TL, Phillips DJ, Vlug A, Harada S, Radl J. Evaluation of monoclonal antibodies having specificity for human IgG subclasses: results of the 2nd IUIS/WHO collaborative study. Immunol. Lett. 31(2),143-68 (1992).

Juneja VR, McGuire KA, Manguso RT, LaFleur MW, Collins N, Haining WN, Freeman GJ, Sharpe AH. PD-L1 on tumor cells is sufficient for immune evasion in immunogenic tumors and inhibits CD8+ T cell cytotoxicity. J Exp Med. 214(4), 895-904 (2017).

Kabat EA, Wu TT, Perry HM, Gottesman KS, Foeller C. Sequences of Proteins of Immunological Interest, 5th ed. NIH Publication No. 91-3242. Washington, D.C.: U.S. Department of Health and Human Services (1991).

Kim YH, Choi BK, Kim KH, Kang SW, Kwon BS. Combination Therapy with Cisplatin and Anti-4-1BB. Cancer Res. 68(18), 7264-7269 (2008).

Klein C, Schaefer W, Regula JT. The use of CrossMAb technology for the generation of bi- and multispecific antibodies. MAbs 8(6), 1010-20 (2016).

Kleinovink JW, Marijt KA, Schoonderwoerd MJA, Hall T, Ossendorp F, Fransen MF. PD-L1 expression on malignant cells is no prerequisite for checkpoint therapy. Oncoimmunology. 6(4), e1294299 (2017).

Kocak E et al. Combination therapy with anti-CTL antigen-4 and anti-4-1BB antibodies enhances cancer immunity and reduces autoimmunity. Cancer Res. 15;66(14), 7276-84 (2006).

Lechner MG et al. Immunogenicity of murine solid tumor models as a defining feature of in vivo behavior and response to immunotherapy. J Immunother. 36(9), 477-89 (2013).

Ledermann JA, Begent RH, Massof C, Kelly AM, Adam T, Bagshawe KD. A phase-I study of

repeated therapy with radiolabelled antibody to carcinoembryonic antigen using intermittent or continuous administration of cyclosporin A to supress the immune response. Int. J. Cancer 47(5), 659-64 (1991).

Lefranc MP et al. IMGT®, the international ImMunoGeneTics information system® 25 years on. Nucleic Acids Res. 43(Database issue):D413-22 (2015).

Lefranc MP et al. IMGT unique numbering for immunoglobulin and T cell receptor constant domains and Ig superfamily C-like domains. Dev. Comp. Immunol. 29(3), 185-203 (2005).

Li F. and Ravetch JV. Antitumor activities of agonistic anti-TNFR antibodies require differential FcγRIIB coengagement in vivo. Proc Natl Acad Sci USA, 110(48), 19501-6 (2013).

Link A et al. Preclinical pharmacology of MP0310: a 4-1BB/FAP bispecific DARPin drug candidate promoting tumor-restricted T cell co-stimulation [abstract]. In: Proceedings of the Annual Meeting of the American Association for Cancer Research; 2018 Apr 14-18; Chicago (IL) Abstract nr 3752 (2018).

Makkouk A, Chester C, Kohrt HE. Rationale for anti-CD137 cancer immunotherapy. Eur J Cancer. 54, 112-119 (2016).

Martins JP, Kennedy PJ, Santos HA, Barrias C, Sarmento B. A comprehensive review of the neonatal Fc receptor and its application in drug delivery. Pharmcol. Ther. 161, 22-39 (2016).

Niu L et al. Cytokine- mediated disruption of lymphocyte trafficking, hemopoiesis, and induction of lymphopenia, anemia, and thrombocytopenia in anti-CD137-treated mice. J Immunol. 178(7), 4194-4213 (2007).

Pérez-Ruiz E, Etxeberria I, Rodriguez-Ruiz, Melero I. Anti-CD137 and PD-1/PD-L1 Antibodies En Route toward Clinical Synergy. Clin. Cancer Res. 23, (18) (2017)

Reichen C et al. FAP-mediated tumor accumulation of a T-cell agonistic FAP/4-1BB DARPin drug candidate analyzed by SPECT/CT and quantitative biodistribution [abstract]. In: Proceedings of the Annual Meeting of the American Association for Cancer Research; 2018 Apr 14-18; Chicago (IL) Abstract nr 3029 (2018).

Schofield DJ et al. Application of phage display to high throughput antibody generation and characterization. Genome Biol. 8(11), R254 (2007).

Segal NH et al. Phase I Study of Single-Agent Utomilumab (PF-05082566), a 4-1BB/CD137 Agonist, in Patients with Advanced Cancer. Clin Cancer Res. 24(8):1816-1823 (2018).

Segal NH et al. Results from an Integrated Safety Analysis of Urelumab, an Agonist Anti-CD137 Monoclonal Antibody. Clin Cancer Res. 23(8):1929-1936 (2017).

Shuford WW et al.I 4-1BB costimulatory signals preferentially induce CD8+ T cell proliferation and lead to the amplification in vivo of cytotoxic T cell responses. J Exp Med. 186(1), 47-55 (1997).

Smith TF, Waterman MS. Identification of common molecular subsequences. J. Mol. Biol. 147(1), 195-7 (1981).

Taraban VY et al. Expression and costimulatory effects of the TNF receptor superfamily members CD134 (OX40) and CD137 (4-1BB), and their role in the generation of anti-tumor immune responses. Eur. J. Immunol. 32, 3617-3627 (2002).

Tello, D, Goldbaum, FA, Mariuzza, RA, Ysern, X, Schwarz, FP, Poljak, RJ. Three-dimensional structure and thermodynamics of antigen binding by anti-lysozyme antibodies, Biochem Soc. Trans., 21(4), 943-6 (1993).

Tolcher AW et al. Phase Ib Study of Utomilumab (PF-05082566), a 4-1BB/CD137 Agonist, in Combination with Pembrolizumab (MK-3475) in Patients with Advanced Solid Tumors. Clin. Cancer Res. 23, 5349-57 (2017)

Wang X, Mathieu M, Brezski RJ. IgG Fc engineering to modulate antibody effector functions. Protein Cell 9(1), 63-73 (2018).

Wen T, Bukczynski J, Watts TH. 4-1BB ligand-mediated costimulation of human T cells induces CD4+ and CD8+ T cell expansion, cytokine production, and the development of cytolytic effector function. J Immunol. 168(10), 4897-906 (2002).

Wolfl M, Kuball J, Ho WY, Nguyen H, Manley TJ, Bleakley M, Greenberg PD. Activation-induced expression of CD137 permits detection, isolation, and expansion of the full repertoire of CD8+ T cells responding to antigen without requiring knowledge of epitope specificities. Blood. 110(1):201-10 (2007).

Won EY, Cha K, Byun JS, Kim DU, Shin S, Ahn B, Kim YH, Rice AJ, Walz T, Kwon BS, Cho HS. The structure of the trimer of human 4-1BB ligand is unique among members of the tumor necrosis factor superfamily. J Biol Chem. 285(12), 9202-10 (2010).

Wozniak-Knopp G et al. Introducing antigen-binding sites in structural loops of immunoglobulin constant domains: Fc fragments with engineered HER2/neu-binding sites and antibody properties. Protein Eng Des Sel. 23(4), 289-97 (2010).

Ye Q, Song DG, Poussin M, Yamamoto T, Best A, Li C, Coukos G, Powell DJ Jr. CD137 accurately identifies and enriches for naturally occurring tumor-reactive T cells in tumor. Clin Cancer Res. 20(1):44-55 (2014).

Yu X, Anasetti C. CH 10 - T-cell costimulation in graft-versus-host disease and graft-versus-leukemia effect. Immune Biology of Allogeneic Hematopoietic Stem Cell Transplantation. 195-222 (2013).

Zanetti M. Tapping CD4 T Cells for Cancer Immunotherapy: The Choice of Personalized Genomics. J Immunol. 194:2049-2056 (2015).

REFERENCES CITED IN THE DESCRIPTION

Cited references

This list of references cited by the applicant is for the reader's convenience only. It does not form part of the European patent document. Even though great care has been taken in compiling the references, errors or omissions cannot be excluded and the EPO disclaims all liability in this regard.

Patent documents cited in the description

- WO2016177802A1 [0013]
- WO2018056821A [0014] [0021] [0021] [0021]
- WO2017123650A [0014]
- WO2019025545A1 [0014]
- EP184187A [0042] [0047]
- GB2188638A [0042] [0047]
- EP239400A [0042] [0047]
- EP0120694A [0043]
- EP0125023A [0043]
- WO2006072620A [0067]
- WO2009132876A [0067]
- WO2011066389A1 [0140] [0141] [0142] [0143]
- US7288638B [0232]
- US20120237498A1 [0236]
- US8217149B2 [0262] [0425] [0435]
- US20120237498A [0362]
- WO1994016730A1 [0391]

Non-patent literature cited in the description

- **HU et al.**Cancer Res., 1996, vol. 56, 133055-61 [0044]
- **KABAT, E.A et al.**Sequences of Proteins of Immunological InterestU.S. Department of Health and Human Services19910000 [0053]

- **LEFRANC, M.-P. et al.**Nucleic Acids Res., 2015, vol. 43, D413-22 [0053]
- **LEDERMANN et al.**Int. J. Cancer, 1991, vol. 47, 659-664 [0192]
- **BAGSHAWE et al.**Antibody, Immunoconjugates and Radiopharmaceuticals, 1991, vol. 4, 915-922 [0192]
- Physician's Desk Reference, 2003, [0192]
- **ALTSCHUL SFGISH WMILLER WMYERS EWLIPMAN DJ**Basic local alignment search tool.J. Mol. Biol., 1990, vol. 215, 3403-10 [0500]
- **ALTSCHUL SFMADDEN TLSCHÄFFER AAZHANG JZHANG ZMILLER WLIPMAN DJ**Gapped BLAST and PSI-BLAST: a new generation of protein database search programs.Nucleic Acids Res., 1997, vol. 25, 173389-402 [0500]
- **BAGSHAWE KDSHARMA SKSPRINGER CJANTONIW PROGERS GTBURKE PJMELTON R**Antibody-enzyme conjugates can generate cytotoxic drugs from inactive precursors at tumor sitesAntibody, Immunoconjugates and Radiopharmaceuticals, 1991, vol. 4, 915-922 [0500]
- **BAIRD JR et al.**Immune-mediated regression of established B16F10 melanoma by intratumoral injection of attenuated Toxoplasma gondii protects against rechallenge.J Immunol., 2013, vol. 190, 1469-478 [0500]
- **BARTKOWIAK TCURRAN MA.**4-1BB Agonists: Multi-Potent Potentiators of Tumor ImmunityFront Oncol., 2015, vol. 5, 117- [0500]
- **BARTKOWIAK T et al.**Activation of 4-1BB on Liver Myeloid Cells Triggers Hepatitis via an Interleukin-27-Dependent PathwayClin Cancer Res., 2018, vol. 24, 51138-51 [0500]
- **BERGMAN IBURCKART GJPOHL CRVENKATARAMANAN RBARMADA MAGRIFFIN JACHEUNG NV**Pharmacokinetics of IgG and IgM Anti-Ganglioside Antibodies in Rats and Monkeys After Intrathecal AdministrationThe Journal of Pharmacology and Experimental Therapeutics, 1998, vol. 284, 1111-115 [0500]
- **BITRA ADOUKOV TWANG JPICARDA GBENEDICT CACROFT MZAJONC DM**Crystal structure of murine 4-1BB and its interaction with 4-1BBL support a role for galectin-9 in 4-1BB signaling.J Biol Chem., 2017, vol. 293, 41317-1329 [0500]
- **BROWN MHBARCLAY AN**Expression of immunoglobulin and scavenger receptor superfamily domains as chimeric proteins with domains 3 and 4 of CD4 for ligand analysisProtein Eng., 1994, vol. 7, 4515-21 [0500]
- **BRUHNS PLANNASCOLI BENGLAND PMANCARDI DAFERNANDEZ NJORIEUX SDAËRON M**Specificity and affinity of human Fcgamma receptors and their polymorphic variants for human IgG subclassesBlood., 2009, vol. 113, 163716-25 [0500]
- **CHACON JAWU RCSUKHUMALCHANDRA PMOLLDREM JJSARNAIK APILON-THOMAS SWEBER JHWU PRADVANYI L**Co-stimulation through 4-1BB/CD137 improves the expansion and function of CD8(+) melanoma tumor-infiltrating lymphocytes for adoptive T-cell therapyPLoS One, 2013, vol. 8, 4e60031- [0500]
- **CHAPPLE SDCROFTS AMSHADBOLT SPMCCAFFERTY JDYSON MR**Multiplexed expression and screening for recombinant protein production in mammalian cellsBMC Biotechnol., 2006, vol. 6, 49- [0500]
- **CHESTER CAMBULKAR SKOHRT HE**4-1BB agonism: adding the accelerator to cancer immunotherapyCancer Immunol Immunother., 2016, vol. 65, 101243-8 [0500]
- **CHESTER CSANMAMED MFWANG JMELERO I**Immunotherapy targeting 4-1BB:

mechanistic rationale, clinical results, and future strategiesBlood, 2018, vol. 131, 149-57 [0500]

- **CLAUS C et al.**A novel tumor-targeted 4-1BB agonist and its combination with T-cell bispecific antibodies: an off-the-shelf cancer immunotherapy alternative to CAR T-cells [abstractCancer Res., 2017, vol. 77, [0500]
- **CROFT M.**Co-stimulatory members of the TNFR family: keys to effective T-cell immunity?Nat Rev Immunol., 2003, vol. 3, 8609-20 [0500]
- **CURRAN MAGEIGER TLMONTALVO WKIM MREINER SLAL-SHAMKHANI ASUN JCALLISON J. P**Systemic 4-1BB activation induces a novel T cell phenotype driven by high expression of Eomesodermin.J. Exp.Med., 2013, vol. 210, 4743-755 [0500]
- **DUBROT J et al.**Treatment with anti-CD137 mAbs causes intense accumulations of liver T cells without selective antitumor immunotherapeutic effects in this organCancer Immunol Immunother., 2010, vol. 59, 81223-1233 [0500]
- **DYSON MRZHENG YZHANG CCOLWILL KPERSHAD KKAY BKPAWSON TMCCAFFERTY J**Mapping protein interactions by combining antibody affinity maturation and mass spectrometryAnal. Biochem., 2011, vol. 417, 125-35 [0500]
- **FISHER TS et al.**Targeting of 4-1BB by monoclonal antibody PF-05082566 enhances T-cell function and promotes anti-tumor activityCancer Immunol Immunother., 2012, vol. 61, 101721-33 [0500]
- **GROSSO JINZUNZA DWU QSIMON JSINGH PZHANG XPHILLIPS TSIMMONS PCOGSWELL J.**Programmed death-ligand 1 (PD-L1) expression in various tumor types.Journal for Immunotherapy of Cancer., 2013, vol. 1, 153- [0500]
- **HASENHINDL CTRAXLMAYR MWWOZNIAK-KNOPP GJONES PCSTADLMAYR GRÜKER FOBINGER C**Stability assessment on a library scale: a rapid method for the evaluation of the commutability and insertion of residues in C-terminal loops of the CH3 domains of IgG1-FcProtein Eng. Des. Sel., 2013, vol. 26, 10675-82 [0500]
- **HEZAREH MHESSELL AJJENSEN RCVAN DE WINKEL JGPARREN PW**Effector function activities of a panel of mutants of a broadly neutralizing antibody against human immunodeficiency virus type 1J Virol., 2001, vol. 75, 2412161-8 [0500]
- **HINNER MJAIBA, RSBWIEDENMANN ASCHLOSSER CALLERSDORFER AMATSCHINER GROTHE CMOEBIUS UKOHRT HEOLWILL SA**Costimulatory T cell engagement via a novel bispecific anti-CD137 /anti-HER2 proteinJ. Immunotherapy Cancer, 2015, vol. 3, 2187- [0500]
- **HOLLIGER PHUDSON PJ**Engineered antibody fragments and the rise of single domains.Nat Biotechnol., 2005, vol. 23, 91126-36 [0500]
- **HU SSHIVELY LRAUBITSCHEK ASHERMAN MWILLIAMS LEWONG JYSHIVELY JEWU AM**Minibody: A novel engineered anti-carcinoembryonic antigen antibody fragment (single-chain Fv-CH3) which exhibits rapid, high-level targeting of xenografts.Cancer Res., 1996, vol. 56, 133055-61 [0500]
- **HURTADO JCKIM YJKWON BS**Signals through 4-1BB are costimulatory to previously activated splenic T cells and inhibit activation-induced cell death.J Immunol., 1997, vol. 158, 62600-9 [0500]
- **IDUSOGIE EEPRESTA LGGAZZANO-SANTORO HTOTPAL KWONG PYULTSCH MMENG YGMULKERRIN MG**Mapping of the C1q binding site on rituxan, a chimeric

antibody with a human IgG1 Fc.J Immunol., 2000, vol. 164, 84178-84 [0500]

- **JAIN T et al.**Biophysical properties of the clinical-stage antibody landscapePNAS, 2017, vol. 114, 5944-949 [0500]
- **JEFFERIS RREIMER CBSKVARIL FDE LANGE GLING NRLOWE JWALKER MRPHILLIPS DJALOISIO CHWELLS TW**Evaluation of monoclonal antibodies having specificity for human IgG sub-classes: results of an IUIS/WHO collaborative studyImmunol. Lett., 1985, vol. 10, 3-4223-52 [0500]
- **JEFFERIS RREIMER CBSKVARIL FDE LANGE GGGOODALL DMBENTLEY TLPHILLIPS DJVLUG AHARADA SRADL J.**Evaluation of monoclonal antibodies having specificity for human IgG subclasses: results of the 2nd IUIS/WHO collaborative studyImmunol. Lett., 1992, vol. 31, 2143-68 [0500]
- **JUNEJA VRMCGUIRE KAMANGUSO RTLAFLEUR MWCOLLINS NHAINING WNFREEMAN GJSHARPE AH**PD-L1 on tumor cells is sufficient for immune evasion in immunogenic tumors and inhibits CD8+ T cell cytotoxicity.J Exp Med., 2017, vol. 214, 4895-904 [0500]
- **KABAT EAWU TTPERRY HMGOTTESMAN KSFOELLER C**Sequences of Proteins of Immunological InterestU.S. Department of Health and Human Services19910000 [0500]
- **KIM YHCHOI BKKIM KHKANG SWKWON BS**Combination Therapy with Cisplatin and Anti-4-1BB.Cancer Res., 2008, vol. 68, 187264-7269 [0500]
- **KLEIN CSCHAEFER WREGULA JT**The use of CrossMAb technology for the generation of bi- and multispecific antibodies.MAbs, 2016, vol. 8, 61010-20 [0500]
- **KLEINOVINK JWMARIJT KASCHOONDERWOERD MJAHALL TOSSENDORP FFRANSEN MF**PD-L1 expression on malignant cells is no prerequisite for checkpoint therapyOncoimmunology, 2017, vol. 6, 4e1294299- [0500]
- **KOCAK E et al.**Combination therapy with anti-CTL antigen-4 and anti-4-1BB antibodies enhances cancer immunity and reduces autoimmunity.Cancer Res., 2006, vol. 66, 147276-84 [0500]
- **LECHNER MG et al.**Immunogenicity of murine solid tumor models as a defining feature of in vivo behavior and response to immunotherapy.J Immunother., 2013, vol. 36, 9477-89 [0500]
- **LEDERMANN JABEGENT RHMASSOF CKELLY AMADAM TBAGSHAWE KD**A phase-I study of repeated therapy with radiolabelled antibody to carcinoembryonic antigen using intermittent or continuous administration of cyclosporin A to supress the immune responseInt. J. Cancer, 1991, vol. 47, 5659-64 [0500]
- **LEFRANC MP et al.**IMGT®, the international ImMunoGeneTics information system® 25 years on.Nucleic Acids Res., 2015, vol. 43, D413-22 [0500]
- **LEFRANC MP et al.**IMGT unique numbering for immunoglobulin and T cell receptor constant domains and Ig superfamily C-like domainsDev. Comp. Immunol., 2005, vol. 29, 3185-203 [0500]
- **LI F.RAVETCH JV**Antitumor activities of agonistic anti-TNFR antibodies require differential FcyRIIB coengagement in vivo.Proc Natl Acad Sci USA, 2013, vol. 110, 4819501-6 [0500]
- **LINK A et al.**Preclinical pharmacology of MP0310: a 4-1BB/FAP bispecific DARPin drug candidate promoting tumor-restricted T cell co-stimulation [abstractProceedings of the

Annual Meeting of the American Association for Cancer Research, 2018, [0500]

- **MAKKOUK ACHESTER CKOHRT HE**Rationale for anti-CD137 cancer immunotherapyEur J Cancer., 2016, vol. 54, 112-119 [0500]
- **MARTINS JPKENNEDY PJSANTOS HABARRIAS CSARMENTO B.**A comprehensive review of the neonatal Fc receptor and its application in drug deliveryPharmcol. Ther., 2016, vol. 161, 22-39 [0500]
- **NIU L et al.**Cytokine- mediated disruption of lymphocyte trafficking, hemopoiesis, and induction of lymphopenia, anemia, and thrombocytopenia in anti-CD137-treated mice.J Immunol., 2007, vol. 178, 74194-4213 [0500]
- **PÉREZ-RUIZ EETXEBERRIA IRODRIGUEZ-RUIZMELERO I**Anti-CD137 and PD-1/PD-L1 Antibodies En Route toward Clinical SynergyClin. Cancer Res., 2017, vol. 23, 18 [0500]
- **REICHEN C et al.**FAP-mediated tumor accumulation of a T-cell agonistic FAP/4-1BB DARPin drug candidate analyzed by SPECT/CT and quantitative biodistribution [abstractProceedings of the Annual Meeting of the American Association for Cancer Research, 2018, [0500]
- **SCHOFIELD DJ et al.**Application of phage display to high throughput antibody generation and characterizationGenome Biol., 2007, vol. 8, 11R254- [0500]
- **SEGAL NH et al.**Phase I Study of Single-Agent Utomilumab (PF-05082566), a 4-1BB/CD137 Agonist, in Patients with Advanced CancerClin Cancer Res., 2018, vol. 24, 81816-1823 [0500]
- **SEGAL NH et al.**Results from an Integrated Safety Analysis of Urelumab, an Agonist Anti-CD137 Monoclonal AntibodyClin Cancer Res., 2017, vol. 23, 81929-1936 [0500]
- **SHUFORD WW et al.**I 4-1BB costimulatory signals preferentially induce CD8+ T cell proliferation and lead to the amplification in vivo of cytotoxic T cell responses.J Exp Med., 1997, vol. 186, 147-55 [0500]
- **SMITH TFWATERMAN MS**Identification of common molecular subsequences.J. Mol. Biol., 1981, vol. 147, 1195-7 [0500]
- **TARABAN VY et al.**Expression and costimulatory effects of the TNF receptor superfamily members CD134 (OX40) and CD137 (4-1BB), and their role in the generation of anti-tumor immune responsesEur. J. Immunol., 2002, vol. 32, 3617-3627 [0500]
- **TELLO, DGOLDBAUM, FAMARIUZZA, RAYSERN, XSCHWARZ, FPPOLJAK, RJ.**Three-dimensional structure and thermodynamics of antigen binding by anti-lysozyme antibodiesBiochem Soc. Trans., 1993, vol. 21, 4943-6 [0500]
- **TOLCHER AW et al.**Phase Ib Study of Utomilumab (PF-05082566), a 4-1BB/CD137 Agonist, in Combination with Pembrolizumab (MK-3475) in Patients with Advanced Solid TumorsClin. Cancer Res., 2017, vol. 23, 5349-57 [0500]
- **WANG XMATHIEU MBREZSKI RJ**IgG Fc engineering to modulate antibody effector functionsProtein Cell, 2018, vol. 9, 163-73 [0500]
- **WEN TBUKCZYNSKI JWATTS TH**4-1BB ligand-mediated costimulation of human T cells induces CD4+ and CD8+ T cell expansion, cytokine production, and the development of cytolytic effector function.J Immunol., 2002, vol. 168, 104897-906 [0500]
- **WOLFL MKUBALL JHO WYNGUYEN HMANLEY TJBLEAKLEY MGREENBERG**

PDActivation-induced expression of CD137 permits detection, isolation, and expansion of the full repertoire of CD8+ T cells responding to antigen without requiring knowledge of epitope specificitiesBlood, 2007, vol. 110, 1201-10 [0500]

- **WON EYCHA KBYUN JSKIM DUSHIN SAHN BKIM YHRICE AJWALZ TKWON BS**The structure of the trimer of human 4-1BB ligand is unique among members of the tumor necrosis factor superfamily.J Biol Chem., 2010, vol. 285, 129202-10 [0500]
- **WOZNIAK-KNOPP G et al.**Introducing antigen-binding sites in structural loops of immunoglobulin constant domains: Fc fragments with engineered HER2/neu-binding sites and antibody propertiesProtein Eng Des Sel., 2010, vol. 23, 4289-97 [0500]
- **YE QSONG DGPOUSSIN MYAMAMOTO TBEST ALI CCOUKOS GPOWELL DJ JR**CD137 accurately identifies and enriches for naturally occurring tumor-reactive T cells in tumorClin Cancer Res., 2014, vol. 20, 144-55 [0500]
- **YU XANASETTI C.**CH 10 - T-cell costimulation in graft-versus-host disease and graft-versus-leukemia effectImmune Biology of Allogeneic Hematopoietic Stem Cell Transplantation., 2013, 195-222 [0500]
- **ZANETTI M.**Tapping CD4 T Cells for Cancer Immunotherapy: The Choice of Personalized GenomicsJ Immunol., 2015, vol. 194, 2049-2056 [0500]

ANTISTOFMOLEKYLER DER BINDER PD-L1 OG CD137

Patentkrav

1. Antistofmolekyle der binder til programmeret dødsligand 1 (PD-L1) og CD137, som omfatter:

(a) en komplementaritetsdeterminerende region (CDR)-baseret antigen-bindingssted for PD-L1; og

(b) et CD137 antigen-bindingssted placeret i et CH3-domæne af antistofmolekylet, hvori CD137 antigen-bindingsstedet omfatter en første sekvens og en anden sekvens henholdsvis placeret i AB og EF hårnålestrukturerne af CH3-domænet, hvori den første sekvens er placeret mellem positionerne 14 og 17 på CH3-domænet og den anden sekvens er placeret mellem positionerne 91 og 99 på CH3-domænet, hvori nummereringen af aminosyrerester stemmer overens med IMGT-nummereringsskemaet, og

hvori antistofmolekylet omfatter VH-domænet, VL-domænet, første sekvens og anden sekvens anført i:

(i) SEQ ID NR. **12**, **14**, **113** og **114**, henholdsvis **[FS22-172-003-AA/E12v2]**;

(ii) SEQ ID NR. **23**, **25**, **113** og **114**, henholdsvis **[FS22-172-003-AA/E05v2]**;

(iii) SEQ ID NR. **23**, **30**, **113** og **114**, henholdsvis **[FS22-172-003-AA/G12v2]**;

(iv) SEQ ID NR. **12**, **14**, **79** og **80**, henholdsvis **[FS22-053-008-AA/E12v2]**;

(v) SEQ ID NR. **23**, **25**, **79** og **80**, henholdsvis **[FS22-053-008-AA/E05v2]**;

(vi) SEQ ID NR. **12**, **14**, **79** og **89**, henholdsvis **[FS22-053-017-AA/E12v2]**;

(vii) SEQ ID NR. **23**, **25**, **79** og **89**, henholdsvis **[FS22-053-017-AA/E05v2]**; eller

(viii) SEQ ID NR. **23**, **30**, **79** og **89**, henholdsvis **[FS22-053-017-AA/G12v2]**,

2. Antistofmolekyle ifølge krav 1, hvori antistofmolekylet omfatter VH-domænet og VL- domænet anført i SEQ ID NR. **12** og **14**, henholdsvis **[E12v2]**.

3. Antistofmolekyle ifølge ethvert af de foregående krav, hvori antistofmolekylet omfatter CH3-domænet anført i SEQ ID NR.: **115 [FS22-172-003]**, SEQ ID NR.: **81 [FS22-053-008]**, eller SEQ ID NR.: **90 [FS22-053-017]**.

4. Antistofmolekyle ifølge ethvert af de foregående krav, hvori antistofmolekylet omfatter den tunge kæde og lette kæde af antistof:

(i) **FS22-172-003-AA/E12v2** anført i henholdsvis SEQ ID NR. **134** og **17**;
(ii) **FS22-172-003-AA/E05v2** anført i henholdsvis SEQ ID NR. **137** og **28**;
(iii) **FS22-172-003-AA/G12v2** anført i henholdsvis SEQ ID NR. **140** og **33**;
(iv) **FS22-053-008-AA/E12v2** anført i henholdsvis SEQ ID NR. **143** og **17**;
(v) **FS22-053-008-AA/E05v2** anført i henholdsvis SEQ ID NR. **146** og **28**;
(vi) **FS22-053-017-AA/E12v2** anført i henholdsvis SEQ ID NR. **152** og **17**;
(vii) **FS22-053-017-AA/E05v2** anført i henholdsvis SEQ ID NR. **153** og **28**; eller
(viii) **FS22-053-017-AA/G12v2** anført i henholdsvis SEQ ID NR. **154** og **33**.

5. Antistofmolekyle ifølge ethvert af de foregående krav, hvori antistofmolekylet omfatter den tunge kæde og lette kæde anført i SEQ ID NR. **134** og **17**, henholdsvis **[FS22-172-003-AA/E12v2]**.

6. Antistofmolekyle ifølge ethvert af de foregående krav, hvori CH3-domænet af antistofmolekylet ydermere omfatter en yderligere lysinrest (K) på den nærmeste C-terminus af CH3-domænesekvensen.

7. Antistofmolekyle ifølge ethvert af kravene 1, 2, 3 og 6, hvori:
(i) antistofmolekylet er modificeret til at reducere eller ophæve binding af CH2-domænet på antistofmolekylet til en eller flere Fcγ-receptorer; og/eller
(ii) antistofmolekylet ikke binder til en eller flere Fcγ-receptorer.

8. Nucleinsyremolekyle eller -molekyler der koder antistofmolekylet ifølge ethvert af de foregående krav.

9. Vektor eller vektorer der omfatter nucelinsyremolekylet eller -molekylerne ifølge krav 8.

10. Rekombinant værtscelle der omfatter nucleinsyremolekylet(erne) ifølge krav 8, eller vektoren(erne) ifølge krav 9.

11. Fremgangsmåde til at producere antistofmolekylet ifølge ethvert af kravene 1 til 7 der omfatter dyrkning af den rekombinante værtscelle i krav 10 under betingelser for produktion af antistofmolekylet.

12. Fremgangsmåde ifølge krav 11 der ydermere omfatter isolering og/eller rensning af antistofmolekylet.

13. Farmaceutisk sammensætning der omfatter antistofmolekylet ifølge ethvert af kravene 1 til 7 og et farmaceutisk acceptabelt hjælpestof.

14. Antistofmolekyle ifølge ethvert af kravene 1 til 7 til anvendelse i en fremgangsmåde til behandling af cancer i et individ.

DRAWINGS

Drawing

															AB																						
IMGT	1.4	1.3	1.2	1.1	1	2	3	4	5	6	7	8	9	10	11	12	13	14	15	16	16.5	16.4	16.3	16.2	16.1	17	18	19	20	21	22	23	24	25	26	27	28
IMGT exon numbering	1	2	3	4	5	6	7	8	9	10	11	12	13	14	15	16	17	18	19	20						21	22	23	24	25	26	27	28	29	30	31	32
EU numbering	341	342	343	344	345	346	347	348	349	350	351	352	353	354	355	356	357	358	359	360						361	362	363	364	365	366	367	368	369	370	371	372
Kabat numbering	361	363	364	365	366	367	368	369	370	371	372	373	374	375	376	377	378	381	382	383						384	385	386	387	388	389	390	391	392	393	394	395
Wt Fcab	G	Q	P	R	E	P	Q	V	Y	T	L	P	P	S	R	D	E	L	T	K						N	Q	V	S	L	T	C	L	V	K	G	F
FS22-053																			N	P	P	Y	L	F	S												
FS22-053-008																			N	P	P	Y	L	F	S												
FS22-053-009																			N	P	P	Y	L	F	S												
FS22-053-010																			N	P	P	Y	L	F	S												
FS22-053-011																			N	P	P	Y	L	F	S												
FS22-053-012																			N	P	P	Y	L	F	S												
FS22-053-013																			N	P	P	Y	L	F	S												
FS22-053-014																			N	P	P	Y	L	F	S												
FS22-053-015																			N	P	P	Y	L	F	S												
FS22-053-016																			N	P	P	Y	L	F	S												
FS22-053-017																			N	P	P	Y	L	F	S												
FS22-172																			R		Y	Y	P	P	Y												
FS22-172-001																			P	F	V	M	P	P	Y												
FS22-172-002																			P	F	Q	M	P	P	Y												
FS22-172-003																			P	Y	I	I	P	P	Y												
FS22-172-004																			N	Y	I	Y	P	P	Y												
FS22-172-005																			Q	Q	V	Y	P	P	Y												
FS22-172-006																			R		Y	Y	P	P	Y			L									

Figure 1A

	IMGT	IMGT exon numbering	EU numbering	Kabat numbering	Wt Fcab	Y	P	S	D	I	A	V	E	W	E	S	N	G	Q	P	E	N	N	Y	K	T	T	P	P	V	L	D	S	D	G	S	F	F	L	Y	S	K
	29	33	373	396	FS22-053																																							
	30	34	374	397	FS22-053-008																																							
	35	35	375	398	FS22-053-009																																							
	36	36	376	399	FS22-053-010																																							
	37	37	377	400	FS22-053-011																																							
	38	38	378	401	FS22-053-012																																							
	39	39	379	402	FS22-053-013																																							
	40	40	380	405	FS22-053-014																																							
	41	41	381	406	FS22-053-015																																							
	42	42	382	407	FS22-053-016																																							
	43	43	383	408	FS22-053-017																																							
	44	44	384	410	FS22-172																																							
	45	45	385	411	FS22-172-001																																							
	45.1	46	386	414	FS22-172-002																																							
	45.2	47	387	415	FS22-172-003																																							
	45.3	48	388	416	FS22-172-004																																							
	45.4	49	389	417	FS22-172-005																																							
	77	50	390	418	FS22-172-006																																							
	78	51	391	419																																							
	79	52	392	420																																							
	80	53	393	421																																							
	81	54	394	422																																							
	82	55	395	423																																							
	83	56	396	424																																							
	84	57	397	425																																							
	84.1	58	398	426																																							
	84.2	59	399	427																																							
	84.3	60	400	428																																							
	84.4	61	401	430																																							
	85.4	62	402	433																																							
	85.3	63	403	434																																							
	85.2	64	404	435																																							
	85.1	65	405	436																																							
	85	66	406	437																																							
	86	67	407	438																																							
	87	68	408	439																																							
	88	69	409	440																																							

Figure 1B

				EF																																	
IMGT	89	90	91	92	93	94	95	96	97	98	99	100	101	102	103	104	105	106	107	108	109	110	112	113	114	115	116	117	118	119	120	121	122	123	124	125	129
IMGT exon numbering	70	71	72	73	74	75	76	77	78	79	80	81	82	83	84	85	86	87	88	89	90	91	92	93	94	95	96	97	98	99	100	101	102	103	104	105	CHS 10
EU numbering	410	411	412	413	414	415	416	417	418	419	420	421	422	423	424	425	426	427	428	429	430	431	432	433	434	435	436	437	438	439	440	441	442	443	444	445	446
Kabat numbering	441	442	443	444	445	446	447	448	449	450	451	452	453	454	455	456	457	458	459	460	461	462	463	464	465	466	467	468	469	470	471	472	473	474	475	476	477
Wt Fcab	**L**	**T**	**V**	**D**	**K**	**S**	**R**	**W**	**Q**	**Q**	**G**	**N**	**V**	**F**	**S**	**C**	**S**	**V**	**M**	**H**	**E**	**A**	**L**	**H**	**N**	**H**	**Y**	**T**	**Q**	**K**	**S**	**L**	**S**	**L**	**S**	**P**	**G**
FS22-053				**Y**	**Y**	**N**				**D**																											
FS22-053-008					**Y**	**W**			**L**	**E**																											
FS22-053-009				**E**	**H**	**T**			**L**	**D**																											
FS22-053-010					**Y**	**M**			**L**	**D**																											
FS22 053 011					**Y**	**W**			**T**	**D**																											
FS22-053-012					**H**	**M**			**L**	**E**																											
FS22-053-013				**G**	**Y**	**E**			**L**	**E**																											
FS22-053-014				**Y**	**H**	**W**			**L**	**D**																											
FS22-053-015					**H**	**W**			**L**																												
FS22-053-016					**Y**	**I**			**L**	**N**																											
FS22-053-017				**Y**	**H**	**W**			**L**	**E**																											
FS22-172				**G**	**A**	**D**			**L**	**E**																											
FS22-172-001				**G**	**A**	**D**			**L**	**E**																											
FS22-172-002				**G**	**A**	**D**			**L**	**E**																											
FS22-172-003				**G**	**A**	**D**			**L**	**E**																											
FS22-172-004				**G**	**A**	**D**			**L**	**E**																											
FS22-172-005				**G**	**A**	**D**			**L**	**E**																											
FS22-172-006				**G**	**A**	**D**			**L**	**E**																											

Figure 1C

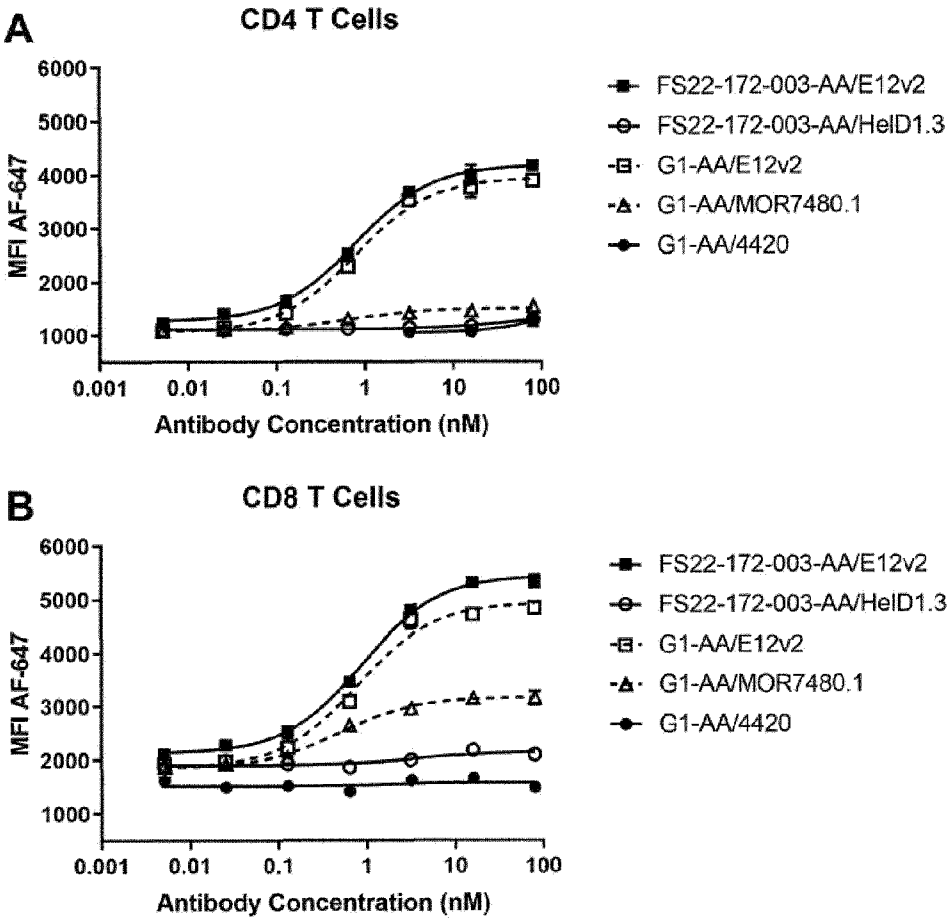
A
CD4 T Cells
MFI AF-647
6000
5000
4000
3000
2000
1000
0.001
0.01
0.1
1
10
100
Antibody Concentration (nM)
FS22-172-003-AA/E12v2
FS22-172-003-AA/HelD1.3
G1-AA/E12v2
G1-AA/MOR7480.1
G1-AA/4420
B
CD8 T Cells
MFI AF-647
6000
5000
4000
3000
2000
1000
0.001
0.01
0.1
1
10
100
Antibody Concentration (nM)
FS22-172-003-AA/E12v2
FS22-172-003-AA/HelD1.3
G1-AA/E12v2
G1-AA/MOR7480.1
G1-AA/4420

Figure 2

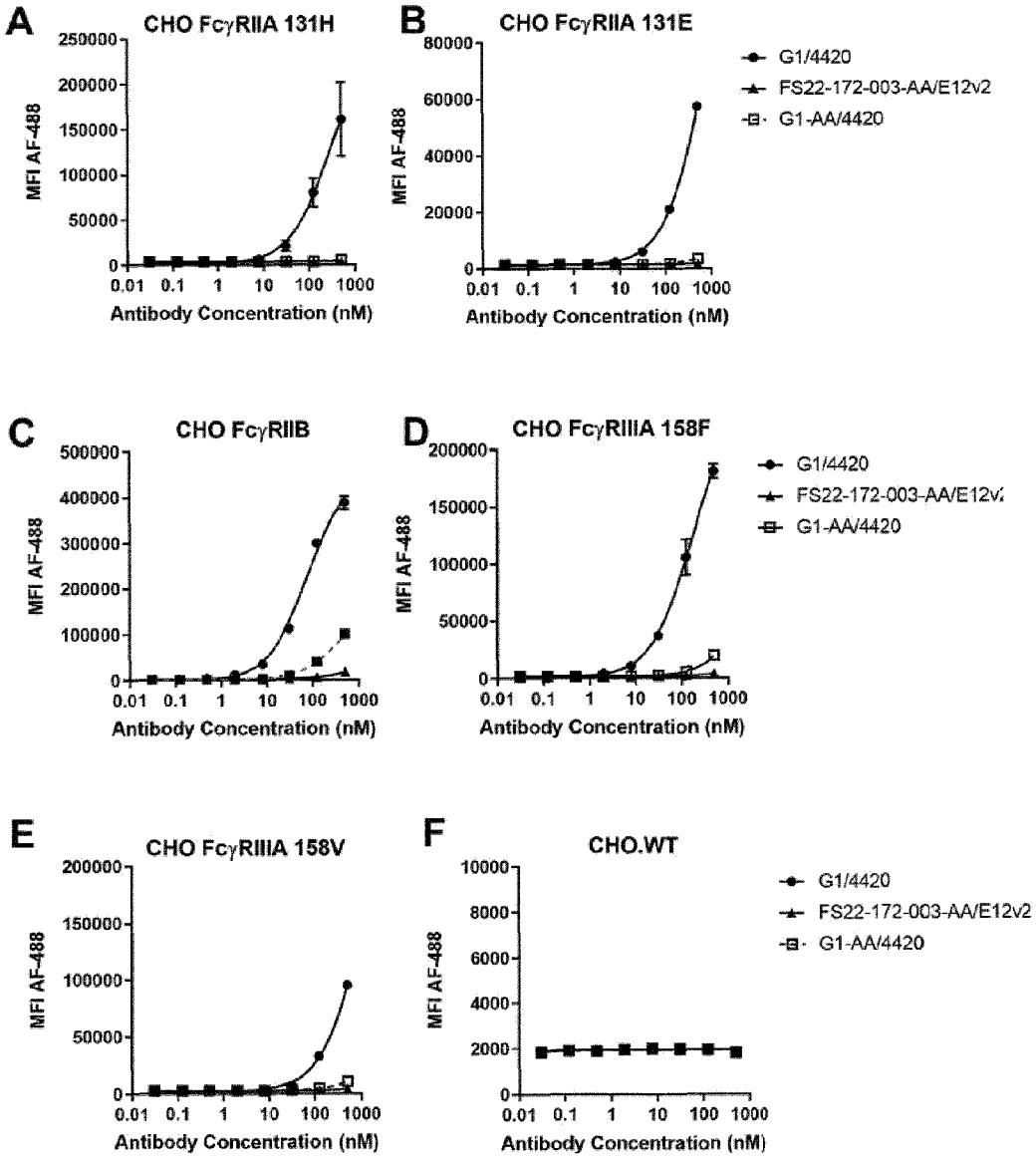
A
CHO FcγRIIA 131H
MFI AF-488
250000
200000
150000
100000
50000
0
0.01 0.1 1 10 100 1000
Antibody Concentration (nM)
B
CHO FcγRIIA 131E
MFI AF-488
80000
60000
40000
20000
0
0.01 0.1 1 10 100 1000
Antibody Concentration (nM)
G1/4420
FS22-172-003-AA/E12v2
G1-AA/4420
C
CHO FcγRIIB
MFI AF-488
500000
400000
300000
200000
100000
0
0.01 0.1 1 10 100 1000
Antibody Concentration (nM)
D
CHO FcγRIIIA 158F
MFI AF-488
200000
150000
100000
50000
0
0.01 0.1 1 10 100 1000
Antibody Concentration (nM)
G1/4420
FS22-172-003-AA/E12v2
G1-AA/4420
E
CHO FcγRIIIA 158V
MFI AF-488
200000
150000
100000
50000
0
0.01 0.1 1 10 100 1000
Antibody Concentration (nM)
F
CHO.WT
MFI AF-488
10000
8000
6000
4000
2000
0
0.01 0.1 1 10 100 1000
Antibody Concentration (nM)
G1/4420
FS22-172-003-AA/E12v2
G1-AA/4420

Figure 3

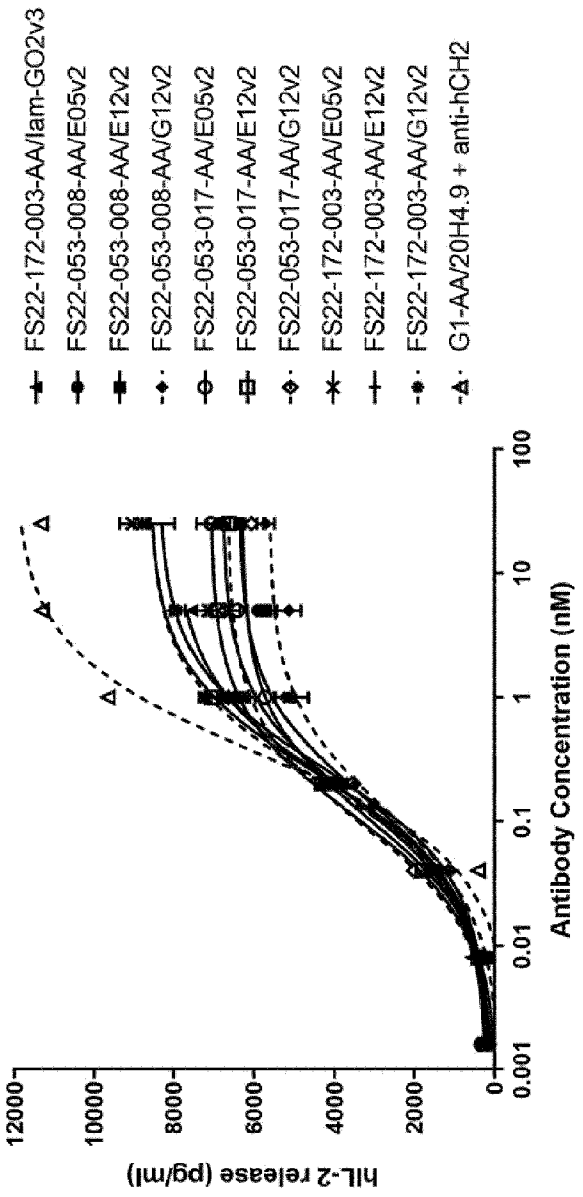
FS22-172-003-AA/Iam-GO2v3
FS22-053-008-AA/E05v2
FS22-053-008-AA/E12v2
FS22-053-008-AA/G12v2
FS22-053-017-AA/E05v2
FS22-053-017-AA/E12v2
FS22-053-017-AA/G12v2
FS22-172-003-AA/E05v2
FS22-172-003-AA/E12v2
FS22-172-003-AA/G12v2
G1-AA/20H4.9 + anti-hCH2
hIL-2 release (pg/ml)
12000
10000
8000
6000
4000
2000
0
0.001
0.01
0.1
1
10
100
Antibody Concentration (nM)

Figure 4

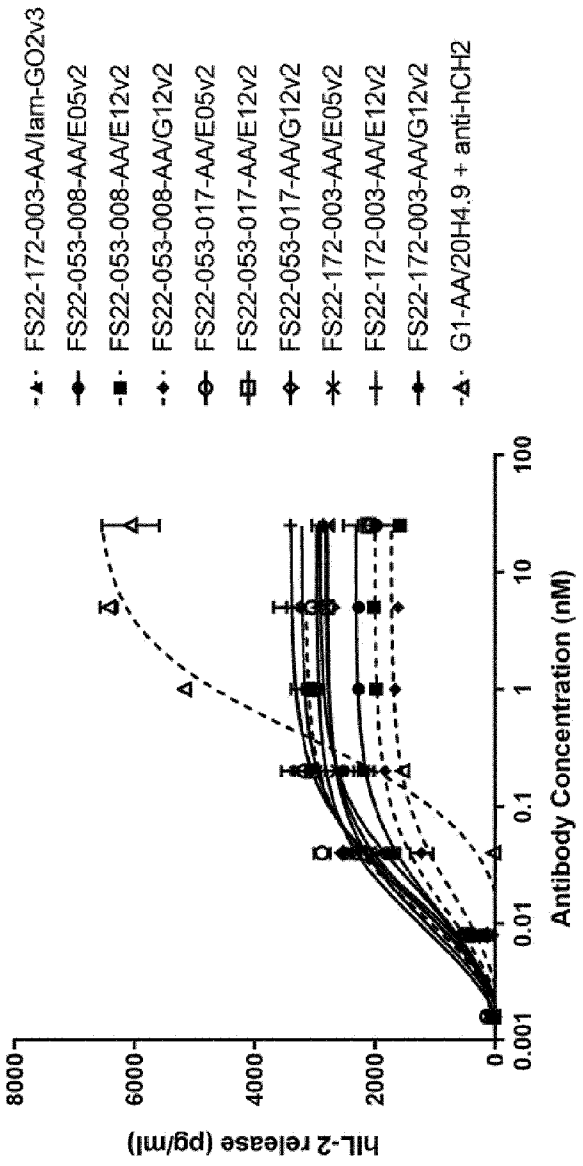
FS22-172-003-AA/Iam-GO2v3
FS22-053-008-AA/E05v2
FS22-053-008-AA/E12v2
FS22-053-008-AA/G12v2
FS22-053-017-AA/E05v2
FS22-053-017-AA/E12v2
FS22-053-017-AA/G12v2
FS22-172-003-AA/E05v2
FS22-172-003-AA/E12v2
FS22-172-003-AA/G12v2
G1-AA/20H4.9 + anti-hCH2
hIL-2 release (pg/ml)
8000
6000
4000
2000
0
0.001
0.01
0.1
1
10
100
Antibody Concentration (nM)

Figure 5

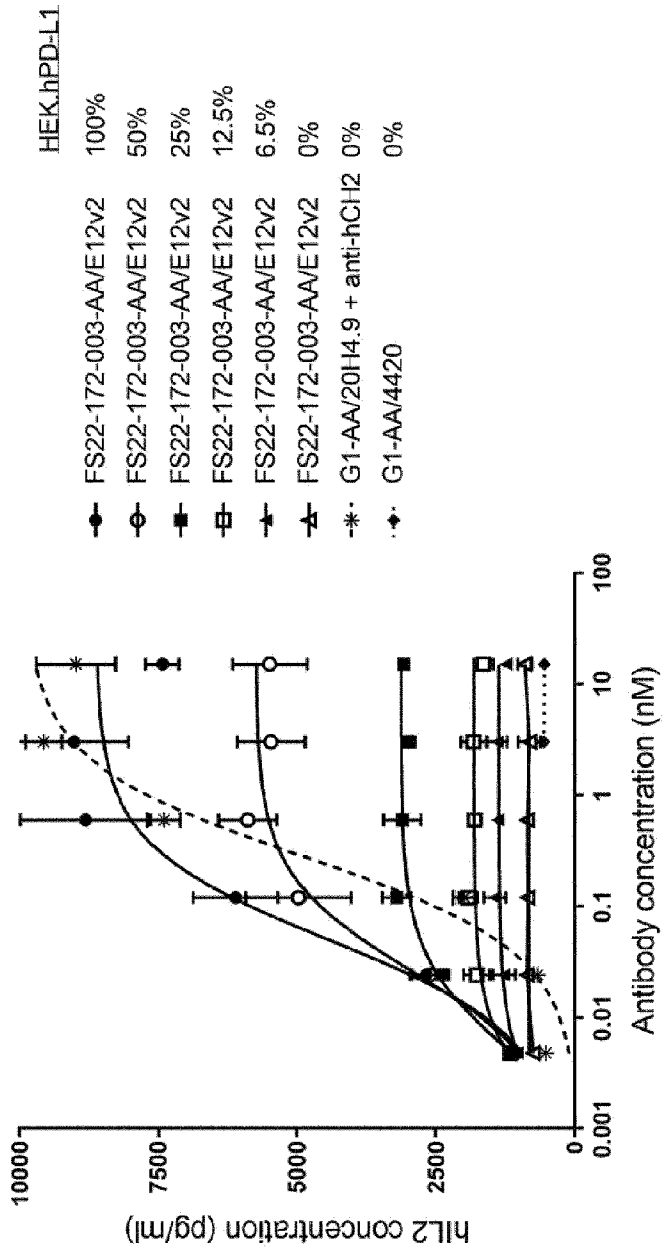
HEK.hPD-L1
FS22-172-003-AA/E12v2 100%
FS22-172-003-AA/E12v2 50%
FS22-172-003-AA/E12v2 25%
FS22-172-003-AA/E12v2 12.5%
FS22-172-003-AA/E12v2 6.5%
FS22-172-003-AA/E12v2 0%
G1-AA/20H4.9 + anti-hCH2 0%
G1-AA/4420 0%
hIL2 concentration (pg/ml)
10000
7500
5000
2500
0
0.001
0.01
0.1
1
10
100
Antibody concentration (nM)

Figure 6

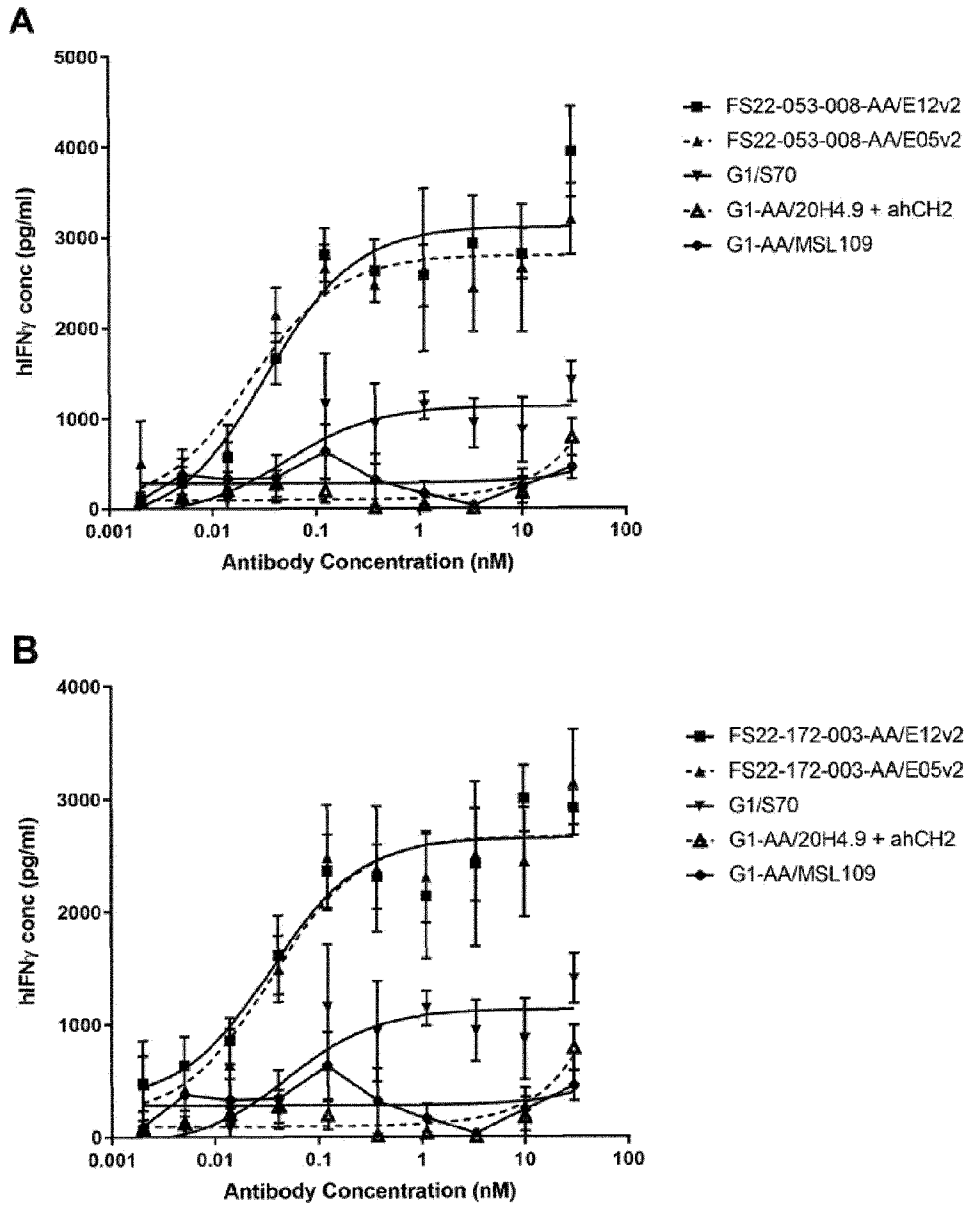
A
hIFNγ conc (pg/ml)
5000
4000
3000
2000
1000
0
0.001
0.01
0.1
1
10
100
Antibody Concentration (nM)
FS22-053-008-AA/E12v2
FS22-053-008-AA/E05v2
G1/S70
G1-AA/20H4.9 + ahCH2
G1-AA/MSL109
B
hIFNγ conc (pg/ml)
4000
3000
2000
1000
0
0.001
0.01
0.1
1
10
100
Antibody Concentration (nM)
FS22-172-003-AA/E12v2
FS22-172-003-AA/E05v2
G1/S70
G1-AA/20H4.9 + ahCH2
G1-AA/MSL109

Figure 7

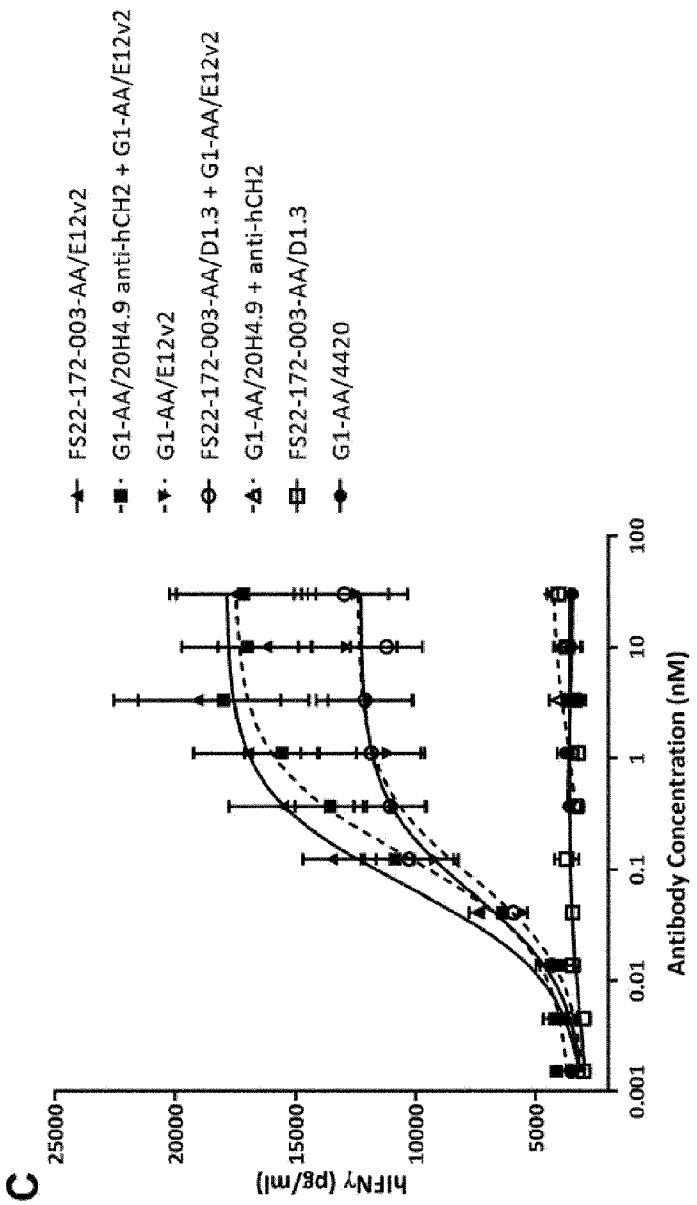

Figure 7 continued

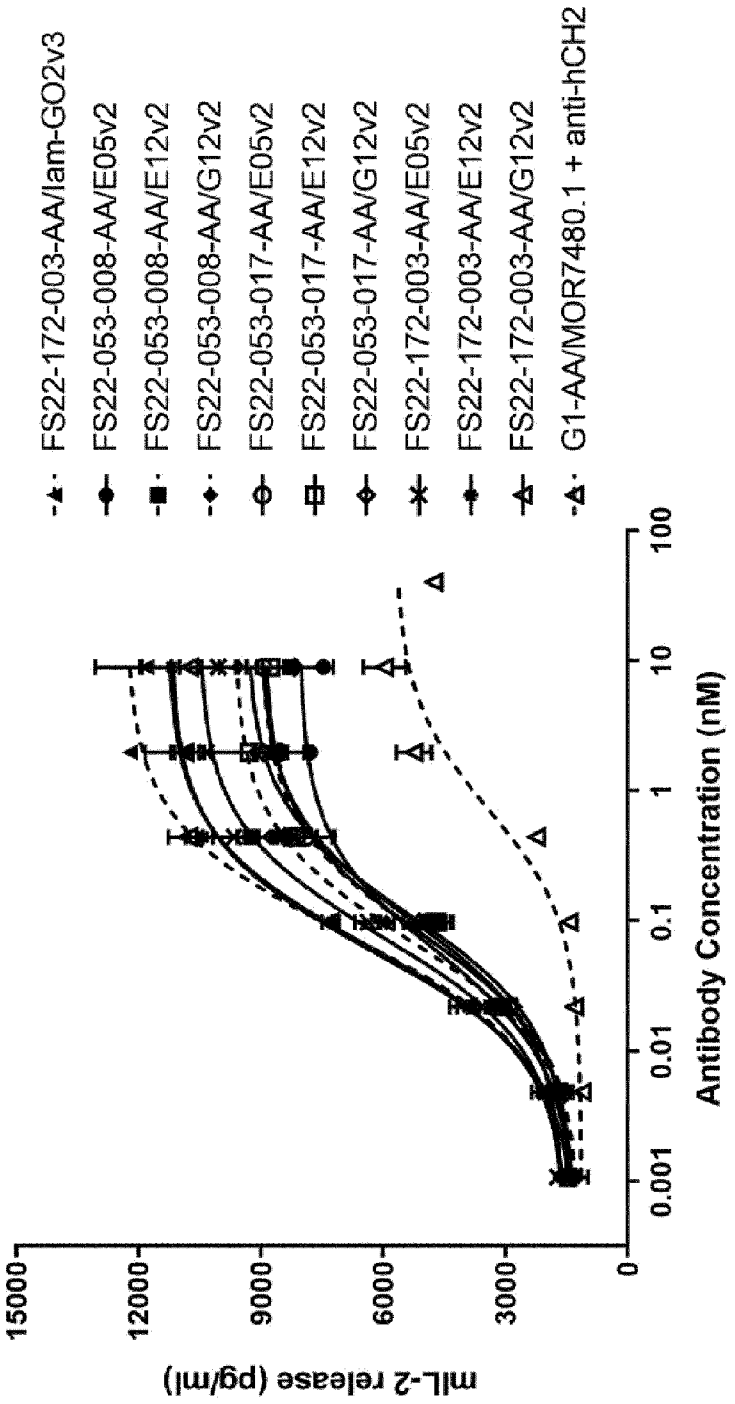
FS22-172-003-AA/Iam-GO2v3
FS22-053-008-AA/E05v2
FS22-053-008-AA/E12v2
FS22-053-008-AA/G12v2
FS22-053-017-AA/E05v2
FS22-053-017-AA/E12v2
FS22-053-017-AA/G12v2
FS22-172-003-AA/E05v2
FS22-172-003-AA/E12v2
FS22-172-003-AA/G12v2
G1-AA/MOR7480.1 + anti-hCH2
mIL-2 release (pg/ml)
15000
12000
9000
6000
3000
0
0.001
0.01
0.1
1
10
100
Antibody Concentration (nM)

Figure 8

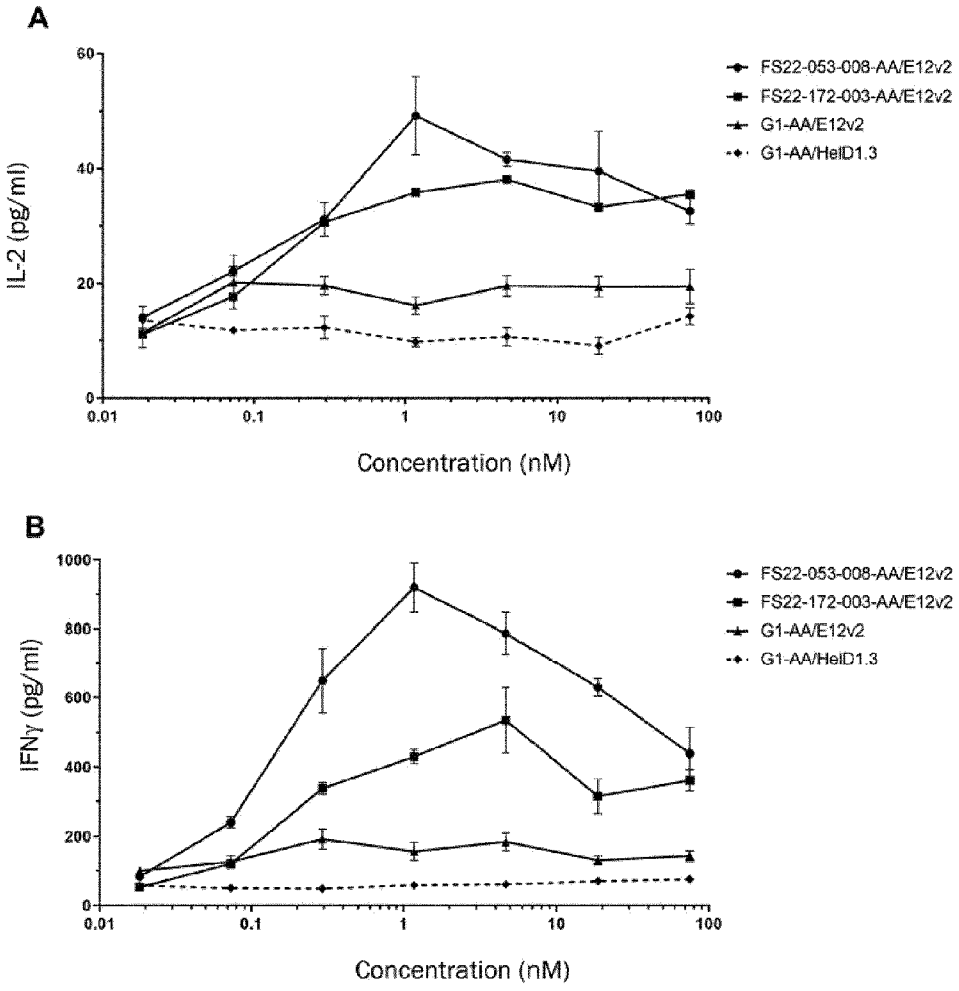
A
IL-2 (pg/ml)
60
40
20
0
0.01
0.1
1
10
100
Concentration (nM)
FS22-053-008-AA/E12v2
FS22-172-003-AA/E12v2
G1-AA/E12v2
G1-AA/HelD1.3
B
IFNγ (pg/ml)
1000
800
600
400
200
0
0.01
0.1
1
10
100
Concentration (nM)
FS22-053-008-AA/E12v2
FS22-172-003-AA/E12v2
G1-AA/E12v2
G1-AA/HelD1.3

Figure 9

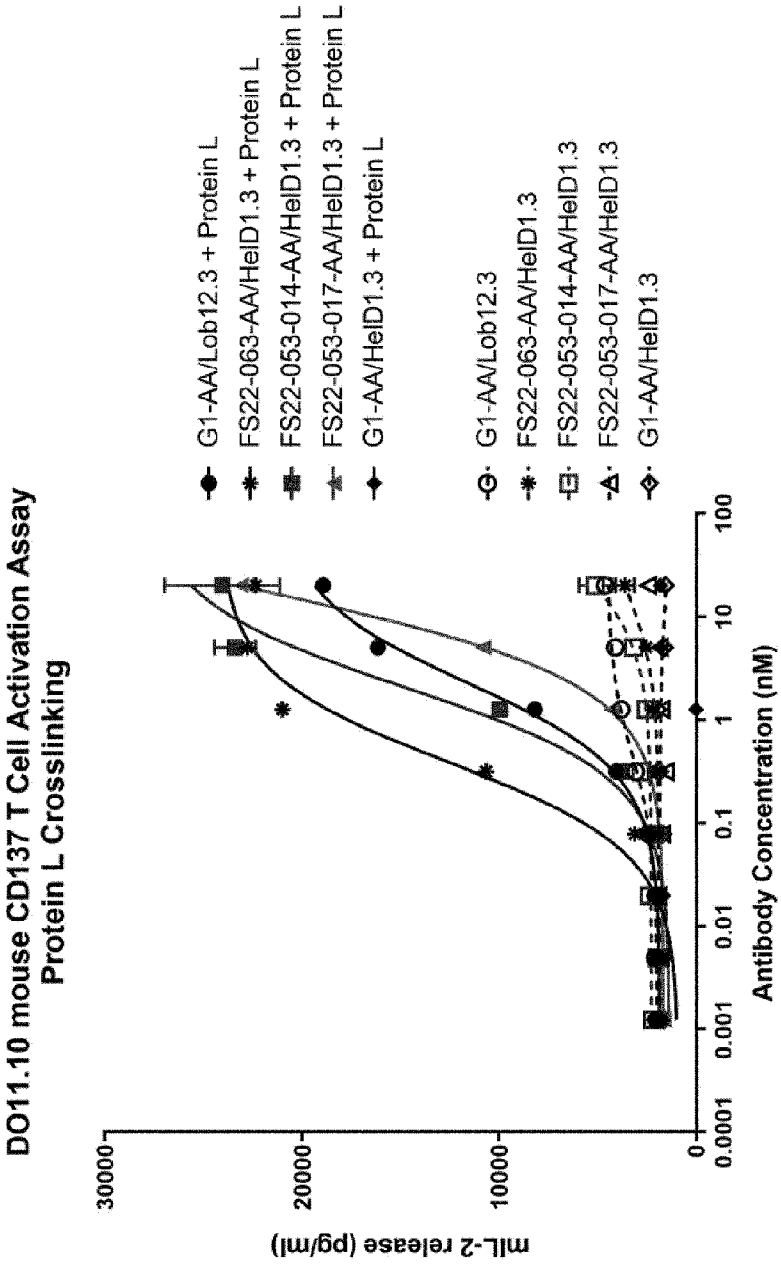
DO11.10 mouse CD137 T Cell Activation Assay
Protein L Crosslinking
mIL-2 release (pg/ml)
30000
20000
10000
0
0.0001
0.001
0.01
0.1
1
10
100
Antibody Concentration (nM)
G1-AA/Lob12.3 + Protein L
FS22-063-AA/HelD1.3 + Protein L
FS22-053-014-AA/HelD1.3 + Protein L
FS22-053-017-AA/HelD1.3 + Protein L
G1-AA/HelD1.3 + Protein L
G1-AA/Lob12.3
FS22-063-AA/HelD1.3
FS22-053-014-AA/HelD1.3
FS22-053-017-AA/HelD1.3
G1-AA/HelD1.3

Figure 10

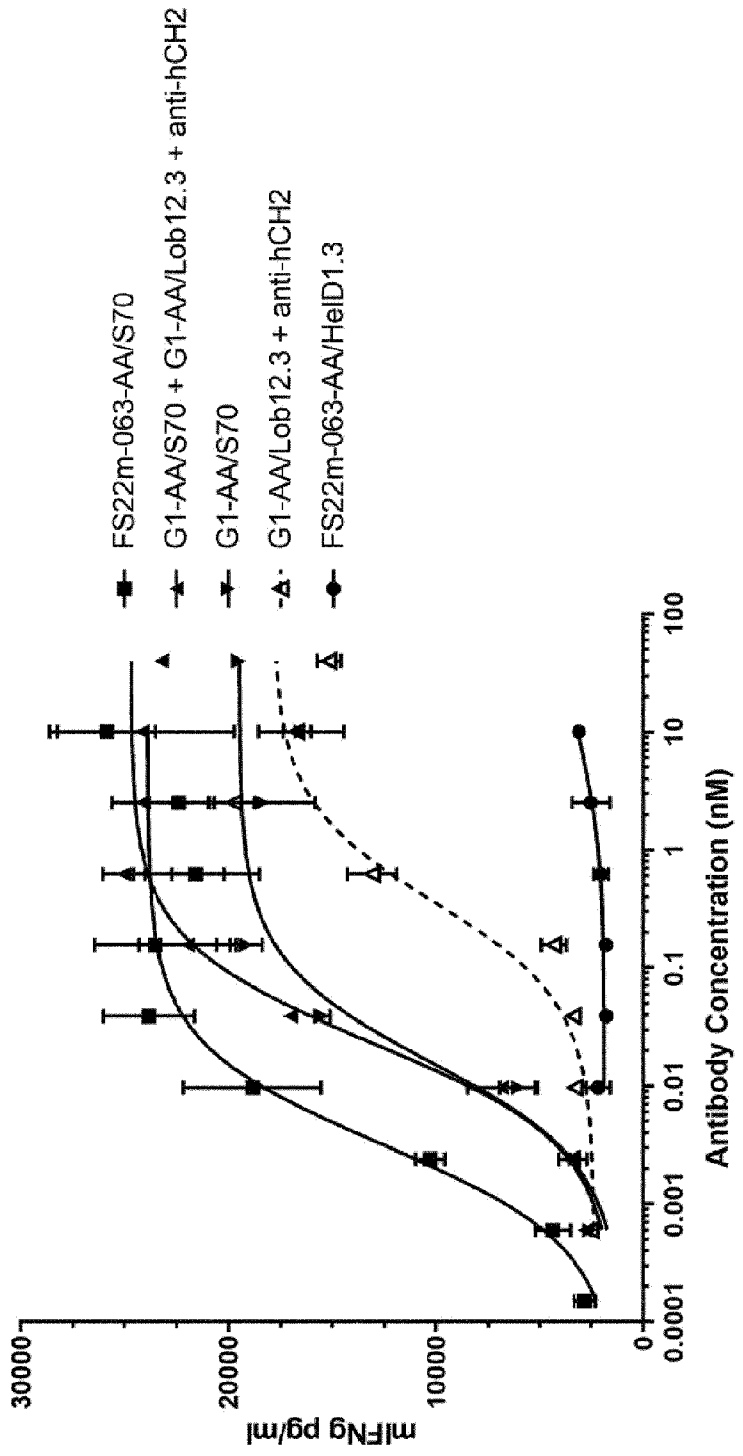
FS22m-063-AA/S70
G1-AA/S70 + G1-AA/Lob12.3 + anti-hCH2
G1-AA/S70
G1-AA/Lob12.3 + anti-hCH2
FS22m-063-AA/HelD1.3
mIFNg pg/ml
30000
20000
10000
0
0.0001
0.001
0.01
0.1
1
10
100
Antibody Concentration (nM)

Figure 11

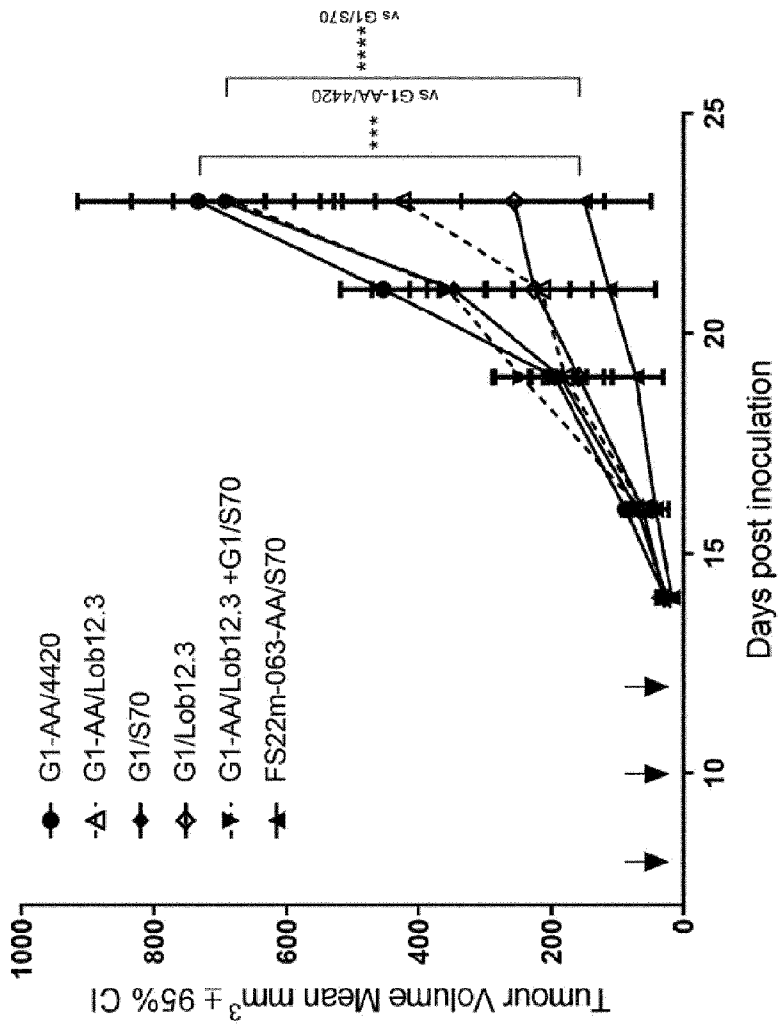
Tumour Volume Mean mm³ ± 95% CI
1000
800
600
400
200
0
10
15
20
25
Days post inoculation
G1-AA/4420
G1-AA/Lob12.3
G1/S70
G1/Lob12.3
G1-AA/Lob12.3 +G1/S70
FS22m-063-AA/S70
vs G1-AA/4420
***
vs G1/S70
****

Figure 12

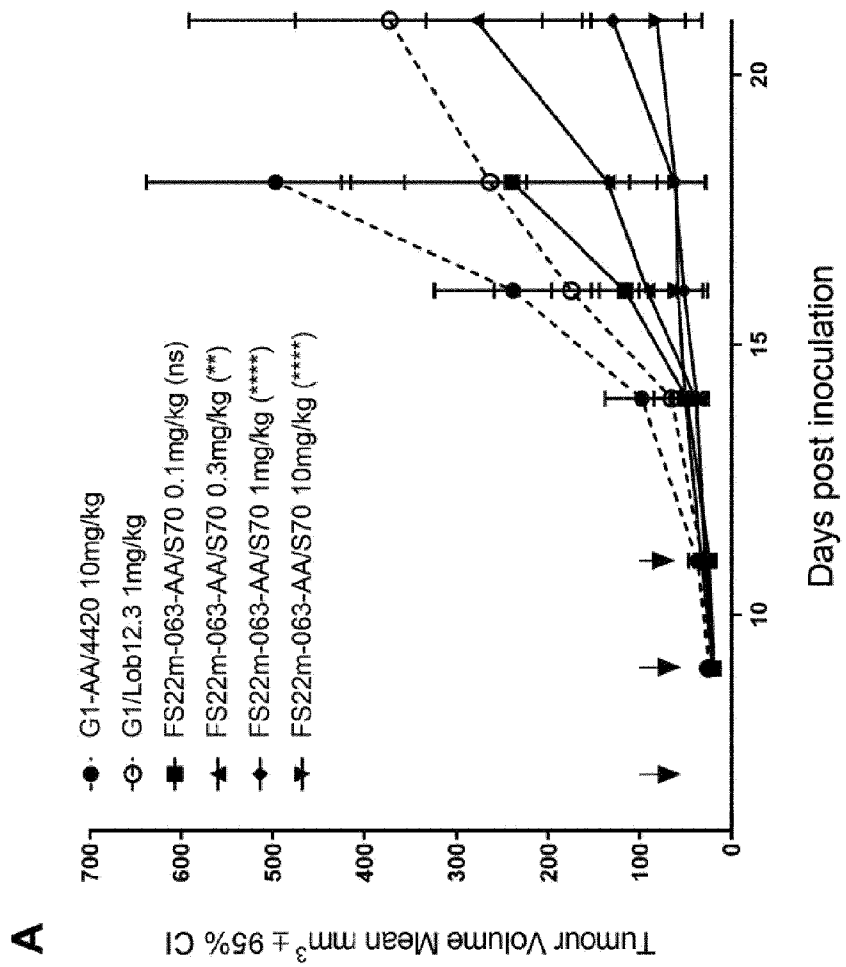
A
Tumour Volume Mean mm³ ± 95% CI
700
600
500
400
300
200
100
0
10
15
20
Days post inoculation
G1-AA/4420 10mg/kg
G1/Lob12.3 1mg/kg
FS22m-063-AA/S70 0.1mg/kg (ns)
FS22m-063-AA/S70 0.3mg/kg (**)
FS22m-063-AA/S70 1mg/kg (****)
FS22m-063-AA/S70 10mg/kg (****)

Figure 13

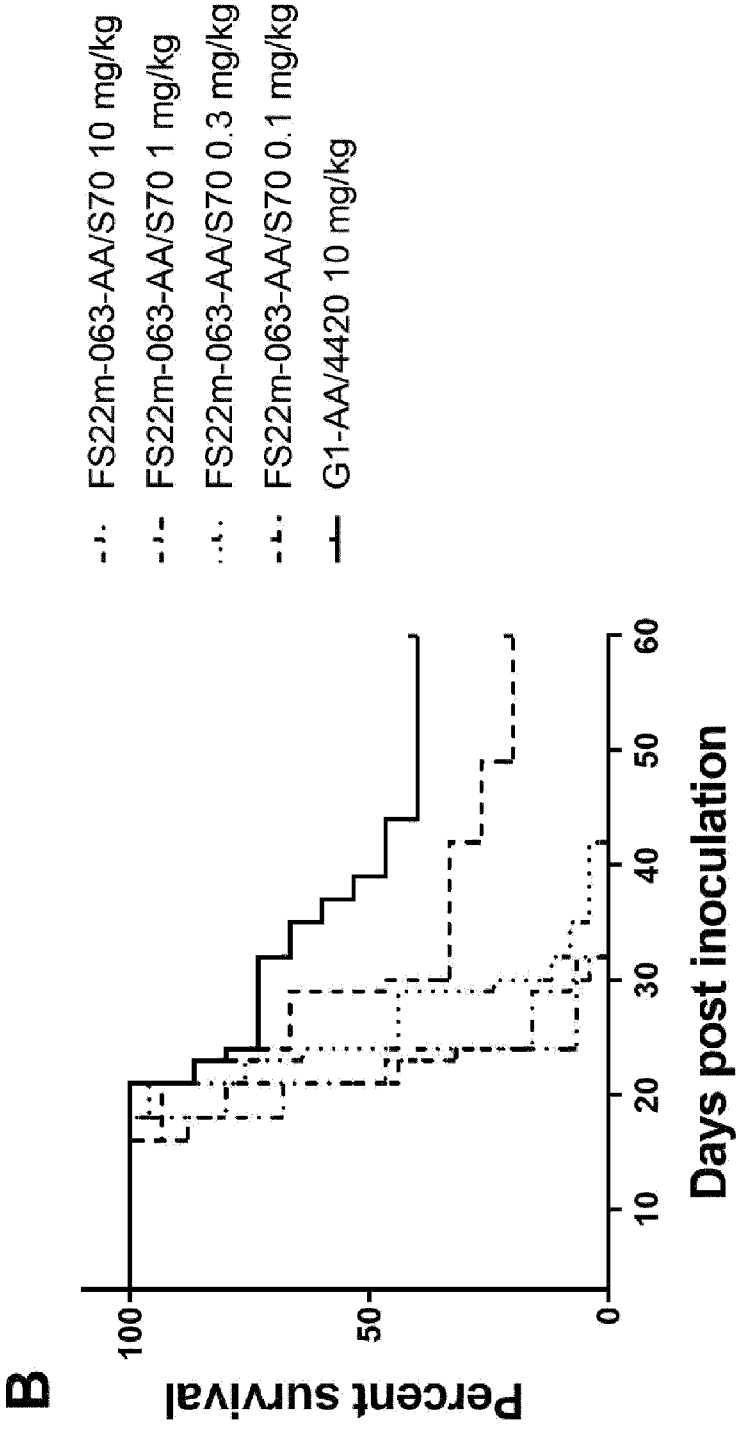

Figure 13 continued

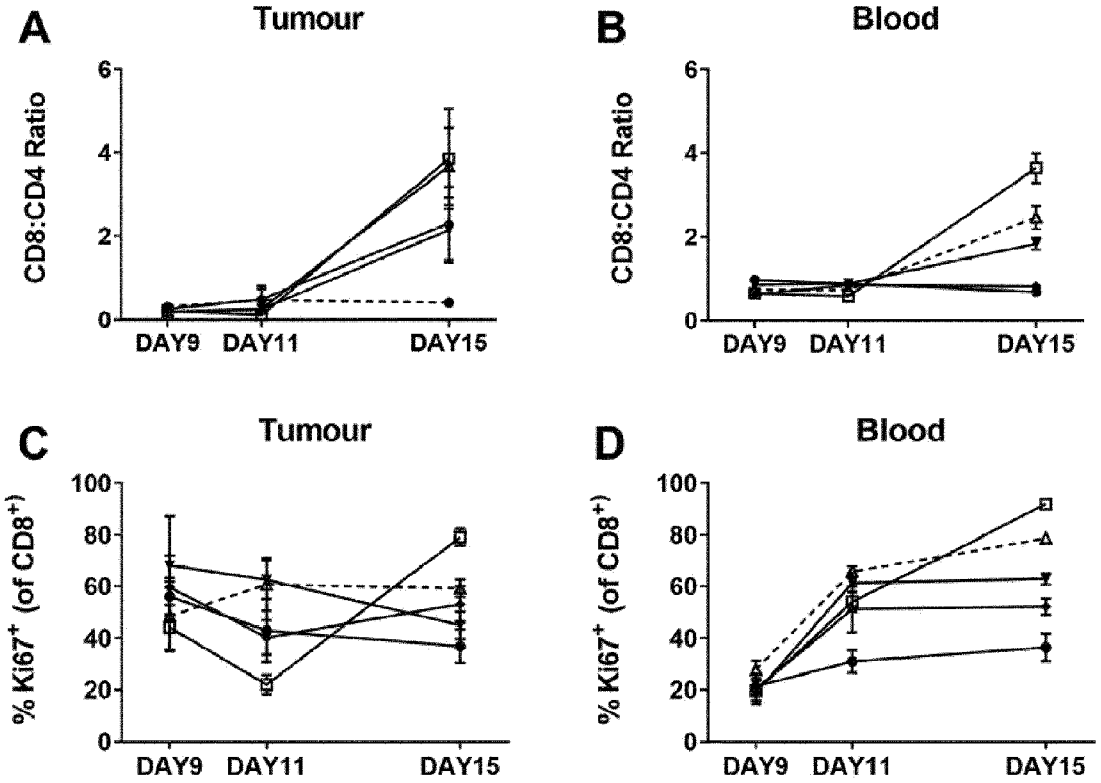
A
Tumour
CD8:CD4 Ratio
6
4
2
0
DAY9
DAY11
DAY15
B
Blood
CD8:CD4 Ratio
6
4
2
0
DAY9
DAY11
DAY15
C
Tumour
% Ki67+ (of CD8+)
100
80
60
40
20
0
DAY9
DAY11
DAY15
D
Blood
% Ki67+ (of CD8+)
100
80
60
40
20
0
DAY9
DAY11
DAY15

Figure 14

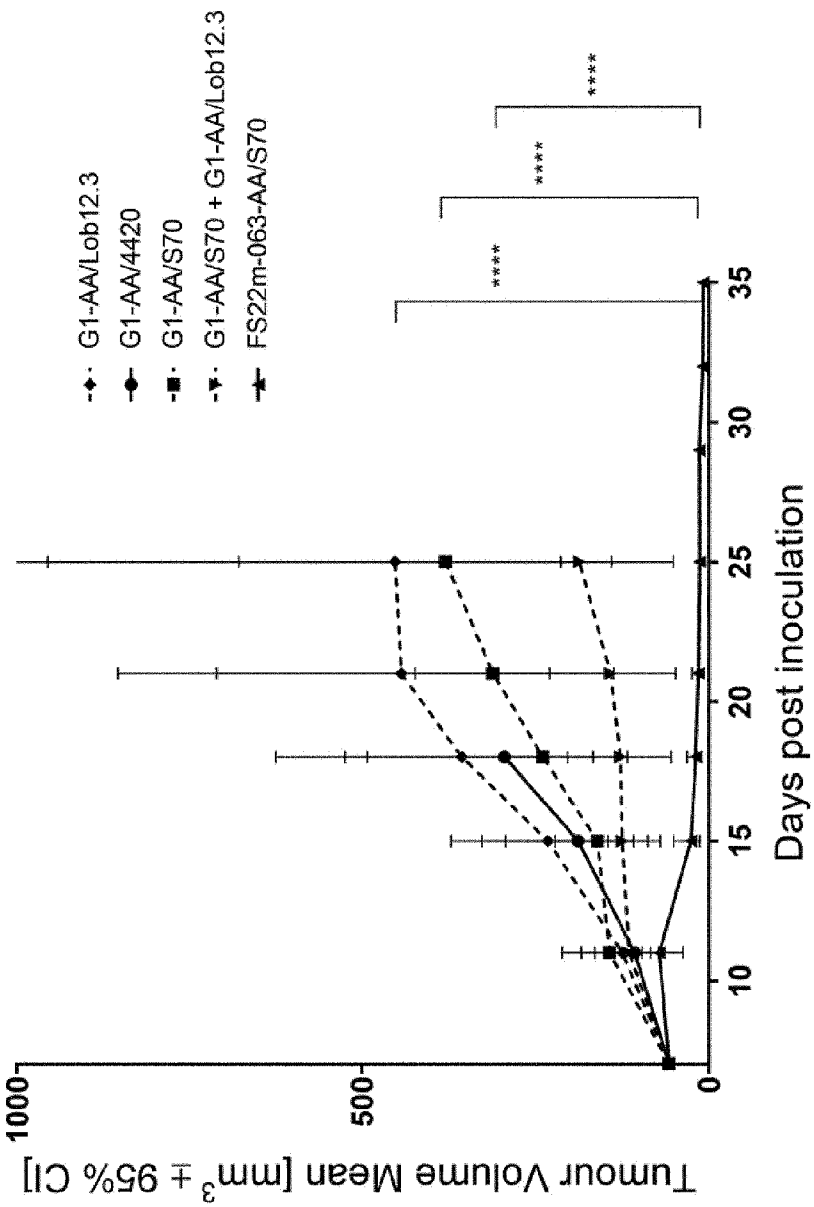
G1-AA/Lob12.3
G1-AA/4420
G1-AA/S70
G1-AA/S70 + G1-AA/Lob12.3
FS22m-063-AA/S70
****
****
****
Tumour Volume Mean [mm³ ± 95% CI]
1000
500
0
10
15
20
25
30
35
Days post inoculation

Figure 15

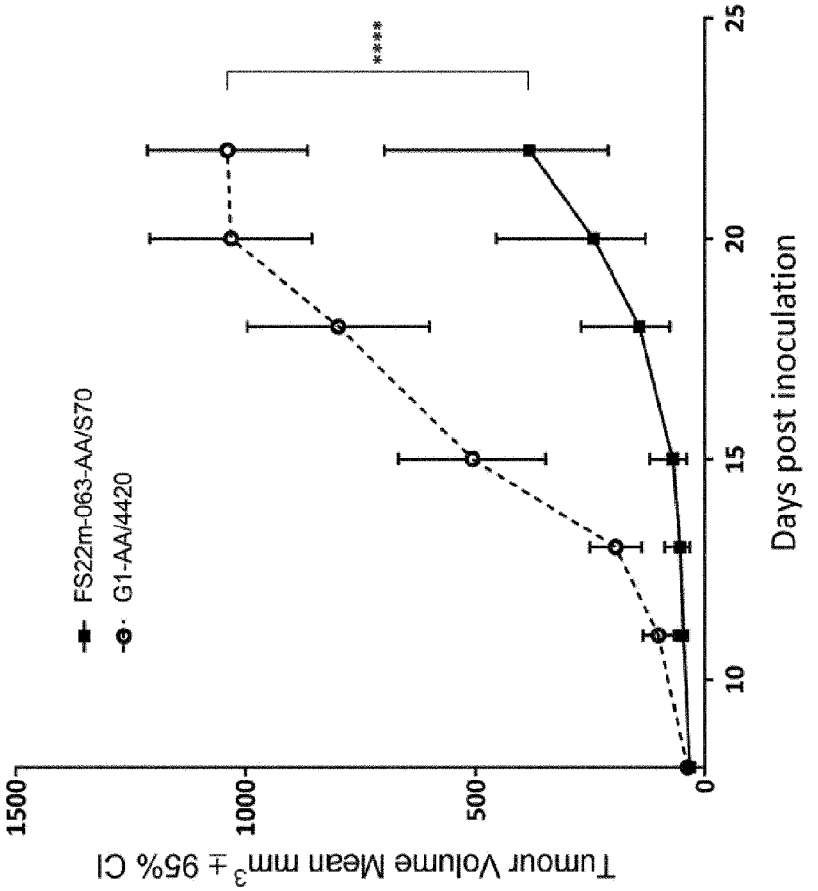
Tumour Volume Mean mm³ ± 95% CI
1500
1000
500
0
10
15
20
25
Days post inoculation
FS22m-063-AA/S70
G1-AA/4420
****

Figure 16

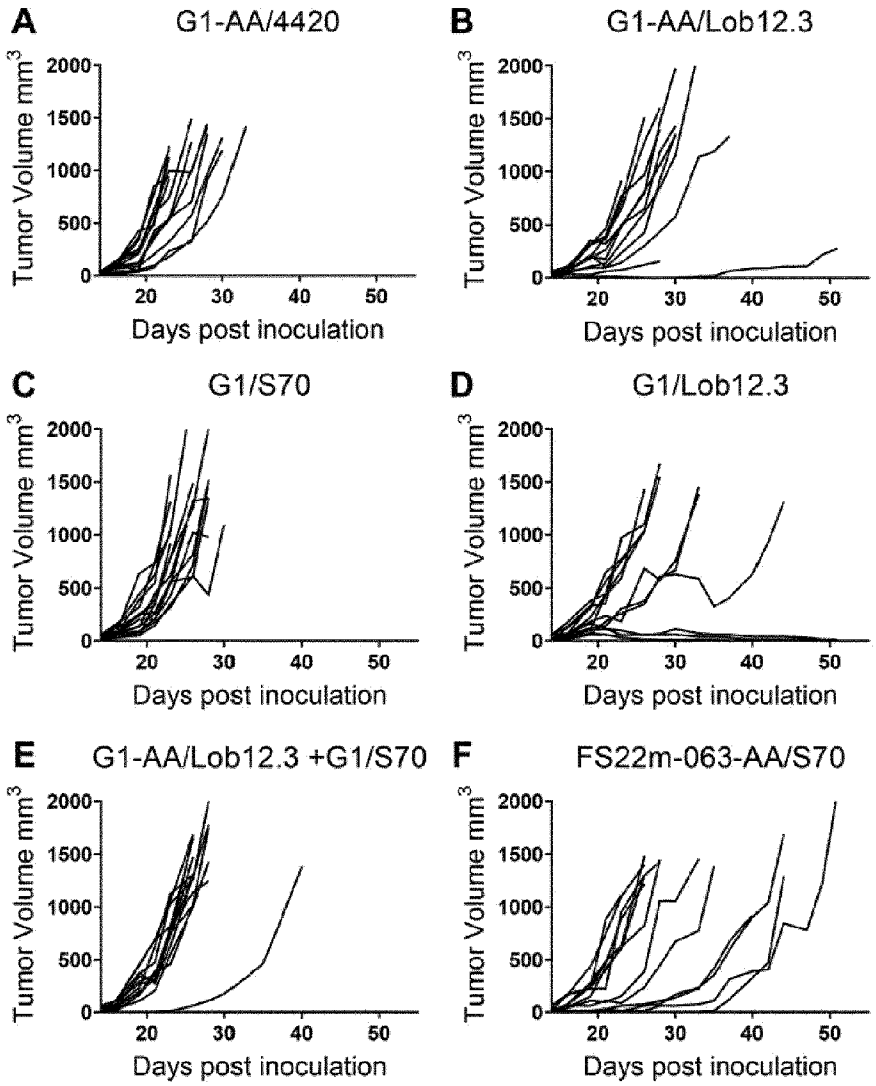
A
G1-AA/4420
B
G1-AA/Lob12.3
C
G1/S70
D
G1/Lob12.3
E
G1-AA/Lob12.3 +G1/S70
F
FS22m-063-AA/S70
Tumor Volume mm3
2000
1500
1000
500
0
20
30
40
50
Days post inoculation

Figure 17

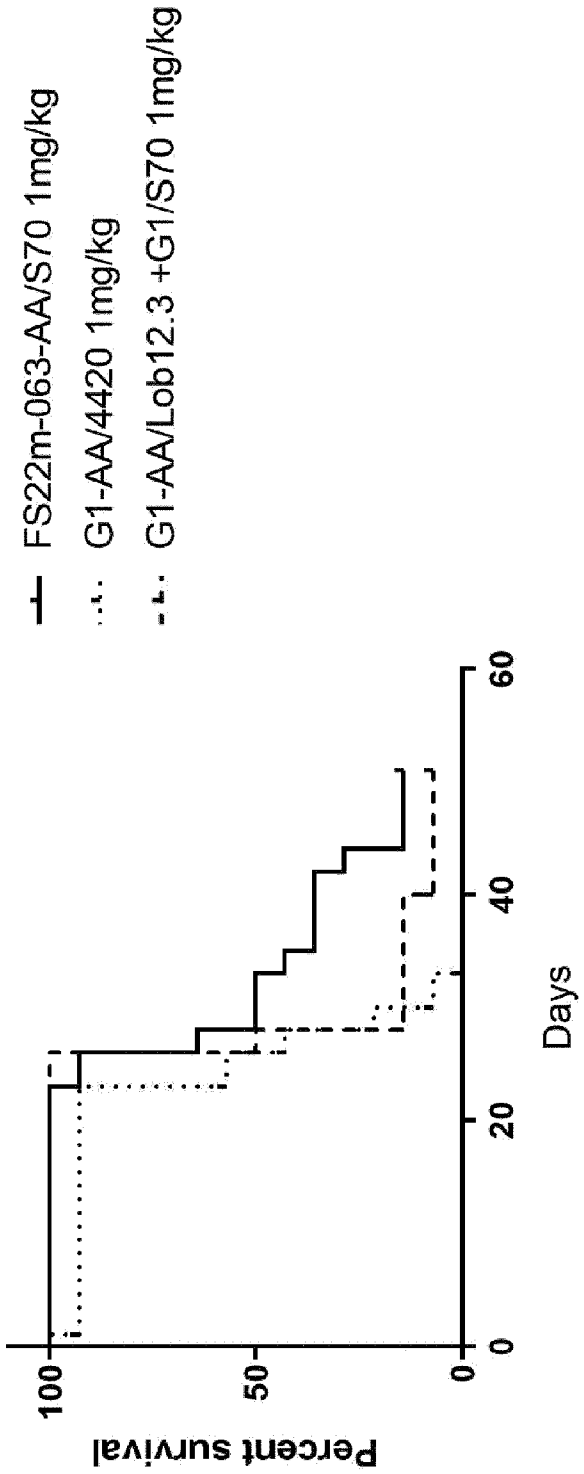
FS22m-063-AA/S70 1mg/kg
G1-AA/4420 1mg/kg
G1-AA/Lob12.3 +G1/S70 1mg/kg
Percent survival
100
50
0
0
20
40
60
Days

Figure 18

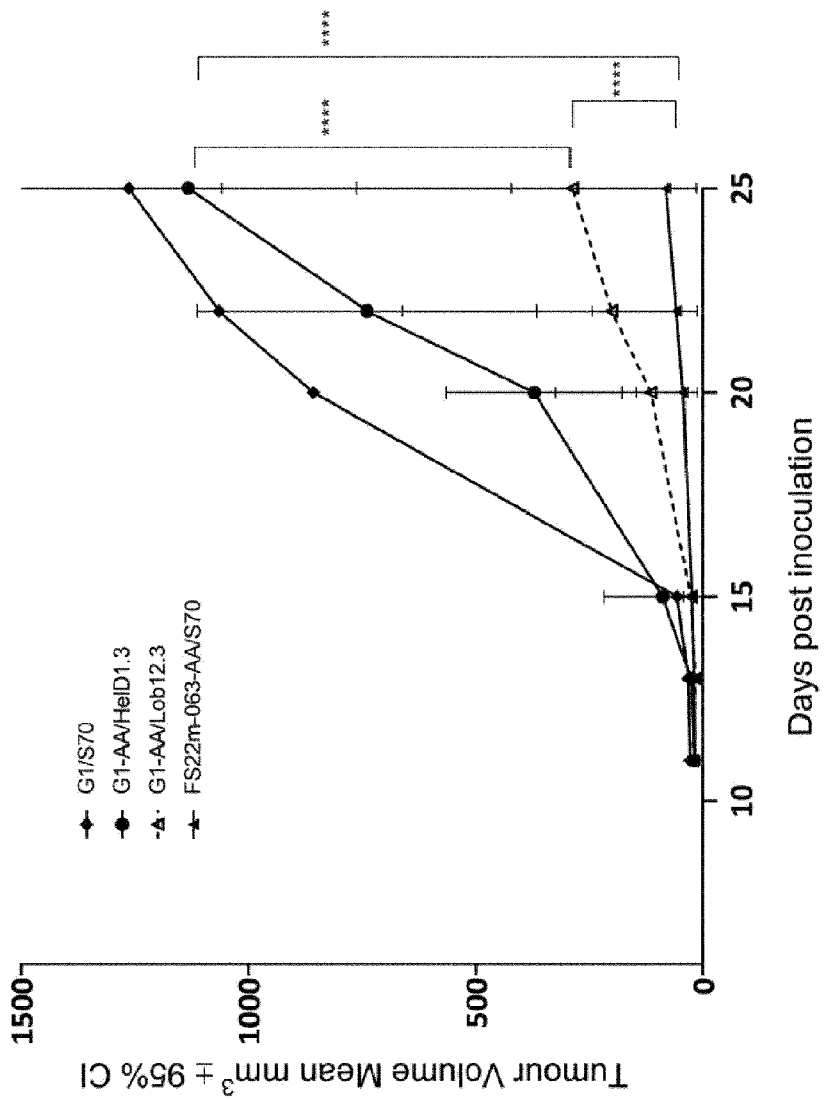
Tumour Volume Mean mm³ ± 95% CI
1500
1000
500
0
10
15
20
25
Days post inoculation
G1/S70
G1-AA/HelD1.3
G1-AA/Lob12.3
FS22m-063-AA/S70
****
****
****

Figure 19

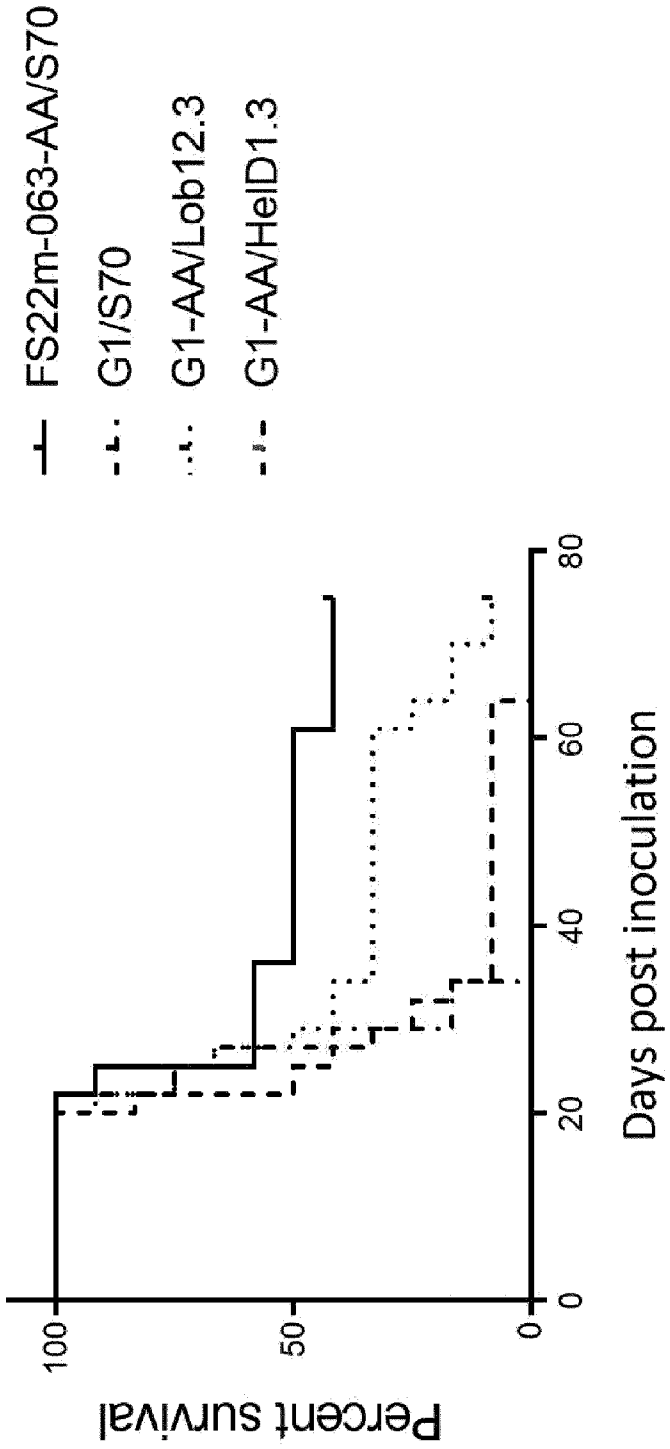
FS22m-063-AA/S70
G1/S70
G1-AA/Lob12.3
G1-AA/HelD1.3
Percent survival
100
50
0
0
20
40
60
80
Days post inoculation

Figure 20

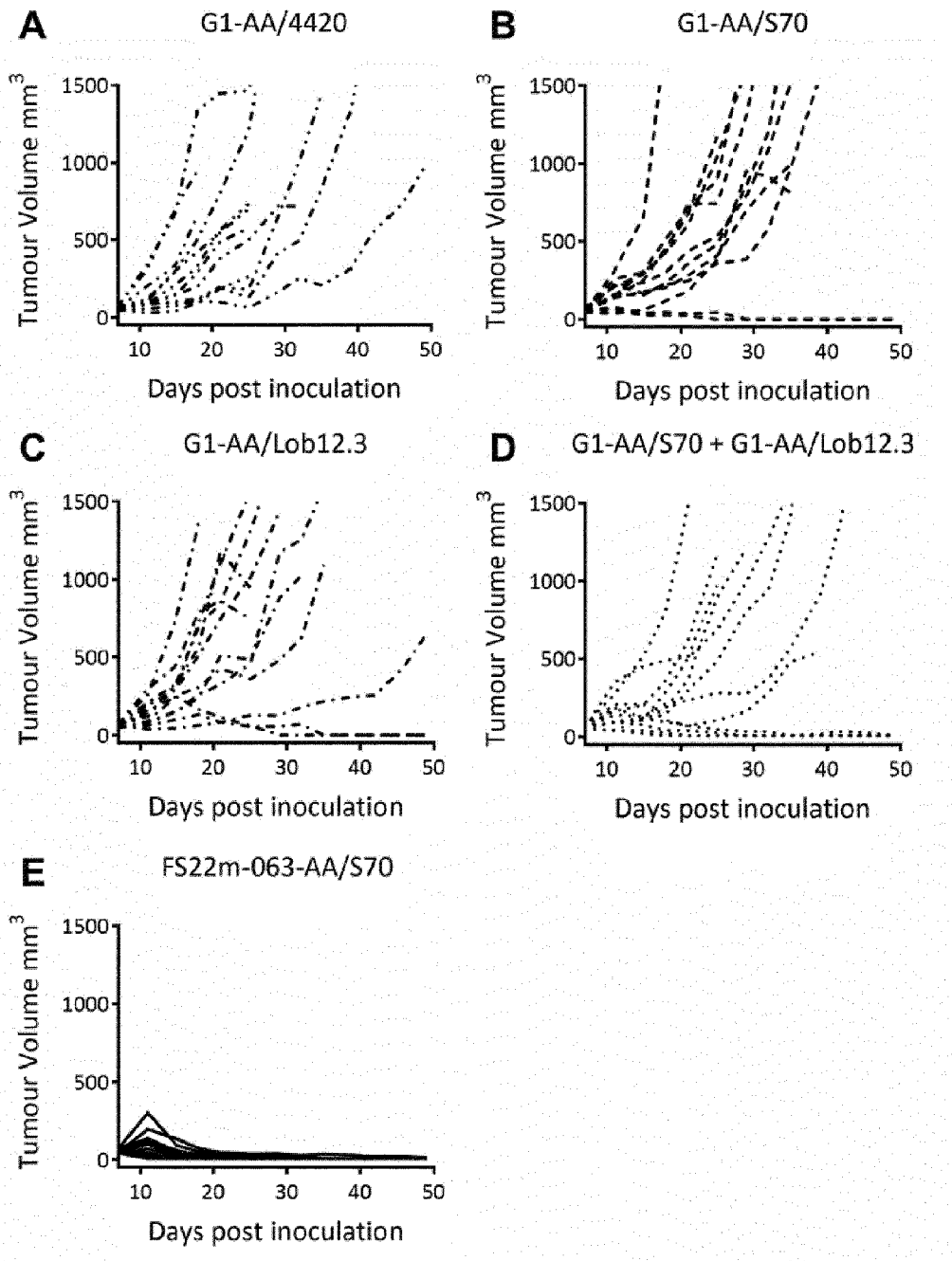
A
G1-AA/4420
B
G1-AA/S70
C
G1-AA/Lob12.3
D
G1-AA/S70 + G1-AA/Lob12.3
E
FS22m-063-AA/S70
Tumour Volume mm3
1500
1000
500
0
10
20
30
40
50
Days post inoculation

Figure 21

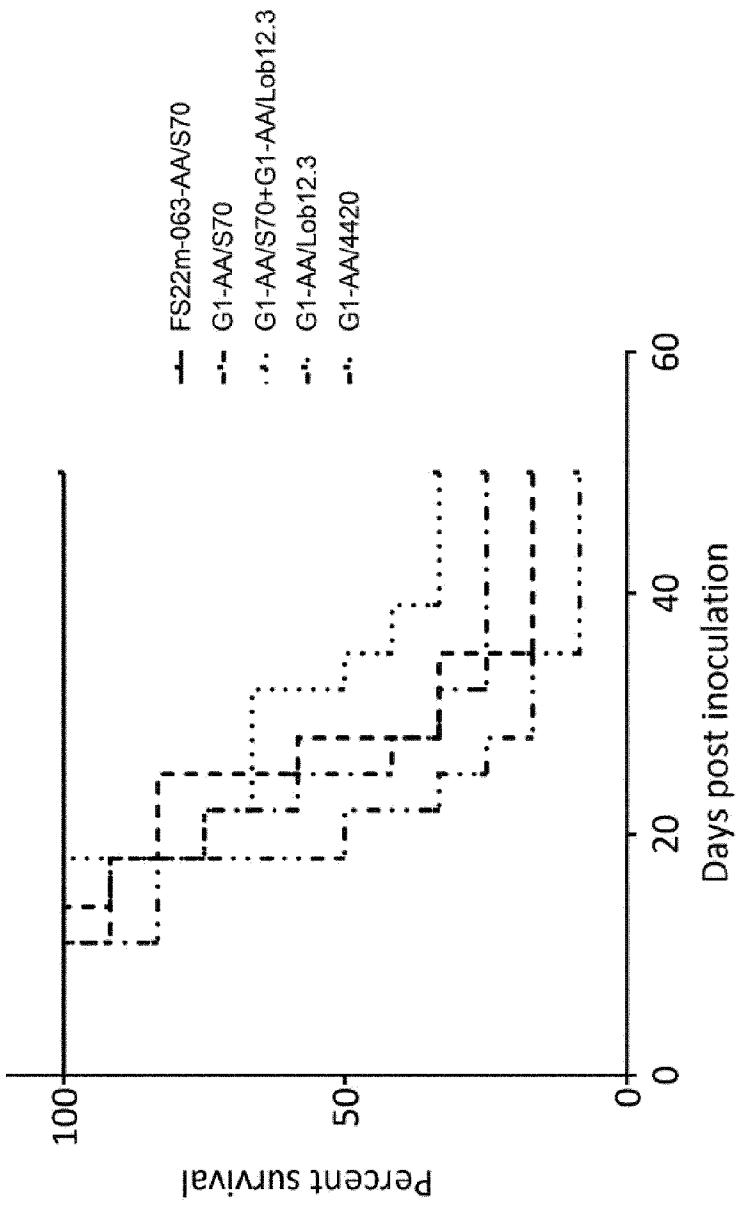
FS22m-063-AA/S70
G1-AA/S70
G1-AA/S70+G1-AA/Lob12.3
G1-AA/Lob12.3
G1-AA/4420
Percent survival
100
50
0
0
20
40
60
Days post inoculation

Figure 22

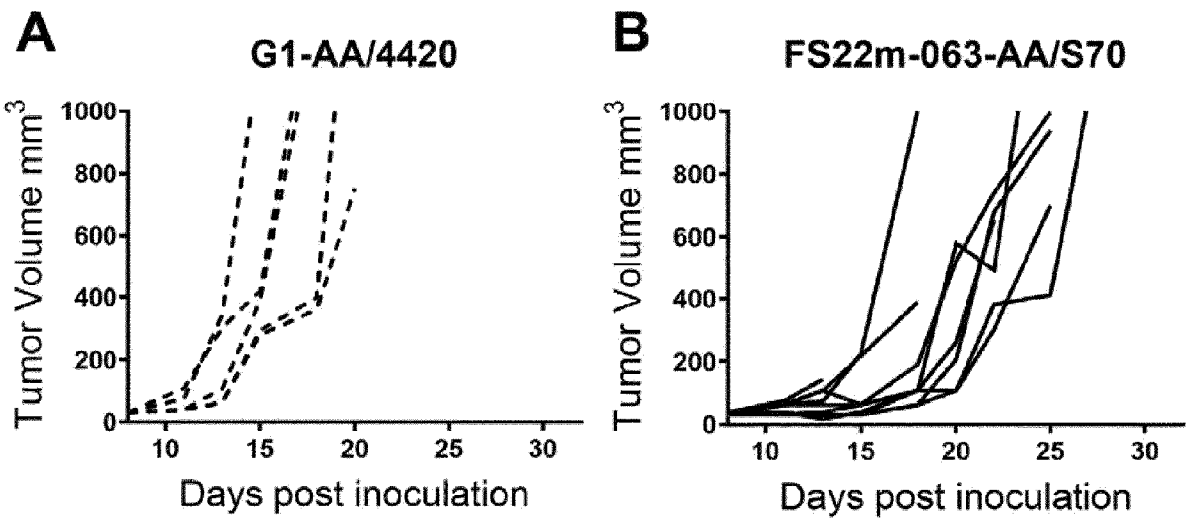

Figure 23

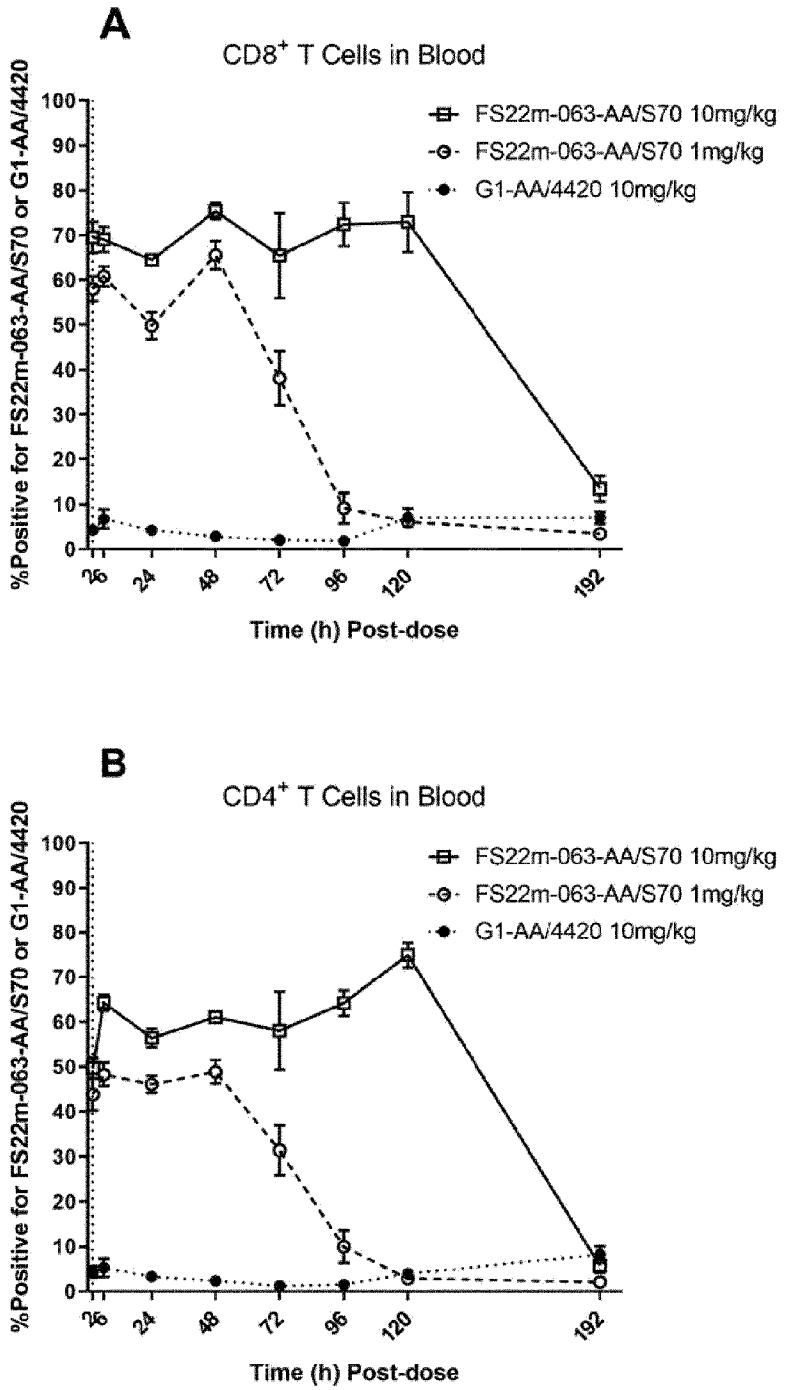
A
CD8+ T Cells in Blood
FS22m-063-AA/S70 10mg/kg
FS22m-063-AA/S70 1mg/kg
G1-AA/4420 10mg/kg
%Positive for FS22m-063-AA/S70 or G1-AA/4420
Time (h) Post-dose
B
CD4+ T Cells in Blood
FS22m-063-AA/S70 10mg/kg
FS22m-063-AA/S70 1mg/kg
G1-AA/4420 10mg/kg
%Positive for FS22m-063-AA/S70 or G1-AA/4420
Time (h) Post-dose

Figure 24

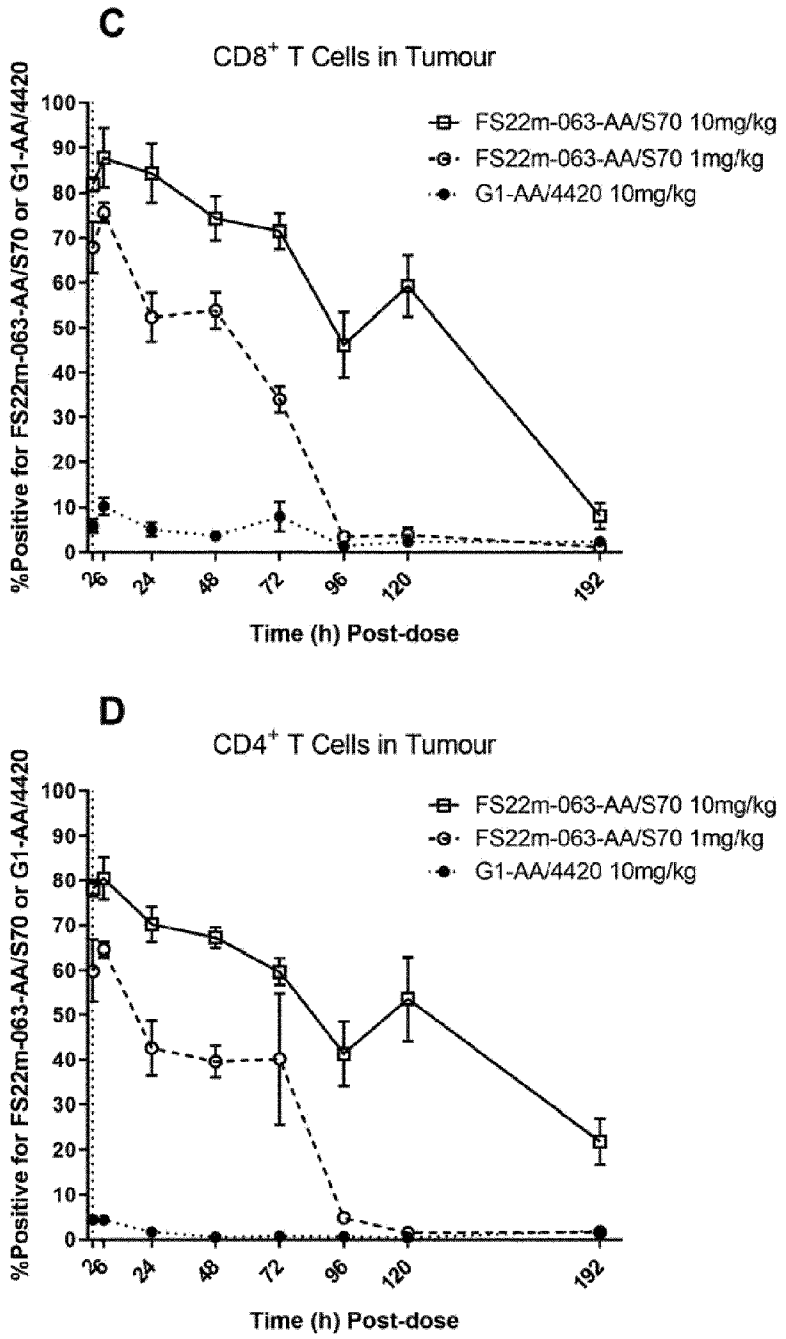

Figure 24 continued

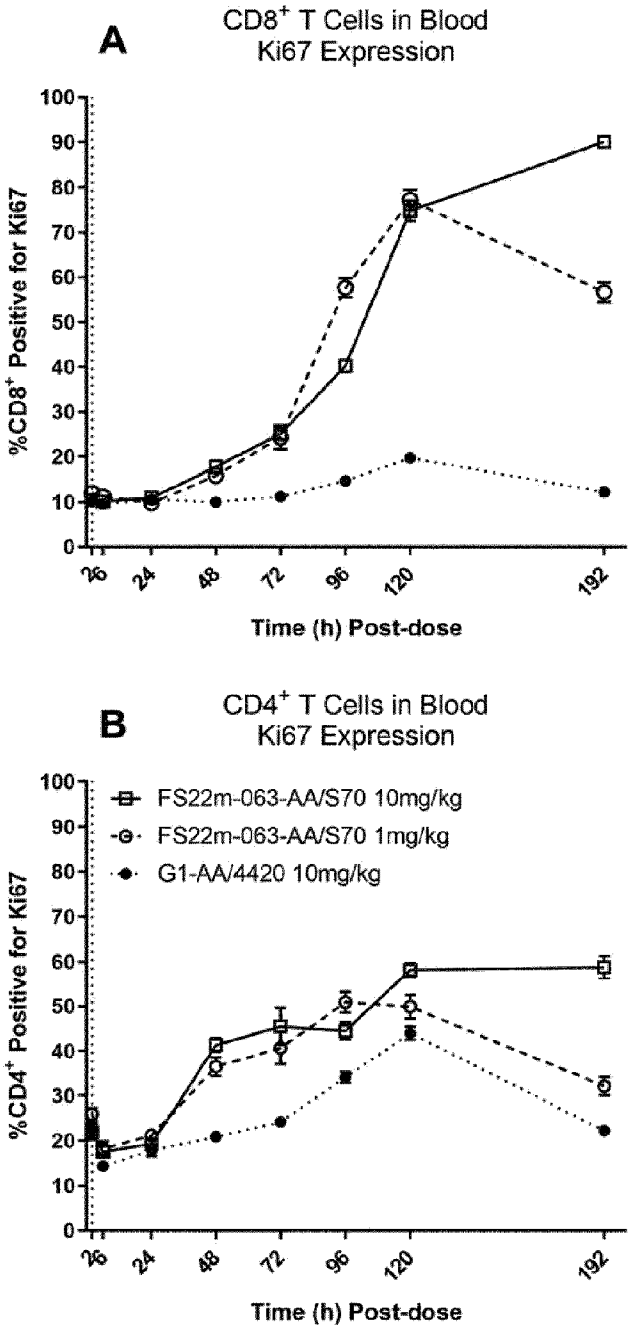
A
CD8+ T Cells in Blood
Ki67 Expression
%CD8+ Positive for Ki67
Time (h) Post-dose
B
CD4+ T Cells in Blood
Ki67 Expression
FS22m-063-AA/S70 10mg/kg
FS22m-063-AA/S70 1mg/kg
G1-AA/4420 10mg/kg
%CD4+ Positive for Ki67
Time (h) Post-dose

Figure 25

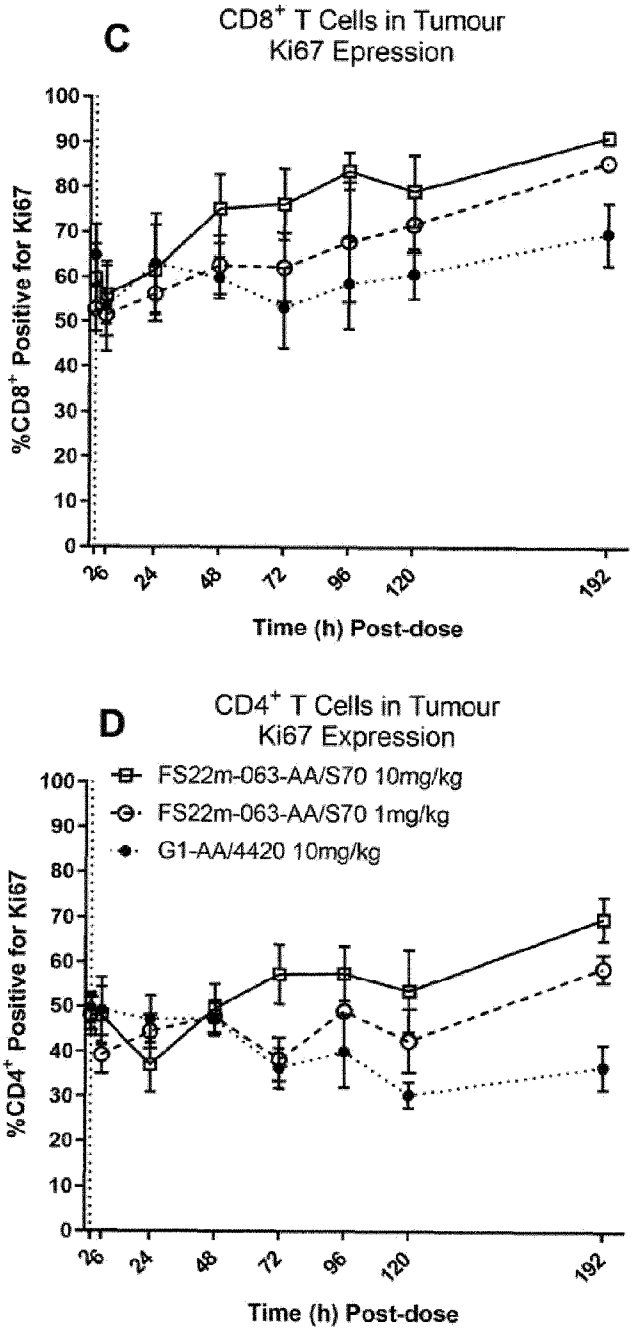

Figure 25 continued

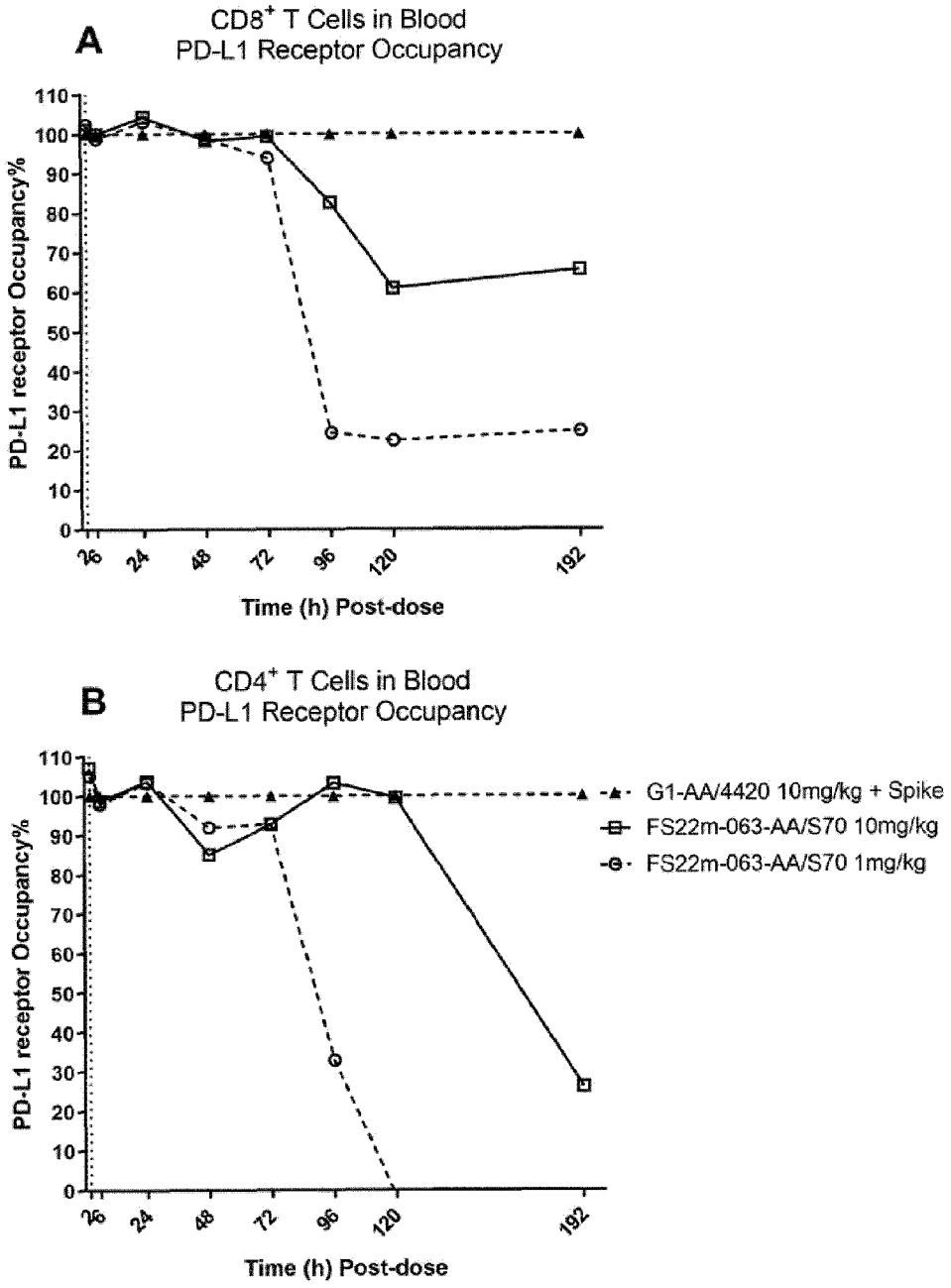
A
CD8+ T Cells in Blood
PD-L1 Receptor Occupancy
PD-L1 receptor Occupancy%
Time (h) Post-dose
B
CD4+ T Cells in Blood
PD-L1 Receptor Occupancy
PD-L1 receptor Occupancy%
Time (h) Post-dose
G1-AA/4420 10mg/kg + Spike
FS22m-063-AA/S70 10mg/kg
FS22m-063-AA/S70 1mg/kg

Figure 26

C

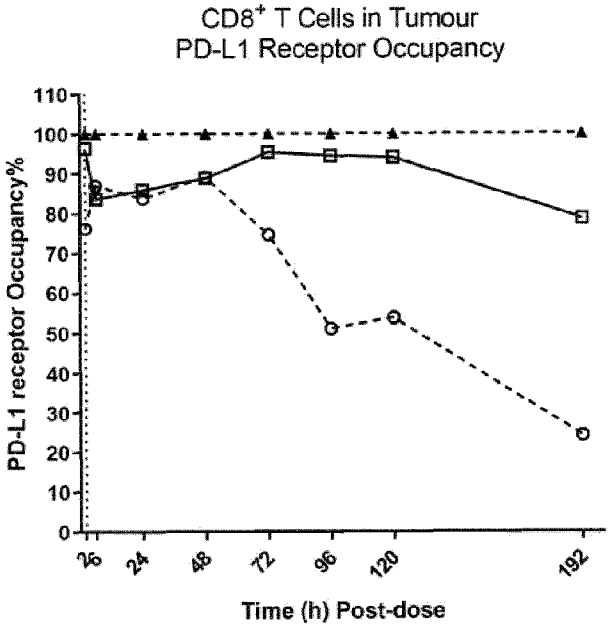

D

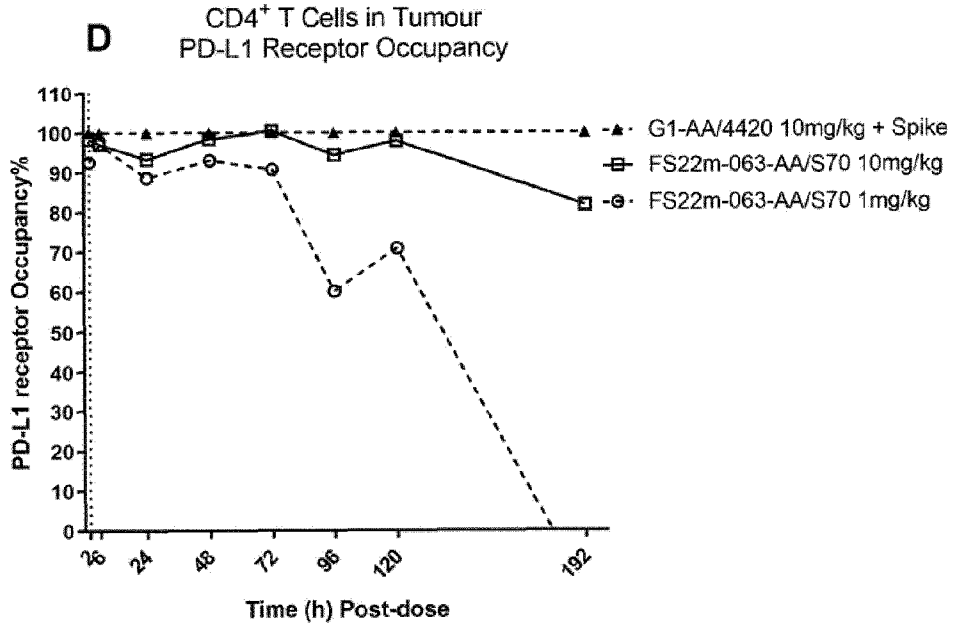

Figure 26 continued

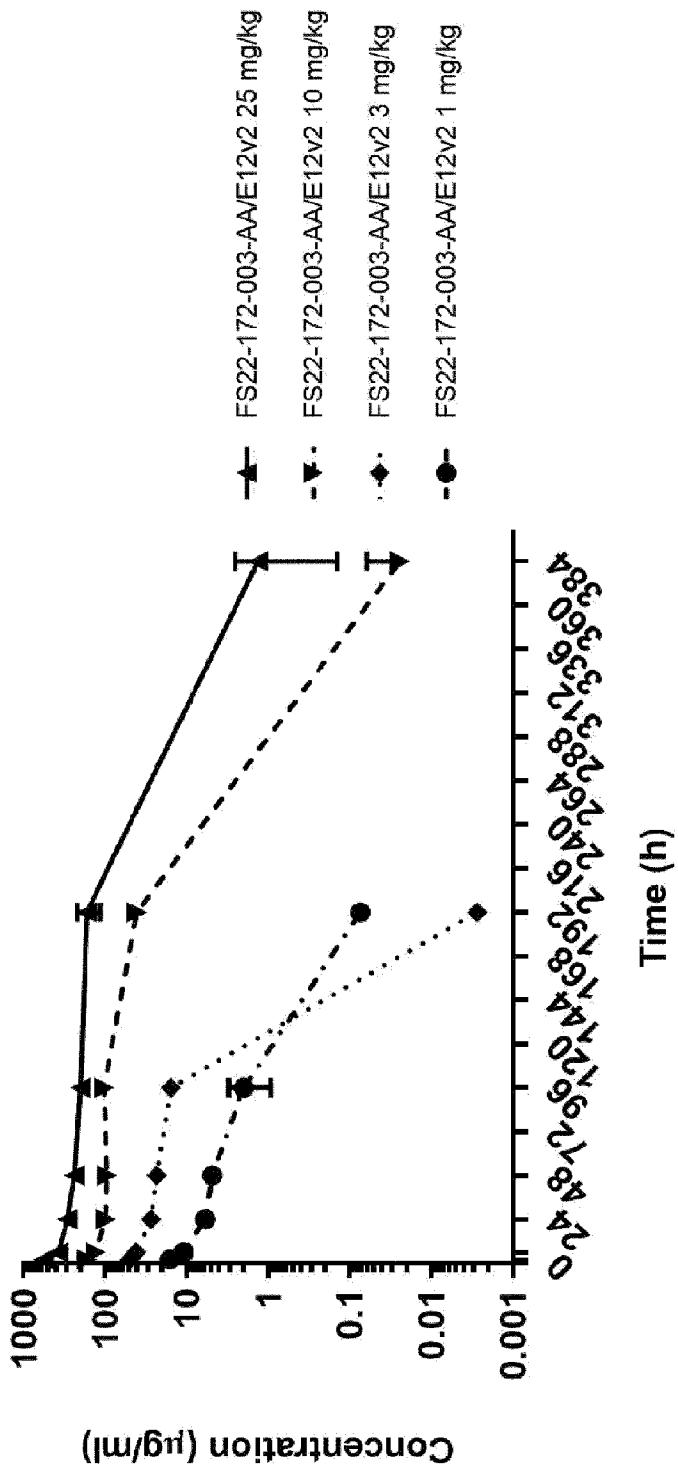
FS22-172-003-AA/E12v2 25 mg/kg
FS22-172-003-AA/E12v2 10 mg/kg
FS22-172-003-AA/E12v2 3 mg/kg
FS22-172-003-AA/E12v2 1 mg/kg
Concentration (µg/ml)
1000
100
10
1
0.1
0.01
0.001
Time (h)
0
24
48
72
96
120
144
168
192
216
240
264
288
312
336
360
384

Figure 27

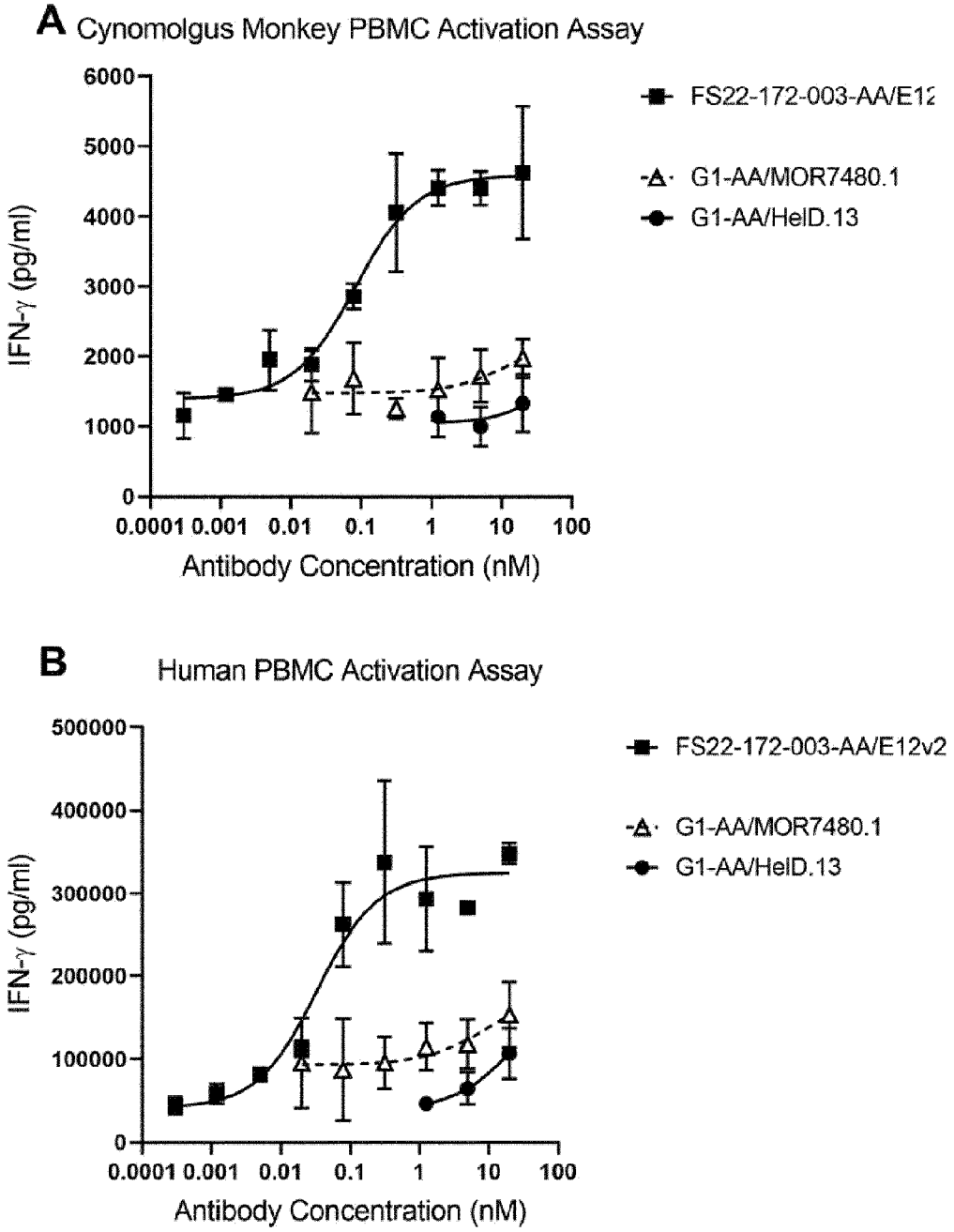
A Cynomolgus Monkey PBMC Activation Assay
IFN-γ (pg/ml)
6000
5000
4000
3000
2000
1000
0
0.0001 0.001 0.01 0.1 1 10 100
Antibody Concentration (nM)
FS22-172-003-AA/E12
G1-AA/MOR7480.1
G1-AA/HelD.13
B Human PBMC Activation Assay
IFN-γ (pg/ml)
500000
400000
300000
200000
100000
0
0.0001 0.001 0.01 0.1 1 10 100
Antibody Concentration (nM)
FS22-172-003-AA/E12v2
G1-AA/MOR7480.1
G1-AA/HelD.13

Figure 28